CELL CYCLE-DEPENDENT CHANGES IN LYMPHOID CELLS INFECTED WITH FELINE LEUKAEMIA VIRUS

by

Sarah R. Toth

Submitted for the Degree of Doctor of Philosophy to the Faculty of Veterinary Medicine, University of Glasgow

January, 1980

CONTENTS

Table of Contents

List of Tables

CHAPTER FOUR

CHAPTER FIVE

List of Figures

INTRODUCTION

CHAPTER TWO

CHAPTER THREE

The figures in Chapter Three are scanning electron micrographs (SEM) and transmission electron micrographs (TEM).

In Figure Nos. 8 to 62, FL74 cells are shown.

CHAPTER FOUR

CHAPTER FIVE

CHAPTER SIX

ACKNOWLEDGEMENTS

During the course of my research I was assisted by many of the staff of the Department of Veterinary Pathology, for which I wish to thank them all. I am particularly grateful to Professor W.F.H. Jarrett, who initiated and supervised my research and gave encouragement and advice throughout. He also generously provided facilities and resources in his department.

I am greatly indebted to Dr. Helen Laird for the unfailing support she gave me at all stages of my work, and for the training she provided on the use of the electron microscope. This helped me considerably in the completion of many parts of my studies.

My thanks are due to Mrs. Carole McLay for her technical assistance in the preparation of the EM material.

The excellent photographic work was done by Mr. Colin Wilson which is gratefully appreciated.

I would like to thank Mrs. Jacquie Grantham and Mrs. Betty Paterson for their thorough and efficient typing of the text.

Finally, I wish to acknowledge the financial support which was provided by the Wellcome Trust.

SUMMARY

The aim of this study was to investigate a variety of cell cycle-related changes in FeLV-infected lymphoid cells.

The cell cycle and the use of synchronised cells played a major role in most of the experiments carried out. The Introduction, therefore, contains an outline of the concept of the mammalian cell cycle and a discussion of some of its practical applications.

In Chapter One, synchronising techniques and life cycle analysis methods are described in general, while the methods used during the course of this study are presented in more detail.

The relationship between a distinct phase of the cell cycle and the release of FeLV is examined in Chapter Two. By using two assay systems and applying two different synchronising methods it was established that virus production is cell cycle-dependent. It occurs in the G_1 period in both homologous and heterlogous cell lines.

Changes in morphology during synchronous growth were examined by transmission (TEM) and by scanning (SEM) electron microscopy (Chapter Three). An analysis of morphological data obtained by TEM and SEM revealed that synchronised cells of the cat lymphoblastoid line, FL74, exhibited distinct ultrastructural variations which were closely related to the cell cycle. It was also established, for the first time, that the surface structure of lymphoid cells showed cell cycle-specific changes which were highly characteristic. When the number of budding C-type particles was

counted on cells which were morphologically characterised in this way it was found that in both TEM and SEM preparations the early-G_1-cells were releasing the highest number of virus particles.

An investigation of the expression of viral antigens and FOCMA in synchronised cells was the subject of a further study described in Chapter Four. By using immunofluorescence techniques, evidence was obtained for the cell cycle-dependent expression of viral and FOCMA antigens. The viral structural antigens, p15 and p30, and the major envelope glycoprotein gp70 reached a peak in the early-G_1 phase, whereas, FOCMA was expressed 14 hours later in the late-G_1 period. FOCMA peaks were detected on FeLV-infected feline but not on FeLV-infected canine cell lines. This suggested that FOCMA was distinct from the viral antigens.

In order to investigate the kinetics of FeLV production and to explore some of the regulatory mechanisms responsible for the expression of antigens in FL74 cells, the effects of various metabolic inhibitors were examined (Chapter Five). It was found that virus production and antigen expression were regulated by a complex cell cycle-dependent synthesis of RNA, mRNA, viral and cellular proteins, which in turn were co-ordinated by mitosis.

Finally, in Chapter Six, the occurrence and distribution of feline leukaemia virus-associated antigens were examined by immuno-electron microscopy. Ferritin labelling of cells prefixed in glutaraldehyde revealed that the cell surface antigens were randomly distributed. gp70

was found to be the most plentiful followed by FOCMA, p30 and p15 in descending order. Antisera to p15 and p30 did not stain intact viral particles, while the non-budding areas of the cell membrane were labelled. Both gp70 and FOCMA antisera stained viral particles as well as the non-budding areas of the cell membrane. In order to investigate the unexpected labelling of viral particles by FOCMA antisera, an immunofluorescence-immunoferritin study in capping conditions and competition experiments were performed. The results indicated that FOCMA was distinct from gp70 and that labelling of virions was possibly due to the undetected presence of neutralising antibodies in the FOCMA antisera used. Ferritin labelling of synchronised FL74 cells showed that in the early-G_1 phase considerably more antigenic sites per unit length were expressed than in the S phase.

INTRODUCTION

INTRODUCTION

1. The Concept of the Cell Cycle

2. Some Practical Applications of the Cell Cycle Model

3. Review of the Literature

In the last few years the theoretical and practical importance of cell cycle-dependent changes in proliferating cells has been recognised to an increasing extent. In many fields of biological sciences, researchers are becoming more and more aware of the interaction between phases of the cycle and certain biochemical events. This is reflected in the growing number of references made to this phenomenon in data analysis and interpretation.

The concept of the cell cycle has contributed to a better understanding of the nature and behaviour of the neoplastic cell and to the therapy of the disease it causes. Similarly, it has a major role to play in the elucidation of the complex relationship between virus production, antigen expression and the infected cell. At a more practical level, a knowledge of this concept may prove useful in the explanation of apparent contradictions in experimental results in a variety of fields, such as virology, immunology, morphology etc. Thus, for example, variations that sometimes occur in cytotoxicity tests may be explained by cycle-specific changes in cell membrane antigen expression. Also, cell cycle-dependence of certain immunological markers may have a profound effect on the actual proportion of cells identified. Moreover, virus detection in low-producer cells can be greatly improved by their synchronisation, and the effectiveness of vaccines may be influenced by the stage in their life cycle of the cells from which they were prepared. In ultrastructural studies also the occurrence of cycle-related changes in cell morphology can be a crucial factor in data interpretation.

When this study was commenced only a limited number of publications were available as to the cell cycle-dependence of oncornaviruses. Most of the investigations were carried out in the avian system. In the murine system, reports were scarce and contradictory, while in the feline system almost no information was obtainable. It was the aim of the present work to fill this gap and to clarify certain aspects of viral carcinogenesis. For this purpose it was decided to investigate several cycle-related changes in feline leukaemia virus-infected lymphoid cells. It was also hoped that in so doing some information might be gained concerning the nature of feline oncornavirus-associated cell membrane antigen (FOCMA). This topic has been the subject of extensive research during recent years, although the molecular nature of the antigen has yet to be determined.

As the present investigations were progressing, a few important findings were published regarding cell cycle-dependent changes mainly in the murine system. These confirmed and in part helped to interpret the results already obtained by me. They will be discussed in the appropriate context.

The cell cycle and the use of synchronised cell cultures are the two common denominators in all the experiments presented in this thesis. The complexity of the cell cycle model and the variety of synchronising techniques and life cycle analysis methods available required a separate research into these matters. This was necessary to enable the projected main experiments to be carried out. This preliminary research is discussed in the Introduction and in Chapter One.

This Introduction has the following aims:

First, to outline the concept and describe the basic postulates of the cell cycle model.

Second, to draw attention to the impact which its application has already made on the therapy of cancer.

Third, to review the results obtained by the use of synchronised cell cultures in the field of viral carcinogenesis and antigen expression.

1. The Concept of the Cell Cycle

The cell cycle has been defined as the interval between one mitosis and the next in one or both daughter cells. Since its formulation, the concept has had a considerable impact on cell biology. Many studies of cell replication have been directed towards defining the fundamental events which characterise the various stages in the life cycle of a cell. Originally, most investigations were concerned with mitosis, since this was the only event in the cycle which could be observed microscopically. It was only in 1953 that Howard and Pelc demonstrated that DNA synthesis in eukaryotic cells was confined to a discrete period of the interphase which they called the DNA synthetic phase (S). Consequently, the cell cycle was divided into four phases, G_1 - S - G_2 - M, where G_1 and G_2 are gaps, S is the period of nuclear DNA synthesis and M is the period of mitosis.

This was the first major step in the evolution of the cell cycle concept. The second, no less important, was the classification of mammalian cells, in relation to DNA synthesis and mitosis, into three distinct populations: (1) continuously dividing cells such as stem cells of the bone marrow and those in the crypts of the small intestine and exponentially-growing cells in cultures; (2) non-dividing cells examples of which are erythrocytes, polymorphonuclear leukocytes and the keratinised cells of the epidermis; and (3) resting cells which can be induced to divide by an appropriate stimulus; such types are liver cells, which regenerate after partial hepatectomy, endometrial cells prior to oestrogen stimulation, lymphocytes before phytohaemagglutinin stimulation and confluent or contact-inhibited cultured fibroblasts. The cell cycle is shown diagramatically in Figure 1.

Tissues in the animal body can grow by two basic mechanisms; by an increase in the size of the cells or in the number of cells. The cell cycle is concerned only with the second mechanism of growth and considering the three distinct cell populations described previously, it may be concluded that the cells of an adult tissue or organ may increase in number in a given time by one of three ways, i.e., (1) by shortening the length of the cell cycle, (2) by increasing the fractions of cells that go through the cycle and (3) by decreasing cell loss.

Since neoplasia is, pathologically, one of the most important aspects of growth, the discovery of the cell cycle was, not surprisingly, a breakthrough in this area. The concept of the cell cycle has not only furthered the development of a whole new field, the biochemistry of the cell cycle, but it has brought about a completely new approach to the factors that control division in mammalian cells, and to the therapy of cancer.

Questions about the kinetics of cell proliferation arise at many stages of an attempt to study the development of malignant cells. Information about the onset and cessation of proliferative activity and the phases of the proliferative cell cycle, makes it possible to compare the growth of normal and cancer cells. Certain populations of cells differ in their proliferative behaviour. As pointed out by Gilbert and Lajtha (1965), the main characteristics of these populations are governed by the input of cells from other populations, the production of cells within the population and the loss of cells. However, cells may divide and increase in number without loss or gain from other populations, a phenomenon known as closed dividing. Cells in tissue culture and in early tumour growth are examples of this.

There are several methods for the analysis of the kinetics of cell proliferation in normal and malignant cells. Tumour growth can be expressed in mathematical terms. In vivo tumour growth must be thought of in basic terms of cell population kinetics. Determination of the degree of production and the growth characteristics of neoplastic cell populations are as important as the analysis of the proliferating cell cycle.

In in vitro tissue culture systems, evaluation of the duration of the cell cycle based on the time taken to double the cell population, usually gives mean values of 20 - 30 hr. according to the type of cell and the medium. The mean duration of the cell cycle can also be calculated from mitotic indices. The more cells which divide per unit of time, the shorter is the generation time. The formula $T = \log_e 2\frac{d}{M} = 0,693\,\frac{d}{M}$ fits best with experimental results, where T = generation time, M = mitotic index, and d = duration of mitosis. In 1971, Lipkin published average times for each phase of the cell cycle in rapidly renewing normal cell populations. The duration of M is short, ranging from 1 - 2 hr; G_2 is generally longer than M, lasting for 1 - 4 hr.; S is about 7 hr. in rodent tissues and approximately 10 - 20 hr. in human cells. The greatest variation is found in G_1, with estimated times ranging from a few hours to several days. The length of the G_1 period is responsible for the variations in the duration of the whole cell cycle, the other periods being more constant.

The concept and terminology of cycling cells actively moving through the cell cycle is well established and documented (Baserga, 1976; Prescott, 1976). More confusing are the various concepts and the terminology of non-cycling cells and their relationship to cycling cells. In 1963, Lajtha proposed that cells can move out of the cycle or become arrested for extended periods

of time but still retain the capability of reactivation. The same author introduced the concept of "G_0", where cells move out of the cycle from the G_1 period; where they can remain indefinitely in a resting state (as far as cell division is concerned); and where upon being recalled by an appropriate stimulus, they exhibit a characteristic delay before entering S phase. In addition, it has been shown (Epifanova and Terskikh, 1969; Tobey et al., 1971; and Pederson and Gelfant, 1970) that a small population of cells can leave the cycle at the G_2 stage. These cells are held up or arrested in the G_2 period, but could enter mitosis immediately, in response to an appropriate stimulus.

A much greater proportion of cells moves out of, and back into, the cell cycle from the G_1 period; and for this reason and because of the behaviour of normal and transformed cells in culture, G_1 and G_0 periods have been subdivided and analysed by a variety of schemes. Temin (1971) subdivided G_1 into $G_{1\ a,b,c}$. Smith and Martin (1973) subdivided the cell cycle into an "A state" and "B phase". The "B phase" includes the conventional S_1 G_2 and M periods and part of G_1; the "A state" is located in G_1. However, the "A state" differs from the G_0 concept in that it implies that cells have a constant probability ("transition probability") of leaving the "A state" and entering the "B phase". Pardee (1974) introduced the concept of a unique fixed restriction point, "R", located in mid-G_1, a critical switching point at which cells shift back and forth from cycling to non-cycling states; he proposed that malignant cells have lost their R-point control. Augenlicht and Baserga (1974) introduced the concept of "deep-deeper G_0 states", in which they postulate that the longer that cells remain quiescent, the deeper they go into G_0, and the longer the pre-replicative phase lasts (i.e., the delay before entering S after stimulation). Prescott (1976) favours the idea of "prolonged arrest" within the cell cycle in

the G_1 and in the G_2 periods. Finally, Gelfant (1977) described a model with four major categories of cells: cycling cells, non-cycling G_1-blocked cells, non-cycling G_2-blocked cells and non-cycling G_0-blocked cells. These represent the potential proliferating pool in cells in culture and in tissues and tumours in vivo.

Most tissues and cell systems are predominantly composed of cycling cells and non-cycling G_0-blocked cells. They also contain small proportions of both G_1- and G_2-blocked cells. G_1- and G_2-blocked cells enter S or M promptly; G_0-blocked cells enter S after a delay (release from the G_0 barrier implies concomitant opening of the G_1 block). The degree, the rate and the point of release of all three categories of non-cycling cells may depend upon the stimulus, on whether cells are immature, adult or chronologically aged, and upon the particular tissue.

There are several procedures for studying and for detecting cycling and non-cycling cells in vivo and in vitro. Cycling, continuously dividing cells, can be identified in a number of ways.

(1) DNA content profiles obtained by Feulgen cytophotometry or by flow cytofluorometry, reveal 3 classes of cells according to their DNA content:

(a) cells in G_1 with a normal resting diploid nuclear DNA content of 2C,

(b) cells in G_2 with 4C DNA, and

(c) cells with intermediate DNA contents between 2C and 4C representing cells in the process of DNA synthesis (i.e., moving through the S phase of the cell cycle).

(2) Cycling cells in S incorporate ^{3}H-thymidine and can be observed as labelled nuclei in autoradiographs or detected by scintillation counting.

(3) Cycling cells can be seen in mitosis.

In general, non-cycling cells can be demonstrated and distinguished from one another only by experimentally opening the G_0 barrier and the G_1 and the G_2 blocks in the same tissue by some form of physical, chemical or biological stimulus.

(1) G_1-blocked cells are arrested late in the G_1 period and are located at the G_1 block (nuclear DNA content, 2C).

(2) G_2 blocked cells are arrested in the late G_2 period and are located at the G_2 block (nuclear DNA content, 4C).

(3) G_0-blocked cells are arrested early in G_1 by a G_0 barrier; these cells have 2C nuclear DNA contents and they are located at a distance in time from the G_1 cell-cycle block.

Most of the authors favour the view that transformed cells arise from non-cycling cells and under certain conditions lose their ability to return to a resting state (Temin, 1971; Pardee, 1974; Baltimore, 1974; and Gelfant, 1977). The point in the cell cycle at which cells rest is somewhere in G_1, but not at the border of the S phase. Pardee's restriction point "R" and Temin's "G_{1b}" phase are located in mid-G_1 and are comparable to Gelfant's out-of-cycle G_0 phase. In addition, Gelfant suggests that transformation can occur in all three categories of non-cycling, blocked cells.

Since the mammalian cell cycle revolves round two major events, DNA synthesis and mitosis, the preparation for both of these processes involves an elaborate sequence of biochemical events. The changes necessary for DNA synthesis occur in the prereplicative (G_1) phase and those required for mitosis occur in the premitotic (G_2) phase. Macromolecular biosynthesis is maximal during S and minimal during M. The main biochemical events which can occur during the various phases of the cell cycle are shown in Table 2, p.28.

Biochemical studies of the cell cycle usually require populations which are "synchronised". The production of these populations in which most of the cells are at a similar stage of biochemical development has thus become an important technique of cell physiology. The usefulness of synchronised cultures in the study of the biochemistry of several phases of the cellular life cycle of mammalian cells has been long recognised and numerous methods have been developed to produce such cultures. The ideal synchronisation method would be one which is purely selective and which could be applied to a growing population without affecting the growth rate. The technique which comes closest to these requirements is "mitotic selection", but, unfortunately, its use is restricted to monolayer cultures. Many of the physical and chemical blocks presently available for preparing synchronised populations can cause a state of unbalanced growth and may even prevent part of the population from carrying out subsequent cell cycle operations. The techniques may still be profitably employed in studies of cell cycle-parameters provided that appropriate allowance is made for non-traversing populations in data interpretation.

2. Some Practical Applications of the Cell Cycle Model

In infectious diseases, especially those due to viruses, prevention is much more spectacular than cure. It may be that prevention will also become the method of control of cancer. Prevention entails a knowledge of causative factors in cancer, i.e., the aetiology of cancer and the mechanism of carcinogenesis. This is one justification for the large investments in viral oncology, chemical carcinogenesis and cell biology. The cell cycle model has already exerted some influence on carcinogenesis and cancer therapy.

Although the work presented in this thesis is concerned mainly with certain aspects of viral carcinogenesis and the cell cycle, restriction of the discussion to this aspect only would result in an incomplete picture. Before reviewing the relevant literature, therefore, it is proposed to outline briefly the influence that the knowledge of the cell cycle has had on the cure of cancer.

While research into the reciprocal relationship of the cell cycle and carcinogenesis is still in an early stage and could be considered a fruitful area for future investigation, the knowledge of the cell cycle has already made its impact on cancer therapy. From the very first studies on cell kinetics, it became quickly apparent that both radiotherapy and chemotherapy could be made more rational if based on the kinetics of the cell cycle and its phases.

The major goal in cancer chemotherapy is to learn how to select drugs, drug levels and intervals between doses or courses that will kill disseminated cancer cells faster than they are being replaced, for long

enough to reduce the number with proliferative integrity to zero, and without ever overdosing the host. Factors which determine the rate at which neoplastic and normal cells are killed by cytotoxic drugs include the proliferative state of the cell populations and the time such cells are exposed to effective concentrations of the drug. This is true both for cells growing in vitro and in vivo. In general, agents which react with DNA have a tendency to render cells non-viable very quickly and in an exponential manner. However, "anti-metabolites" which show varying degrees of cell-cycle-stage specificity, with or without self-limitation, usually require longer periods to render dividing cells permanently incapable of proliferation, regardless of the drug concentration.

One of the major advances in cancer chemotherapy has been the application to treatment of humans of animal-derived data on cellular and drug kinetics. Selective toxicity of anti-tumour drugs has been demonstrated for rapidly growing large growth fraction tumours occurring in patients under age 30. Attempts to improve chemotherapy of large and small growth fraction tumours by kinetic observations in vivo in humans, have been disappointing. Recent evidence suggests that the heterogeneity of cells within tumours has prevented precise observation of the relation of cellular and drug kinetics. Nevertheless, the availability of xenografts, flow cytometry and tumour markers presents an opportunity to isolate subpopulation of tumour cells; to characterise their cellular and drug kinetics and to correlate these with values obtained in vivo.

The rationale of the radiotherapy of cancer rests upon two important observations of cells moving through the cell cycle. First, cells in certain

phases of the cycle are much more sensitive to the action of X-rays than they are when in other phases. Secondly, and even more importantly, cells which are not in the cell cycle may be more resistant to X-rays than cells moving around the cycle. If one could synchronise a population of cells and then hit them with X-rays, it might be possible to achieve the goal of cancer therapy, i.e., a maximal effect on cancer cells with a minimum of damage to normal cells. The problem here, of course, is the fact that synchronisation of cells, while feasible in vitro, has not been accomplished in vivo. Repeated doses of X-rays and subsequent use of certain drugs like vincristine do increase the degree of synchronisation of a population of tumour cells but not effectively enough. In the methodology of synchronising in vivo tumour cells, immunology may play a role.

Non-cycling cells are quite resistant to X-rays. It has been proposed that these G_0 tumour cells may be the ones that cause the defeat of therapeutic measures, whether chemotherapy or radiotherapy, because they can escape both and then start tumour growth anew when they return to the cycle after the cessation of the therapeutic measures. De Casse and Gelfant (1968) have shown that tumour cells can be brought back to the cycle by immunosuppressive agents, indicating that immune mechanisms may be responsible for shifting tumour cells to a non-cycling G_0 state, and the removal or inhibition of these mechanisms may make it possible for G_0 cells to switch back to the proliferative cycling state and start tumour growth again. Presently, the combination of chemotherapy, radiotherapy and immunology seems to be the most promising approach to the cure of cancer.

3. Review of the Literature

In in vitro studies, it has been found that the production of many cellular products, including proteins, RNA and new cellular DNA is cell-cycle related. Various cell surface markers appear to be preferentially expressed in certain phases of the cycle, which is, in most cases, the G_1 phase.

There are reports indicating a relationship between the phase of the cell cycle and the ability of carcinogenic agents to effect neoplastic transformation. Frei and Ritchie (1963) have shown that 7, 12-dimethylbenz (a) anthracene, a polycyclic aromatic hydrocarbon, is more effective in inducing cancer of the skin of mice when applied at the time of day in which the number of skin cells in DNA synthesis is at a maximum.

1-p-D-Arabinofuranosylcytosin (ara-C) is a powerful inhibitor of DNA synthesis and is widely used as a chemotherapeutic agent. It has been shown that ara-C is capable of causing malignant transformation in cultured hamster embryo cells and also in rat cells (Jones et al., 1972; Kouri et al., 1975). More recently, Jones et al., (1977) have reported that the C3H/10T½ CL8 line of mouse embryo cells have been transformed by the agent and the transformation was cell cycle, more precisely, S-phase specific. This cell line has been recently utilised in several laboratories to study the oncogenic potential of various other chemotherapeutic agents.

In the field of viral carcinogenesis, it has been shown that a close relationship exists between the cell cycle, on the one hand, and, on the other, (a) viral transformation, (b) virus induction or activation, (c) virus infection, (d) virus production and (e) viral antigen expression. These various relationships are discussed below, in turn.

(a) Todaro and Green (1965) found that when cells in culture were exposed to an oncogenic virus such as SV-40, neoplastic transformation occurred only when the cells were allowed to divide at least once after exposure to the virus.

(b) Human lymphoblastoid cells latently infected with the Epstein-Barr herpesvirus (EB virus) contain numerous, apparently complete copies of the repressed virus genome. Virus activation in cultured lymphoblastoid cells occurs spontaneously in producer cells, and may be induced in some producer and non-producer cells by the incorporation into the DNA of thymidine (dT) analogues. Activation of the repressed Epstein-Barr virus in human lymphoblastoid cells by halogenated pyrimidines is cell cycle-dependent in that the analogue must be incorporated into DNA during the early S-phase to initiate the virus activation sequence (Hampar et al., 1973, 1974a). Replication of the resident EB virus genome in non-producer cells also occurs during the S-1 period (Hampar et al., 1974b), suggesting a temporal relationship with virus activation.

Drugs other than halogenated pyrimidines have been employed for activating repressed virus genomes. Inhibitors of protein synthesis or media deficient in specific amino-acids, for example, may induce activation of latent DNA (Kaplan et al., 1972) or RNA viruses (Aaronson and Dunn, 1974). Hampar et al., (1976) were able to induce EB virus activation in synchronised non-producer Raji cells with inhibitors of protein synthesis or with arginine-deficient medium.

Activation of SV-40 virus by UV irradiation is cell cycle-dependent, in that maximum activation levels are observed when cells are treated during the late S-G_2 phase (Kaplan et al., 1972).

Evidence to suggest cell cycle-dependence for drug induced activation of type-C RNA viruses has been reported (Greenberger and Aaronson, 1975; Schwartz et al., 1975). The thymidine analogue -5-bromodeoxyuridine (BrdU) induced the synthesis of a latent type C virus in secondary cultures of normal rat embryo cells. The optimal virogenic dose of BrdU was 0.1 mM; when the concentration was reduced to 0.1 μM ^{3}H BrdU was incorporated predominantly into the repetitive and intermediate repetitive DNA sequences (Schwartz et al., 1975). The same researchers demonstrated that the 30,000 molecular weight group-specific antigen (p30) of Friend mouse leukaemia virus, was expressed in synchronised rat embryo cell cultures treated with 0.1 μM BrdU. Treatment with BrdU during the late synthetic (S) phase was sufficient for the expression of the p30 antigen and ^{3}H-BrdU was preferentially incorporated into the intermediate repetitive DNA of rat embryo cells during the synthetic phase of the cell cycle (Schwartz et al., 1975).

These findings indicate that BrdU-specific effects may stem from the incorporation of BrdU into a few critical regulatory sequences responsible for the control of specialised gene expression in animal cells.

In the light of these results, one has to take into account the possibility of cell cycle-dependence in attempts to activate viruses by drugs. If the drug employed inhibits the cell from traversing the cycle, activation may not occur and one may conclude, erroneously, that the drug in question cannot activate virus.

(c) There is a close relationship between murine leukaemia or sarcoma virus infection and the cell cycle (Joshikura, 1968, 1970; Joshikura et al., 1968). A similar phenomenon has been reported for Rous sarcoma virus

(RSV) infection (Bader, 1966a). In both cases, the efficiency of virus infection was at its maximum in the DNA synthetic period. It was supposed that cellular DNA synthesis is required for the establishment of virus infection. According to Temin (1967), new DNA is required for the establishment of the virus infection, and the "provirus" thus formed is activated by cell division. The necessity of cell division for RSV infection was also reported by Bader (1968).

(d) Hobom-Schnegg et al., (1970) have shown that in synchronised chicken embryo cells infected many hours before mitosis, RSV production did not begin before the end of mitosis. Temin (1967) observed that colchicine in concentrations which arrest cells in mitosis, blocks or delays RSV production. He went further, suggesting that cell division is necessary for activation of any new cellular differentiation in vertebrates.

Humphries et al., (1972) have demonstrated that neither viral-specific RNA nor avian leukosis viral gs antigens are produced in stationary cells and that, until cell cycle-dependent activation, transcription of the provirus does not occur.

In synchronised chick fibroblasts transformed by and producing the Schmidt-Ruppin strain of RSV, virus-specific RNA, viral protein synthesis and virus release occurred in the early S and G_1 phases of the cell cycle, respectively. This would be a second control of viral transcription once the transcription was activated by the initial cell division.

Viruses of the avian sarcoma-leukosis group are released from synchronised chick cells after mitosis, irrespective of whether the cells are infected during the first gap (G_1) period or during the synthetic phase of the cell cycle (Temin, 1967; Hobom-Schnegg, 1970; Leong, 1972). Such a

correlation between virus production and a distinct phase of the cell cycle is less clear for the murine sarcoma-leukaemia viruses. In 1971, Lerner et al., reported that viral antigen and budding virus particles were present in mouse cells infected with Moloney leukaemia virus, throughout all cellular growth phases and also in metaphase arrested cells. The release of Kirsten mouse sarcoma leukaemia virus from synchronised rat cells coincided with mitosis, according to Panem and Kirsten (1973). Stimulation of stationary mouse fibroblasts chronically infected with Moloney leukaemia virus to re-enter the growth cycle synchronously, was followed by two waves of virus release. The first wave occurred in G_1 and the second wave coincided roughly with the mitotic period of the following cell cycle. The first wave of released virus appears to have contained viral RNA already present in the resting cells, while the second wave of released virus particles carried newly formed viral RNA (Paskind et al., 1975).

(e) Virus release and major group-specific antigen expression has been examined in heterologous rat cells chronically producing murine leukaemia virus (MuLV) and the Kirsten isolate of murine sarcoma virus. Mitosis has been shown to be required for virus release and the major viral protein was in highest amounts during the G_2 phase of the cell cycle (Panem and Schauf, 1974).

Infectious M-MuLV production was completely dependent on the first mitosis after release from synchrony and, in contrast to studies in rat cells chronically infected with MuLV, it was shown that in a de novo infection of synchronised mouse cells with MuLV, the three viral proteins examined were produced not during the G_2 phase of the cycle, but only after mitosis (Fischinger et al., 1975).

When the synthesis and cleavage of virus precursor proteins were investigated in synchronised mouse cells chronically infected with Rauscher murine leukaemia virus (R-MuLV), synthesis was shown to occur in three distinct waves corresponding to the G_1, middle S and late S-G_2 phases of the cell cycle. The G_1 wave of viral precursor synthesis did not require new viral RNA synthesis, while the two later waves were apparently dependent upon the presence of newly made viral RNA (Naso and Brown, 1977). If virus release occurs around mitosis, these observations are consistent with a synchronised synthesis of viral protein precursors prior to mitosis.

Apparently, not only the induction of viruses is cell cycle-dependent, but also the induction of differentiation and the synthesis of specialised products.

Murine erythroleukaemia cells (MELC) can be induced to erythroid differentiation in culture by several agents. Differentiation is associated with the expression of erythroid characteristics including α and β globin mRNA, globins and haemoglobins. It has been demonstrated with other cell systems that there is a differential expression of genes during the cell cycle. Studies with synchronised cell cultures have shown that certain genes appear to be transcribed primarily in G_1, while others are transcribed throughout the cell cycle (Prescott, D.M., 1976 and Melli et al., 1977). Gambari et al., (1978) examined the relationship between globin mRNA synthesis, DNA replication and the G_1 phase of the cell cycle in synchronised and induced MELC. Accumulation of newly synthesised globin mRNA was first detected when cells were in the first prolonged G_1 phase of the cycle, which follows release of the cells from block at the G_1/S boundary and progression of cells through the first S - G_2 - M, implying that a round of DNA synthesis is required prior to the accumulation of globin in MELC.

In the last few years, several cell surface markers have been detected and characterised by the application of recently developed and more refined immunological techniques. Significantly, the importance of the timely co-ordination of complex biochemical events and their relatedness to the cell cycle in the expression of the cell surface markers is being recognised.

Evidence for the cell cycle-dependent expression of cell surface antigens has been obtained in several studies with synchronised cell cultures.

An established line of mouse lymphoma, induced by M-MuLV showed considerable variations in complement-dependent, antibody-mediated cytotoxic sensitivity to anti-H-2 and anti-M-MuLV sera. These variations were also observed when cells were tested with the same sera in an indirect membrane immunofluorescence test (Cikes, 1970a). Experiments designed to elucidate the mechanism of this phenomenon revealed an inverse correlation between growth rate and cell volume on the one hand and expression of surface antigens on the other. Quantitative absorption studies showed that the decrease in surface antigen concentration was not merely due to a dilution of antigenic receptors on the surface of larger cells, but to a decrease in the number of antigenic receptors per cell (Cikes, 1970a). This conclusion was substantiated in further experiments (Cikes, 1970b). When the expression of H-2- and virus-determined surface antigens was monitored during synchronous cell growth, the highest proportion of antigen-positive cells was found during the G_1 period of the cell cycle. Interestingly, the H-2- and virus-determined surface antigens were temporally co-expressed (Cikes et al., 1971).

Shipley (1971) synchronised U79-753B-3 Chinese hamster cells by incubating them with 2 mM hydroxyurea for 3.5 hrs. which synchronises cells at the G_1/S boundary. The sensitivity of the synchronised cells to complement-

dependent immune damage has been tested by their colony-forming ability following exposure to a heterologous antiserum and complement. It has been found that the cells in the middle of the S period were maximally resistant to specific immune lysis.

Pasternak (1971) used zonal centrifugation to synchronise P 815 Y mouse mastocytoma cells. This procedure separates cells according to their size which, in turn, is dependent on the position of cells within the cell cycle. The extent of complement-dependent cytolysis in cells harvested from different regions of the gradients was measured by the ^{51}Cr-release test using a suitable dilution of H-2 antiserum. The cytotoxic sensitivity was high during the early G_1 period, decreased progressively during the G_1/S transition, reached its lowest value in the middle of S, and was restored in G_2.

Changes in the extent of cell surface antigen expression seem to be the most convincing explanation to account for the changes in cytotoxic sensitivity during the cell cycle.

Thomas (1971) has studied the expression of blood groups B and H activities in synchronised mouse mastocytoma cells and in mitogen induced mouse lymphocytes. It has been found that these two activities behaved reciprocally; during the G_1 phase, cells were B- and H+, whereas in the S phase, they were B+ and H-. It has also been shown that B-negative mouse lymphocytes, which are normally in G_0 phase, acquired B-positive activity upon stimulation with mitogen.

Pellegrino et al., (1972) examined HL-A antigen expression in synchronised cultures of long established human cell line (WIL_2) derived from splenic lymphocytes of a normal donor. The synchronisation in G_1 was

achieved by growing cells to saturation density. It was found that maximal antibody absorptive capacity occurred in early S.

Summer et al., (1973) assayed the expression of H-2 antigens in Ficoll gradient fractions of P 815 Y mastocytoma cells using complement-dependent immune cytolysis, the binding of radiolabelled antibody and the inhibition of specific immune cytolysis. In addition, the fragility of cells was assayed by their resistance to detergents, hypotonicity and freeze-thawing. Immune cytolysis and cell fragility reached minimal values during the S phase. H-2 antigen expression was highest in the G_1 phase of the cell cycle. It was concluded that H-2 antigens were synthesised and inserted into the cell membrane during the G_1 period and their concentration did not change during the S and G_2 periods.

No cell cycle-dependent changes in HL-A antigen expression was found in synchronised normal human lymphoid cell line (WIL_2) by examining the sensitivity of these cells to complement-dependent immune lysis (Ferrone et al., 1973).

The discrepancy between this result and those showing cell cycle-dependent changes in the expression of antigens was explained by the fact that in this study, normal and not transformed cells were used. However, Pellegrino et al., (1972) and Rosenfeld et al., (1973a, b) have demonstrated cell cycle-related changes in antigen expression on cells derived from normal donors. The findings of Thomas and Phillips (1973) give an additional and more plausible explanation for the above described discrepancies. They have found that dividing lymphoid cells possess membrane antigens which are not present on normal resting lymphocytes. Thomas (1974) has also demonstrated that the cell surface antigen (i antigen), which is only expressed in foetal tissues,

transformed cell lines and mitogen stimulated lymphocytes, was recognised by anti-i serum. This i antigen is maximally expressed in human lymphoblastoid cell lines during the S and G_2 periods.

The rat basophilic leukaemia cells have histamine-containing granules and receptors for IgE. It has been observed that the IgE-binding capacity of cultured cells varies quite widely from culture to culture. When experiments were undertaken to elucidate this phenomenon, it was found that the variations could be accounted for by changes in the number of receptors during the cell cycle and the distribution of cells in different phases of their cycle in cultures at various stages of growth. The cells showed an inverse relationship between growth rate and expression of receptor activity for IgE, active receptors being acquired in the G_1 phase of the cell cycle. No accumulation of receptors occurred during S and G_2 phases, though the average cell volume increased. During mitosis, receptors were simply distributed to daughter cells (Isersky et al., 1975).

Olsen et al., (1976) found that the feline oncornavirus associated cell membrane antigen (FOCMA) expression on the feline lymphoblastoid cell line FL74 is cell cycle-dependent and that the rate at which a cell passes through the cell cycle determines the pattern and intensity of the fluorescence of the cell membrane. Highest anti-FOCMA titres were detected in the G_1 phase of the cell cycle.

The use of cell surface markers to identify subpopulations of lymphocytes has received wide application in the evaluation of the role of lymphocytes in the immune response. Thymic-derived lymphocytes (T cells) may be identified by their ability to form non-immune rosettes with erythrocytes of heterologous or, in some cases, homologous species. Bursal or bone marrow-

derived lymphocytes (B cells) possess a receptor for the third component of complement and are identified by their ability to form rosettes with an erythrocyte-antibody-complement (EAC) complex.

Krakowka et al., (1977) examined two continuous lines of lymphoid cells. FL74 cells have T cell markers whereas canine CT45-S cells express EAC markers on their surfaces. They showed that synchronisation has a profound effect on the expression of these markers and, in fact, can affect the actual proportion of cells identified as T cells, B cells or non-rosetting null cells. One hundred per cent of FL74 cells were expressing the T cell markers in the G_1 phase of the cell cycle, whereas 100% binding of EAC to CT45-S cells was never observed. Lowest percentages of EAC-binding cells were found in the G_1 phase, highest values being obtained during the cellular exponential growth phase.

Recently, the phenotypic expression of blood group H and its specific gene product α-2-fucosyl transferase enzyme (FT) have been demonstrated in HeLa cells. In synchronised cells, FT assay values were found to be maximal in S and early G_2 phases and minimal in early G_1 phase. It has been suggested that cell cycle-related enzyme discontinuity may explain the previously demonstrated low transferase enzyme values in untreated acute leukaemic cells, where significant proportions of the total cell mass are believed to be non-cycling in G_0 or G_1 (Kuhns, 1978).

The results of studies on cell surface antigen expression in synchronised cell cultures obtained in various laboratories provide convincing evidence for the existence of cell cycle-dependent antigenic expression. The most likely explanation for some divergent results is the

use of different cell lines, heterologous and not precisely defined antisera, and the application of different synchronising techniques.

TABLE 1

The Mammalian Cell Cycle

Phase	Meaning	Functional State	Duration
G_1	First gap	Stable amount of DNA = 2C	Few hours - several days
S	Synthetic	DNA doubles its amount = 2C→4C	7 hours
G_2	Second gap	Stable amount of DNA = 4C	1 - 4 hours
M	Mitosis	DNA is halved = 2 x 2C	1 - 2 hours

TABLE 2.

BIOCHEMICAL EVENTS OCCURRING DURING THE VARIOUS PHASES OF THE CELL CYCLE

G_1 Phase

Reformation of polysomes, nucleoli and the nuclear membrane.
Altered membrane function, with increased uptake of amino acids and nucleosides.
Increased cellular Na^+ content and decreased cellular K^+ content.
Restoration of protein synthesis.
Synthesis of specific proteins, non-histone chromosomal proteins and immunoglobulins.
Increase in the specific activity of alkaline phosphatase in isolated plasma membranes.
Increase in the specific activity of RNA polymerase.
Glycoprotein synthesis.
Increased rate of synthesis and utilisation of ATP.
Synthesis of histone messenger RNA
Complete cessation of histone synthesis.

S Phase

DNA and simultaneous histone synthesis.
Synthesis of non-histone chromosomal proteins.
High rate of protein synthesis.
Increased synthesis of enzymes related to nucleic acid metabolism.
Increased synthesis of glycoproteins.
Continuation of RNA synthesis.
Decrease in alkaline phosphatase activity.
Peak rate of uptake of oxygen.
Microtubular protein synthesis (in mid-S).

G_2 Phase

Decreased protein synthesis, but continuation of non-histone chromosomal protein synthesis.
Decreased RNA synthesis.
Completion of microtubular protein synthesis.
Synthesis of special class of division-related proteins.
Synthesis of glycolipids and lipids.
Decreased uptake of oxygen.
Degradation and disappearance of some enzymes responsible for metabolism of deoxynucleotides, e.g., DNA polymerase III.
Persistence of elevated levels of thymidine kinase, DNA polymerase I and ribonucleotide reductase.
Cessation of histone synthesis.

M Phase

Markedly reduced rate of protein synthesis.
Complete cessation of histone synthesis.
Synthesis of non-histone chromosomal proteins continues unabated.
Reduced rate of RNA synthesis.
DNA transcription ceases, with a marked decrease in chromatin template activity.
Reduced ability of ribosomes to incorporate amino acids into proteins.
Changes in cell surface, loss of Ca^{++}, elevated electrophoretic mobility, decreased gelation.
Decreased uptake of oxygen.
Disaggregation of polysomes, nucleoli and nuclear envelope.
Chromatin condensation, centriole migration and spindle formation.
Decreased activity of RNA polymerase.
Synthesis of glycolipids and lipids.

Data collated from Baserga, (1968, 1974); Lieberman (1970); Mueller (1971); Tobey et al., (1971).

FIGURE 1. Compartments of the Cell Cycle

1. Continuously dividing, cycling cells traversing the sequence $G_1 \longrightarrow S \longrightarrow G_2 \longrightarrow M$.

2. Non-dividing cells which leave the cycle permanently after M, and will never synthesise DNA.

3. Resting cells which leave the cycle transiently:

   (a) from G_1, and enter a resting state in G_0 or in an "extended G_1" phase. Following appropriate stimulus they will resume DNA synthesis.

   (b) from G_2, and enter a resting state called "G_2-arrest". Following appropriate stimulus they will enter mitosis.

THE CELL CYCLE

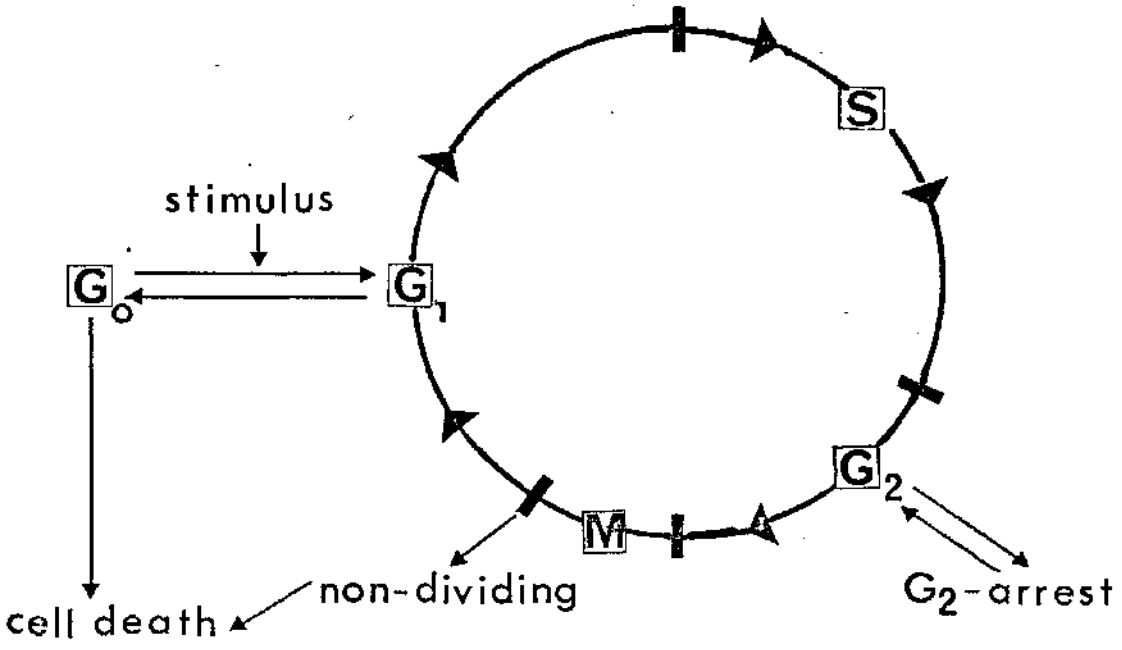

CHAPTER ONE

CELL SYNCHRONISATION AND LIFE CYCLE ANALYSIS

CHAPTER ONE: CELL SYNCHRONISATION AND LIFE CYCLE ANALYSIS

1. Materials and Methods

2. Synchronising Techniques in General

3. Life Cycle Analysis in General

4. Synchronising Techniques Used during the Course of this Study

5. Life Cycle Analysis of FL74, F422 and CT45-S Cell Lines

1. Materials and Methods

Cells

FL74 is a pseudodiploid feline lymphoid leukaemia cell line. It was established in a static suspension culture from a solid infiltrate of a leukaemic cat's kidney by Theilen et al., (1969). These cultures are infected with, and continually produce, the Kawakami-Theilen strain of FeLV, subgroups A, B and C (FeLV-ABC/KT), and are used as standard target cells to detect feline leukaemia antibodies by the indirect immunofluorescence test. The cells express the T-lymphocyte marker for the feline species (Cockerell et al., 1976).

F422 is an established cell line growing in suspension isolated originally from a thymic lymphoma of a kitten inoculated with the second passage of Rickard strain of FeLV, subgroup A (FeLV-A/R).

CT45-S cells are canine thymocytes originally isolated by Dr. J. Mitchell. The cells were derived from a primary culture of normal canine thymus tissue, but express only the EAC (B cell) surface marker.

Media

Growth medium: suspension cultures (FL74, F422, CT45-S) were maintained in medium consisting of equal proportions of Liebovitz L-15 and McCoy's 5A media (Gibco Bio-Cult Ltd.) supplemented with antibiotics and 15% foetal bovine serum (FBS).

Media for synchronising cells:

(1) (a) For thymidine blockage the growth medium described above is used with the addition of 2mM thymidine.

(1) (b) Release medium is the growth medium with the addition of 2×10^{-3} M deoxycytidine.

(2) Growth medium was used for the cold treatment of cells at $4^{o}C$.

(3) Isoleucine-deprived medium was prepared from Select-Amine Kit Lyophilised (Gibco Bio-Cult Ltd.) which contains the amino acids individually packaged, vitamins and balanced salt solution, in sterile lyophilised form. The medium was supplemented with 15% dialysed isoleucine-free foetal calf serum and antibiotics.

Cell culture

Cells were grown in stationary suspension cultures in 8 ounce glass bottles. They were subcultured every three days. Cells were pelleted by low speed centrifugation (500 rpm) for 5 minutes and resuspended in fresh pre-warmed growth medium. Cells were generally seeded at the density of 5×10^{5} cell per ml.

Chemicals

Chemicals were purchased from Sigma Company, London, and from British Drug Houses (B.D.H.).

Tritiated thymidine (^{3}H-TdR) was obtained from the Radiochemical Centre, Amersham.

Pulse labelling with ^{3}H-TdR

Replicate cultures of known cell number were synchronised by a double thymidine block. After release from the block, at two hourly intervals, the release medium was replaced with fresh release medium containing 0.2μ Ci/ml ^{3}H-TdR and cells were incubated in it for 30 minutes. Incorporation was terminated by chilling rapidly to 0 - $4^{o}C$. Cells were centrifuged and washed by resuspending in the same volume of cold incomplete medium or PBS. The washed cells were resuspended in about 20 times their volume of 10% trichloracetic acid (TCA) and were kept on ice for at least 30 minutes to extract

the acid-soluble materials. The precipitates were drained by filtration through Whatman GF/C glass-fibre filter discs inserted into Millipore 3025 sampling manifold. Before removal, the filters were washed with ethanol. The filters were dried in a hot air oven and placed in scintillation fluid : toluene with 0.4% 2, 5 diphenyloxazole (PPO) and 0.04% 1, 4 di-2-(5 phenyl-oxazolyl)-benzene (POPOP).

Samples were counted in an Intertechnique SL40 scintillation counter. DNA synthesis was expressed as counts per minute ^{3}H-TdR/cell.

Mitotic index (MI) determination

0.5 - 1 ml. of suspension culture was centrifuged for 3 minutes at 500 rpm. The medium was decanted and the cells were resuspended by drop-wise addition of 1 - 2 ml. of cold hypotonic buffer (0.002 M phosphate buffer) with continuous gentle agitation. Cells were allowed to swell for 2 minutes in the case of F422 and CT45-S cells, and for 5 minutes in the case of FL74 cells. After fixation with Carnoy's fixative (3 parts methanol : 1 part acetic acid) for 5 minutes, cells were air-dried and stained with Giemsa stain for 30 minutes.

500 to 1,000 cells were scored routinely for mitotic figures. The percent of nuclei in metaphase was taken as the percent of cells in mitosis.

Trypan Blue Exclusion Test

0.1 ml. of cell suspension and 0.1 ml. of 0.1% Trypan Blue solution (in PBS) were mixed. After 2 minutes, a haemocytometer was filled with the mixture by a capillary tube. Cells were counted in the four corner squares, and from the number of live cells and dead cells (the latter stain blue) the viability of the cell culture in percentage could be calculated.

2. Synchronising Techniques in General

Techniques which accumulate or select cultured cells in short, specific segments of the cell cycle are extremely useful in studies of periodic biochemical events and regulatory mechanisms controlling macromolecular biosynthesis. Synchronously growing populations of mammalian cells have been obtained by two general approaches.

A. The first method involves the blocking and accumulation of cells in a particular stage of the division cycle, followed by release of this block.

B. The second method of obtaining synchronously growing populations involves selection of a group of cells in or close to a particular stage of the cell cycle.

The most frequently used synchronising techniques belonging to both methods are discussed below.

A. (1) Techniques for blocking cells in the G_1 phase

(a) Low temperature treatment

In 1959, Newton and Wildy reported that HeLA cells could be induced to undergo parasynchronous division by chilling ($4^{\circ}C$) for a short period. They suggested that the effect of chilling is to place all those cells not actually in mitosis in a state corresponding to that at the end of telophase.

Miura and Utakoji (1961) proposed that only a certain population of cells is affected by chilling in logarithmically growing populations. Analysis of their data reveal that the G_1-cells were affected by the low temperature treatment. The cells were delayed and divided only after one generation time.

In practice, if stationary cells (most of which are in the G_1 phase) are subjected to chilling for an appropriate length of time, after the release of the cold block, they will be accumulated in the G_1 phase in much higher percentage and will divide synchronously one generation time later.

(b) Establishment of stationary-phase cultures by a variety of means

There is experimental evidence that stationary cells are arrested in the G_1 phase of the cell cycle (Tobey and Ley, 1970).

Serum starvation, isoleucine and glutamine deprivation, contact inhibition and growth to high cell densities are all known to establish stationary phase cultures, in other words, to block cells in the G_1 phase.

Littlefield (1962) reported partial synchronisation of L-cells after diluting stationary-phase suspension cultures with fresh medium, but the medium components responsible for these observations were not determined. Mohberg and Johnson (1963) showed that isoleucine, glutamine, and leucine were the only amino acids depleted from the medium after growth of mouse L-cells had ceased in monolayer cultures. Temin (1971) reported stimulation of multiplication of stationary chicken cells by the addition of serum. Ley and Tobey (1970) presented evidence that components of the growth medium were responsible for the induction of DNA synthesis and cell division in G_1-arrested cells independently of addition of fresh serum. Amino acid analysis of spent medium revealed that it was completely devoid of isoleucine and addition of isoleucine and glutamine to cells in spent medium brought about synchronous cell division without addition of fresh serum. The results presented suggest that, in the absence of isoleucine, cells in S-G_2-M continue to traverse the cell cycle and accumulate in G_1, whereas in glutamine-deficient medium, most cells synthesising DNA at the time of transfer to deficient medium, never divide.

Essentially, all cells in a culture maintained for 20 hrs. in isoleucine-deficient medium possess the G_1 DNA content. Experimental evidence is provided by biochemical measurements of DNA mass and standard cell cycle analysis techniques (Enger and Tobey, 1972). The mechanisms by which isoleucine and glutamine induce DNA synthesis in cells arrested in G_1, is not known.

A. (2) Technique for blocking cells in the S-phase: Inhibition of DNA synthesis

The synthesis of DNA in mammalian cells is inhibited by a high concentration of thymidine in the medium, apparently by the inhibition of the reduction of cytidine diphosphate to deoxycytidine diphosphate (Xeros, 1962). This effect forms the basis of a method for the synchronisation of DNA synthesis and cell division and is known as the thymidine block (Rueckert, 1960; Xeros, 1962; Petersen and Anderson, 1964; and Bootsma, 1964). Usually, two consecutive additions and removals of an excess of thymidine in medium are used in order to increase the degree of synchrony. This is called the double thymidine block. According to Petersen and Anderson (1964) no significant differences in the quality of the synchrony were observed with blocking concentrations of thymidine ranging from 2 to 25 mM.

It is often assumed that the excess thymidine blocks DNA synthesis completely and the cells are blocked at the G_1/S border. However, cells subjected to the double-thymidine procedure accumulate in the S phase. Galavazy and Bootsma (1966), Studzinski and Lambert (1969) and Bostock et al., (1971) have showed by various techniques, that cells enter the S phase and complete replication of part of their genome.

The thymidine block is a useful technique, but interpretation of results must take into account two points: (1) the thymidine block does not accumulate cells at the G_1/S border and (2), it does not completely inhibit DNA synthesis. This effect of a double thymidine block gives a plausible explanation for the observations that the first S + G_2 period after release from the thymidine block is shortened in comparison with untreated cells (Galavazi and Bootsma, 1966; Studzinski and Lambert, 1969).

B (1) The use of gentle shearing forces to collect or remove mitotic cells

The method proposed by Terasima and Tolmach (1963) is by far the most attractive synchronisation procedure for monolayer cultures. It is based on the fact that cells, when growing in a monolayer culture, are tightly bound to the glass during interphase, but become tenuously attached and round up after they enter mitosis. Division occurs while in the loosely bound state, and, later, in early G_1, the daughter cells spread out into the typical interphase morphology. During the mitotic period, the cells can be selectively removed by gentle washing or shaking.

This method is reported (Mitchison, 1971) to interfere less than other methods with the biochemical events in the cell cycle. Further support for the advantages of this method came from Terasimova et al., (1966, 1968).

In order to increase the yield of mitotic cells, several modifications of the technique were introduced. A relatively high mitotic index was obtained by Sinclair and Morton (1963) working with Chinese hamster cells treated with cold trypsin which caused little detachment of non-dividing cells from glassware. Robbins and Marcus (1964) demonstrated the importance of low calcium concentration in the medium; by their method they increased the yield up to 95%. Lindahl and Sörenby (1966) have been able to produce large quantities of mitotic HeLa cells by the use of a rather complicated mechanical system. Mittermayer et al., (1968) and Petersen et al., (1969) found that repeated harvesting increased the yield of mitotic cells. Ooka and Daillie (1974) developed a combined method of selective detachment following by natural gravity sedimentation and Yamaguchi et al., (1977) designed a special cylindrical culture flask for the selection of mitotic cells.

B. (2) Temporary inhibition of mitosis by colcemide, with subsequent gathering of the inhibited cells

The observation that Chinese hamster fibroblasts can be blocked in mitosis by colcemid, and that the block can be reversed by removal of this agent, provided a means for the synchronisation of large populations of cells (Stubblefield et al., 1965).

B. (3) Selection of synchronous cell populations by the repeated addition of vinblastine sulphate (VS04) to monolayer cultures

The mitotic cell collection method is limited by the relatively small fraction of cells which is in mitosis at any randomly dividing population. The mitotic removal method requires frequent rinsing or shaking of the monolayer cultures. Pfeiffer and Tolmach (1967) introduced a method for obtaining large, synchronous populations which were relatively unperturbed and were not contaminated by dead or damaged or metabolically altered cells.

By this technique, randomly growing cultures were treated with VS04, which caused metaphase arrest and blocked the passage of cells through mitosis. Any fraction of the population could be accumulated in mitosis and subsequently washed away, leaving behind cells in only the latter part of the division cycle. After the removal and the second addition of the drug, the position of the remaining cells in the cell cycle could be sharply defined.

B. (4) Killing of the DNA synthesising cell population by high specific activity ^{3}H-TdR

By this method (Whitmore and Gulyas, 1961), high specific activity tritiated thymidine (^{3}H-TdR) was used to kill selectively cells synthesising DNA so as to leave alive only a "window" of cells in the latter part of the G_1 phase of the cell cycle. Although the ^{3}H-TdR method can yield large populations,

they are contaminated with dead or damaged cells, making most biochemical studies impossible.

The synchronising techniques discussed above usually produce only one synchronous wave of growth. In biological situations, variability in the proliferative behaviour of the cells leads to the rounding off of the first wave and to desynchronisation and decline in size of succeeding waves. In practice, complete desynchronisation occurs after the second or third wave.

The decay of synchrony is caused by variations in generation times among cells as pointed out by Engelberg (1964), using mathematical models. Generation times normally differ among cells belonging to the same clone and even between daughter cells. The G_1 phase of the cell cycle seems to be the main variable responsible for this spread.

Genetic heterogeneity may account for the rapid reversion of synchronised cultures to random growth. The capacity of a population of cells to desynchronise may be a fundamental property of the growing cell. This mechanism could play a role in survival, and could be considered a defence against any insult to which cells in a certain phase of the cell cycle were susceptible, but to which, cells in other phases were relatively insensitive.

Similarly, the degree of synchrony attainable may be an inherent property of the cell. Time lapse cinematography of different cell lines, notably HeLa and Chinese hamster ovary cells, revealed that synchrony in HeLa cells with approximately 9% variation in generation times (Puck and Steffen, 1963) was superior to that observed in hamster cells for which the variance was about 13% (Anderson and Petersen, 1964).

3. Life Cycle Analysis in General

The use of specific radioactive precursors which are incorporated into DNA, RNA and protein of the cell, has led to additional advances in cell proliferative kinetics. The most widely used precursor has been the deoxyribonucleoside thymidine (TdR) which is incorporated specifically into the DNA that is being synthesised at the time of the labelling. The incorporation of TdR into DNA has made possible the identification of the DNA synthesis phase of the cell cycle, in addition to mitosis. Prior to incorporation, the thymidine is converted to its triphosphate derivative which is then incorporated as monophosphate into DNA together with the phosphates of the other three deoxyribonucleosides dATP, dGTP and dCTP.

A number of theoretical models have been developed and used to follow the progress of a group of cells through the proliferative cycle.

(1) By the standard percent labelled mitosis method, the duration of the cell cycle phases can be measured by pulse labelling the cells with ^{3}H-TdR and using autoradiography. After cells are so labelled, their passage through mitosis and the phases of the cell cycle can be followed and analysed. This method has been widely used to determine cell cycle characteristics of tissue culture, animal and human cell types. In order to use the method, the frequency of mitoses must be high, as in bone marrow, skin, intestine and it can be anticipated that a great deal of time will be spent in counting ^{3}H-TdR-labelled mitoses.

In addition, the following methods have also been developed to analyse the duration of the cell cycle phases:

(2) "Double labelling" of cells with ^{3}H-TdR followed after a short period by labelling with ^{14}C-TdR (Baserga, 1963).

(3) "Continuous labelling" with ^{3}H-TdR (Robinson et al., 1965).

(4) Timelapse cinematography and autoradiography (Sisken, 1964).

(5) The combination of ^{3}H-TdR and colchicine (Puck and Steffen, 1963).

(6) The use of the above methods normally takes several days. Gray et al., (1975) and Gray and Mendelsohn (1975) have reported a rapid technique of cell cycle analysis utilising sequential sampling, electronic sorting of S phase cells and liquid scintillation counting.

(7) Barranco et al., (1977) have recently published a rapid and accurate technique which allows the determination of cell cycle parameters within 1 hour of the end of the experiments. The procedure involves ^{3}H-TdR pulse labelling of asynchronous monolayer cultures and liquid scintillation counting of sequentially collected mitotic cells.

4. Synchronisation Techniques Used during the Course of this Study

Throughout this study, lymphoid cell lines (FL74, F422, CT45-S) were used which were growing in suspension culture. This fact restricted greatly the choice of synchronisation procedures and life cycle analysis methods. It was decided that three classes of synchrony-induction techniques would be used:

(a) reversible suppression of DNA synthesis with excess thymidine (double thymidine ((TdR) block),

(b) removal of an essential component from the culture medium (isoleucine deprivation) and

(c) low temperature treatment of cells at $4^{o}C$.

The combination of these synchronisation techniques offered two advantages.

Firstly, it produced a tightly synchronised cell population in both the $S + G_2 + M$ and the G_1 phases of the cycle. As previously described, the double TdR block arrests cells at the G_1/S border or in the early S phase. After release from the block, the cells synchronously traverse through the $S + G_2 + M$ phases, the duration of which is fairly constant and during which the synchrony is tight. Due to the variations in the generation time of individual cells and to the presence of a non-traversing population in the G_1 phase, cells gradually lose their synchrony. Especially, in the FL74 cell line, the G_1 phase is very long ranging between 22 - 25 hours; therefore, in order to be able to examine a more tightly synchronised population in the G_1 phase, isoleucine deprivation and cold treatment of cells were applied. Although both techniques accumulate cells in the G_1 phase, the mechanisms responsible for producing synchrony are different. The time of the block

within G_1 is not the same. Isoleucine deprivation blocks cellular maturation at the end of G_1 (Yen and Pardee, 1978), while cold treatment of cells produces a block at the beginning of the G_1 phase (Miura and Utakoji, 1961).

Secondly, the results of the same experiments using the different synchronising methods could be compared. This, in turn, helped to exclude possible artefactual phenomena in data interpretation and played a confirmatory role in the case of similar results.

The detailed synchronisation procedures are presented in Tables 3, 4 and 5, p.48, 49 and 50 respectively.

5. Life Cycle Analysis of the FL74, F422 and CT45-S Cell Lines

Life cycle analysis of the cells was performed to determine the optimum times for nucleoside addition and removal. For the analysis of the various lymphoid cell lines growing in suspension cultures, the following method was used:

A. Determination of the population doubling time

The time it takes for an entire culture to double in number when all cells are dividing is called the population doubling time. When all cells are dividing the cell number increases exponentially with time, and the average doubling time of a single cell can be derived from a plot of the log of cell number versus time, which will be a straight line.

Population doubling times were computed from growth curves. Viable cell counts were done daily by the trypan blue exclusion test. The doubling time was that time in which the population increased by a factor of 2 during the logarithmic growth phase.

Alternatively, population doubling time was determined by the formula -

$$\text{Log } N = \text{Log } No + kt \log 2$$

where N is the number of cells at time t, No is the number of cells at time o, and k is the regression constant. The population doubling time is the reciprocal of k. (Hayflick, 1973).

The doubling times of the FL74 cell line which has the lowest saturation densities (1.2×10^6/ml) ranged between 28 and 32 hours. The mean doubling time of 30 hrs. was used throughout the experiments.

The cell lines F422 and CT45-S have higher saturation densities, 2.5×10^6/ml and 2.8×10^6/ml, and faster doubling times, 20 - 23 hrs. and 18 - 20 hrs. respectively.

B. Synchronisation of cells by a double TdR block

Cells were synchronised using standard recommended times. A 16 hr. block was applied twice with an 8 hr. release period in between. The time after the release from the second block will be designated as post-release - 0 hour (PR -0 hr), and the following times as PR - 2 hr, PR - 4 hr. and so on.

After PR - 0 hr. the cells resumed growth and traversed the following phases of the cell cycle ($S + G_2 + M$) in a synchronous fashion.

C. Determination of the time of mitosis and the degree of synchrony

Cells were synchronised and grown in duplicate cultures. At two hourly intervals, after PR - 0 hr, cells were removed, treated with hypotonic buffer, sedimented on coverslips by cytospin, fixed with Carnoy's fixative and stained with Giemsa stain. One thousand cells were counted for the estimation of the mitotic index.

The mitotic index (MI) of FL74 cells reached a peak at PR - 8 hr. 22 - 25% of the synchronised cells were in metaphase at that time, and at least 50 - 60% of the cells passed through mitosis between 7 and 9 hr. post release.

Both the F422 and CT45-S cell lines have their mitotic peaks at PR - 8 hr.

The duration of the mitotic period can be calculated from mitotic indices.

In a population of dividing cells, the fraction of cells within each period at any time is about equal to the fraction of the average cycle time taken up by that period. For example, in an asynchronous log-phase culture of FL74 cells, about 3.2% of the cells are in mitosis, so mitosis must take about 95 minutes for that population which doubles every 30 hrs.

Throughout the experiments, 1.5 hr was used as a mean value for the duration of the mitotic phase of FL74 cells. In CT45-S and F422 cell lines, mitosis takes about 1 hr.

The mean duration of the cell cycle can also be calculated from mitotic indices. The more cells divide per unit of time, the shorter the generation time.

Not only can the position of the mitotic phase in the cell cycle be calculated, but at the same time, the degree of synchrony can be monitored by counting mitotic indices. The higher the percentage of cells in metaphase, the better the synchrony.

During each experiment where synchronised cells were used, the mitotic index was determined in order to see the degree of synchrony and the time of the mitotic peak. In the latter, there were variations, due to the different times needed for the manipulations of the cells.

D. Determination of the DNA synthetic phase

Cellular DNA synthesis was measured by the incorporation of ^{3}H-TdR into acid precipitable material. Replicate cultures were synchronised by a double TdR block. After release, cells were pulse-labelled for 30 minutes with ^{3}H-TdR at 2 hr. intervals. Cells were precipitated, precipitates were drained, dissolved and counted in a scintillation counter. DNA synthesis was expressed as counts per minute ^{3}H-TdR/cell (see Fig. 2).

Cellular DNA synthesis was maximal at 4 hr after release from the TdR block.

Determination of the DNA synthetic phase was done only in FL74 cells; this cell line was used for studies with metabolic inhibitors (see Chapter Five), and therefore the knowledge of the exact duration of the S phase was crucial.

From the data of A, B, C and D, the phases of the cell cycle can be estimated as follows :

The phases of the FL74 cell cycle are:

$S + G_2 / M / G_1 = 7.5 + 1.5 + 21 = 30$ hr.

The phases of the F422 cell cycle are :

$S + G_2 / M / G_1 = 7 + 1 + 11 = 19$ hr.

The phases of the CT45-S cell cycle are:

$S + G_2 / M / G_1 = 7 + 1 + 13.5 = 21.5$ hr.

During the first synchronising experiments, using standard blocking and release times, the degree of synchrony was not very high. The life cycle analysis of cells revealed the exact durations of the cell cycle phases whereupon a new synchronising time schedule was designed which, in turn, considerably improved the degree of synchrony.

For example, in the case of the FL74 cells, using the values for the major segments of the life cycle, the following general procedure for inducing synchrony in suspension culture was devised.

On the first day after subculturing, 5×10^5/ml cells were blocked for a period equivalent to $G_2 + M + G_1$ (24 hr.) by addition of 2 mM of thymidine. The block was released for a period slightly in excess of the duration of S (about 6 hr.). A second block was added for a period of 24 hr. Release from the second block resulted in all the cycling cells proceeding through S phase as a synchronised wave.

Cultures were afterwards sampled at intervals and mitotic indices determined to assess the degree and stability of synchrony. Results are shown in Table 7 and Fig. 3.

As a result of better synchrony, at PR - 8 hr, 48% of the FL74 cells were in metaphase, and between PR - 7 hr. and PR - 9 hr. all the cycling cells went through mitosis.

TABLE 3

Synchronisation Procedure

Using Double Thymidine Block

Time (hr)[a]	Treatment	Cell no./ml x 10^5
0	Harvest and resuspend logarithmically growing cells[b] in fresh pre-warmed growth medium containing 2 mM TdR.[c]	5.0
24	Wash 2 x with pre-warmed medium. Resuspend in fresh pre-warmed growth medium containing 10 μM dCTP (release medium).	
30	Wash 1 x with pre-warmed medium. Resuspend in fresh pre-warmed growth medium containing 2 mM TdR.	
54	Wash 2 x with pre-warmed medium. Resuspend in fresh pre-warmed release medium. This time represents zero hour after release from the double thymidine block (PR - 0 hr). The cells are in the S phase.	5.0

a This time schedule was designed for the FL74 cell line.

b Cells are growing logarithmically during the first and second day after subculturing.

c Abbreviations : thymidine (TdR); deoxycytidine (dCTP).

TABLE 4

Synchronisation Procedure

Using Cold Block

Time (hr)	Treatment	Cell no./ml x 10^5
0	Harvest and resuspend cells at the end of their logarithmic growth phase[a] in pre-cooled (4°C) growth medium and keep at 4°C.	5 - 5.5
24 - 30	Harvest and resuspend cells in fresh pre-warmed growth medium (37°C). This time represents zero hour after release from the cold block (PR - 0 hr). The cells are in the early G_1 phase.	5 - 5.5

a At the end of the third day after subculturing.

TABLE 5

Synchronisation Procedure

Using Isoleucine Deprivation

Time (hr)	Treatment	Cell no./ml x 10^5
0	Harvest, wash and resuspend cells at the end of their logarithmic growth phase in isoleucine deficient medium, supplemented with 15% dialysed isoleucine free foetal calf serum.	5 - 5.5
24 - 30	Harvest and resuspend cells in pre-warmed growth medium[a]. This time represents zero hour after release from the deficiency block, (PR - 0 hr). Cells are in the late G_1 phase.	5 - 5.5

a The complete growth medium can be the isoleucine deficient medium, but supplemented with isoleucine (0.26 g/litre in triple distilled water).

CHAPTER TWO

VIRUS RELEASE AND THE CELL CYCLE

CHAPTER TWO : VIRUS RELEASE AND THE CELL CYCLE

1. General Properties of Feline Leukaemia Virus

2. Review of the Literature

3. Materials and Methods

4. Experiments and Results

   A. Measurement of FeLV release from synchronised FL74 cells by the C81-assay

   B. Measurement of FeLV release from synchronised FL74 cells by electron microscopy

   C. FeLV release during logarithmic cell growth

   D. FeLV release from synchronised F422 cells

   E. FeLV release from synchronised CT45-S cells

5. Discussion

At the time this work was started, there was little knowledge of the cell cycle-dependence of oncornaviruses. Although, in a few studies, the close relationship between the cell cycle and avian oncornavirus release had already been indicated, in the murine system results were contradictory and almost no information was available concerning feline leukaemia viruses. The purpose of this chapter is to investigate whether FeLV release is cell cycle-dependent. First, the general properties of FeLV will be briefly discussed.

1. General Properties of Feline Leukaemia Virus

Feline leukaemia virus (FeLV) is a member of the RNA tumour virus group. It was discovered in 1964 (Jarrett et al.,) and later demonstrated in field cases (Laird et al., 1967). RNA tumour viruses or oncornaviruses are usually classified on the basis of the host species from which they were isolated, and by the type of malignancy that they cause.

The leukaemia and sarcoma viruses have very similar morphologies. Each virion comprises a nucleoid containing the RNA genome associated with protein, enclosed in a lipid-containing membrane, called the envelope. Oncornaviruses replicate without killing the host cell, which continues to multiply after infection. In thin sections of infected cells in the EM, progeny virus can be seen budding from the cell surface.

Frequently, sarcoma and leukaemia viruses are collectively described as "C-type particles". This term and two others, "A-type particles" and "B-type particles" were coined by Bernhard in 1958 to distinguish the different sorts of tumour virus particles he had observed in thin sections in the EM.

C-type particles have a centrally placed and spherical nucleoid and they can be seen budding or found extracellularly.

B-type particles have an excentric nucleoid, they are vacuolar or extracellular (mouse mammary tumour virus).

A-type particles can be found only intracellularly and they are often located in the area of the Golgi apparatus.

FeLV appears in two structural forms in the electron microscope.

(1) The so-called "immature" or type-1 virions are circular and have three concentric electron-dense layers. The outer membrane or envelope has a diameter of 100 - 120 nm and the intermediate structure and the dense inner core or nucleoid have a diameter of 80 - 90 nm and 50 - 65 nm respectively. Budding and immature FeLV particles have surface projections, "spikes" on the outer surface of their outer membrane, but these are not nearly as prominent as those seen on avian virions. The immature or type-1 virions are usually seen near the cell surface, very often next to the budding forms.

(2) In the "mature" or type-2 virus particles, no intermediate membrane can be seen. The particles very often have a cuboidal shape and generally tend to vary in shape and size. Spikes mostly disappear, although intermediate structures, that is, type-2 particles with spikes, can also be frequently observed. Mature particles can be found in any position, often intercellularly in clumps.

In the murine leukaemia virus system, the maturation process has been attributed to cleavage of a precursor polypeptide in the released virion (Yoshinaka and Luftig, 1977).

There is no doubt that the immature type converts into a mature one, but the relative infectivity of the two types has not yet been established. Nevertheless, there is evidence to suggest that the type-1 particles may be the

more infectious ones. Smith (1974) found that rapidly harvested virus is more infectious, with an optimum of 20 minutes for RSV. FL74 cells produce a large number of budding and type-2 particles, but type-1 particles are extremely rarely seen. This finding indicates that the conversion from type-1 to type-2 particles must be a very rapid process, and the low infectivity rate of the FL74 virus may be partly due to the lack of the more infectious type-1 particles. These observations with FL74 cells were made during the course of the various experiments presented in this thesis. Budding, type-1 and type-2 FeLV can be seen in Fig. 2.

The genome of FeLV is a single stranded, rapidly sedimenting 70S RNA molecule (Jarrett et al., 1971), which dissociates on heating into smaller 35S sub-units. FeLV, like all oncornaviruses, possesses the RNA-dependent DNA polymerase or reverse transcriptase enzyme by which the viral genetic information is converted into double stranded circular DNA (provirus). The viruses replicate via this provirus, which enters into a stable genetic relationship with the host cell chromosomes.

The genome of the oncornaviruses is coding for four genetic functions.

(1) gag for the group-specific antigens or internal viral polypeptides.

(2) pol for the reverse transcriptase,

(3) env for the envelope glycoprotein, and

(4) onc or src for a cell transformation protein.

FeLV has no onc coding potential. The onc or src gene is expressed in the mammalian sarcoma viruses, most of which appear to be defective mainly due to the loss of the env function. Sarcoma viruses require the presence of helper viruses to provide missing replicative functions. The helper virus is usually a leukaemia virus.

By in vitro translation of viral RNA, the gene products of RNA tumour viruses have been established (Von der Helm and Duesberg, 1975; Kerr et al., 1976; Salden et al., 1976). FeLV has four structural proteins : p10, p12, p15 and p30, which are coded by the gag-gene and are derived from a common precursor (Okasinski and Velicer, 1977). The glycoprotein gp70 is coded by the env-gene.

p10 is a basic protein; it is found in the viral core and is strongly associated with the viral RNA. It has group-specific antigenic determinants and is poorly antigenic.

p12 is an acidic molecule located in the viral core. MuLV p12 carries type-specific determinants.

p15 is, like p30, close to neutral in overall charge. Its exact location in FeLV has not yet been established. It is not associated with the core and is not expressed on the envelope of the virion. It may be involved with the hexagonal shell which possibly constitutes the intermediate membrane in the EM. p15 is the subgroup-specific antigen for R-MuLV, and carries the FMR (Friend, Moloney, Rauscher MuLV) cell surface antigen (Friedman et al., 1974).

p30 is the major structural protein of the viral core. It has group, type and interspecies antigenic determinants. It is not expressed on the surface of the virion.

gp70 is the only glycoprotein of FeLV established so far (Bolognesi et al., 1974). Antibodies to gp70 are virus-neutralising and mostly subgroup-specific and they generally correspond with the classification of FeLV into subgroup A, B and C indicated by interference test. This is the receptor for cell infection. FeLV-A strains grow only in feline cells, while FeLV-B and C

have a wider host range (Jarrett et al., 1978). FeLV-A is present in all known isolates, half of the isolates contain FeLV-B and only 1% of the isolates contain FeLV-C as FeLV-AC or FeLV-ABC (Jarrett et al., 1978).

After the transcription of the provirus and the translation of the viral polypeptides, the viral RNA, viral proteins and glycoprotein assemble at the cell membrane. Newly formed virions are released by budding at the cell surface where they acquire an envelope containing cell membrane components. In this way, an infected cell can be transformed and may continue to proliferate while releasing virus progeny.

Due to the fact that oncornaviruses replicate in cells without causing any cytopathic change, rapid detection of the virus in cell culture requires indirect methods. There are several methods to isolate and assay FeLV, e.g., labelling with ^{3}H-uridine; density gradient centrifugation (FeLV bands at the density of 1.16 g.m^{-3} in sucrose); electron microscopy of cultures; complement fixation test; fluorescent test for group-specific antigen; immunodiffusion; interference test; reverse transcriptase assay; radio-immunoassay. FeLV is frequently assayed on sarcoma-positive, leukaemia-negative C81 cells by focus inducing activity.

2. Review of the Literature

Oncornavirus production proceeds through a DNA "provirus" intermediate and is closely dependent on normal cellular functions (Temin, 1971). In the avian oncornavirus system, the close relationship between the cell cycle and virus release has been established. It has been found that virus production and virus release are completely dependent on the ability of the infected cell to traverse through the cell cycle, that is, to synthetise new DNA and to complete mitosis.

Temin (1967) carried out a series of experiments with partially synchronised G_1 phase chicken embryo fibroblasts which were grown in serum-depleted medium. To improve the degree of synchrony, cells were treated with 2.5 mM thymidine at the time of subculture. Cells were exposed to RSV at different stages of the cell cycle in the presence or absence of inhibitors of mitosis and DNA synthesis. One of the findings was that circumstances which prevented or interfered with mitosis immediately after exposure to virus also prevented virus production. It was concluded that mitosis after infection might be related to activation of virus production and that virus production was synchronised by mitosis. No attempt was made to define the specific events necessary for virus production in or after mitosis (e.g., loss of polysomes and decrease of protein synthesis during mitosis; formation of the new interphase nucleus, or entrance into the metabolically active G_1 period).

The results of Hobom-Schnegg et al., (1970) confirmed Temin's findings. They demonstrated, using partially synchronised chick embryo cells, that RSV production starts at the same point in the cell cycle (after mitosis) and at the same rate whether cells were infected in the G_1 phase or in the S phase of the cell cycle. Leong et al., (1972) found, using RSV infected chick

fibroblasts synchronised by exposure to serum-free medium, that not only virus release, which occurred in the G_1 phase, but also the synthesis of the virus-specific RNA and of the viral proteins were cell cycle-dependent. The latter two occurred in the S phase of the cycle. In all the experiments described above, RSV was assayed by focus formation in tissue culture. When stationary chick fibroblasts were infected with RSV, they remained infected for at least 5 days, but they did not release infectious virus or become transformed until after cell division. The stationary cells did not contain group-specific antigens or viral RNA detectable by hybridisation (Humphries and Temin, 1972).

The finding that in synchronised avian cells, mitosis was required not only for virus production, but also for the appearance of virus-specific RNA and for the formation of group-specific antigens, is suggesting that the newly formed virion RNA also serves as a mRNA; accordingly, no viral protein is made prior to mitosis unless some were made from the input virus RNA as "early" proteins.

In the murine oncornavirus system, the correlation between virus release and a distinct phase of the cell cycle, has not been uniformly established. Originally, Lerner et al., (1971) reported that viral antigen and budding virus particles were present in mouse cells infected with Moloney leukaemia virus throughout the cell cycle. In 1973, Panem and Kirsten examined the release of the Kirsten mouse leukaemia virus and the Kirsten mouse sarcoma-leukaemia virus from synchronised rat cells. The chronically infected cells were synchronised by a double thymidine block and virus release was monitored by focus forming and focus inducing assays. It was found that virus release coincided with mitosis.

The dependence of Moloney murine leukaemia virus production on cell growth has been reported by Paskind et al., (1975). Infected cells were made stationary by serum starvation. Stimulation of the cells to re-enter the growth cycle synchronously, was followed by two waves of virus release. The first wave was in the middle of the G_1 phase and the second roughly coincided with the mitotic phase of the following cycle. The first wave of released virus appears to have contained viral RNA already present in the resting cells, while the second wave of virus carried newly formed viral RNA. Virus release was monitored by reverse transcriptase and XC plaque assays. The analysis of their results obtained by using metabolic inhibitors suggested that virus production is controlled in a complex way by cell cycle-dependent RNA and protein synthesis.

Fischinger et al., (1975) examined the first cycle of infection (de novo infection) of Moloney MuLV in synchronised, cloned 3T3 FL cells. The eclipse period of virus could be varied at will in synchronised cells. Virus was assayed on S + L- mouse cells by focus inducing activity. Infectious virus production was completely dependent on the first mitosis after release from the synchrony inducing block.

3. Materials and Methods

Cells

FL74, F422 and CT45-S cells are described in Chapter One.

FEA are feline embryo cells (Jarrett et al., 1973).

C81 is a relatively flat subclone of the cloned 8C cat cell line. The 8C line is derived from the Crandell feline kidney cell line (CCC) and transformed by a single hit Moloney-MSV infection. The cells were obtained from Dr. P.J. Fischinger.

Media and cell culture

The medium and the culturing of the suspension cultures are described in Chapter One.

Monolayer cultures (FEA, C81) were maintained in Eagle's minimal essential medium (MEM) - Glasgow modification (McPherson and Stoker, 1962) which was prepared at the Institute of Virology, University of Glasgow. The medium was supplemented with 10% foetal bovine serum (FBS) (Gibco Bio-Cult Ltd.) and called EFC 10 medium.

Monolayer cells were grown in 8 ounce glass bottles or in 2.5 litre rotating glass bottles. Cells were subcultured after reaching confluence. The culture fluid was decanted and the cells were removed from the glass by washing first with versene, then with a mixture of versene and trypsin (20 : 2). Cells were resuspended in fresh EFC 10 medium and transferred to new bottles, which were flushed with 5% carbon dioxide in air before sealing.

Virus assays

A. FeLV assay on S+ L- cells by focus inducing activity

(a) Preparation of samples

Samples were taken from logarithmically and synchronously growing

cells. In the former case, unconcentrated, spent tissue culture fluids were collected on the first, second and third day after subculturing the cells. In the latter case, after release from the synchrony inducing block, at 2-hourly intervals, tissue culture fluids of duplicate cultures were replaced with fresh, pre-warmed growth medium and after 2 hours the medium was collected.

In both cases, samples were first centrifuged at low speed followed by clarification (10,000 r.p.m. for 10 minutes at $4^{o}C$) or filtration through 0.45 μm Millipore filters. Subsequently, they were stored at $-70^{o}C$.

(b) Assay of samples

Samples were assayed on the sarcoma-positive leukaemia-negative C81 cell line according to the method of Fischinger et al., (1974). After the addition of a large amount of FeLV, the C81 cell layer rounds up completely, but at higher dilutions of the virus, discrete focal lesions can be seen and the rounded, loosely attached cells in their centre can easily be removed by washing.

The C81 assay was performed as follows :-
The mixture of 3×10^{7} FEA and 3×10^{6} C81 cells (10 : 1) was seeded into 5 cm. plastic plates. On the following day, replicate cultures were infected with 0.5 ml. absorption medium (4μg/ml. polybrene) and 0.5 ml. of the FeLV-containing sample. This should be done before the plates become confluent because, for FeLV production, cell multiplication is necessary. After 1.5 hours incubation, the inoculum was replaced by fresh EFC 10. The cells were fed every second or third day. The first foci appeared on days 7 to 10 after infection and were counted under the microscope.

B. Detection of FeLV by electron microscopy (EM).

(a) Preparation of cells for EM

Cells were seeded and grown in suspension cultures at a density of

5×10^5 cell/ml. When synchronisation was required, replicate cultures were first synchronised by one of the synchronising methods described in Chapter One. At the end of the synchronising procedure, at 2-hourly intervals, 5 ml. of the cultures were removed, washed and pelleted by low-speed centrifugation.

In preliminary experiments, it had been established that a short centrifugation of 2 - 3 minutes at 300 r.p.m. was the optimal time to obtain pellets in which the cells were not too tightly packed and in which the cells best retained their original surface morphology. Using this method, the observation of the cell morphology and the detection and counting of the budding viral particles were performed without difficulty.

(b) Fixation, dehydration and embedding

Pellets were fixed in a mixture of paraformaldehyde and glutaraldehyde for 4 - 6 hours at 4^{o}C. After fixation, the pellets were rinsed twice in Cacodylate-buffer (0.1 M) and post-fixed for 1 hour in osmium tetroxide (1% osmic acid in Millonig's phosphate buffer, pH 7.2 - 7.4).

The fixed pellets were dehydrated in an ascending series of 70%, 90% and 100% alcohol and further dehydrated in propylene oxide. The dehydrated pellets were soaked for 1 hour in a mixture consisting of equal parts of propylene oxide and resin (Araldite) and left overnight in a mixture of 20% propylene oxide and 80% Araldite. They were transferred to gelatine capsules containing Araldite and were allowed to polymerise at 57^{o}C for 48 hours. In this way, six blocks were prepared from each individual pellet.

(c) Cutting and staining of thin sections

Thin sections, approximately 500 A^{o} in thickness, were cut on an

LKB Mark 3 Ultramicrotome, using glass and diamond knives, and were mounted on copper specimen grids (obtained from Smethurst High-Light Ltd., Bolton, Lancs.). The thin sections were stained:

(1) with uranyl acetate (Watson, 1958) for 20 minutes and rinsed in (a) concentrated methanol, (b) 50% methanol, twice, (c) distilled water, twice; and dried on filter papers.

(2) with lead citrate (Reynolds, 1963) for 10 minutes and rinsed in (a) 0.02 N sodium hydroxide, (b) distilled water, twice; and dried on filter paper.

Finally, the sections were examined with an AEI 6B or AEI 801 electron microscope at the instrumental magnifications of 5,000 - 60,000.

4. Experiments and Results

A. Measurement of FeLV release from synchronised FL74 cells by the C81 assay.

Replicate cultures of FL74 cells were synchronised by a double thymidine block and the appearance of FeLV in culture fluids was determined at 2-hourly intervals after release from the second TdR block. Unconcentrated, spent tissue culture fluids were collected and assayed on S + L- cells. From the same cultures, cells were prepared for electron microscopy and samples were taken for mitotic index determination.

The results shown in Table 6, p.73 are representing the mean values of three separate experiments. Virus release increased significantly at PR - 8 hr., reaching a peak at PR - 10 hr. in the early G_1 phase of the cycle. The release of FeLV then decreased in the later part of the G_1 phase indicating that the viral peak was a function of the cell cycle and not simply a result of the repeated addition of fresh medium.

B. Measurement of FeLV release from synchronised FL74 cells by electron microscopy

Replicate cultures of FL74 cells were synchronised by excess thymidine or chilling. At the end of the synchronising protocols and at a range of time intervals, pellets were obtained and processed for electron microscopy as described in the Materials and Methods part of this Chapter. From the same cultures, tissue culture fluids were collected for virus assay and samples were taken for mitotic index determination. Six blocks were made from each sample and thin sections were cut from each block. One hundred cell profiles from each block were examined and the budding C-type particles were counted.

The data obtained are presented as the number of budding C-type particles per 100 cell profiles, and represent the mean values of 5 separate experiments. As shown in Fig. 3 and Table 7 on cells synchronised by TdR, the number of budding particles increased sharply and reached a peak at PR - 10 hr. declining later in the cycle. The viral peak was preceded by a peak of DNA synthesis at PR - 4 hr. and by a mitotic peak at PR - 8 hr.

The pattern of virus release measured by EM closely followed the pattern obtained by focus-inducing activity; this is a significant finding and its importance and application will be explained in more detail in the Discussion part of this Chapter.

Cells synchronised by cold treatment accumulate in the G_1 phase of the cycle. When FL74 cells were examined by EM after release from the cold block, it was found that the rate of virus release was about the same during the following mid- and late- G_1 phase of the cell cycle. Virus production increased later, reaching a peak at PR - 34 hr. in the early G_1 phase of the cycle (Table 8, p.75). This PR - 34 hr. is equivalent to the PR - 10 hr. in the TdR method. The mitotic indices showed that the synchrony achieved was not very high.

Nevertheless, by this method, too, a significant viral peak was detected and it was in the same period of the cell cycle (early G_1) as that found by the TdR synchronising method.

In Fig. 4 an FL74 cell is shown with numerous budding C-type particles on the cell membrane. In Fig. 5 the morphology of the cell is demonstrated.

C. FeLV release during logarithmic cell growth

In order to examine the rate of virus release during the exponential

growth phase, tissue culture fluids and cell pellets were obtained on the first, second and third days after subculturing the FL74 cells. At the same time, samples were taken for mitotic index determination. Culture fluids were assayed on C81 cells and the pellets were processed for EM.

The results represent the mean values of three separate experiments.

As can be seen in Tables 9 and 10, p.76 & 77, by both assays, virus release was highest on the first day after subculturing the cells. When cells were examined in the EM for multiple buds per cell profiles, it was found that more cells had multiple buds on their surfaces on the first day than on the second and third day after subculturing. The number of budding C-type particles ranged between 2 and 16 per cell profile. Extracellular groups of viruses were located near the budding sites and consisted almost entirely of type-2 or intermediate-type viral particles. Type-1 particles were rarely seen. For example, in one sample, 300 cell profiles were examined; 64 budding particles and large clumps of type-2 particles were found; only 4 type-1 particles were seen.

Similarly, higher percentages of cells were in mitosis on the first day (3.2%) than on the second and third days (2.2%, 1.0% after subculturing.

D. FeLV release from synchronised F422 cells

F422 cells were synchronised by a double thymidine block and by chilling. After release from the blocks, at time intervals, cell pellets were obtained and prepared for EM. Samples were taken from the same cultures for mitotic index determination.

After release from the double thymidine block, F422 cells were examined during the S - G_2 - M periods of the cell cycle. As judged by the

mitotic indices, the synchrony was tight, i.e. there was a sharp mitotic peak at PR - 8 hr. (Table 11, p.78). However, no budding C type particles were observed during the above-mentioned time intervals.

To investigate more closely the G_1 phase of the cell cycle, F422 cells were synchronised by cold treatment. When the cells were released from the cold block and examined by EM, a distinct viral peak was found in the mid-G_1 phase of the cell cycle. Using this synchronising method, budding viral particles were found not only during the G_1 phase, but also during the following S and M periods. This, at first, might appear contradictory to the findings obtained by the TdR block, where, during S and M, no budding particles were observed. However, this can be explained by the fact that the degree of synchrony was not high (the mitotic peak was not sharp enough) In other words, in such partially synchronised population, there is always a certain group of cells which is out of synchrony and these cells release virus.

In Fig. 6 an F422 cell is shown with budding and released virus particles which have type-1 morphology. Note the uropod morphology which is typical of this cell line.

E. FeLV release from synchronised CT45-S cells

CT45-S cells infected with FeLV subgroup AB were synchronised by the double thymidine procedure. After the cells were released from the synchrony-inducing thymidine block, cell pellets were prepared at time intervals and processed for EM examination. At the same time, samples were collected for mitotic index determination.

Cells were examined for budding C-type particles during the different phases of the cell cycle. As shown in Table 12, p79 the degree of synchrony was high; at PR - 8 hr., 45% of the cells were in metaphase. Virus release coincided with mitosis, reaching a peak at PR - 8 hr. Contrary to the observations made on the feline FL74 and F422 cells where no budding C-type particles were observed on the membranes of mitotic cells, in these heterologous canine cells a large number of budding FeLV particles were seen, not only on the smaller G_1 cells, but also on mitotic cells. Contrary to the FL74 virus, a large proportion of the extracellular particles had the type-1 morphology.

In Fig. 7 CT45-S cells are shown with budding C-type particles.

5. Discussion

To establish the relationship between a distinct phase of the cell cycle and the release of feline leukaemia virus, two feline and one canine lymphoid cell lines chronically infected with FeLV have been investigated after synchronisation.

FL74 cells, which express the feline oncornavirus associated cell membrane antigen (FOCMA), were selected for further experiments described in the following Chapters, and for that reason, they have been examined in the greatest possible detail.

The results of the experiments clearly indicate that feline oncornavirus production is cell cycle-dependent. In this, FeLV is similar to the avian and murine oncornavirus systems. Virus release occurs in both feline cells in the G_1 phase of the cell cycle, although there is some difference between them concerning the exact time of the viral peak in the G_1 phase itself.

FL74 cells release virus in the early part of the G_1 phase just after mitosis. There is only a 2 -3 hour gap between the mitotic and the viral peak. Both synchronising techniques produced similar results.

Virus production in F422 cells occurs in the mid-G_1 phase of the cell cycle. When F422 cells were synchronised by the double thymidine block, no virus was detected in the S - G_2 - M periods of the cycle. Only after synchronisation by cold treatment after which most of the cells were accumulated in the G_1 phase, was it possible to detect virus release.

In the case of both feline cell lines, no budding C-type particles were detected on the membranes of mitotic cells, even after treatment with vinblastine sulphate or colchicine, which drugs block cells in metaphase.

In addition to the synchronised cells, exponentially growing FL74 cells were examined on the first, second and third days after subculturing.

In my hands, FL74 cells underwent one division and reached saturation density on the third day. On the third and fourth days, the mitotic index was very low. By the re-addition of fresh growth medium, a certain degree of synchrony was induced because most of the cells completed mitosis during the first day. The highest mitotic index detected was at the end of the first day, and consequently the number of cells doubled on the second day. Highest virus titres and highest number of budding C-type particles were found on the first day. Similarly, more cells had multiple budding particles on their membranes on the first day than on the second and third days, which was the consequence of the high mitotic rate found on the first day as virus release seems to be dependent on mitosis.

In CT45-S cells, virus release coincided with the mitotic peak. When cells were examined in the electron microscope, a large number of budding C-type particles were observed on metaphase cells and on the smaller early G_1 cells. This finding indicates that the dependence of oncornavirus production on the cell cycle is more complex than previously envisaged. Apparently, the time sequence varies in every cell system, especially so in a heterologous host cell which might not exhibit identical temporal control responses for virus production. This observation made on CT45-S cells is very similar to that of Panem and Kirsten's (1973) who have found that murine leukaemia virus production coincided with mitosis in heterologous rat cells, while other investigators (Paskind et al., 1975; Fischinger et al., 1975), using mouse cells, have reported that MuLV release occurs in the G_1 phase of the cell cycle.

When the first experiments were designed, the obvious choice for the detection of FeLV release seemed to be the C81-assay. Due to the fact that FL74 virus has a low infectivity rate and that during the time of the experiments frequent contaminations occurred, the results were not always conclusive and the experiments had to be repeated several times. Fortunately, from each experiment, cell pellets were processed for electron microscopy, and after comparing the data obtained by both methods, it became clear that the EM results were similar to those of the C81-assay. Experiments were repeated several times to ascertain the reliability of the EM method. The results appeared to be fairly similar and always repeatable. My experience over the years made it possible for me to carry out the EM work without difficulty. It was therefore decided that the monitoring of virus release in all future experiments would be performed by electron microscopy.

As stated above, I was particularly interested in the relationship between virus release and the cell cycle concerning the FL74 cell line. Using two assay systems and applying two different synchronising techniques, it was convincingly established that virus production was cell cycle-dependent and occurred after the mitotic peak, but the question still remained, which particular cells were releasing most of the virus? Although the synchrony achieved, especially with the TdR block, was considerably high, the cell population was far from being completely synchronous. At the time (PR - 10hr.) when the viral peak occurred, there were cells traversing through mitosis, early G_1 cells just emerging from telophase and even cells belonging to the G_2 population. As mentioned earlier, metaphase cells, which are easily recognisable by EM, appeared to have no virus particles. Therefore, the virus-producing cells must have belonged to some other sequence of the mitotic

phase or to the early G_1 or G_2 phase of the cell cycle. Which phase precisely however, was not possible to determine by transmission electron microscopy alone. The only conclusive observation made during the procedure of counting budding C-type particles was that the cells releasing most virus were smaller than the rest of the population. This indicated the likelihood of their belonging to the early G_1 phase.

To establish which particular cells were releasing the highest number of virus particles, it was necessary to be able morphologically to identify individual cells or a group of cells belonging to a distinct phase of the cell cycle. For that purpose, techniques were developed and experiments performed to study the ultrastructure of synchronised FL74 cells. These will be discussed in the next Chapter.

TABLE 6

Release of Infectious Virus from

Synchronised FL74 Cells

Hours (post release)	FIU/ml. x 10^3	M.I. in %
2	1.0	0.01
4	1.7	0.05
6	2.3	2.5
8	6.3	48.0
10	12.3	24.0
12	5.6	17.0
14	4.6	1.4

TABLE 7

Detection of FeLV Release

from Synchronised FL74 Cells by Two Assays.

Hours (post release)	FIU/ml. x 10^3	M.I. in %	Number of buds per 100 cell profiles
2 (S)	1.0	0.01	20
4	1.7	0.05	30
6 (G_2)	2.3	2.5	50
8 (M)	6.3	48.0	100
10 (E-G_1)	12.3	24.0	140
12	5.6	17.0	70
14	4.6	1.4	40

TABLE 8

Release of FeLV from FL74 Cells

Synchronised by Chilling

Hours (post release)	No. of buds/ 100 cell profiles	M.I. in %
6 (Mid-G_1)	30	1.8
22 (Late-G_1)	36	2.4
26 (S)	75	5.0
30 (M)	100	20.0
34 (Early-G_1)	138	3.2

TABLE 9

Growth Characteristics of FL74 Cells

in Static Suspension Culture

Time (days)	No. of cells/ml. x 10^5	Viability in %	Saturation density	Doubling time (hr.)		FIU/ml. x 10^3	M.I. in %
				mean ±	SD		
0	5.0						
1	5.6	86				5.3	3.2
2	10.05	87	1.2×10^6	30	1.8	2.6	2.2
3	12.0	80				2.0	1.0
4	12.0	75					

TABLE 10

Appearance of Budding C-Type Particles on FL74 Cells

During the Exponential Growth Phase

Time (days)	No. of buds/ 100 cell profiles	No. of multiple buds/ 100 cell profiles	M.I. in %
1	40	19	3.2
2	29	12	2.2
3	28	11	1.0

TABLE 11

Release of FeLV from Synchronised F422 Cells

Synchronisation by TdR block			Synchronisation by cold block		
Hours (post release)	No. of buds/ 100 cell profiles	M.I. in %	Hours (post release)	No. of buds/ 100 cell profiles	M.I in %
2	0	0.01	2 ($E\text{-}G_1$)	4	1.4
4 (S)	0	0.03	4	12	1.6
6 (G_2)	0	1.2	8 ($M\text{-}G_1$)	36	1.6
8 (M)	0	33.0	10 ($L\text{-}G_1$)	24	NT
10 ($E\text{-}G_1$)	2	1.8	16	3	4.0
			20 (M)	20	18.0

TABLE 12

Release of FeLV from Synchronised CT45-S Cells

Hours (post release)	No. of buds/ 100 cell profiles	M.I. in %
2	NT	1.2
4	16	5.0
6	40	12.0
8	120 (M)	45.0
10	60	12.0
16	24	10.0

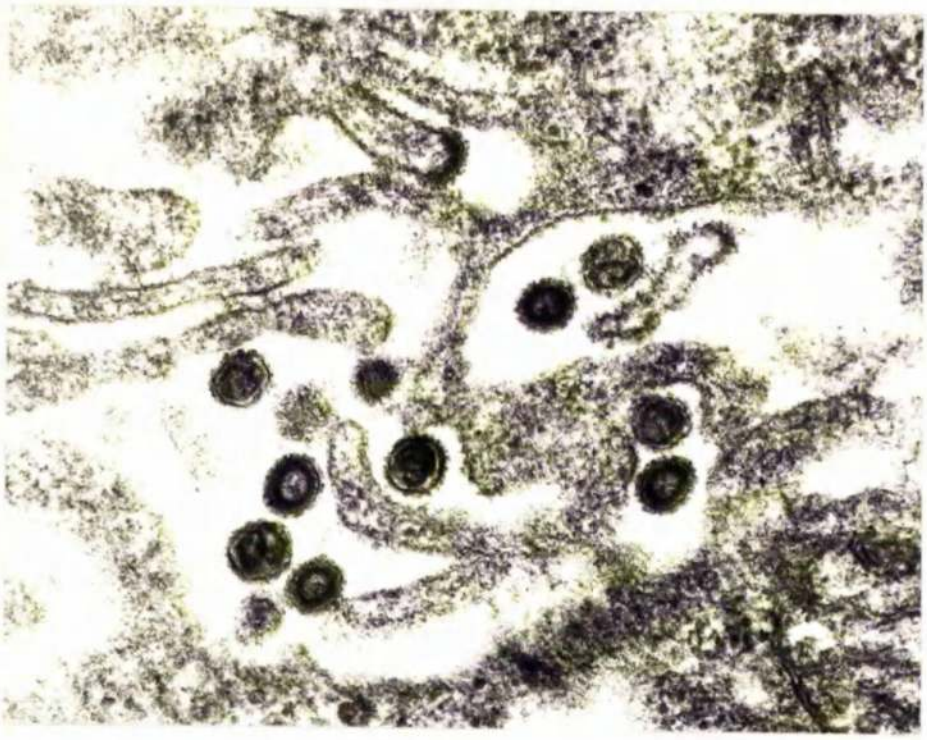

FIGURE 2 : Budding, type-1 and type-2 forms of FeLV

FIGURE 3 : Release of FeLV from Synchronised FL74 Cells

RELEASE OF FeLV FROM SYNCHRONISED FL-74 CELLS

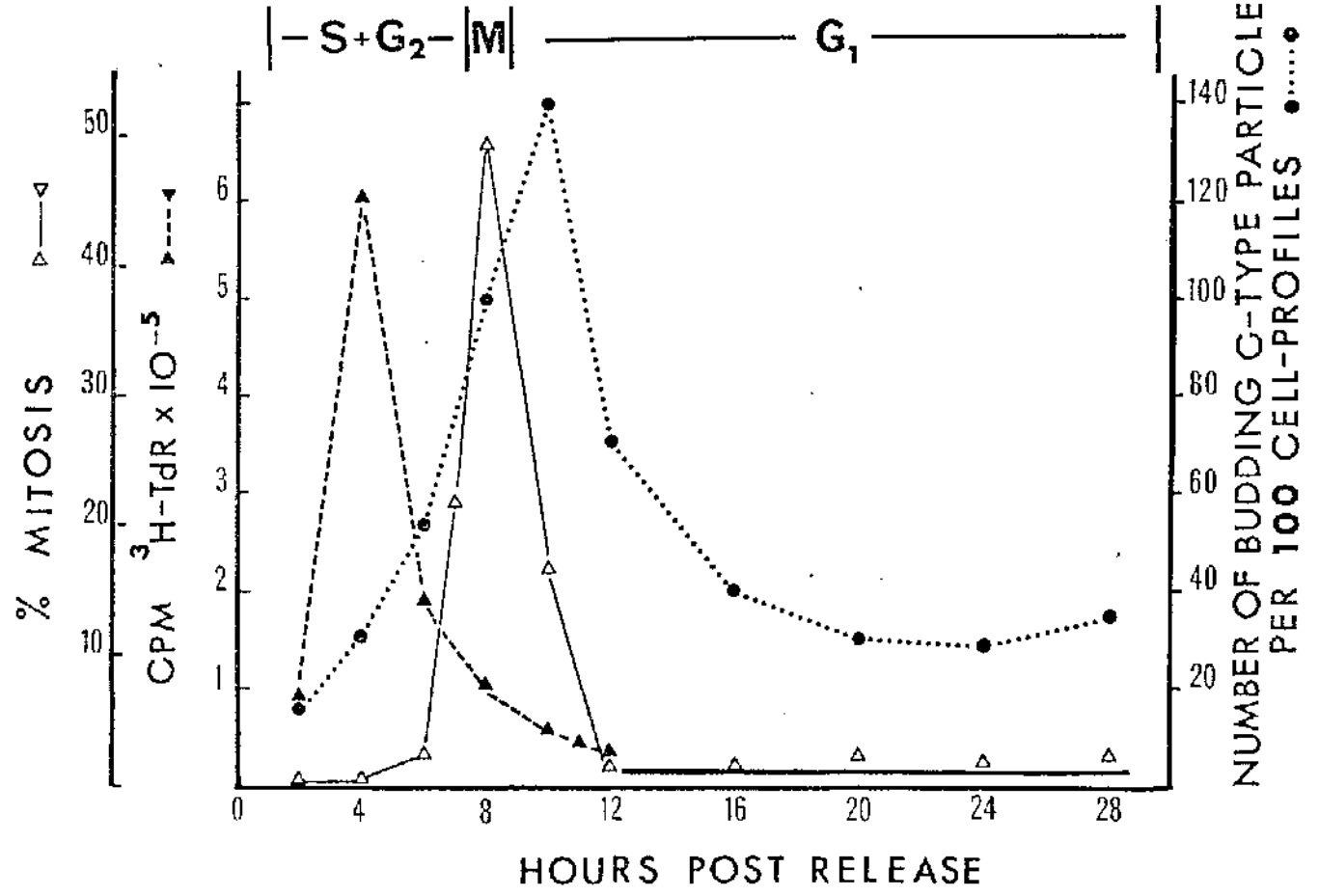

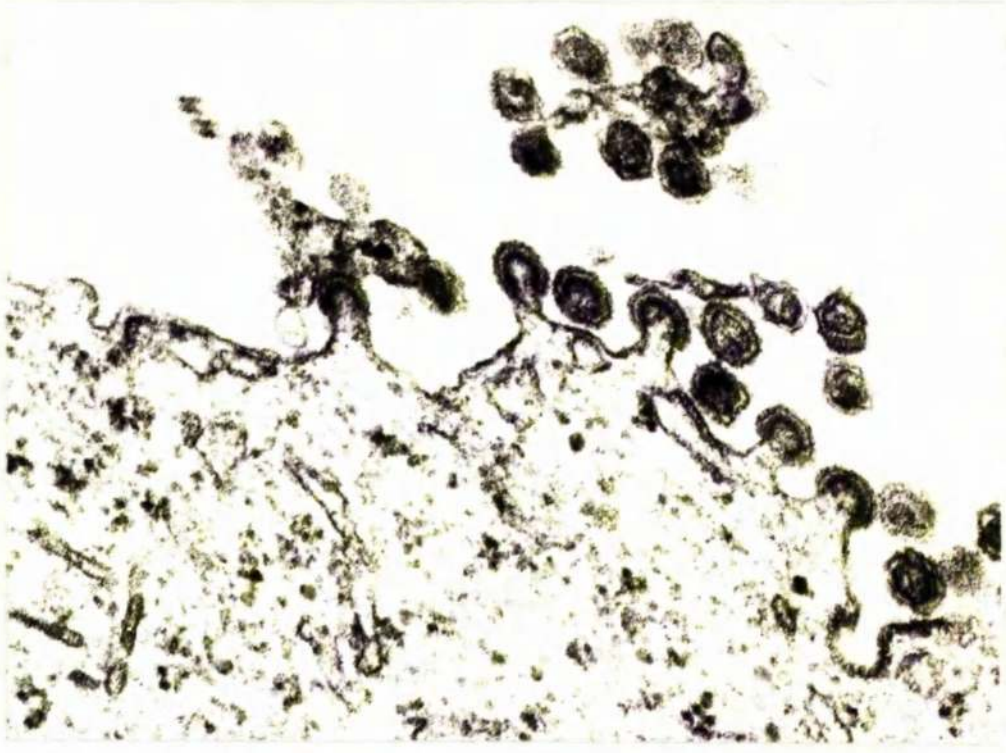

FIGURE 4 : FL74 cell membrane with numerous budding C-type particles at the time of the viral peak

FIGURE 5 : An FL74 cell with budding and released Cltype particles

FIGURE 6 : F422 cells with budding and released virus particles. The cells have uropod morphology which is characteristic of this cell line

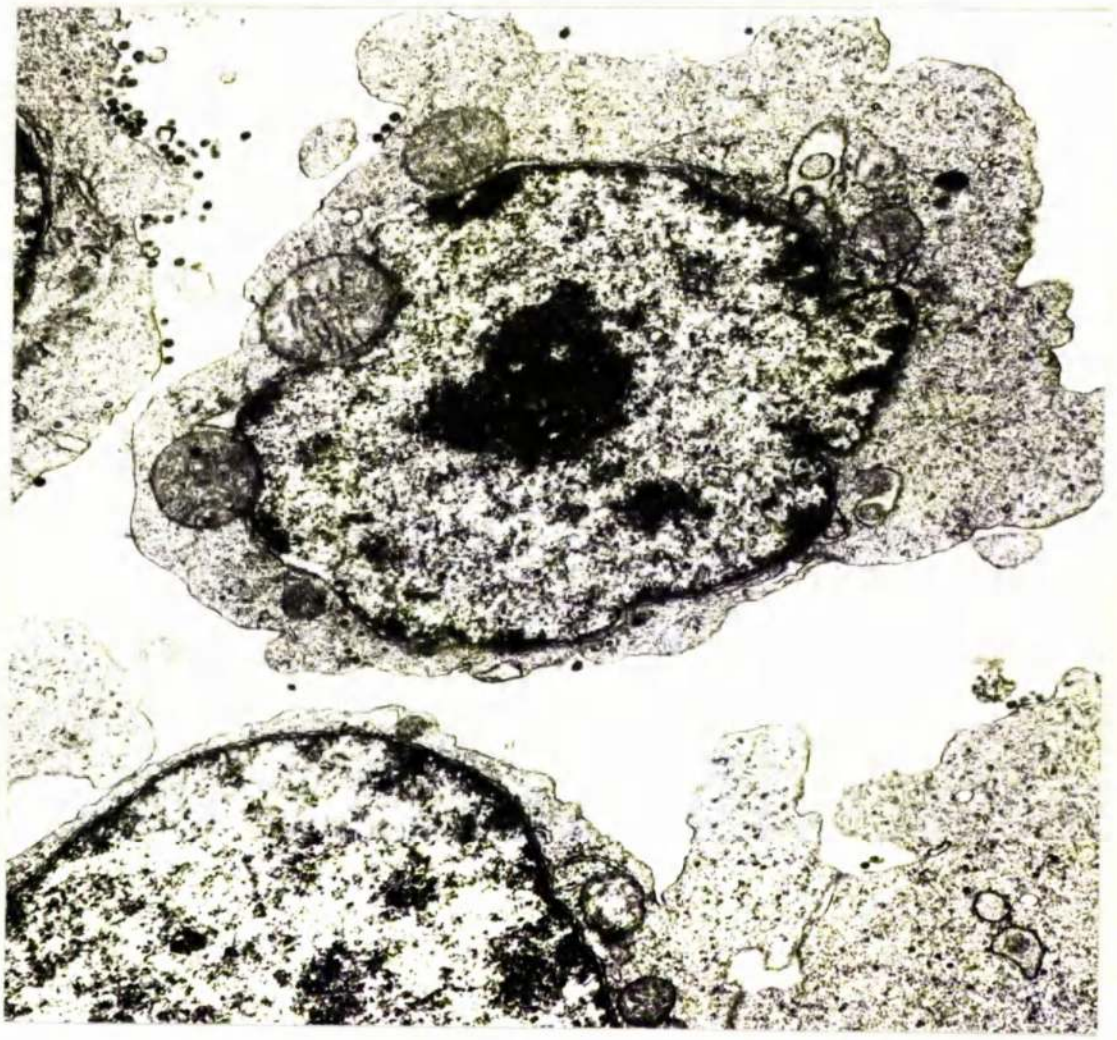

FIGURE 7 : CT45-S cells with budding and released C-type particles

CHAPTER THREE

ULTRASTRUCTURAL STUDIES OF SYNCHRONISED FL74 CELLS BY TRANSMISSION AND SCANNING ELECTRON MICROSCOPY

CHAPTER THREE : ULTRASTRUCTURAL STUDIES OF SYNCHRONISED FL74 CELLS BY TRANSMISSION AND SCANNING ELECTRON MICROSCOPY.

1. The Scanning Electron Microscope
2. Review of the Literature
3. Materials and Methods
4. Experiments and Results
5. Discussion

This study of the morphology of synchronised FL74 cells was intended to examine another aspect of the changing character of these cells through the course of their life cycle. An attempt was made to relate ultrastructural changes of cells to known phases in the cell cycle. Until recently, when structural information about cells was required, it was gained from thin sections. For answering many kinds of questions, especially those concerning internal structure, there is no substitute for this approach. However, for observations of the overall form of cells and particularly of the surface morphology of cells, the thin section, representing only a small part of the surface, is less than adequate. Fortunately, thanks to the improvements in scanning electron microscopy, and in biological specimen preparation techniques (Porter et al., 1972; Boyde et al., 1972), the scanning electron microscope (SEM) has become a most valuable tool for the observation of surface morphology. Therefore, it was decided that, in addition to transmission electron microscopy (TEM), scanning electron microscopy would be used for a detailed exploration of changes in surface morphology and cell shape associated with the cell cycle.

1. The Scanning Electron Microscope

In the scanning electron microscope, the specimen is irradiated by a finely focused electron beam. This releases secondary electrons, back-scattered electrons, characteristic X-rays, and several types of radiation, from a small part of the specimen. There are two ways in which these signals can be used. Either the beam remains stationary at a point to give, for example, an X-ray analysis, or it is scanned in a television raster to obtain information over an area.

The information detected varies with the mode of operation of the microscope. The emissive mode, detecting secondary electrons emitted from the specimen surface, is the one most commonly employed. The secondary electron image is very similar in appearance to a light optical image, except that there is no colour and both the resolution and the depth of focus are greatly improved. Because the SEM has a depth of focus several hundred times that of the light microscope, the images have a three-dimensional appearance.

Until recently, most SEM studies have been concerned with hard specimens. Biological materials presented problems, e.g., distortion was produced by fixation, water removal or drying of the specimen. These problems have to a large extent, been overcome by freeze-drying or by critical point-drying of suitably fixed material.

Critical point-drying which was employed in this study, is a method which attempts to overcome the damage caused by the passage of a phase boundary (liquid/gas or solid/gas) through the specimen. The specimen water is replaced by acetone; acetone is, in turn, replaced by liquid carbon dioxide in a suitable high pressure apparatus. The apparatus is sealed off and its

temperature is raised above the critical point of CO_2 ($31^{\circ}C$). The liquid CO_2 changes to gas without change of volume and without the passage of phase boundary. The gaseous CO_2 is then allowed to escape : the specimen is dried. To prevent the build-up of charge, the specimen is coated with gold.

The preparation of suspended cells for scanning electron microscopy created an additional problem. In earlier studies, blood cells were processed on metallic filters which led to artificial surface changes. However, this problem was overcome by the method of Mazia et al., (1975) described in the Materials and Methods part of this Chapter.

2. Review of the Literature

The surface morphology of the normal, mature lymphocyte has been adequately defined by SEM. The surface of the lymphocyte is covered with microvilli which are randomly distributed. The surface alterations so far described seem to result from environmental, functional or malignant changes rather than taxonomic differences, although thymocytes have consistently been shown to be smoother than peripheral blood lymphocytes regardless of preparatory methodology, which is known to cause variations in the surface of the lymphocytes (Polliack et al., 1975).

There are relatively few publications concerning abnormal lymphocyte states and/or disorders of lymphoid tissues. In chronic lymphatic leukaemia, lymphocytes appear to have fewer microvilli than their normal counterparts (Cohen et al., 1976). In acute lymphocytic and other leukaemias, idiosyncratic cell forms are described (Polliack, 1976). The hairy-cell leukaemias seem to be morphologically diagnostic by their "hybrid" monocytoid/lymphoid appearance (Roath and Newell, 1976) and so are the characteristic cells seen circulating in the Sezary syndroma (Golomb et al., 1975).

It has been shown, by using pokeweed mitogen (PWM) and anti-β_2-microglobulin, that sequential changes occur during the culture period (usually 72 hrs.), i.e., there is an increase in cell size, uropod formation takes place, microvilli which are well developed in the early period of the culture gradually decrease and the cells tend to clump together. There is a certain variability in the appearance of individual cells, which has been explained by the differences in the cells' specific responses to the various mitogens. (It should be mentioned that the above changes are reminiscent of those found in the course of this study on cells traversing through the cell cycle, and they might reflect

cell cycle-dependent changes rather than specific responses to various mitogens.) There is no information available about cell cycle related changes in the surface morphology of lymphoid cells, although several transformed cell lines are obtainable.

Distinct changes in cell surface morphology have already been described as a function of the cell cycle in synchronised cells grown in monolayers (Porter et al., 1973; Hale et al., 1975). One of the important observations made was that transformed cells, not contact inhibited in the usual sense did go through a sequence of phenotypic expression which approached that shown by normal cells. Consequently, two questions arise. Firstly, to what extent are these changes in surface morphology brought about by external influences?; and, secondly, what is the relationship between surface changes and changes in structural and biochemical phenomena within the cell?

As regards the first question, Rubin and Everhard (1973) have established that the variations in surface structure observed during the cell cycle are dependent on direct cell-to-cell contact; cells in cultures where there is no intercellular contact move through the cycle without exhibiting any apparent surface changes except in mitosis. Furthermore, the cell surface is modulated by cell-to-cell interactions even in transformed cells.

It has also been shown that changes in morphology can be caused by temperature, osmotic effects, and in vitro culture conditions (Lin et al., 1973; Brunk et al., 1975; Westbrook et al., 1975; Amos et al., 1976).

To answer the second question requires the investigation of several parameters, such as the role of the cytoskeletal elements and levels of cyclic nucleotides in the cytoplasm. These factors are briefly discussed below.

It has been established by a number of observations that cytoskeletal elements, that is, microtubules and microfilaments, play a paramount role in the maintenance of cell shape, locomotion, cytoplasmic streaming and movements or impedance of movements of certain plasma membrane components.

Microtubules are large rather rigid tubular structures with an outside diameter of approximately 25 nm and an inner core of 15 nm in diameter. They are composed of a 55,000 daltons molecular weight protein, tubulin, which associates into dimers and polymers to form the microtubules (Kirschner et al., 1974). These structures have been found in the nucleus, the cytoplasm and also often in close association with the plasma membrane in a variety of cells. Cytoplasmic microtubules undergo rapid, reversible assembly and disassembly and their polymerisation is sensitive to temperature, Ca^{2+} concentration, cyclic nucleotide concentrations, pH, and pressure (Kirschner et al., 1974; Kirschner and Williams, 1974). Several drugs, such as the alkaloids colchicine, colcemid, vinblastine sulfate and vincristine, are effective in causing depolymerisation of microtubules.

Microtubules are often found in association with another class of membrane-associated cytoskeletal components, the cytoplasmic microfilaments.

Microfilaments are thin protein polymers arranged in double helical filaments with a diameter of 6 - 8 nm and a variable length. They occur either immediately beneath the plasma membrane with the microfilament "bundles" penetrating deep into the cell or they form a lattice or network in the cytoplasm. Microfilaments contain actin and tropomyosin (Lazarides, 1975a; 1975b). Microfilament assemblies are sensitive to cellular cyclic nucleotide concentrations (Willingham and Pastan, 1975), and they can be disrupted to varying degrees by a class of mould metabolites collectively called the cytochalas

Cyclic AMP (adenosine 3':5'-cyclic monophosphate) and cyclic GMP (guanosine 3':5'-cyclic monophosphate) have repeatedly been implicated as regulators of cell proliferation (Pardee, 1975, Review). Cyclic AMP is formed from ATP by adenylate cyclase and destroyed by phosphodiesterase. Adenylate cyclase is localised at the plasma membrane and has an important role in the regulation of hormone activity (Robinson et al., 1972).

Cyclic AMP varies during the cell cycle (Zeilig et al., 1972, 1976). There is evidence that these fluctuations reflect discrete periods in the cell cycle during which elevated cyclic AMP may enhance or retard cell cycle progression (Zeilig et al., 1974, 1976). Zeilig and Goldberg (1977) reported that cyclic GMP levels varied independently and reciprocally with cyclic AMP levels during the cell cycle and that cyclic GMP levels increased up to tenfold at the onset of mitosis. Normal cells show a decreased cyclic AMP level during mitosis (Burger et al., 1973). Also, agents that stimulate cell division decrease the level of cyclic AMP.

Transformed cells show lower levels of cyclic AMP than normal cells (Bürk, 1968; Otten et al., 1971, 1972). The lowered levels of cyclic AMP in the cells are considered to induce abnormal morphology (Johnson et al., 1971; Hsie and Puck, 1971), rapid growth (Bürk, 1968; Otten et al., 1971), decreased adhesiveness (Johnson and Pastan, 1972) and increased agglutinability by plant lectins (Sheppard, 1971; Sheppard and Lehman, 1972).

The underlying mechanisms responsible for the cell cycle-associated fluctuations of cyclic nucleotides are not well understood. They might be regulated by changes in the activity of their anabolic and catabolic enzymes. It has been found that both cyclic AMP and GMP phosphodiesterase activity are fluctuating during the cell cycle (Jeter Jr. et al., 1978).

It has been demonstrated that there is an inverse relationship between growth rate and endogenous levels of cyclic AMP in 3T3 mouse and other cell lines (Otten et al., 1971). Cyclic AMP concentrations increase during contact inhibition, and it has been suggested that some of the properties that are characteristic of contact inhibition, such as loss of blebs might be mediated through cyclic AMP. Electron microscopy of dibutyryl cyclic AMP treated cells has revealed that, in most instances, when the form of the cells becomes more anisometric and growth slows or stops, the number of microtubules increases (Otten et al., 1971, 1972). Cyclic AMP encourages tubulin assembly and consequently microtubule formation, thus no disassembled tubulin will be available to facilitate the changes associated with cell motility or with mitosis (Vasilier et al., 1972; Johnson et al., 1972). When cell proliferation is active, as in transformed cells, cyclic AMP levels are lower (Otten, 1971).

The observation that contact between cells grown in vitro leads to the establishment of tight junctions or gap junctions (nexus) (Johnson and Sheridan, 1971) prompted Porter et al., (1973) to suggest the following theory: the establishment of contact between cells initiates a membrane propagated event (excitation) which spreads over the cells involved and activates the adenyl cyclase responsible for the synthesis of cyclic AMP and this, in turn, initiates the microtubule assembly.

It is widely claimed that the cell surface plays a critical role in the regulation of cell growth, and the number of reports which link cell surface changes to growth control and malignant transformation is increasing. In recent years, SEM has been used to study the surface architecture of a variety of transformed cells and to study virus infection of cultured cells (Porter and Fonte, 1973; Porter et al., 1973, 1974; Vesely and Boyde, 1973; Gonda et al.,

1976). It has been shown that transformed and malignant cells have a surface morphology different from their normal counterparts. Changes in cell surface morphology have also been observed as a function of the cell cycle (Porter et al., 1973; Hale et al., 1975), temperature (Lin et al., 1973), intercellular contact (Rubin and Everhart, 1973), osmotic effects (Brunk et al., 1975) and in vitro culture conditions (Westbrook et al., 1975; Amos et al., 1976).

SEM has also been employed in the study of virus infection of cells and to resolve the morphology of virions on the surface of cells (Carteaud et al., 1973; Panem and Kirsten, 1975; White and McManus, 1975; Fonte and Porter, 1974; Enlander et al., 1974; Perecko et al., 1973; Holmes, 1975).

Hale et al., (1975) examined the surface morphology of chick cells transformed by RSV and found a remarkable resemblance of the transformed cell surface to that of the cell in mitosis. In both cases, the cells become rounded and covered by extensive microvilli. Ambros et al., (1975) demonstrated that chick embryo fibroblasts infected with a temperature-sensitive mutant of RSV, rounded up and developed surface ruffling during the shift to the permissive temperature for transformation.

Based on the findings that transformed cells and mitotic cells display similarities in the binding of lectins to the cell surface and that after infection with polyoma virus, cellular DNA synthesis is required for the appearance of enhanced agglutinability by plant lectins (Eckhard, 1971; Burger, 1973; Noonah et al., 1973), Burger (1973) suggested a model that requires passage through mitosis in order for cells to undergo permanent

surface alterations. He proposed that the transformed cell's surface is in a "permanent mitotic" state. This model was further supported by the observation that both transformed and mitotic cells have reduced internal pools of cyclic AMP (Noonan et al., 1973).

There are certain ultrastructural changes which correlate to the cell cycle and which can be recognised by transmission electron microscopy alone. These include variations in cell size, changes in nuclear and nucleolar morphology and changes in the pattern of chromatin organisation. These can be used as ultrastructural markers to relate other characteristic variations obtained by different techniques to the phases of the cell cycle.

Although cell size per se is not a good indicator of cell cycle phase, relative increase in cell size within each lymphoblast population is directly related to progression through interphase (Everson et al., 1973). By velocity sedimentation, cells can be partly separated according to their phase of growth.

It has been indicated that the nucleolus has a major role in regulating cell proliferation (Baserga et al., 1976). The nucleoli of lymphoid and other cells undergo many distinct morphological changes that appear to coincide with phases of the cell cycle (Gani, 1976; Gonzales and Nardone, 1968; Potmesil and Goldfeder, 1977; Potmesil and Smetana, 1969), and cell maturation (Potmesil and Goldfeder, 1972, 1973; Smetana et al., 1969). Mitogen induced lymphocytic transformation leads to the enlargement of the nucleolus and to the dispersion of nucleolar components (Gani, 1976; Potmesil and Smetana, 1969). In resting mature lymphoid cells the nucleolar structures are smaller and more segregated (Potmesil and Smetana, 1969;

Potmesil and Goldfeder, 1977). Nucleolar variations in leukaemic lymphoblasts have been detected by light and transmission electron microscopy (Smetana et al., 1970; Potmesil and Goldfeder, 1972), and cell cycle-specific nuclear and nucleolar changes of human leukaemic lymphoblasts have been described by Parmley et al., (1977).

It has also been suggested that in interphase, nuclei of cells active in division, chromatin may undergo sequential changes in distribution which relate to the cell cycle (Milner, 1969; Pederson, 1972; Pederson and Robbins, 1972; Rao and Johnson, 1974). According to the hypothesis which emerged from the above studies, the large-scale condensation of chromosomes in mitosis is just one aspect of a continuous cycle of chromatin rearrangements. Cyclical interphase chromatin changes could be important in gene transcription, nuclear growth, ordered chromosome replication and preparation for cell division.

Electron microscopy of transformed lymphocytes revealed marked disaggregation of condensed chromatin during S phase (Tokuyasu et al., 1968; Milner, 1969). Results of several electron microscope-autoradiographic studies of animal cells, after short labelling of DNA with ^{3}H-TdR, indicate that the sites of precursor incorporation are in the dispersed chromatin, often at the periphery of the condensed chromatin masses. This is particularly so in transformed lymphocytes (Tokuyasu et al., 1968; Milner, 1969). These microscopic observations are consistent with the concept of a cyclic sequence of chromatin disaggregation, replication and reaggregation associated with the cell cycle.

3. Materials and Methods

Cells, cell cultures, the synchronising techniques and the preparation of cells for transmission electron microscopy are described in the First and Second Chapters.

Preparation of cells for scanning electron microscopy

(a) Attachment of cells to coverslips

At time intervals, after release from the synchrony inducing block, cells were washed in serum-free growth medium or in Hank's balanced salt solution (Ca^{++}, Mg^{++} free). Alternatively, cells growing in suspension cultures were used without washings to avoid the introduction of changes in their morphology by the subsequent centrifugations.

The method used for attachment of cells was recommended by Mazia et al., (1975). Briefly, round glass coverslips, about 6 mm in diameter, were soaked in a 0.1% solution of poly-l-lysin (70,000 molecular weight, from Sigma) in double distilled water for 30 minutes. The coverslips were rinsed under running tap water for one hour and kept in distilled water for a few minutes before use. Small specimen boxes were used as moist chambers for cell attachment. A few drops of distilled water were placed in the bottom of the box. Coverslips were first dipped in serum-free medium and then placed on the top of the small stalks in the box. Immediately afterwards, a drop of the cells suspended in medium was placed in the centre of the coverslip. The box was closed and left undisturbed for 30 minutes, after which time the unattached cells were rinsed off. The coverslips were transferred into individual bijou bottles containing fixative. At this step, and during the following procedures as well, care was taken to keep the cell-covered side of the coverslips always facing upwards.

The principle behind this method is that the polycationic polylysin molecules strongly adsorb to various solid surfaces leaving cationic sites free which combine with the anionic sites on cell surfaces. The attached cells are not detached by treatment with fixatives or by further processing such as critical-point drying.

(b) Fixation and Dehydration

After attachment, cells were fixed for 30 minutes at room temperature in 2.5% glutaraldehyde in Cacodylate buffer, pH 7.2. The fixative was freshly prepared on every occasion by mixing 2 ml. of 70% glutaraldehyde (Ladd, Burlington) with 54 ml. of buffer. After this initial fixation, the samples were stored in the refrigerator overnight. Before dehydration, cells were rinsed 3 times with Cacodylate buffer and postfixed with 1% osmium tetroxide for 30 minutes. In later experiments, the post-fixation step was omitted.

Dehydration was performed in graded concentrations of acetone (30 - 50 - 70 - 90 - 100 - 100%) for 5 minutes each. In a holder, the coverslips, always covered with 100% acetone, were quickly transferred to a high pressure chamber in which the CO_2 critical point was obtained.

The critical-point-dried cells, on the coverslips, were stuck into aluminium stubs by means of a conductor-silver paint, they were coated with a thin layer of gold, 10 - 20 nm in thickness, in a Polaron E 5000 SEM diode sputter coater and examined in a Philips PSEM 500 scanning electron microscope at an accelerating voltage of 20 - 30 kV.

Assessment of morphological changes was facilitated by viewing 200 - 300 cells per preparations on a television monitor.

4. Experiments and Results

Synchronised populations of FL74 cells were obtained by using three different synchronising methods (double TdR block, cold treatment and isoleucine-deprivation of cells). A combination of these methods offered two main advantages. Firstly, it made it possible to obtain well synchronised populations in different phases (G_1 and $S + G_2 + M$) of the cell cycle. Secondly, the morphological changes found by using these various techniques could be compared. Thus, the methods played a confirmatory role in relation to one another.

After synchronisation, at time intervals, cells from the same cultures were processed for transmission and scanning electron microscopy as described in the Materials and Methods part of the Second and Third Chapters. At the same time, samples were taken for mitotic index determination.

Initially, cells were synchronised by a double thymidine block, after which a good synchrony was achieved in the $S + G_2 + M$ phases.

In the scanning electron microscope, the majority of cells exhibited variations in their surface morphology which were characteristic of each phase of the cell cycle. These were selected and evaluated. Routinely, 200 - 300 cells were examined in each preparation. Furthermore, measurements of the cell size were performed on scanning electron micrographs, and variations in cell shape were noted.

In the transmission electron microscope, thin sections of cell profiles which had no nuclei or nucleoli were not used for ultrastructural study. The knowledge of the cell surface morphology obtained by SEM helped greatly to interpret many of the observations concerning cell size, cell shape and cell surface configurations.

Several other characteristics were evaluated in this study such as nuclear shape, nuclear chromatin distribution, nucleolar position and size, the state of the nucleolus-associated chromatin, and the degree of segregation in the components of the nucleolus.

Cells morphologically characterised and known to belong to a certain period of the cell cycle, were also examined for budding C-type particles.

After mitosis, the synchrony gradually deteriorated and the cells exhibited great diversity in their morphology. In order to examine morphological characteristics in the G_1 phase, cells were synchronised by cold treatment or by isoleucine deprivation. Samples were taken during the G_1 phase and also during the following $S + G_2 + M$ phases.

In addition to the synchronised cells, logarithmically growing and density inhibited cells were also examined by scanning and transmission electron microscopy.

The majority of the cells belonging to a distinct phase of the cell cycle exhibited the same characteristic ultrastructural variations regardless of the synchronising methods used.

The only difference observed was that cells synchronised by the double TdR method, after mitosis, in the early G_1 phase had an extensively "blebbed" surface morphology. On the other hand, density inhibited cells and cells synchronised in the G_1 phase by chilling or isoleucine deprivation were villous or smooth and had no blebs on their surfaces. Only after reaching the next mitotic and early-G_1 phase did the cells exhibit the "blebbed" morphology again. This is in accordance with the observations made by others (Porter et al., 1973; Hale et al., 1975) on cells grown in monolayer, that the blebbed morphology of

early G_1 cells precedes the villous and smooth morphology of density inhibited or late G_1 cells in the normal cell cycle progression.

The experiments were repeated twice. The observations on cell populations from both experiments were essentially identical.

The observations made in each phase of the cell cycle by transmission- and scanning electron microscopy are described and demonstrated below and also shown in Table 13, p 122.

The progression of the FL74 cell through the cell cycle and the associated morphological changes will be described and demonstrated in the following order : early-G_1; mid - late G_1; early - S; mid - late S; G_2; Prophase - Metaphase - Telophase - Cytokinesis. (No attempt was made to identify cells in Anaphase since its estimated duration is only 3 - 5 minutes.) This particular order enables all the morphological changes to be shown at their most striking.

Changes in Morphology during the Cell Cycle:

Early-G_1 Phase

SEM

The cells were often in the late stages of cytokinesis and were associated in pairs. These were the smallest cells with diameters ranging between 7.8 - 8.2 μm.

The surface of the cells was covered with blebs intermingled with microvilli and other small projections. The blebs displayed a great variety in size, measuring 0.5 to 2.0 μm in diameter. The smaller ones might represent the early stages of the formation of larger ones (Figs. 8, 12, 14).

There was a number of smooth spheres and elongated, cytoplasm-

filled bodies in both TEM and SEM preparations, which presumably represented fragments of the cells that had broken away during mitosis (Fig. 10).

A large number of budding virusparticles were present on the cell surface, located preferentially on the various projections of the cells (Figs. 8, 12, 14, 16, 18).

In order to examine the appearance and size of the FL74 virus, initially, purified FL74 virions, in PBS, were placed on poly-l-lysin coated coverslips, fixed, critical-point-dried, and examined in the SEM. At high magnifications (5 - 10,000) the virions were easily recognisable. However, they appeared to be slightly smaller than in thin sections, which was due to the drying process. Similar observations were made concerning the size of the cells.

Very often cells remained in pairs even later in the G_1 phase although their size increased and the ultrastructure of their nuclei and nucleoli showed the typical mid-G_1 characteristics (Figs. 12, 13).

Three to four hours after mitosis, microvilli became the dominating feature of the cell surface. They were fairly uniform in diameter (about 0.1 μm), but varied greatly in length. Some appeared to be small, stub-like, especially when viewed from the top, while others had a considerable length.

TEM

The cytoplasm of the cells was small, containing few organelles. The nucleus was round, with dispersed nuclear chromatin (euchromatin). A given nuclear profile usually contained one, but sometimes two or three nucleoli.

The components of each nucleolus were distinctly segregated into granular component (particles up to 14 nm in diameter), dense fibrillar component or nucleolonema (consisting predominantly of fibrils 5 to 8 nm wide),

and pars amorpha or fibrillar centre (containing less dense, amorphous materials). When the pars amorpha was located in the centre of the nucleolus, it appeared to be ring-shaped.

Examination of thin sections revealed that the ultrastructure of blebs varied. There were basically two types of blebs. The first type was filled with cytoplasm, some of them containing large numbers of polyribosomes, but usually devoid of cytoplasmic organelles (Figs. 13, 15, 19). The second type was empty and had a minimal thickness consisting of two plasma membranes. These seemed to be formed by membrane assembly and produced by the active Golgi apparatus. Several small vesicles were present at the base of every such bleb (Fig. 11). The smaller ones tended to fuse to form larger ones. Thus, the cell is apparently easily able to increase its surface which might be necessary for a variety of reasons, i.e., growth, nutrition, contact, change in form.

The highest numbers of budding C-type particles were seen on these early-G_1 cells (Figs. 9, 15, 17).

Mid - Late - G_1 Phase

SEM

The diameter of cells ranged between 8.2 - 8.5μm. Microvilli seemed to be the characteristic cell surface feature during the mid- and late-G_1 phase of the cell cycle, although their number and size became smaller in late G_1 (Fig. 21). By the end of the G_1 phase, cells appeared to be smooth or undulated and free of blebs and microvilli, although a small number of microvilli occasionally could be seen. Cells, especially in stationary cultures, shed off their surface structures completely (Figs. 26, 27). These "nude" cells then came to dominate the population (Fig. 28).

TEM

The cells in this phase had larger cytoplasm with more numerous cytoplasmic organelles than the early G_1 cells. The nucleus was round, later becoming slightly indented (Figs. 22, 24). The cytoplasm facing the nuclear indentation contained the Golgi apparatus, centrioles and many of the cellular organelles (Fig. 24). The nuclear chromatin was dispersed.

The paucity of nucleolus-associated chromatin was unique to this cell type (Fig. 25). The nucleolar components were segregated, small foci of pars amorpha were present. Small amounts of fibrillar components were often adjacent to the foci, but the granular component was the predominant nucleolar constituent (Figs. 22, 23, 24, 25).

Early-S Phase

SEM

Immediately after release from the thymidine block, the cell surface was smooth or undulated and microvilli were almost completely absent (Fig. 29). Two hours post release, cells appeared to have more microvilli varying in length (Fig. 30). The diameter of the cells was ranging between 8.5 and 11.2 μm.

TEM

The cells contained a moderate amount of cytoplasm. The nucleus was indented. The majority of the nuclear chromatin was dispersed. The nucleoli were large, round and eccentric (Fig. 31). The perinucleolar chromatin had attached again and was intimately associated with the nucleoli. The nucleoli contained a moderate amount of granular and dense fibrillar components (Fig. 32).

Mid - Late-S Phase

SEM

By this time, the cells became noticeably larger than those in the G_1 phase. The diameter of the cells ranged between 11.2 - 12μm.

In the mid- and late-S phase, for the first time, cells showed ruffles or lamellipodia (Figs. 33, 35). Ruffles were present on free edges of the cells. In places, where the cell was in contact with another cell, generally no ruffle was present. These extraordinary surface structures were thin folds and tended to have minimal thickness consisting of two plasma membranes and two internally opposed cytoplasmic cortices (Figs. 34, 36). The vertical dimensions of ruffles were highly variable, in places they extended around the cell as far as 8 - 10μm (Fig. 37). Since cells often possessed several ruffles, the latter could comprise a substantial proportion of the total cell surface at any one time.

Generally, the first small ruffles appeared in the mid-S phase (Fig. 33). The number and size of these surface structures later increased (Figs. 35, 37). In the late-S phase, the surface of the cells became very wavy and ruffled and often the cell surface had ridge-like profiles (Fig. 40).

TEM

The cells contained abundant cytoplasm and the Golgi region was very active (Figs. 38, 42).

The nucleus was indented or sharply folded. The nuclear chromatin was dispersed. Euchromatin was extending to the nuclear pores, clumps of heterochromatin occasionally extended into the central part of the nucleus.

The nucleoli were large, had irregular shapes and usually were

located peripherally. The nucleoli were always surrounded and often penetrated into by perinucleolar chromatin (Fig. 39). At this stage, the dense fibrillar component became very prominent and in the late-S phase, the nucleoli had a trabecular appearance (Fig. 41).

G_2 Phase

SEM

These were the largest cells in the population. They measured up to 13.5 μm in diameter. As the cells progressed through the G_2 phase, their surface features became more and more elaborate which eventually culminated during mitosis.

The cells were covered in varying degrees with microvilli which, in turn, varied greatly in length. However, the most striking feature was the appearance of the very long slender filopodia and a small number of fairly large, round blebs (Figs. 43, 44, 47). The number of filopodia was increasing and also the ruffling of cells was considerable. At the end of the G_2 phase, the cell surface was thickly covered with filopodia, microvilli, small and large blebs intermingled with one another (Fig. 47). The cells contacted each other and were clumped together by means of these surface structures.

TEM

The cells contained abundant cytoplasm with active Golgi region. The nucleus was large and sharply folded (Figs. 45, 48). The nuclear chromatin was aggregated into clumps which were gradually increasing in size.

The nucleolus-associated chromatin infiltrated the nucleolus (Fig. 46).

The nucleoli were large and had a flattened appearance. Aggregates of nucleolar components, including pars amorpha, were frequently seen (Figs. 45, 46). The fibrillar centre of pars amorpha was also observed during mitosis.

Mitosis

During mitosis, the cells had an active surface which was most striking in appearance and which underwent a series of distinct changes corresponding to the successive phases of the mitotic period.

The fact that the population was morphologically fairly homogeneous, due to the high degree of synchrony achieved, as well as the combination of TEM and SEM, made it possible to identify cells during the process of mitosis and cytokinesis right up to the last step when the separating daughter cells appeared at the end of the telophase.

Prophase

SEM

Cells in prophase displayed the most diverse surface features. A great number of long filopodia, small and large blebs, microvilli and extensive ruffling were all present (Fig. 50).

Interestingly, when individual cells were allowed to adhere to the poly-l-lysin coated surface, the cells made contact with the surface by means of their long filopodia which frequently arborised at their tips and by doing so, behaved exactly the same way as monolayer cells do during mitosis as described by Porter et al., (1973) (Fig. 50).

TEM

Fixation of cells in suspension preserved the surface morphology extremely well, and in thin sections, the cell surface protrusions were well recognisable (Fig. 51).

The process of chromatin aggregation into individual chromosomes could be observed (Figs. 48, 49, 51, 52, 55, 57).

At the beginning of the prophase, the nuclear membrane and the nucleoli were still present. The nucleoli were segregated with foci of pars amorpha (Fig. 49).

The last part of the prophase was marked by the disintegration of both nucleolus and the nuclear membrane (Figs. 51, 52).

Metaphase - Anaphase

SEM

Metaphase cells were large, round cells. The surface structure was dominated by medium-sized blebs, but small microvilli and large blebs were also present (Fig. 53).

When the cells were viewed in aggregates, they appeared to cling together by long filopodia and by the extensive surface of their ruffles.

TEM

The cells at this stage had no nuclear membrane. The nuclear chromatin were aggregated into individual chromosomes, and the thin slices of these chromosomes could well be recognised. In Fig. 55, one centriole is shown with the spindle fibrils extending from the centriole towards the chromosomes.

Fig. 55 also illustrates two examples of centrioles. The upper one is cut across, showing the cylindrical form of the centriole. The lower one is cut obliquely through one end of the cylindrical centriole, hence it appears as a dark horse-shoe-shaped structure.

In Fig. 54, in addition to the slices of chromosomes, the cross section of the empty type blebs can be seen, which corresponds to the surface morphology observed by SEM and illustrated in Fig. 53. This is a good

example for the complementary role of the TEM and SEM observations. The finding of round, empty-looking and membrane-bound holes in the surface region of cells which otherwise had the ultrastructure of a typical metaphase cell, made it possible to identify the surface morphology of metaphase cells in the scanning electron microscope.

In Fig. 57, a cell is shown in anaphase or early-telophase. The chromatids of chromosomes separated and moved toward opposite ends of the cell.

Telophase - Cytokinesis

SEM

Individual cells showed strong polarisation, which might represent the first stage of cell division (Fig. 56). Fig. 58 illustrates a dividing cell which is supported and attached to neighbouring cells by filopodia and ruffles. The cell apparently used all its excess cell surface stored in these projections for this supporting purpose, hence, in regions where cell contact was not present, the cell was completely smooth.

The characteristic smooth cell surface can be observed on daughter cells in the very early stage of their separation. Examples for this are the cells in Fig. 59, on the left hand side, while cells in the upper right corner represent separating cells in a later stage. The later ones show extensive blebbing and this bleby surface as described earlier, will be the most characteristic cell surface feature of the early-G_1 cells.

TEM

The ultrastructural characteristics of separating daughter cells in thin sections are illustrated in Fig. 60. The cells were small and had a

slightly elongated shape. The round nucleus was surrounded by a small amount of cytoplasm which tended to bulge out at one pole of the cell. Few cytoplasmic organelles were present.

The nucleus contained condensed chromatin (heterochromatin) distributed alongside the nuclear membrane.

The nucleolus was closely attached to the condensed chromatin and its position was eccentric. The nucleolar components were well segregated with foci of pars amorpha and had often a "ring-shaped" appearance (Fig. 60).

Scanning- and Transmission Electron Microscopy of F422 and CT45-S Cell Lines

Synchronised F422 and CT45-S cells were not included in this detailed ultrastructural study. However, exponentially growing F422 and CT45-S cells were examined by both TEM and SEM.

F422 Cells

These cells had the morphology of a typical uropod. The uropod form was well recognisable not only in the SEM, but also in thin sections when the sectioning was favourable (Figs. 6, 63, 64, 65, 66, 67).

Surface protrusions, mainly blebs, varying in size, were accumulated at one pole of the cell, while the remaining part appeared to be undulated or smooth.

In both TEM and SEM preparations, budding C-type particles were seen only on the blebbed area of the cell. The budding viral structures, like the cross-linked surface molecules in the capping process, were moved

to the uropod part of the cell. In Fig. 66, accumulation of budding particles and thick, parallel-oriented microfilaments, can be seen. Fig. 68 shows that, characteristically, the tail of the uropod is opposite to the nuclear indentation which contains the Golgi apparatus and a prominent centriole cut obliquely.

Generally, uropod formation is associated with cell locomotion, cap-formation, contact with cells or substrate. The name "uropod" originated from McFarland et al., (1966) who observed that cap formation was often accompanied by stimulation of cell motility and change in cell shape which consisted of cell elongation and formation of a more or less pronounced protrusion called a "uropod". The shape of the uropods is similar to the "hand-mirror" shape of lymphocytes moving on substrates or interacting with other cells.

The formation of a uropod has often been described as being accompanied by the formation of small protrusions and membrane ruffles at the front of the cell (Kornovsky et al., 1975). Microvilli are often associated with the uropod, and they may move to the uropod during capping, whereas the rest of the cell remains relatively smooth or undulated.

F422 cells formed uropods spontaneously and permanently, probably as a result of cell-to-cell contact or contact with a solid substrate.

CT45-S Cells

The morphology of the CT45-S cells in both TEM and SEM preparations appeared to be completely different from that of the FL74 and F422 cells.

The presence of giant cells, which amongst other things, was one of the characteristics of this cell line, could be observed by light, scanning- and transmission- electron microscopy (Figs. 69, 70).

In SEM preparations, the cell surface had a bizarre, cauliflower-like structure and almost all the cells had a few, very long and thick, finger-like protrusions (Fig..69).

In TEM preparations, the large nucleus was surrounded with a small rim of cytoplasm containing few cytoplasmic organelles. The cell profiles had an irregular wavy appearance which corresponded well with the SEM image of these cells (Fig. 70).

As shown in Fig. 7 and 70, budding C-type particles were present on cells even in metaphase, and the majority of the released virus particles had the type-1 morphology.

5. Discussion

An analysis of morphological data obtained by TEM and SEM revealed that synchronised FL74 cells exhibited distinct ultrastructural variations which were closely related to the cell cycle.

In the early-G_1 phase, cells were relatively small and had an extensively blebbed surface and segregated nucleoli. Segregated nucleoli, such as the ring-shaped nucleoli in Fig. 9, have been associated with resting, G_0 or early-G_1 phase (Gani et al., 1976; Potmesil and Smetana, 1969). On the other hand, less segregated and often dense nucleoli have been associated with cell proliferation (Potmesil and Goldfeder, 1977). Studies using the demonstration of nucleoli and autoradiographic labelling of cells, have shown that nucleolar morphology is applicable for classification, proliferating and non-proliferating cells in normal tissue, and for studies of their kinetics (Potmesil and Goldfeder, 1972, 1973). It has also been demonstrated that segregation of nucleolar components reflects inhibition of RNA synthesis (Potmesil and Smetana, 1969).

As for the role of the nucleolar components; pars amorpha contains protein, RNA and DNA (Love and Walsh, 1968; Swift, 1963, Goessens, 1976) and it is present in the small G_1 and in the large G_2 cells, and also throughout mitosis (Goessens and Lepoint, 1976; Parmley et al., 1977). It has been proposed that the pars amorpha is the nidus for nucleolar reformation in early interphase (Goessens, 1976; Parmley et al., 1977).

A close relationship has been suggested between RNA synthesis and the granular components, the latter containing RNA precursors (Narayan et al., 1966).

The dense fibrillar components are known to contain ribonuclear protein and some DNA (Narayan et al., 1966; Lettre and Sieles, 1954).

The observations made on the formation of empty-type blebs and also on the formation of ruffles are in accordance with those of Palade (1959), who has proposed, on the basis of extensive EM evidence on secretory mechanisms, that plasma membranes are formed via an assembly line process. Polypeptides are synthesised initially on the rough endoplasmic reticulum and transferred to the smooth endoplasmic reticulum and then to the Golgi apparatus, where they are formed into vesicles. The vesicles migrate to the cell cortex and eventually fuse with the pre-existing plasma membrane. In addition, in electron micrographs of a variety of cell types, vesicles of unknown function have often been observed in the cytoplasm near the plasma membrane (Bennett and Leblond, 1970).

However, the most convincing evidence for the assembly-line mechanism, comes from data on the addition of saccharides during glycoprotein synthesis. In many cell types, the predominant carbohydrate residues attached to polypeptide back-bones are incorporated into nascent molecules at the level of the rough endoplasmic reticulum (RER) or in the smooth endoplasmic reticulum and the Golgi apparatus. When nascent proteins are labelled with radioactive precursors, the labels appear first in the RER and later at the cell surface (Leblond and Bennett, 1974).

In the mid- and late-G_1 phase, cells shed off their blebs and were covered with microvilli. If the in vitro observation of shedding of blebs, and consequently of surface components, reflect the in vivo situation, this may have important immunological consequences. The "shedding" of antigenic material may provide the tumour with "soluble antigenic camouflage" by which it escapes host immunological control. These materials may also participate in the formation of "blocking factors", such as specific immune complexes which are protective towards the tumour in the case of an active cell-mediated immune

response. Furthermore, host responses to acellular forms of tumour antigen in body fluids may lead to a "deviation" of the immune response to these antigens, instead of those expressed upon tumour cells, with the consequence that tumour rejection reactions will diminish.

The predominance of nucleolar granular material might reflect active synthesis of r RNA as suggested by Narayan et al., (1966).

The detachment of nucleolus-associated chromatin from the granular component might facilitate the dislodgement of r RNA precursors into the euchromatin from where their transport through the nuclear pores to the cytoplasm would follow. These ultrastructural findings are in conformity with light microscopy observations of the uniform distribution of basophilic ribonucleoprotein in cultured G_1 lymphocytes (Gani, 1976).

Cells traversing through S phase were increasing in size and showed characteristic cell surface extensions, the ruffles. Ruffles were formed by cell membrane assembly process in a way similar to the formation of blebs described previously. The vesicles fused into the plasma membrane and the cytoplasm flowed into the extensions, which are shown in Figs. 34 and 36. The extensive ruffling occurred at the same time as the cells in culture began to clump together. Thus, the cell-to-cell contact, which seems to be important in cell proliferation was facilitated by this process. Ruffles are likely to have other functions as well: in addition to pinocytosis, they provide the cell with considerable extra surface for metabolite uptake by diffusion.

The decrease of granular component in the S phase nucleoli may correspond to a decrease in RNA synthesis.

The dense fibrillar component is known to contain ribonucleoprotein (Narayan et al., 1966; Recher et al., 1970). Therefore, the increase in the

dense fibrillar component and its association with the nucleolus-associated chromatin may suggest DNA synthesis.

The prominence of the nucleolus-associated chromatin and dense fibrillar component may correspond to the increase in nucleolar trabeculation and staining intensity of cultured S phase lymphoblasts reported by Gani (1976).

In the G_2 phase, cells reached their maximum size. At this stage, new surface structures, the long filopodia and the first blebs, appeared.

The components of the nucleoli were segregated with foci of pars amorpha whose presence was also observed during mitosis. The latter finding was similar to that found in Ehrlich tumour cells (Goessens and Lepoint, 1974) and in human leukaemic lymphoblasts (Parmley et al., 1977).

During mitosis, the shape and the surface structure of the cells underwent a series of morphological variations, being very elaborate and covered with all kinds of surface extensions in prophase; large and round, possessing mainly a few scattered blebs during metaphase; becoming smaller and elongated with rather smooth surface during cell division; developing blebs at the end of the telophase; and finally, exhibiting the characteristic extensively blebbed phenotype in the early-G_1 phase.

When the number of budding C-type particles was counted on FL74 cells morphologically characterised, it was found that in both SEM and TEM preparations, the early-G_1 cells were releasing the highest number of virus particles.

The application of SEM and TEM in this study originated from the need to gain morphological data on synchronised cells in order to identify them in the various compartments of the cell cycle. Not only has this task been satisfactorily achieved, but information was obtained which might prove to have further significance.

To the best of my knowledge, no data exist at present on cell cycle-dependent cell surface changes of lymphoid cells. No doubt, it is a matter of conjecture whether lymphoid cells from special tissues and from animals or subjects with lympho-proliferative disorders may have a surface morphology which is reflected in these in vitro changes. However, scanning electron micrographs are frequently seen which are believed to demonstrate a certain homogeneous population of cells, but which almost always exhibit one or more "odd" cells with completely different (mainly bleby) morphology. Often no explanation is given for the existence of these cells, or various theories are put forward to justify their presence, yet, it is conceivable that these cells are early-G_1 cells which are just emerging from the telophase. Depending on the mitotic rate, in rapidly growing population with short life cycle time, these early-G_1 cells might represent a greater proportion of cells, and in this case, large numbers of cells would appear with extensively blebbed surface morphology. In slow growing population with long generation time, or in population where most of the cells are quiescent and mitosis is sporadic, the majority of the cells would represent the mid-G_1 phenotype (short microvilli, randomly distributed) and the "odd" bleby, early-G_1 phenotype would be seen only occasionally.

Alternatively, or parallel to what has been suggested above, physiological processes, like the relationship between the ring-patch-cap transition phenomenon, cell surface villous control (Loor, 1975), and other processes not yet identified, may be reflected in the range of morphology seen in lymphoid cells. These variations in morphology may also be due to the state of activity of any cell, i.e., whether it has recently contacted other cells or antigen-antibody complexes or is undergoing differentiation.

One of the most interesting observations made during the course of this morphological study, was that these virally transformed lymphoblastoid

cells (FL74) grown in suspension culture, in many instances, showed cell cycle-dependent surface changes similar to those reported by Porter et al., (1973) and Hale et al., (1975) on monolayer cells. Such changes include the following :- the presence of blebs on the early-G_1 cells; the disappearance of blebs and the prevalence of microvilli in the mid-late G_1 phase; the appearance and behaviour of the long filopodia in the late-G_2 phase and during mitosis.

The above findings may further be analysed in the light of the observations made by Folett and Goldman (1970). According to the latter, the differences between transformed cells and normal cells of an equivalent type are only differences in the degree to which cells exhibit morphological variations. Accordingly, it might not be unreasonable to suggest that cells, normal or transformed, go through a sequence of phenotypic expression which is cell cycle-dependent. Furthermore, it would seem that the morphology of the cell surface is dependent upon cell contact, and that cell-to-cell interactions play an important role even between transformed cells.

It would be interesting to investigate the morphological changes of mitogen-induced, synchronised lymphocytes to see the differences and/or similarities between them and transformed cells during the cell cycle.

Recently, the use of SEM has gained much popularity among haematologists and immunologists. The early reports claimed that this method permitted differentiation of T and B lymphocytes and monocytes. The surface morphology of T cells was reported to be smooth or undulated; the B cells to have mainly villous surfaces, while monocytes were described as having ruffled appearance (Lin et al., 1973; Polliack et al., 1973). However, criticism of the above categorisation soon followed after the discovery that T cells had, similarly to B cells, villous cell surface structures (Alexander and Wetzel, 1975; Belpomme et al., 1975).

A number of studies have been performed to classify normal and pathological human mononuclear leukocytes on the basis of their cell surface morphology (Lin et al., 1973; Polliack et al., 1973). It has also been suggested that the different morphological types based on SEM should only be interpreted by comparison with the corresponding immunological membrane phenotypes (Belpomme et al., 1976; Dantchev and Belpomme, 1977). Following this line, morphological and immunological studies have been carried out by Dantchev and Belpomme (1977) and several main morphological types of normal and pathologic mononuclear cells have been described, such as, smooth, undulated, villous, ruffled and bleby. Although in the majority of B cell disorders investigated, cell surfaces were found to be villous or bleby, in many other leukaemias and lymphomas the correlation between immunological findings and cell surface structure could not be established. However, cells in hairy cell leukaemias and in the Sezary syndrome appear to have characteristic morphology and it has been demonstrated that SEM can be used as an adjunct in the diagnosis of hairy cell leukaemia (de Harven et al., 1978).

Interestingly, in the present study, synchronised FL74 cells exhibited all the cell surface variations which were described by Dantchev and Belpomme (1977) and the morphological changes observed were highly cell cycle specific. Therefore, it is possible that the prevalence of one morphological type in a certain leukaemic population reflects the position of the cells in the cell cycle. Similarly, the heterogeneity of cells in many disorders can also be explained by cell cycle dependent variations in the cell surface structure, although morphological changes may be associated with other processes as well, i.e., whether the cells have recently contacted other cells or antigen-antibody complexes or are undergoing differentiation.

The role of the scanning electron microscope in the biological sciences is now well established. Its application has enabled valuable information to be gained in a variety of fields. Further improvements in the resolving power of the SEM, in coating and preparative techniques, and the use of X-ray analysis and of small markers, such as ferritin, may lead to a better understanding of the changing nature of the lymphocyte surface structure in response to physiological events or abnormal states.

TABLE 13

Changes in Morphology of FL74 Cells during the Cell Cycle

Phases of the Cell Cycle

Cell Characteristics	Early G_1	Mid-Late G_1	Early S	Late S	G_2	Prophase Meta-Anaphase Telophase — Mitosis —		
Cell diameter in μm.	7.8 - 8.2	8.2 - 8.5	8.5 - 11.2	11.2 - 12.0	12.0 - 13.5			
Cell surface features	Extensively blebbed. Blebs are empty or filled with cytoplasm 0.5 - 2.0 μm in diameter.	No blebs, few microvilli in various density and length. In static cultures complete exfoliation	Smooth, undulated surface, few villi, small ruffles	Wavy surface. Prominent marginal ruffling. Ruffles are 10 - 12 μm in length	Ruffles, few blebs. Appearance of long filopodia	Many filopodia, blebs and ruffles		Few large cytoplasm filled blebs
Cytoplasmic organelles	Few	Variable	Abundant →					Few
Nuclear shape	Round →			Indented or folded →				Round
Nuclear chromatin	Dispersed →			Dispersed with clumps	Size of clumps increased	Aggregated into large clumps		Condensed alongside the nuclear membrane
Nucleolar shape	Round →			Irregular	Large, flattened			Round
Nucleolar position	Central →		Peripheral →				Absent	Peripheral
Nucleolus associated chromatin	Adjacent, not penetrating the nucleolus	Decreased	Attached with some penetration of the nucleolus	Surrounding and penetrating the nucleolus →				
Dense fibrillar component	Small amount	Multiple small foci	Moderate amount	Prominent →				Small amount
Granular component	Small amount	Abundant	Moderate amount	Not prominent →				Small amount

FIGURE 8 : TdR-synchronised cells soon after division. The cell surface is covered with blebs of many sizes.

SEM x 5,000

FIGURE 9 : Early-G_1 phase cell. The nucleus is round with dispersed chromatin. The components of the nucleoli are segregated and have a characteristic ring-shaped appearance. On the cell membrane numerous budding C-type particles can be seen.

TEM x 5,000

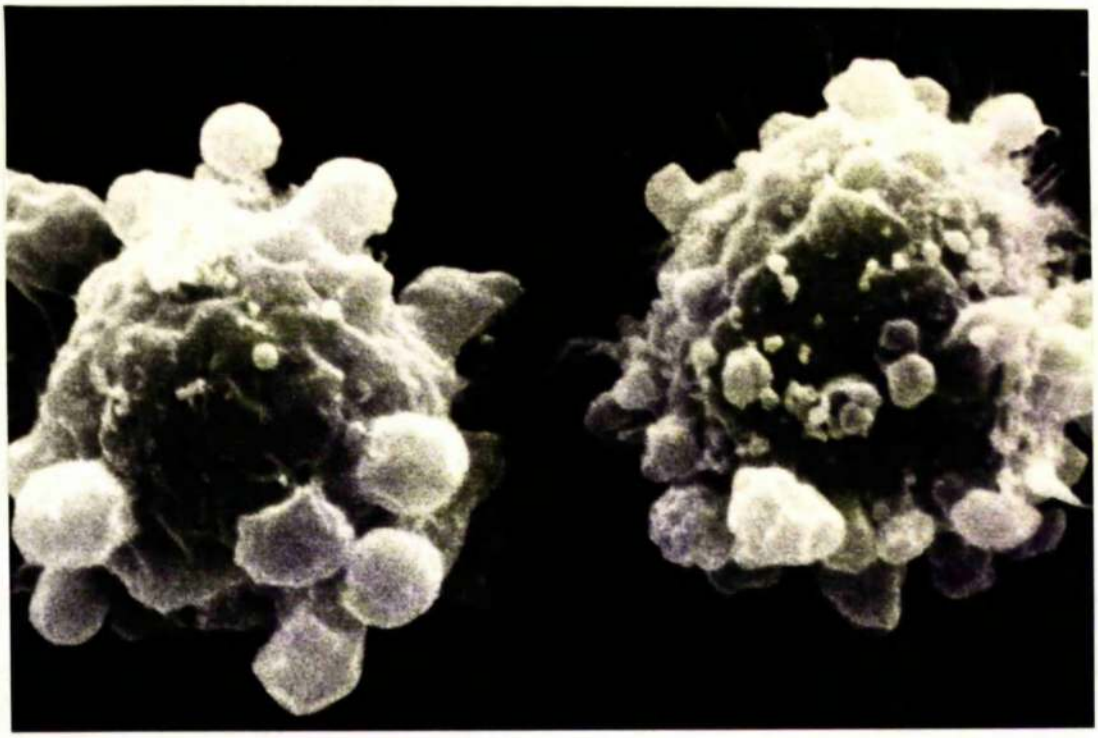

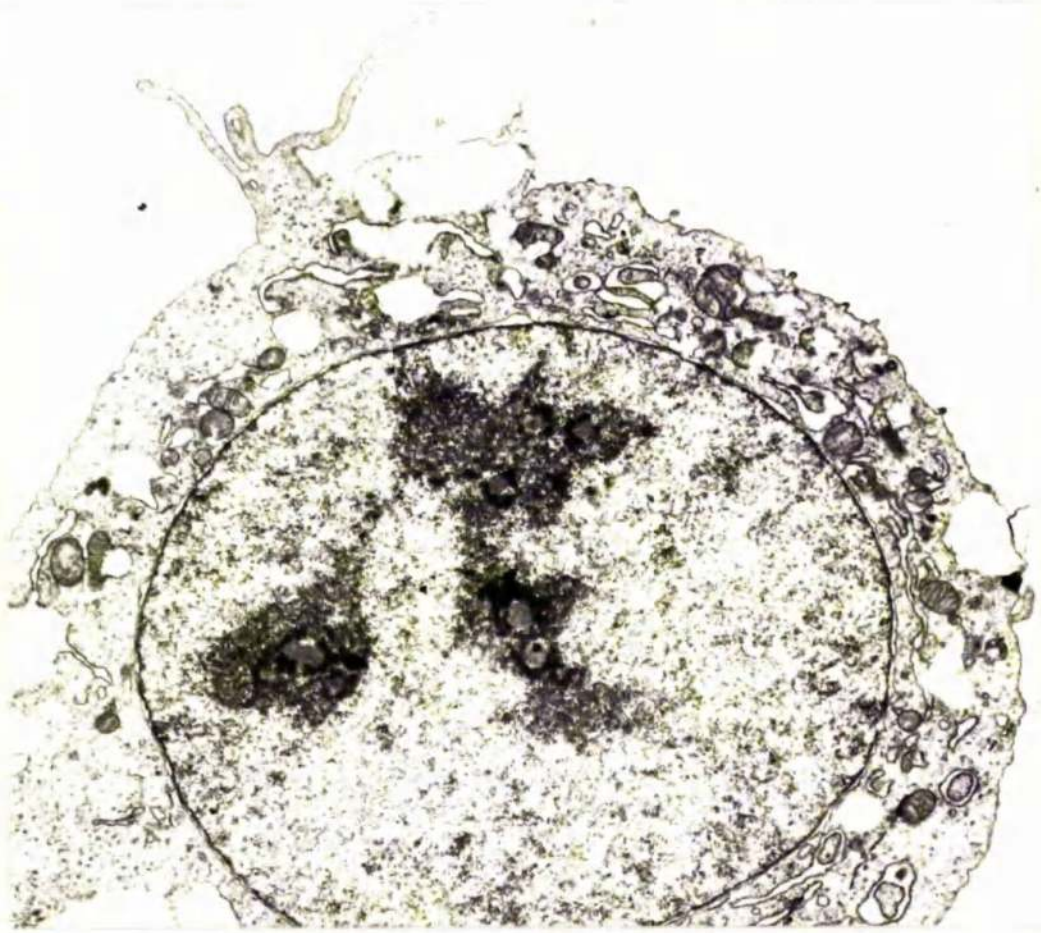

FIGURE 10 : Spheres and elongated bodies which have broken away during cytokinesis are shown among early-G_1 cells.

TEM x 7,500

FIGURE 11 : A membraneous type of bleb is shown. Note the number of small vesicles at the base of the bleb.

TEM x 16,000

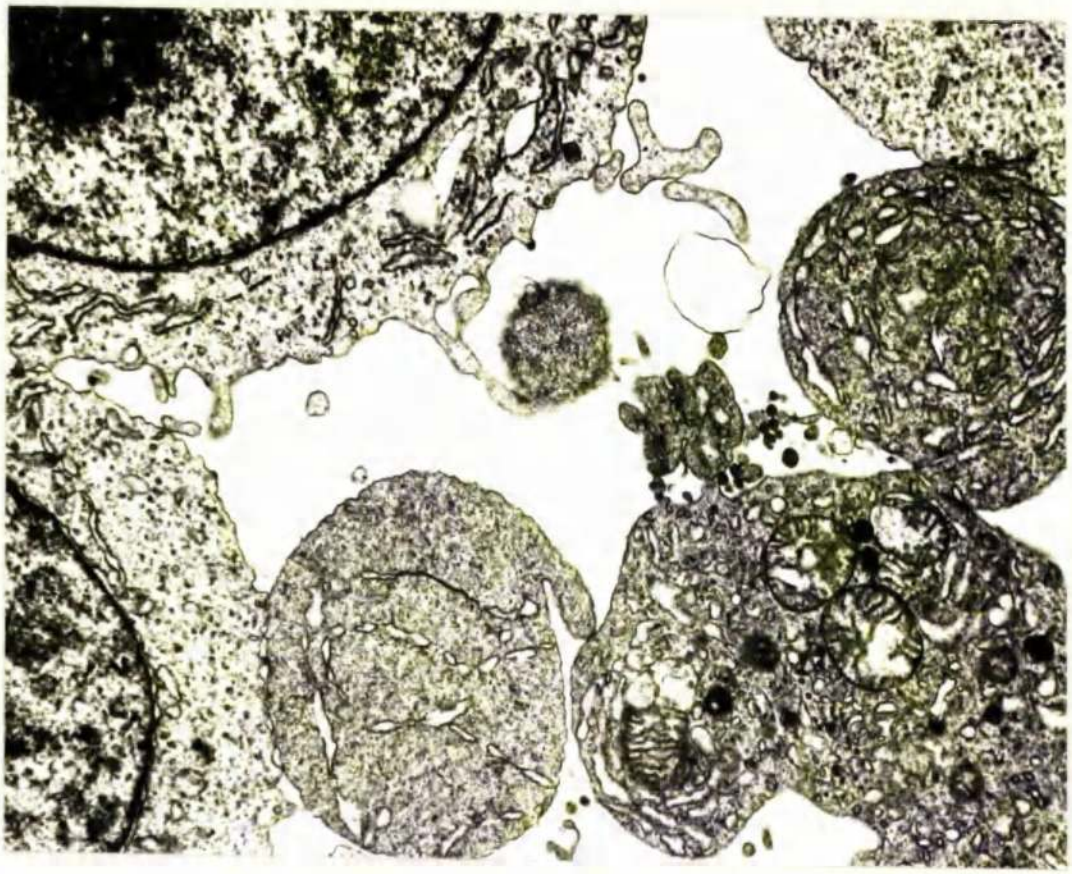

FIGURE 12 : Early - mid - G_1 phase. Daughter cells in contact.

SEM x 5,000

FIGURE 13 : Early- mid - G_1 phase cell. The shape of the cell indicates that it is one of the daughter cells shown in Fig. 12. Round, cytoplasm-filled blebs can also be seen some of which, on the upper right hand side, are shed off.

TEM x 7,500

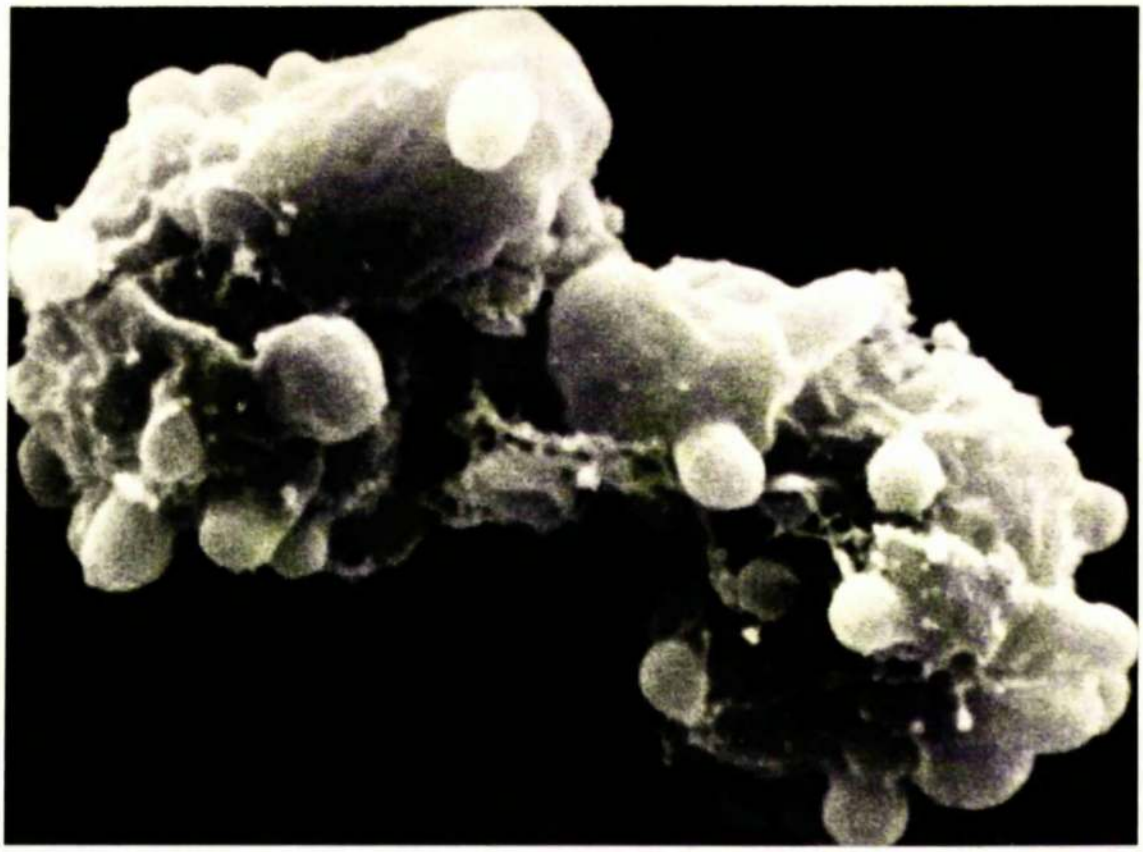

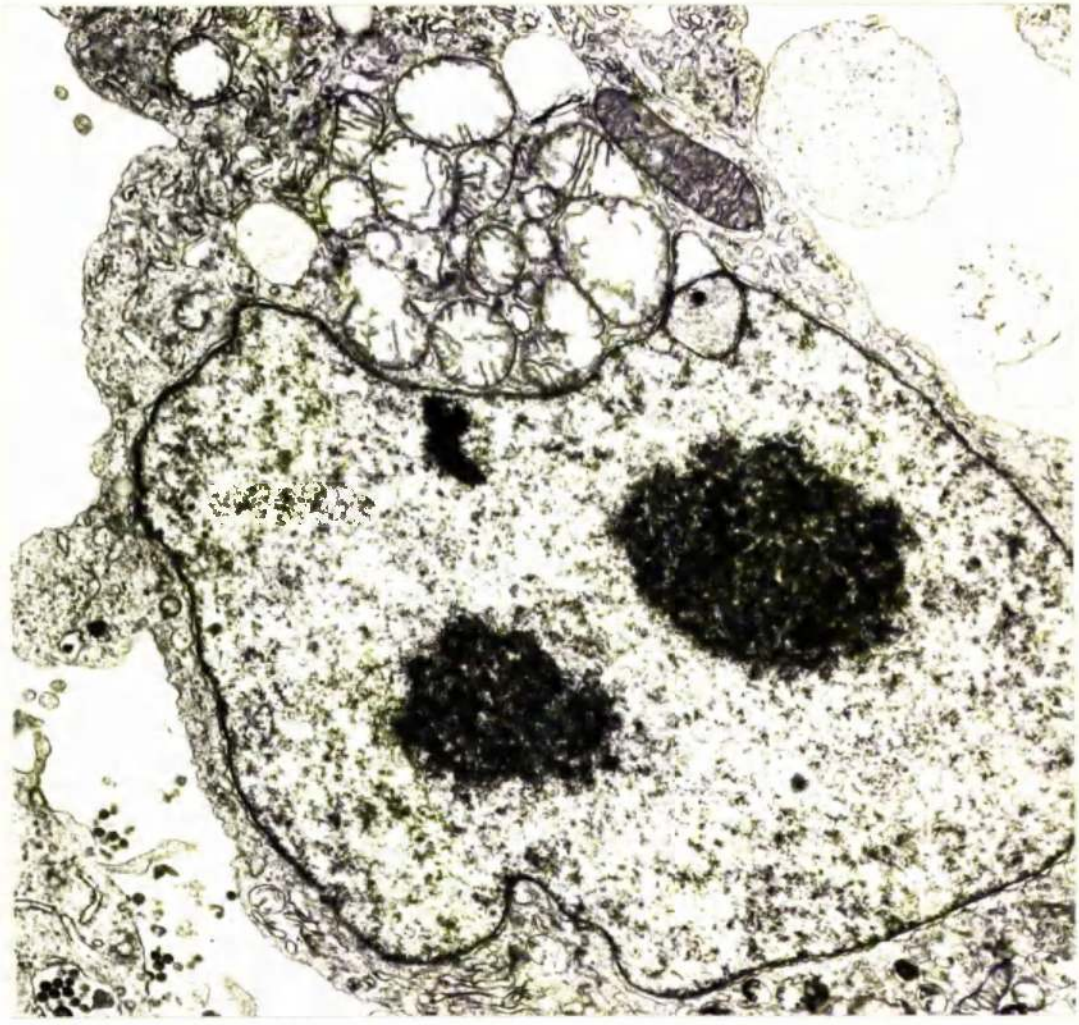

FIGURE 14 : Early - G_1 phase-cell with large blebs, microvilli and numerous budding C-type particles (arrows).

SEM x 5,000

FIGURE 15 : Early - G_1 phase - cell with cell surface protrusions which correspond to the blebs of Fig. 14. On the right hand side, a number of budding and type-1 virions can be seen.

TEM x 7,500

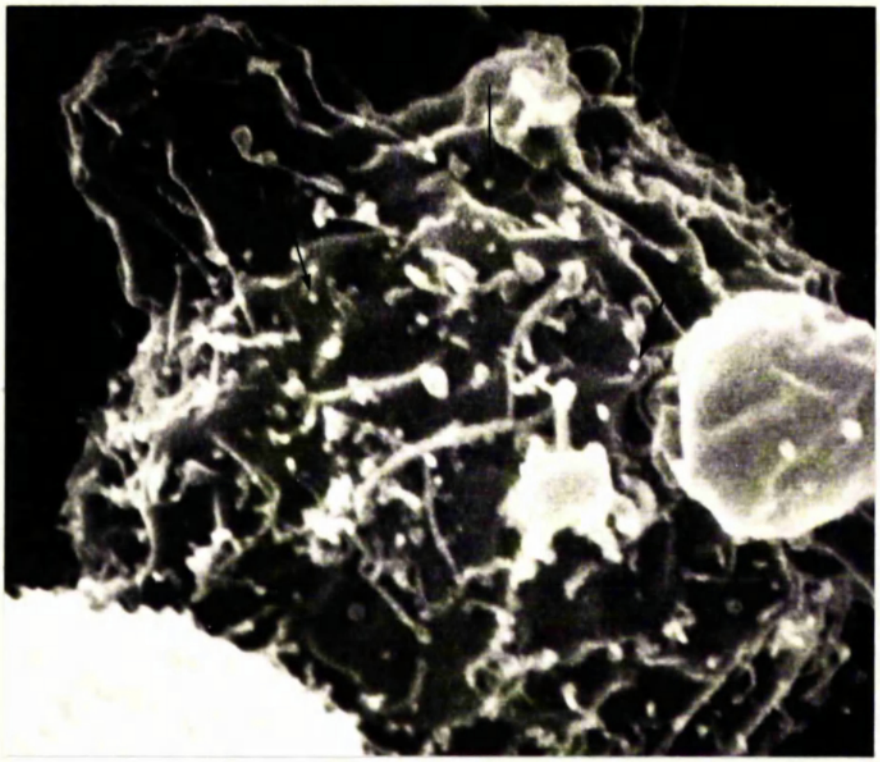

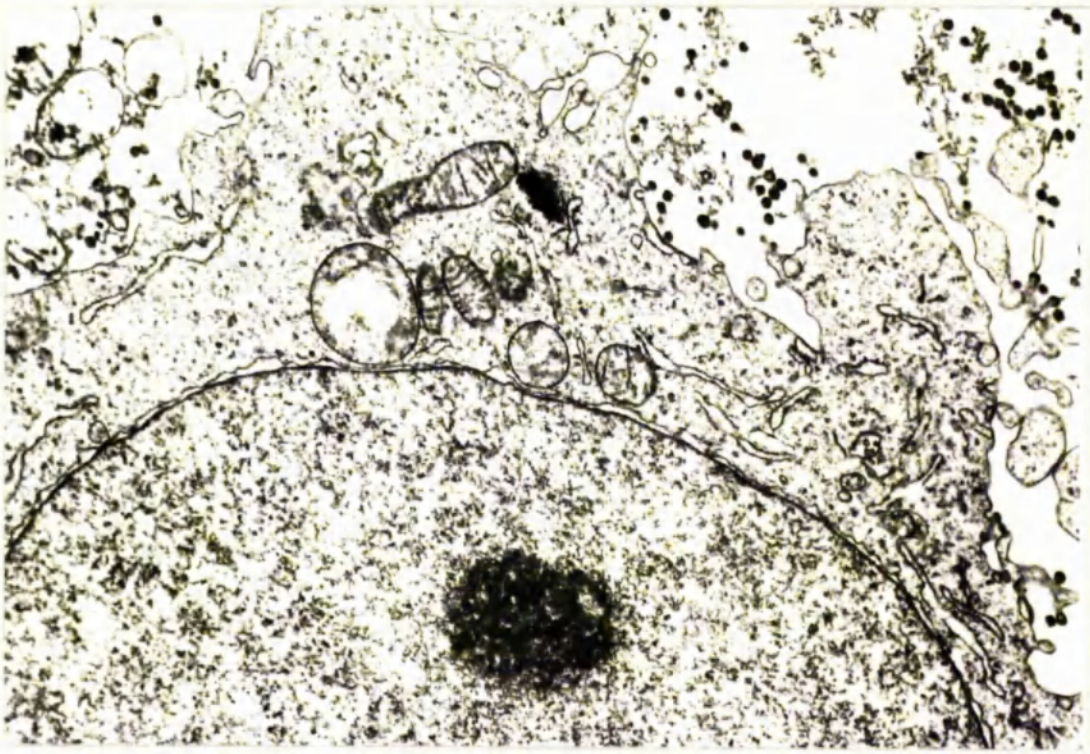

FIGURE 16 : High-power electronmicrograph of an early - mid- G_1 - cell. It is covered with microvilli, small blebs and budding virions (arrows).

SEM x 10,000

FIGURE 17 : High-power electronmicrograph of an early - mid-G_1 - cell. The structure of the cell surface is similar to that in Fig. 16 with long microvilli and budding virions.

TEM x 20,000

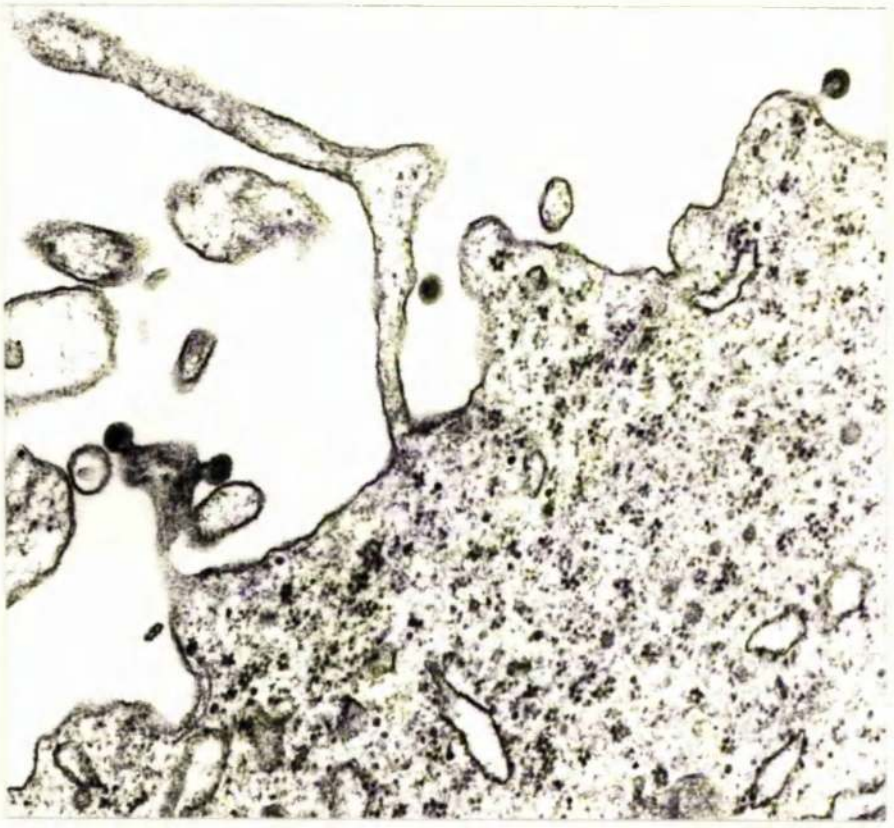

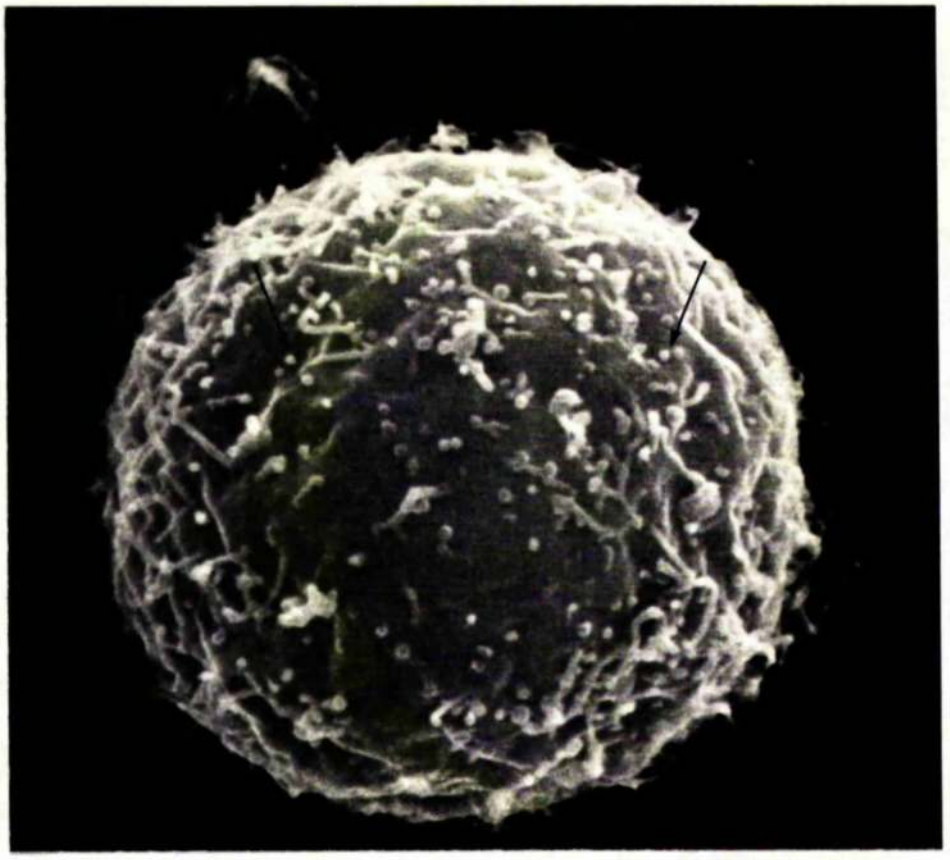

FIGURE 18 : Early - mid - G_1 - cell synchronised by cold treatment. In contrast to TdR-synchronisation, no blebs are present. Note the large number of budding virions (arrows).

SEM x 5,000

FIGURE 19 : Mid - G_1 phase - cell with spherical bodies resulting in the shedding off of blebs. See also Fig. 20.

SEM x 5,000

FIGURE 20 : Shed off blebs among mid - G_1 - cells.

TEM x 7,500

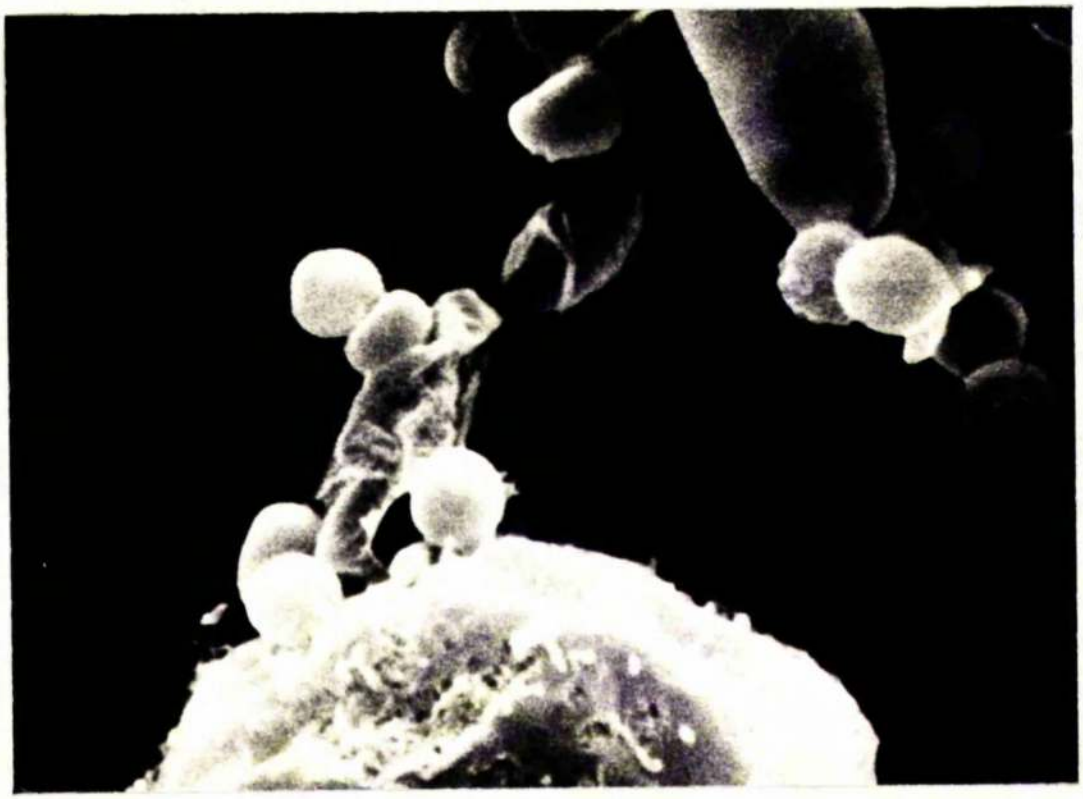

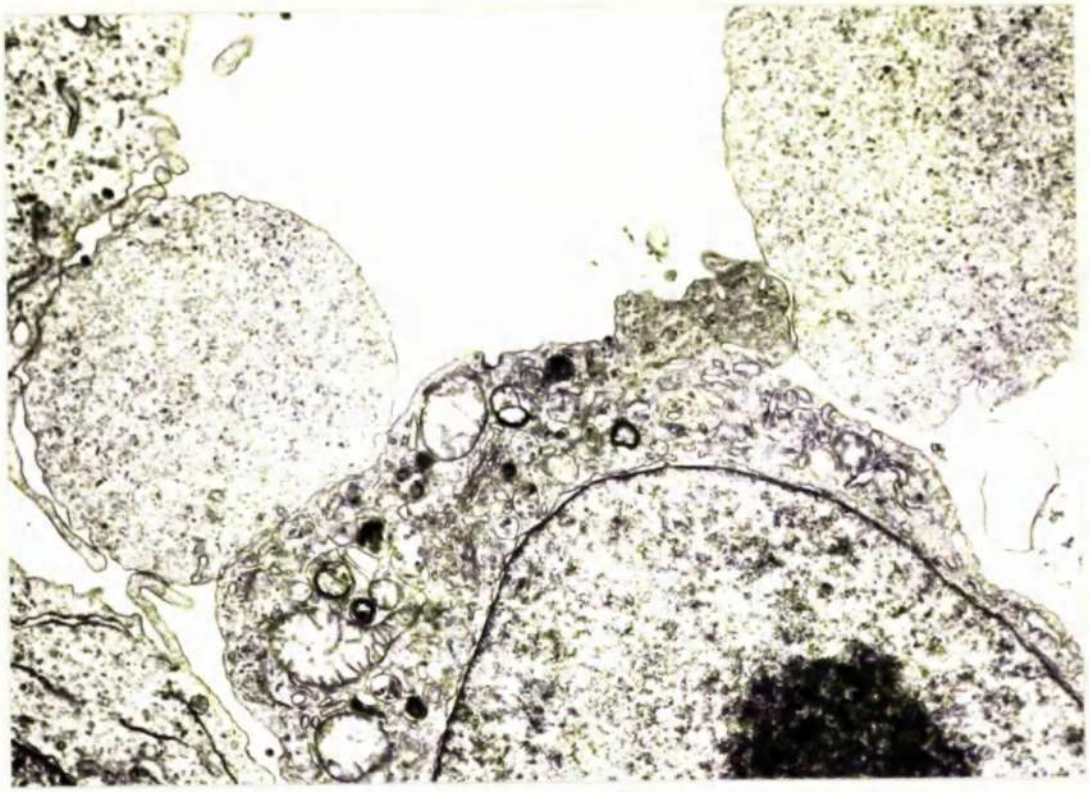

FIGURE 21 : Mid - G_1 phase-cell. The cell surface is almost free of blebs and covered with short stub-like and long microvilli.

SEM x 5,000

FIGURE 22 : Mid - G_1 phase- cell. The nucleus is round with dispersed chromatin. The centrally located nucleolus is well segregated.

TEM x 5,000

FIGURE 23 : Mid - G_1 phase-nucleolus. At high power, the predominant granular component (g) of the nucleolus is shown.

TEM x 20,000

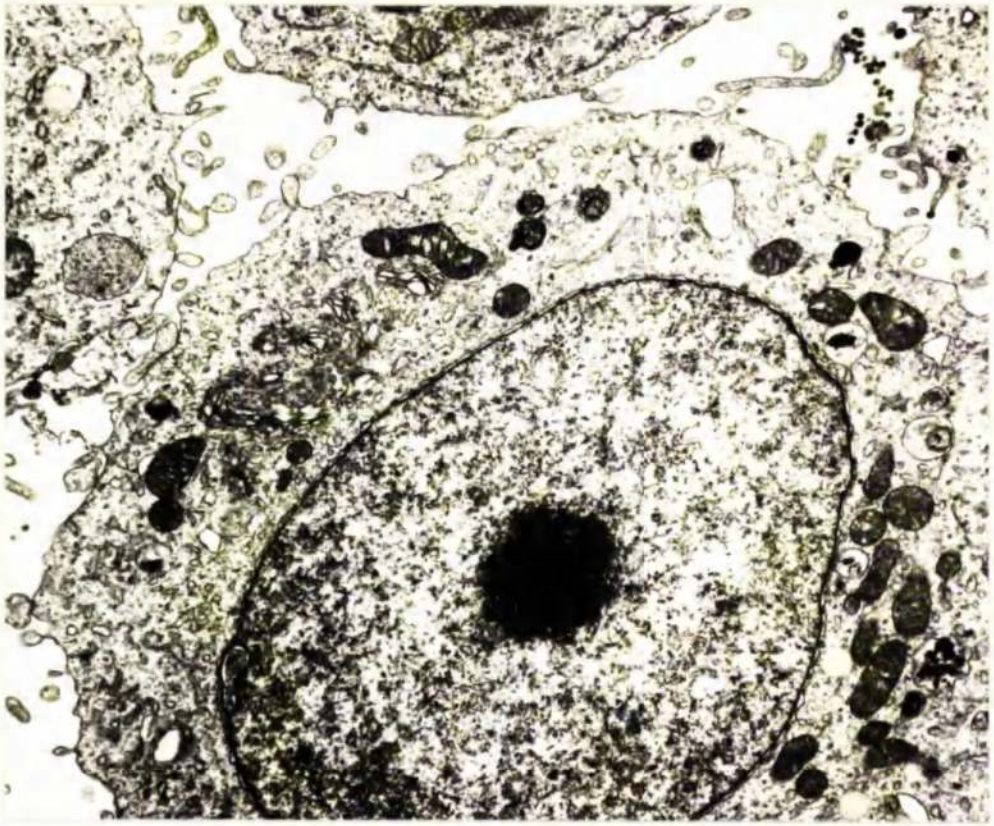

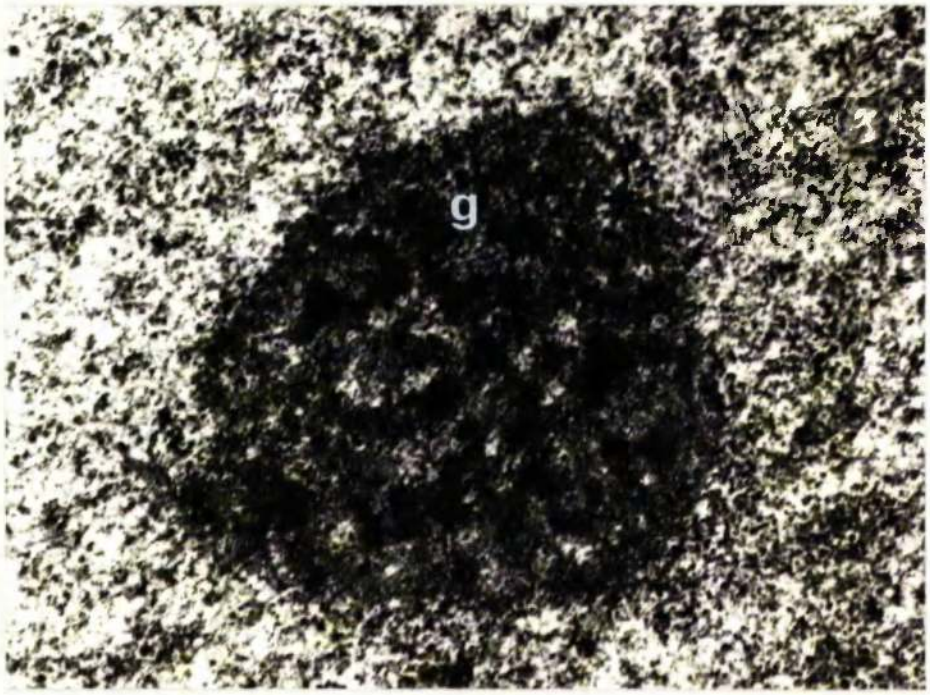
g

FIGURE 24 : Late - G_1 phase - cell. The nucleus is slightly indented. The cytoplasm facing the nuclear indentation contains the Golgi apparatus, centrioles and many of the cytoplasmic organelles. The centrally located nucleolus is well segregated.

TEM x 7,500.

FIGURE 25 : Late - G_1 phase - nucleolus. The granular component is the predominant nucleolar constituent. The paucity of nucleolus associated chromatin is shown (arrows).

TEM x 20,000

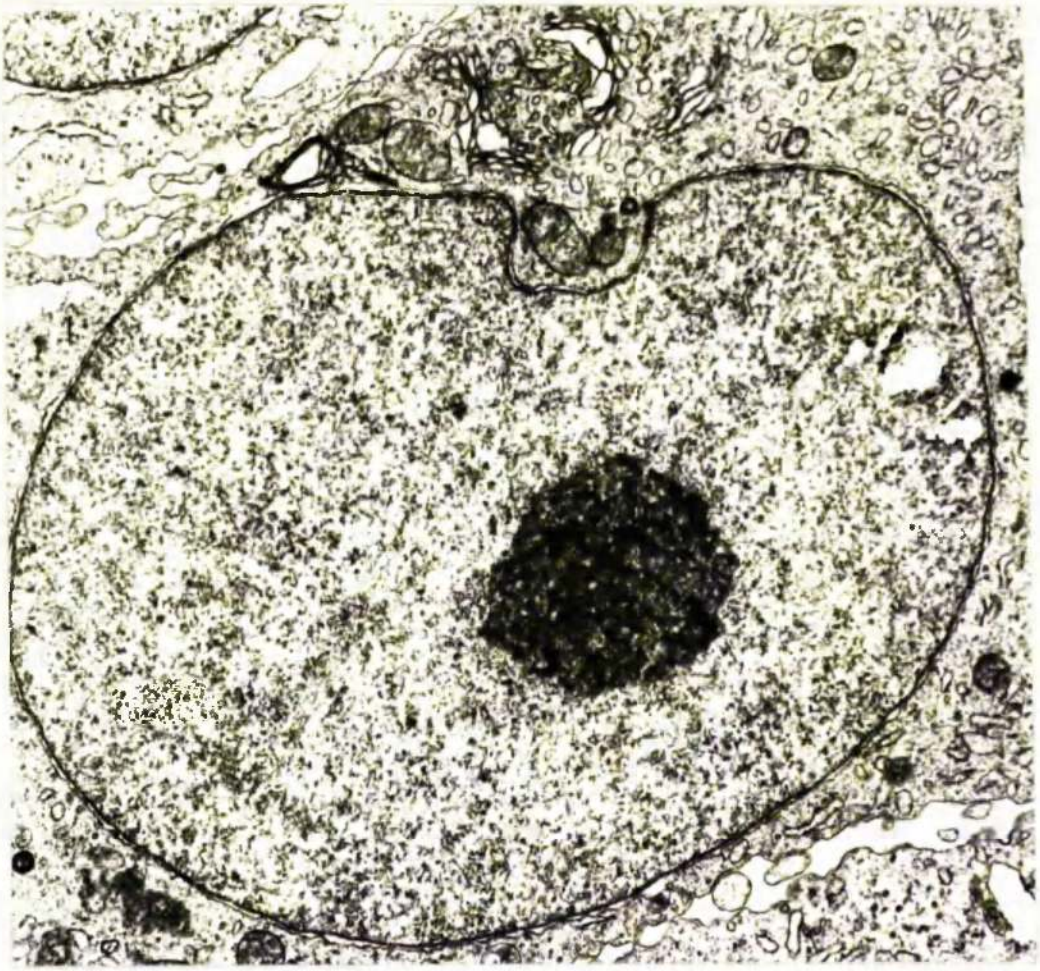


g

FIGURE 26 : Cell from stationary culture. Shed off surface material is shown.

SEM x 5,000

FIGURE 27 : Membraneous and cytoplasm-filled cell surface features shed off from stationary cells.

TEM x 7,500

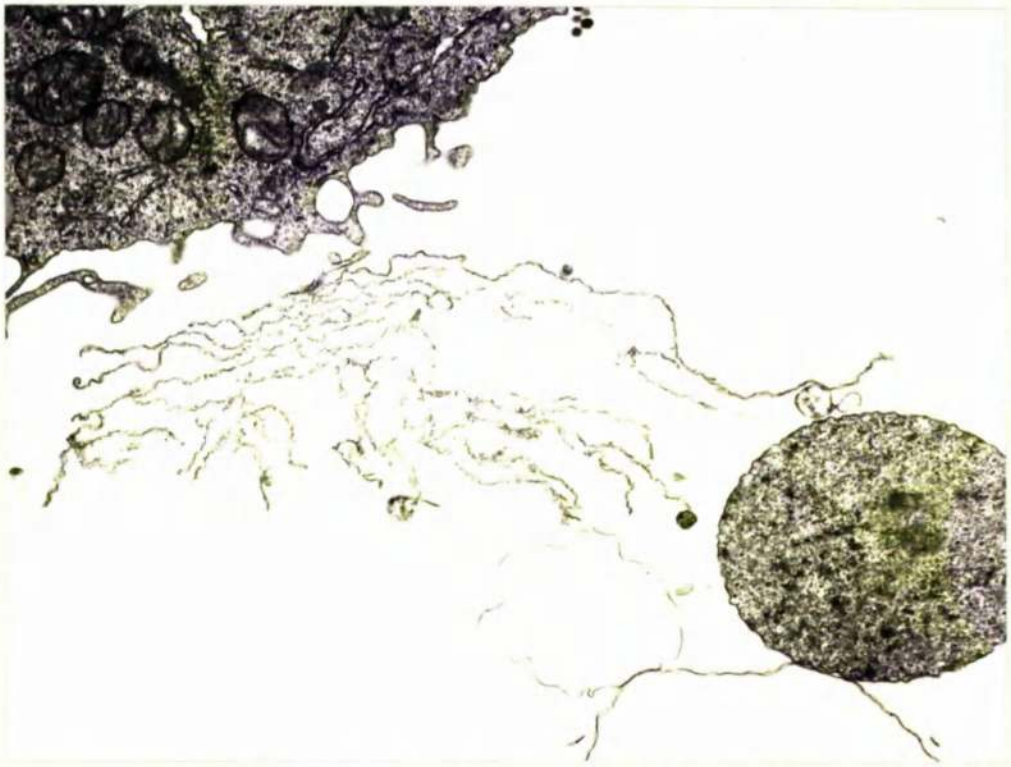

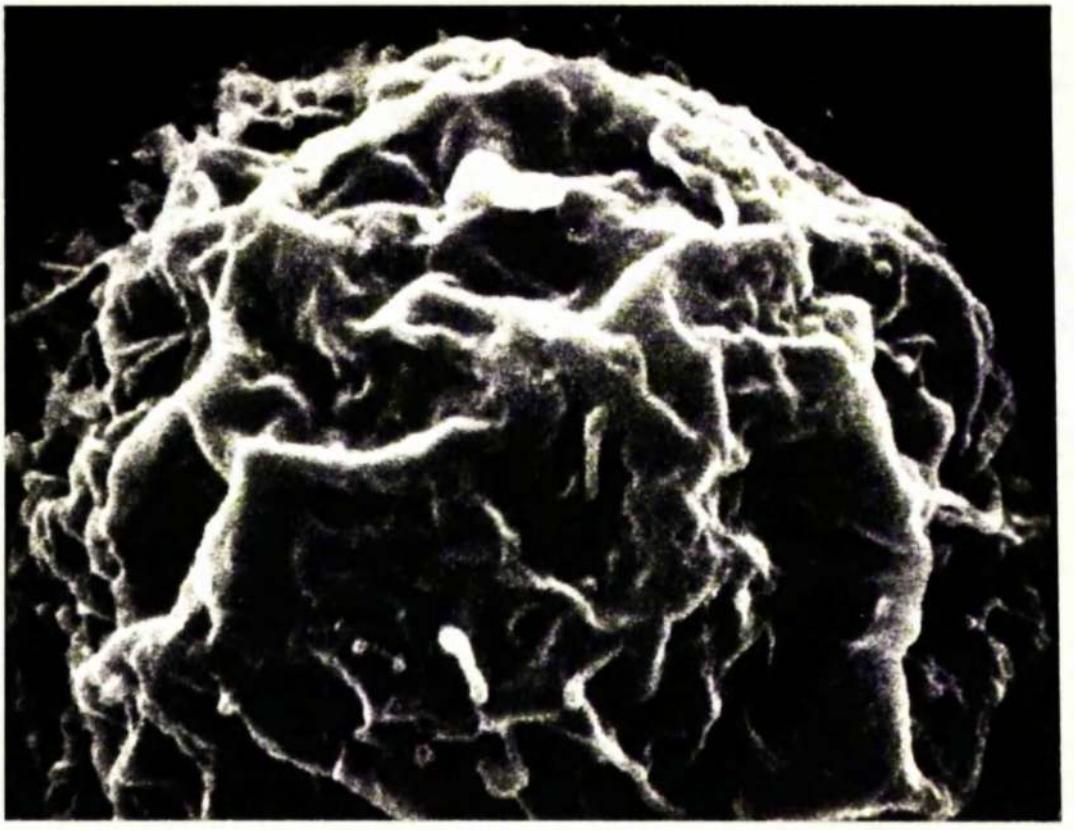

FIGURE 28 : Stationary culture "nude-cell" with deep indentations in its body and without any surface protrusions.

SEM x 10,000

FIGURE 29 : Cell immediately after release from the second TdR block. The cell surface is undulated and only a few short microvilli are present.

SEM x 5,000

FIGURE 30 : Early - S phase. The surface of the cells are more elaborate than the cell shown in Fig. 29.

SEM x 2,500

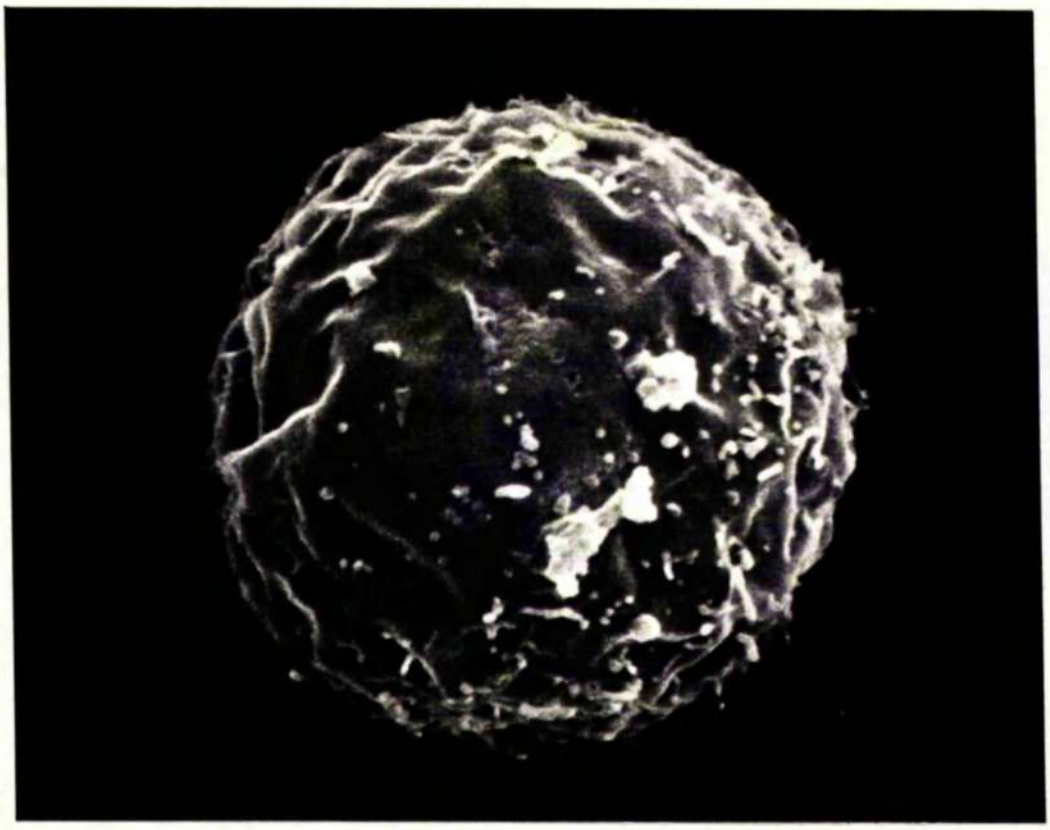

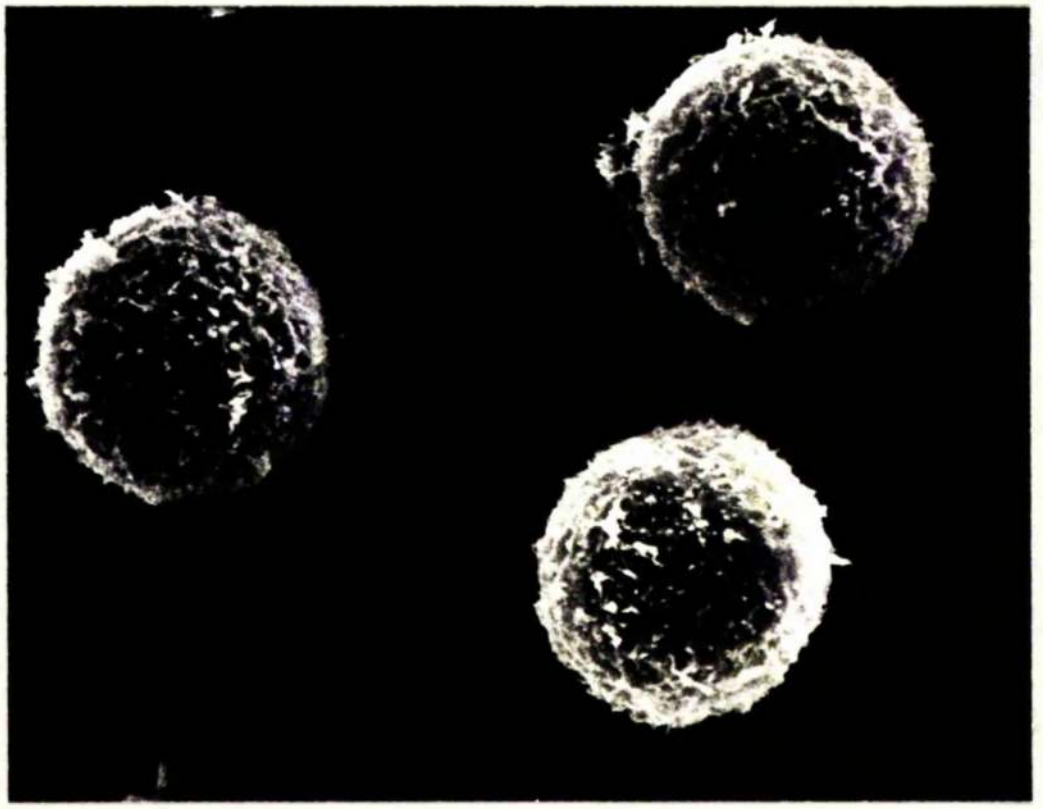

FIGURE 31 : Early - S phase - cell. The nucleus is indented with dispersed chromatin. The eccentric nucleolus is large and round.

TEM x 7,500

FIGURE 32 : Early - S - nucleolus containing moderate amounts of granular (g) and dense fibrillar (f) material. The perinucleolar chromatin is intimately associated with the nucleolus (arrows).

TEM x 20,000

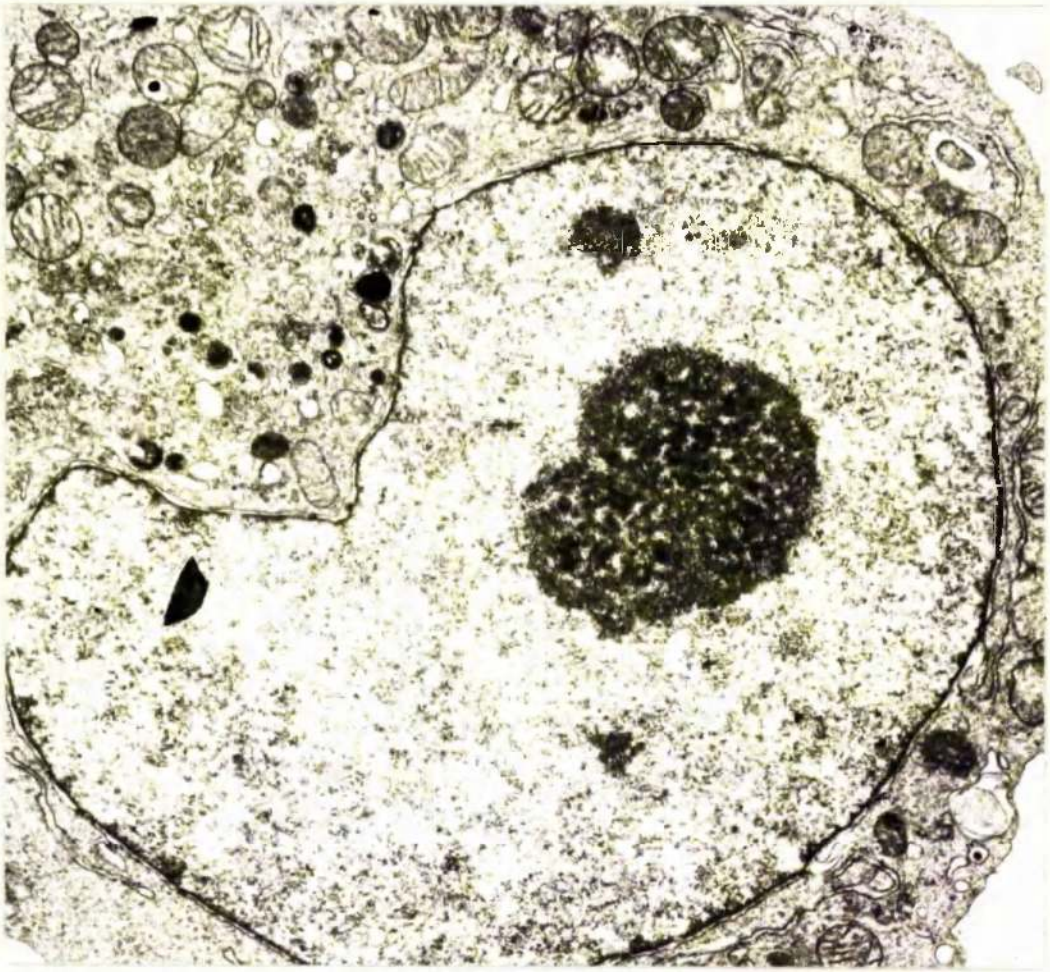

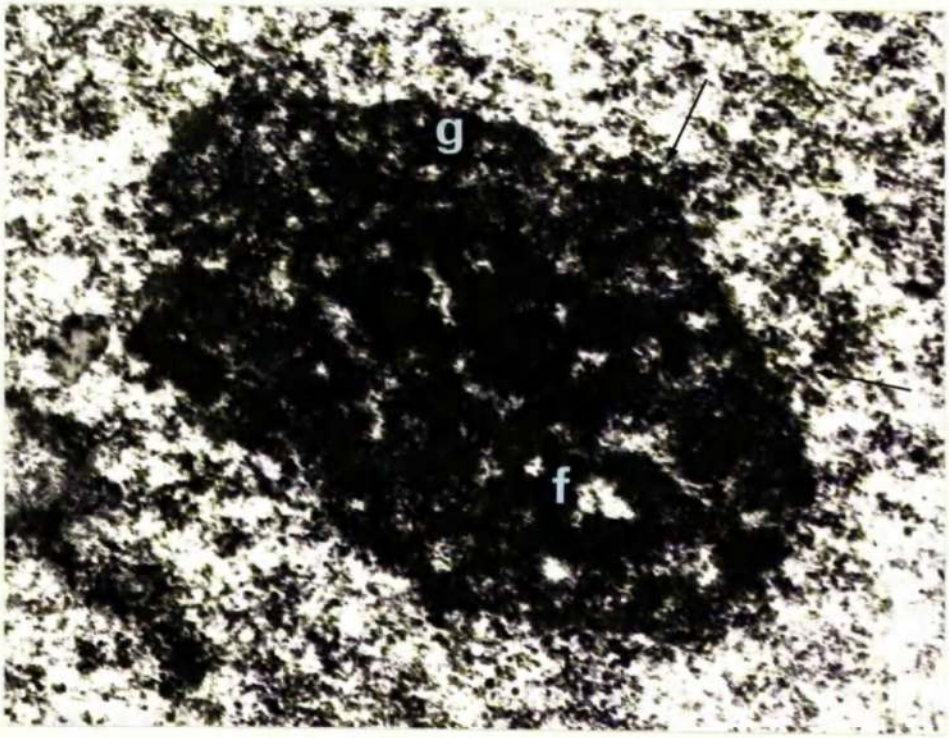
g
f

FIGURE 33 : Mid - S phase- cell. A thin fold of the cell membrane called ruffle or lamellipodium is shown on the free edge of the cell.

SEM x 10,000

FIGURE 34 : Mid - S phase - cell with ruffle. At the base of the ruffle a number of vesicles can be seen.

TEM x 16,000

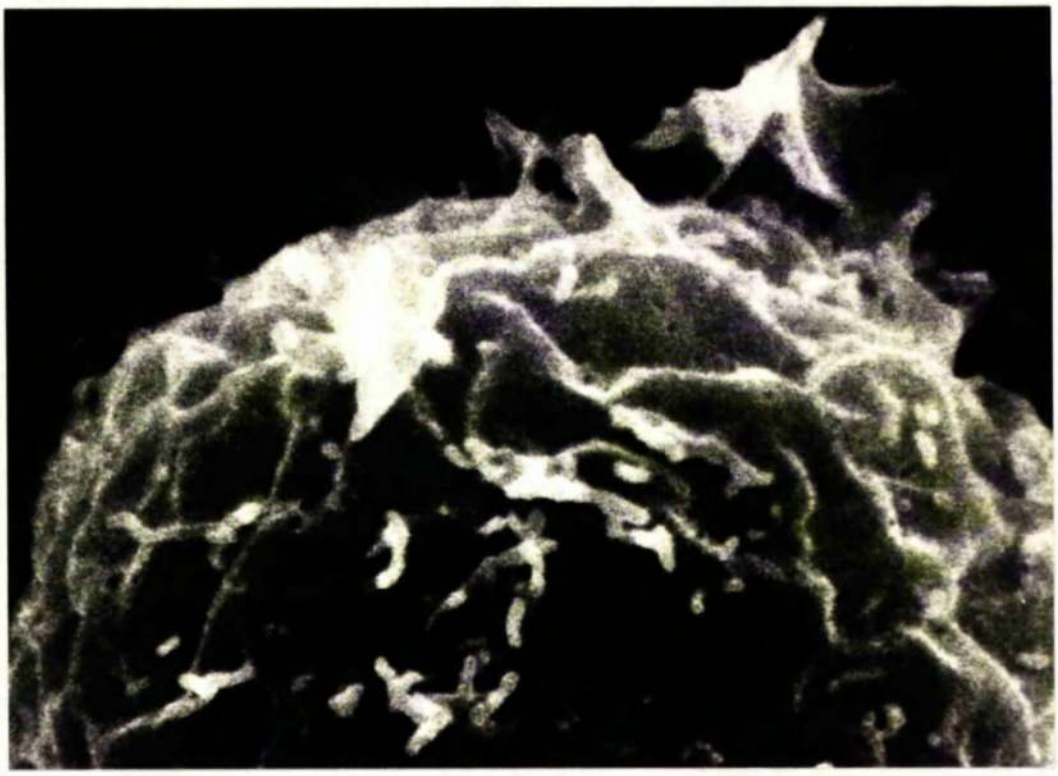

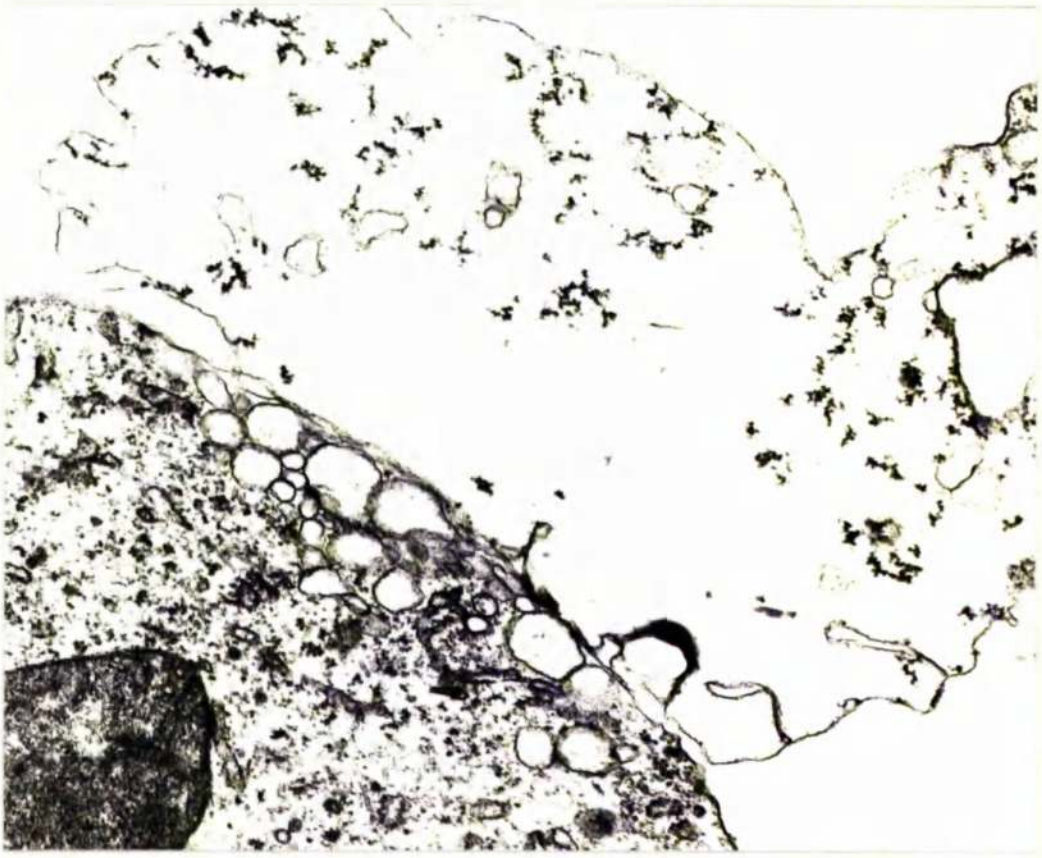

FIGURE 35 : Late - S phase - cell with a number of medium sized ruffles.

SEM x 5,000

FIGURE 36 : Ruffle-formation. Small vesicles fusing to form larger ones. The cytoplasm, containing mainly ribosomes, is seen extending into the membraneous fold.

TEM x 6,300

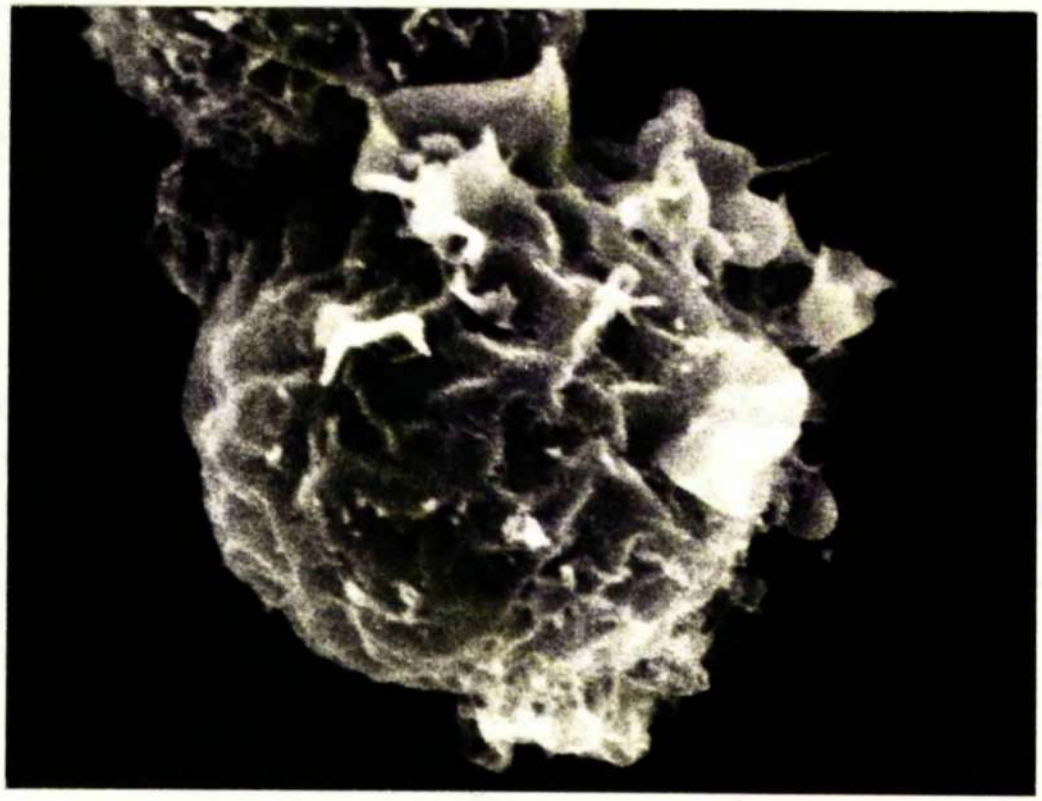

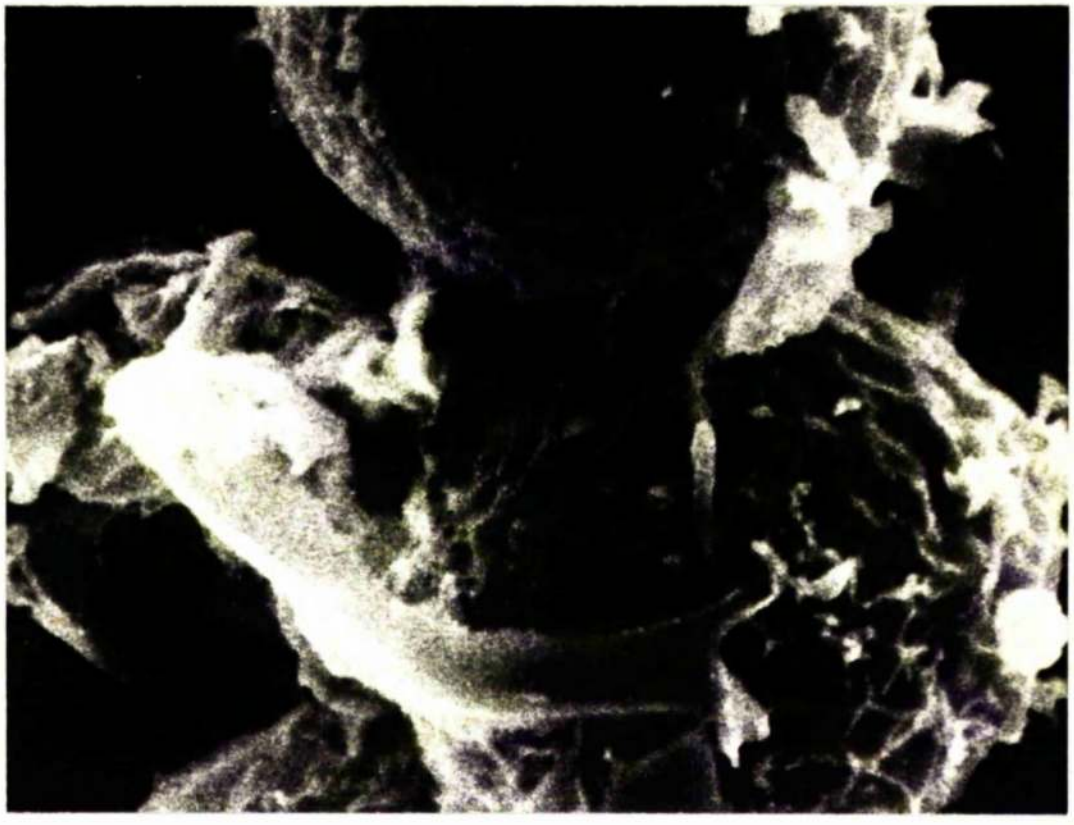

FIGURE 37 : A group of cells with cell-to-cell contact provided by ruffles. On the left hand side, a very large ruffle can be seen.

SEM x 5,000

FIGURE 38 : Mid - S phase - cell. The nucleus is indented with dispersed chromatin. Euchromatin extends to the nuclear pores. This cell has an atypically centrally located nucleolus. The cytoplasm is abundant and the Golgi region is very prominent.

TEM x 7,500

FIGURE 39 : Mid - S phase nucleolus with prominent, dense, fibrillar material (f). It is surrounded and penetrated by perinucleolar chromatin (arrows).

TEM x 20,000

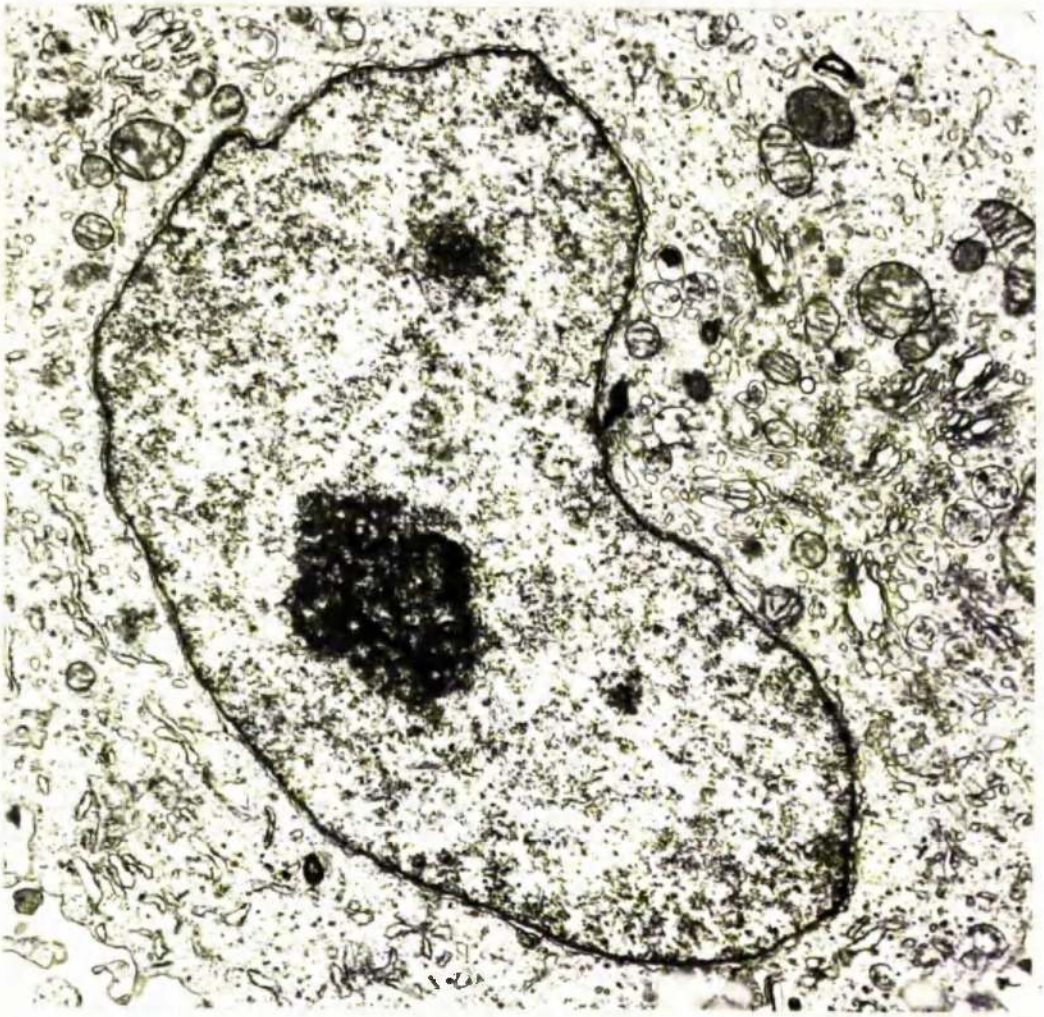

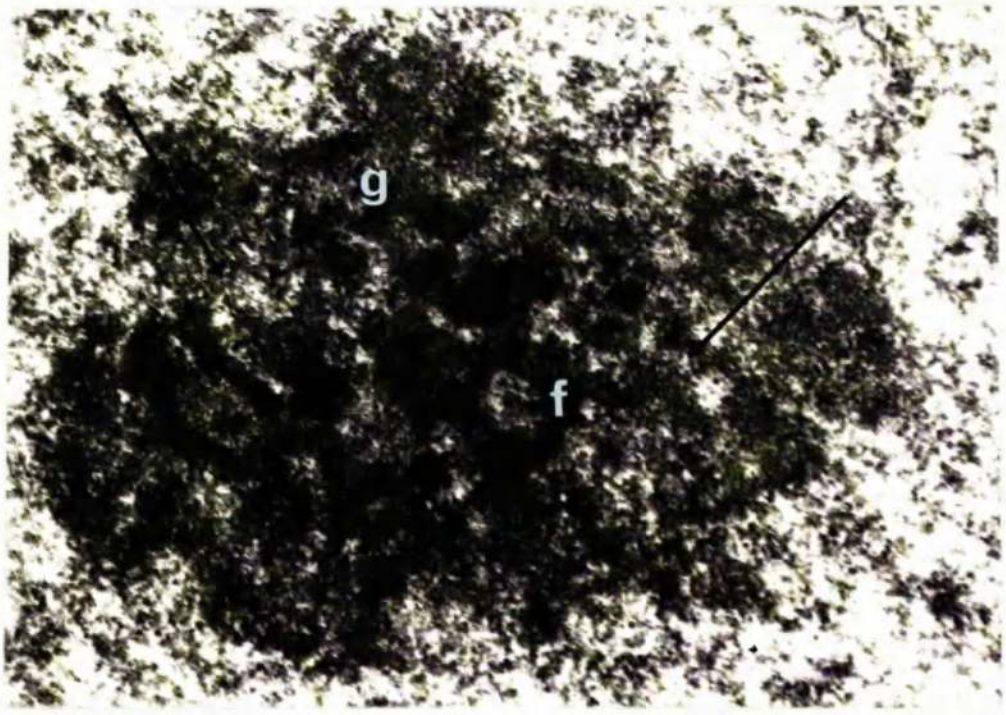
g
f

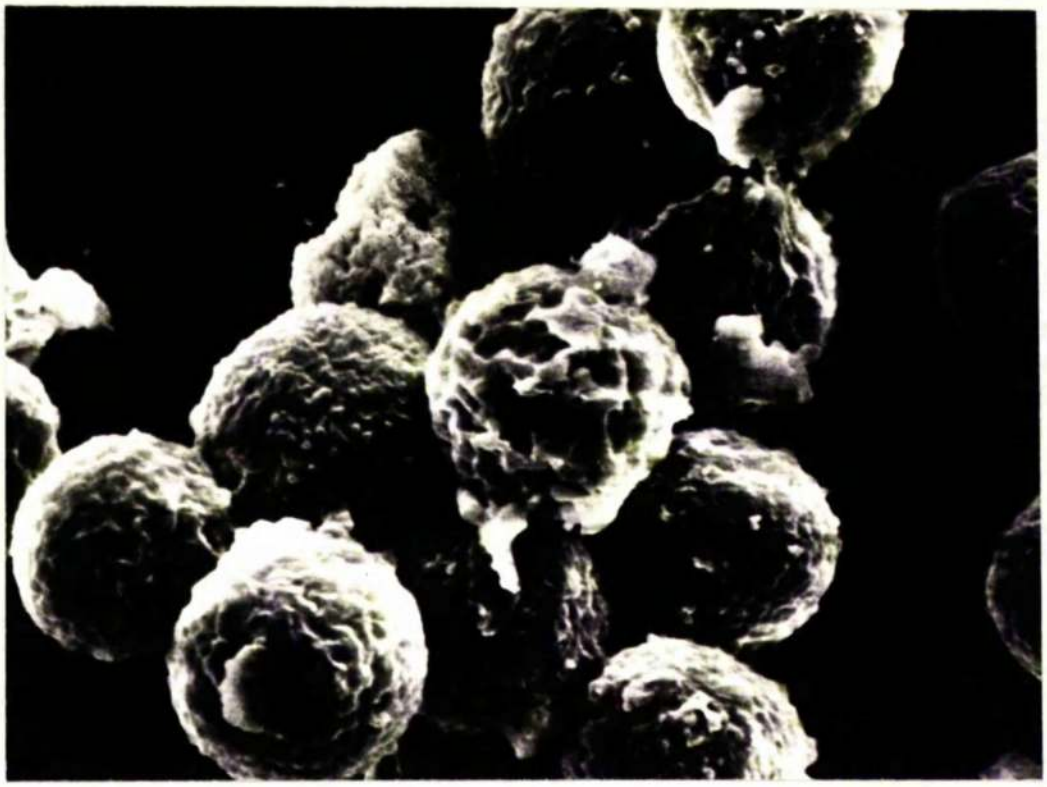

FIGURE 40 : Group of late - S phase - cells with very wavy and ruffled surfaces. The cell, in the middle, has characteristic ridge-like profiles.

SEM x 2,500

FIGURE 41 : Late - S phase - nucleolus which has a trabecular appearance. It is penetrated by perinucleolar chromatin (arrows).

TEM x 20,000

FIGURE 42 : High-power electronmicrograph of a prominent Golgi region characteristic of S- and G_2 - cells.

TEM x 20,000

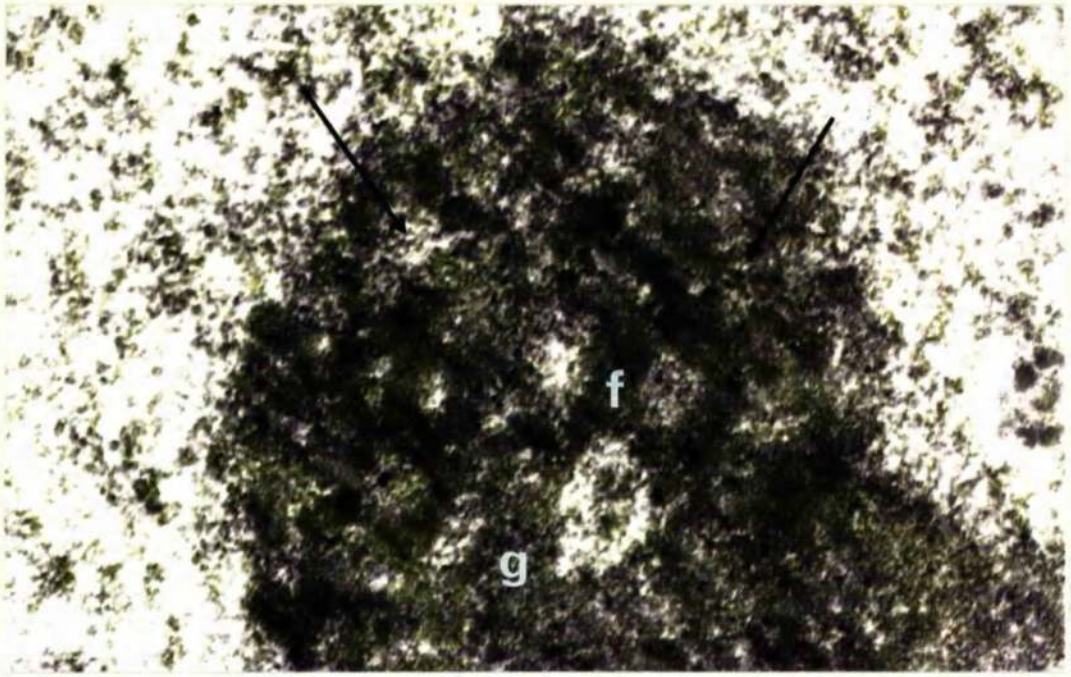
f
g

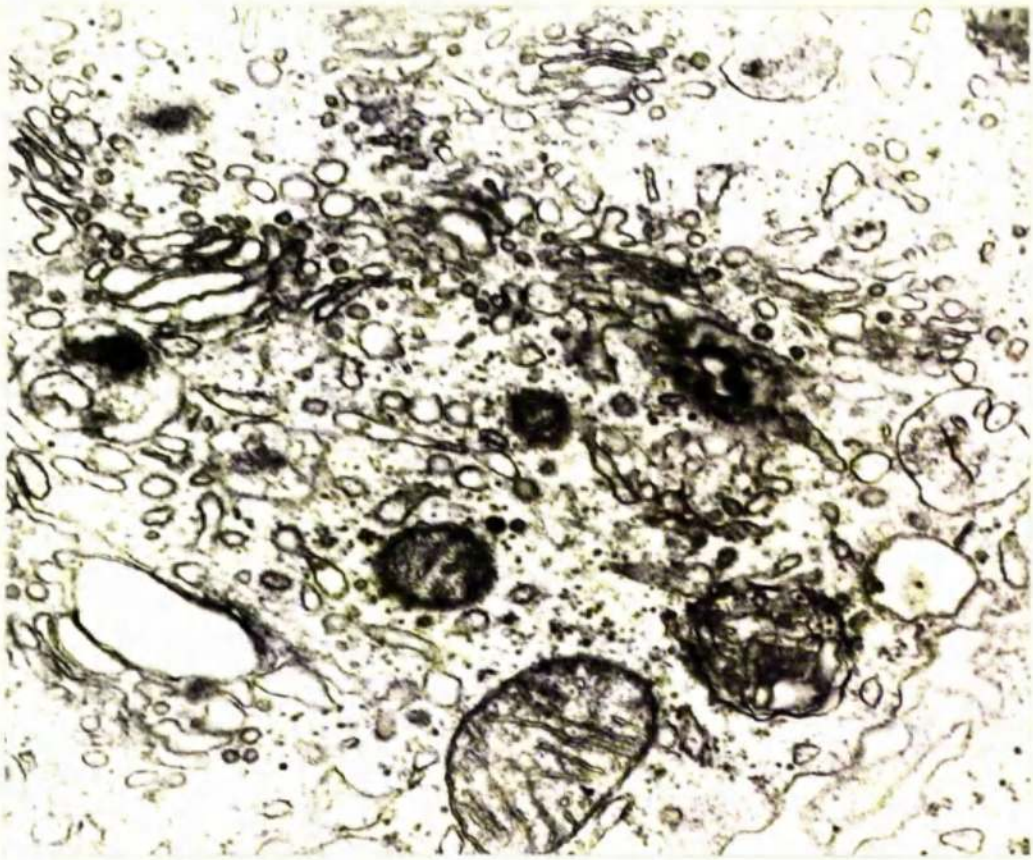

FIGURE 43 : Early -G_2 phase- cells. The shape and the size of the ruffles are characteristic of this phase.

SEM x 2,500

FIGURE 44 : A G_2 phase - cell, on the left hand side, with an elaborate surface structure. It is covered with microvilli, small blebs and large ruffles. Cell-to-cell contact is made by the extensive surface projections.

SEM x 2,500

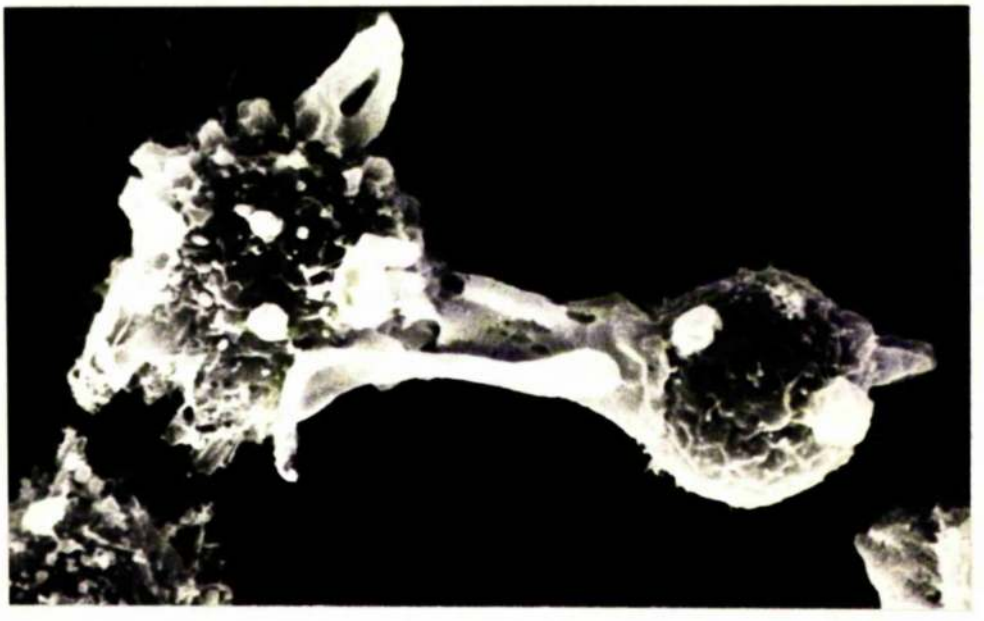

FIGURE 45 : Late - G_2 phase-cell. The cytoplasm is abundant and the Golgi apparatus is very prominent. The nucleus is folded with nuclear chromatin aggregated into small clumps. The eccentric nucleolus is large and has a flattened appearance.

TEM x 7,500

FIGURE 46 : G_2 phase - nucleolus infiltrated throughout with perinucleolar chromatin (arrows).

TEM x 20,000

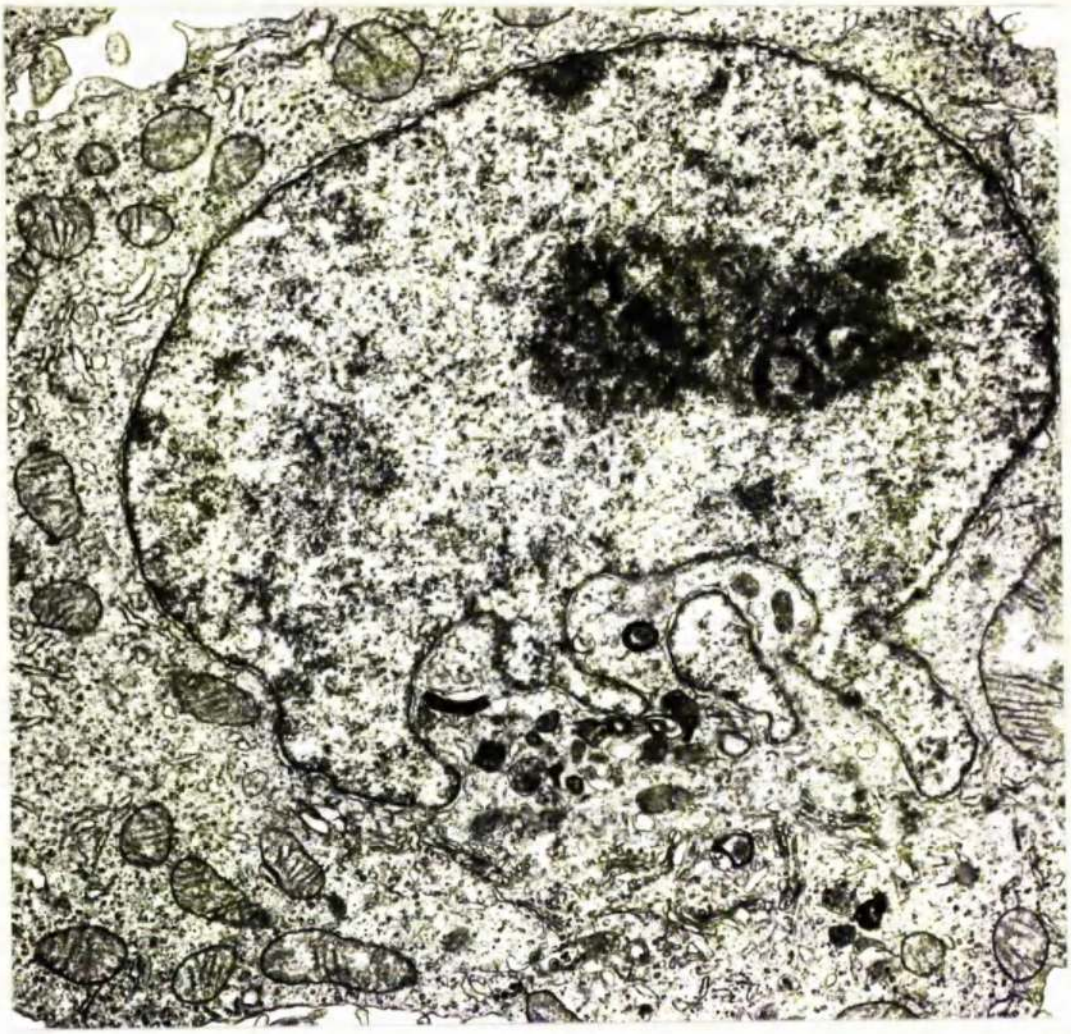

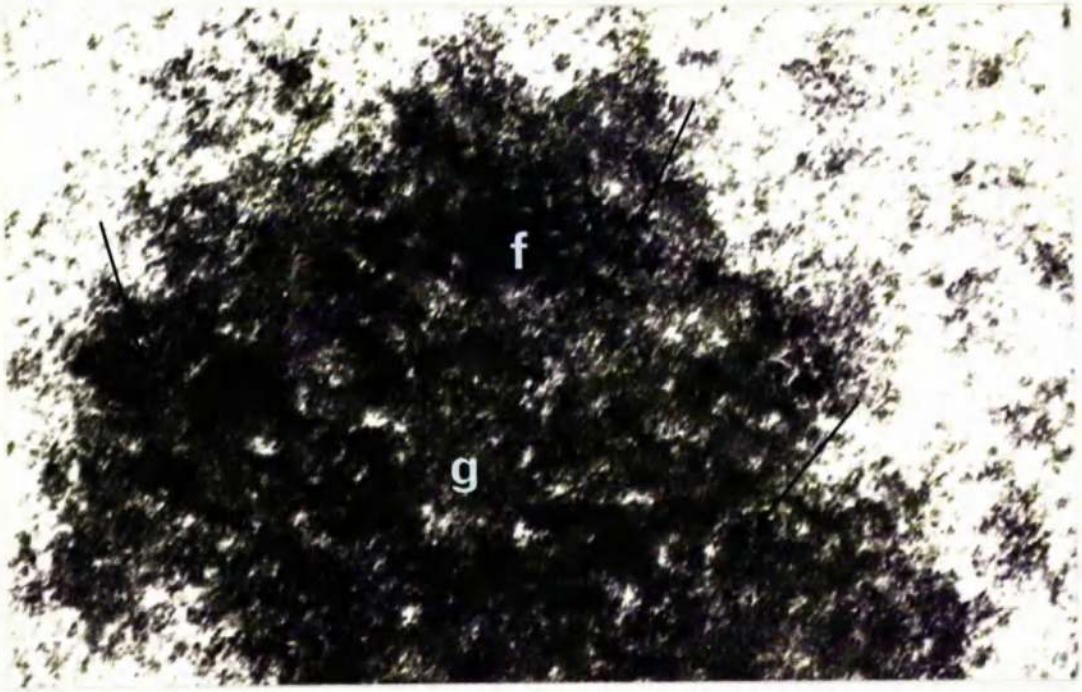
f
g

FIGURE 47 : Late - G_2 phase - cell thickly covered with surface protrusions. Note the presence of the phase specific long and slender filopodia.

FIGURE 48 : Late - G_2 phase cell with abundant cytoplasm and sharply folded nucleus. The nuclear chromatin is aggregated into fairly large clumps. The plane of section does not include the nucleolus.

TEM x 7,500

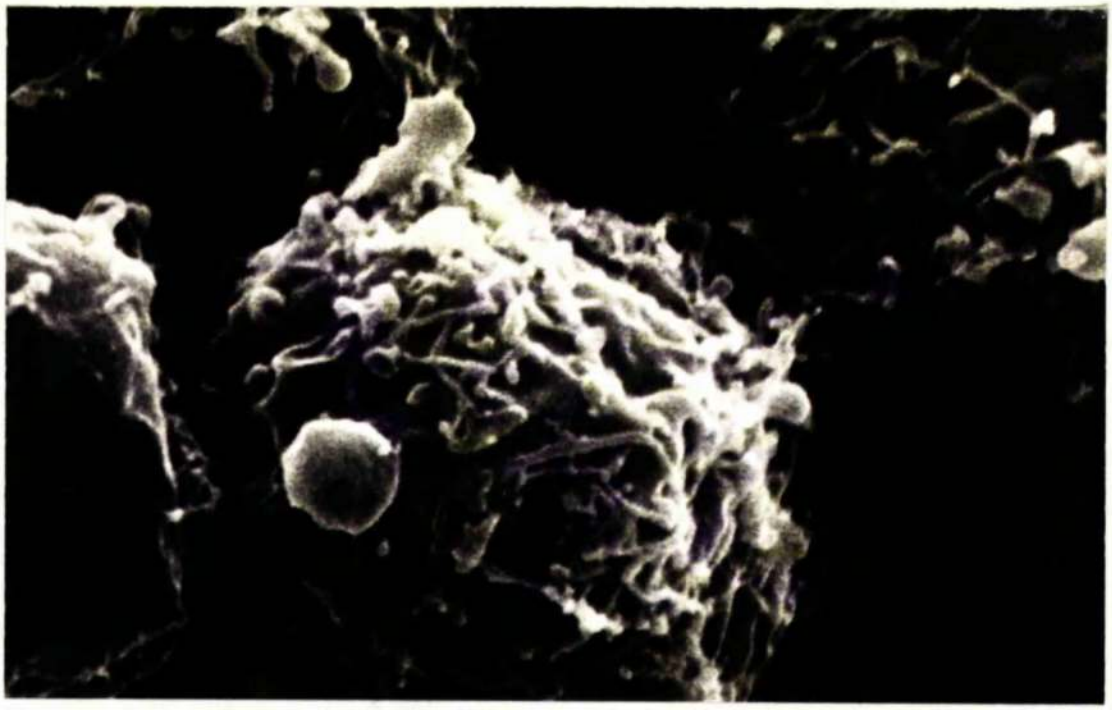

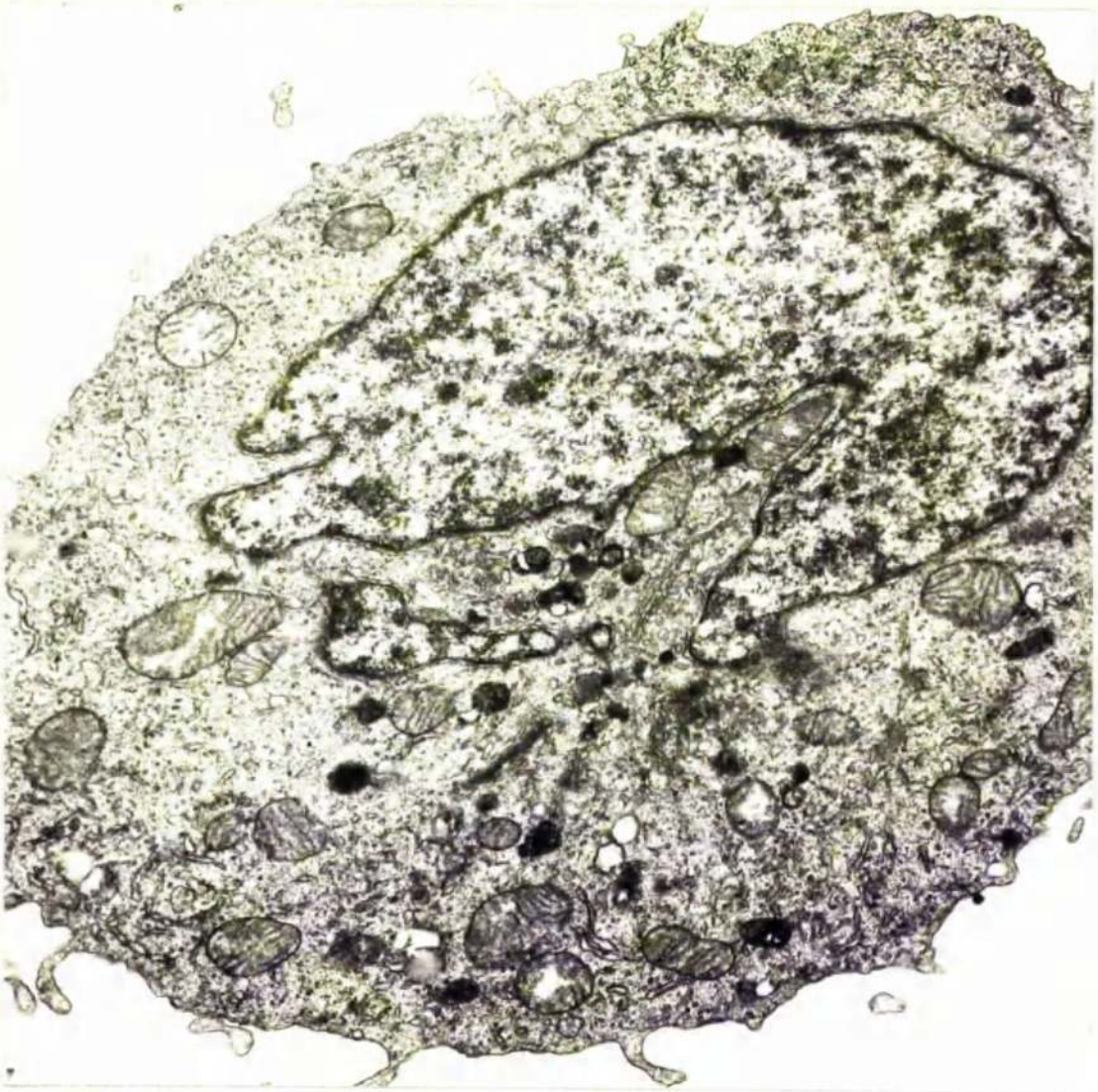

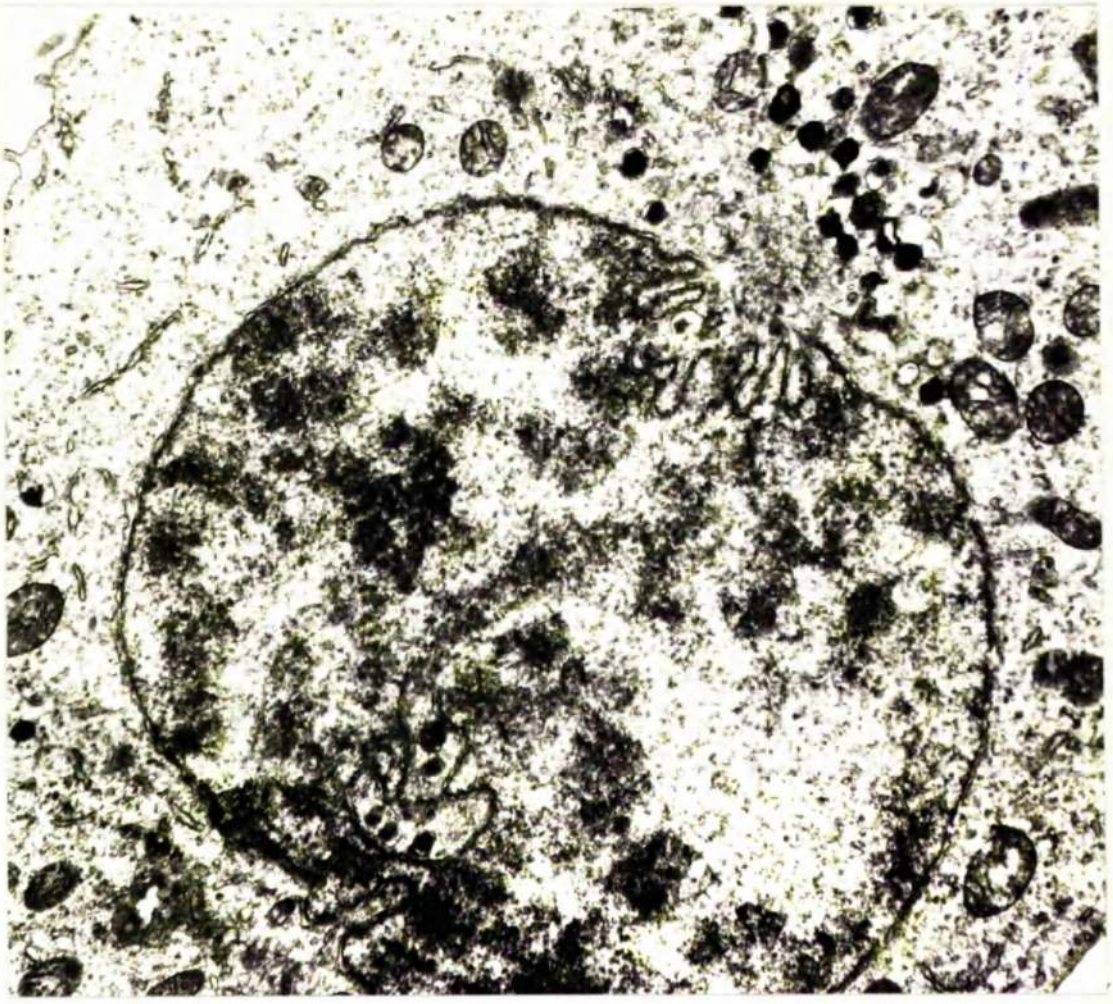

FIGURE 49 : Early - prophase - cell. The nuclear wall and the segregated nucleolus with pars amorpha are seen. The chromatin is aggregated into large clumps.

TEM x 7,500

FIGURE 50 : Cell in mitosis attached to the substrate by its numerous long filopodia some of which are arborised at their tips.

SEM x 10,000

FIGURE 51 : Late - prophase - cell. A remaining small part of the nuclear wall (arrow) and large aggregates of nuclear chromatin are seen. The cell surface features bore striking resemblance to those in Fig. 50.

TEM x 7,500

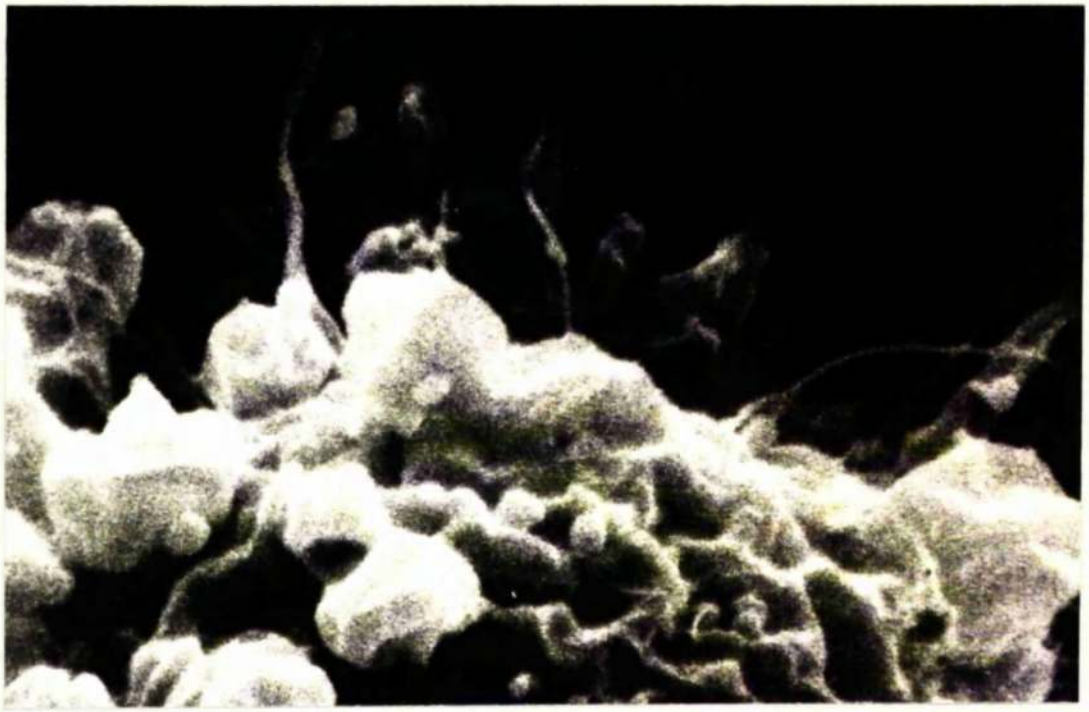

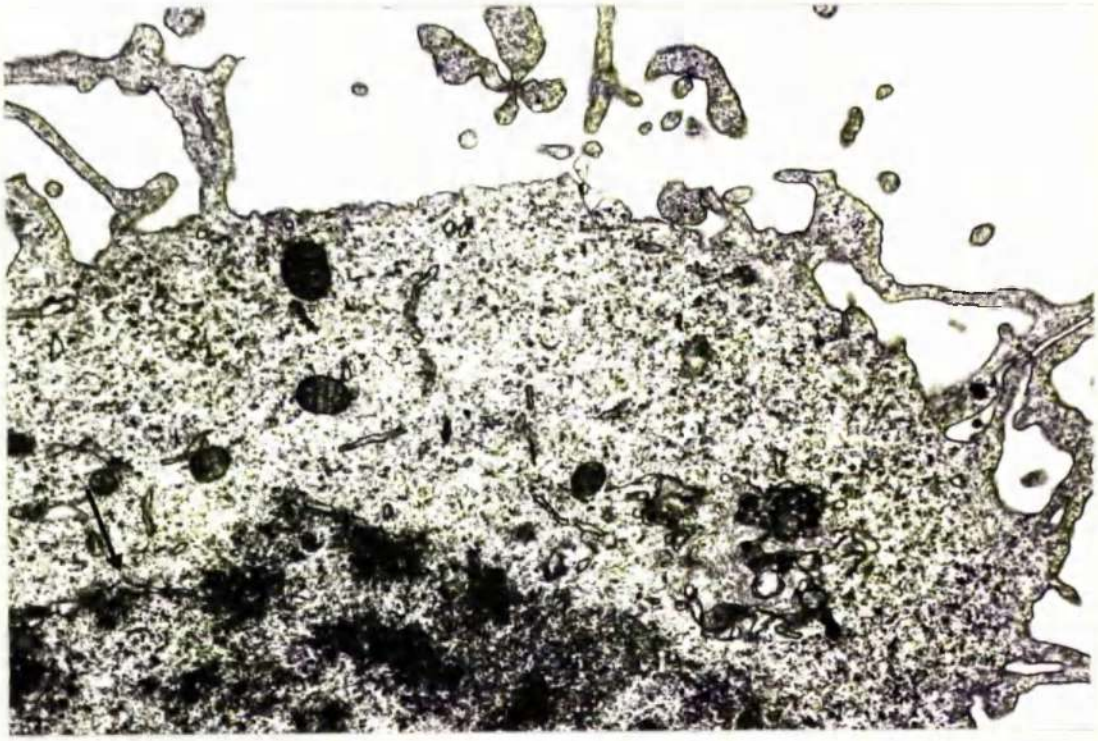

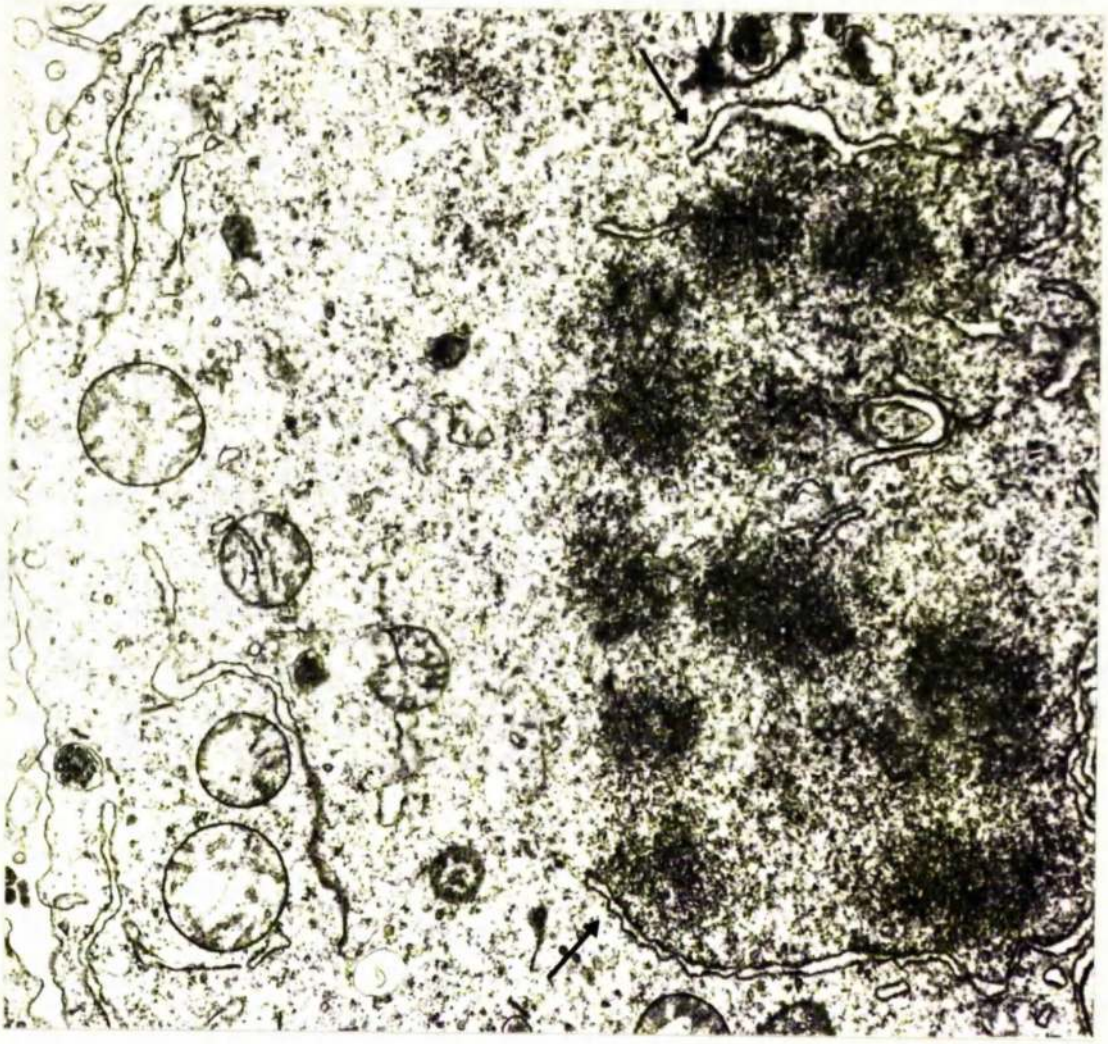

FIGURE 52 : Late-prophase - cell. The partial disappearance of the nuclear wall (arrows) and thin slices of chromosomes are shown.

TEM x 10,000

FIGURE 53 : Metaphase - cell. The surface structure is dominated by medium-sized blebs. Small microvilli and ruffles are also present.

SEM x 5,000

FIGURE 54 : Metaphase - cell. Note the presence of round, membrane-bound holes in the surface region of the cytoplasm. Compare with blebs seen in Fig. 53.

TEM x 20,000

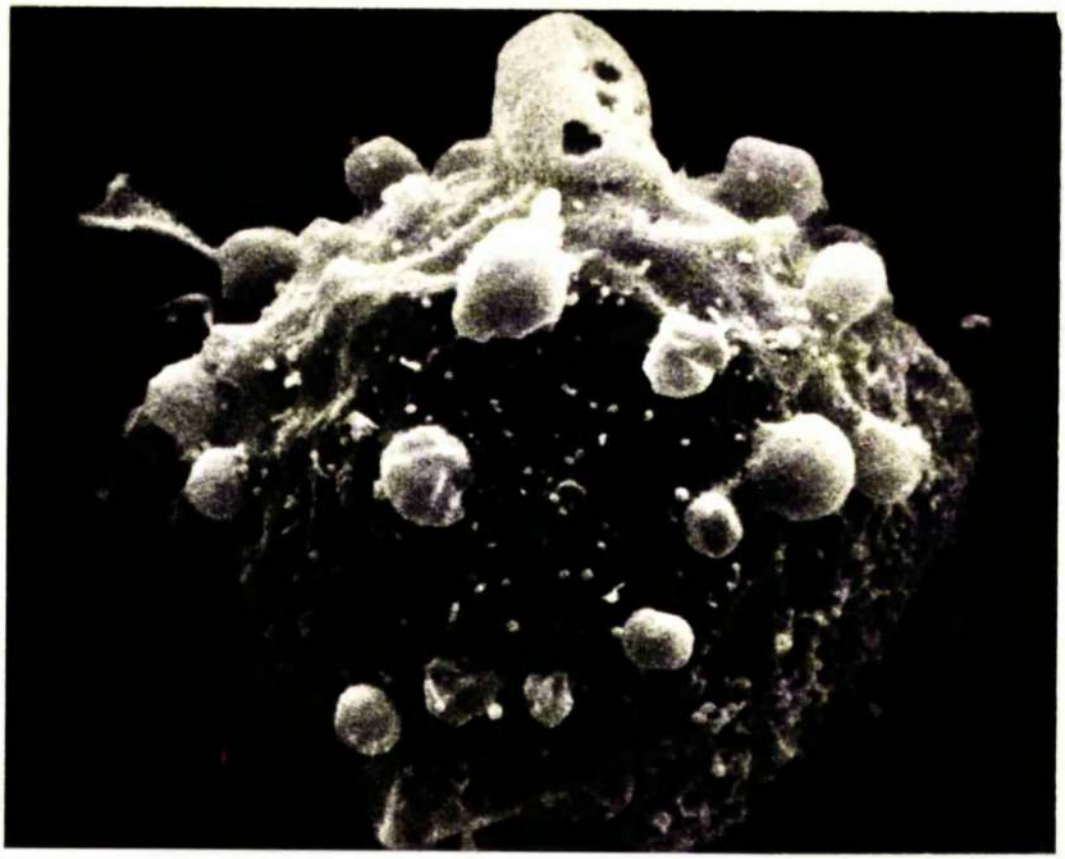

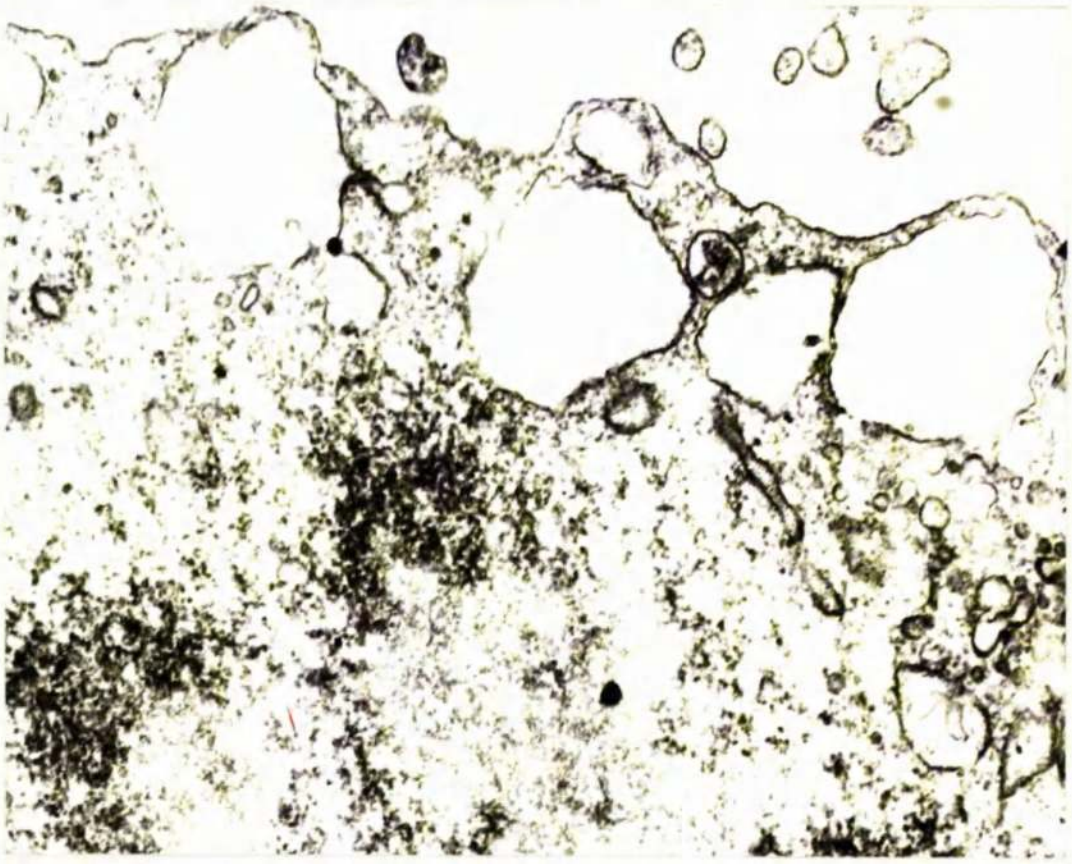

FIGURE 55 : Metaphase cell with centrioles. The upper one is cut across, the lower one is cut obliquely and appears as a dark horseshoe-shaped structure. Spindle fibrils extending from the centrioles towards the chromosomes can also be seen (arrow).

TEM x 7,500

FIGURE 56 : Cell in the early phase of cell division.

SEM x 5,000

FIGURE 57 : Cell in anaphase or in early - telophase. The separated chromatids of the chromosomes are in the opposite ends of the cell.

TEM x 7,500

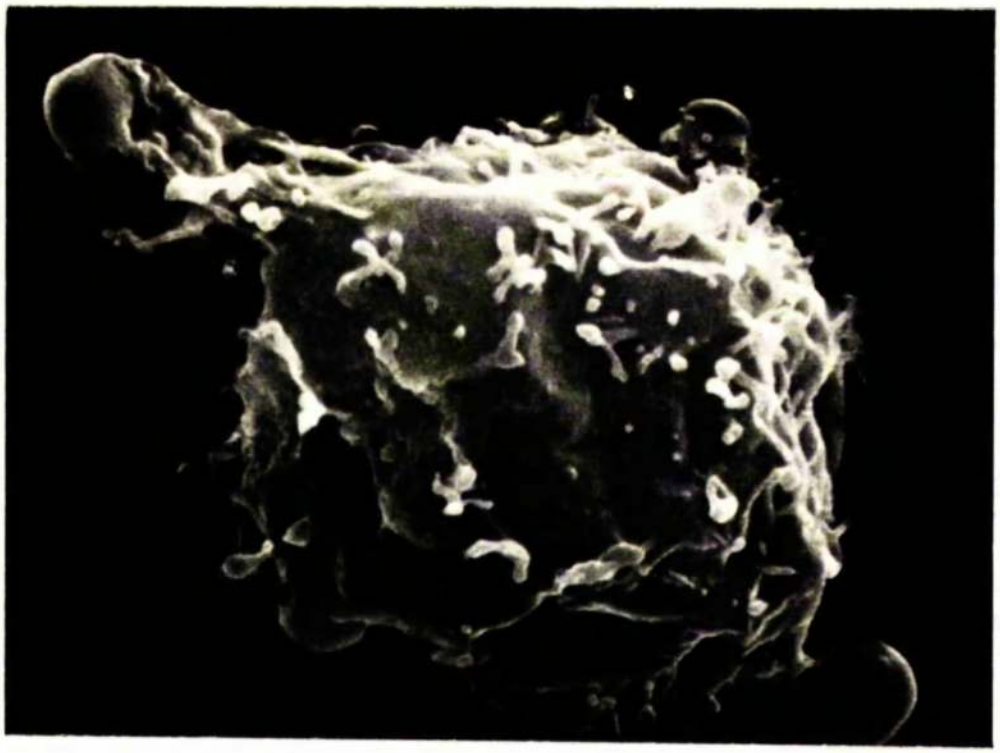

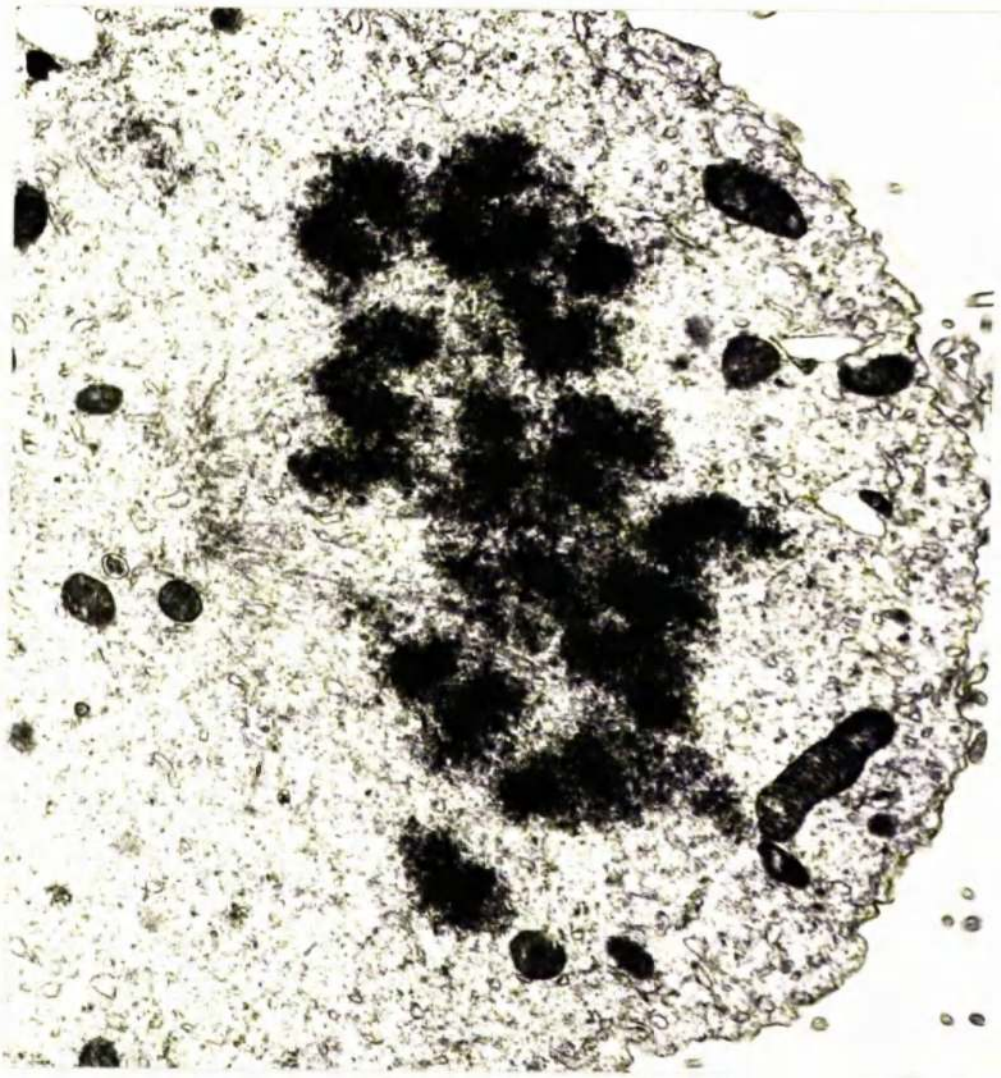

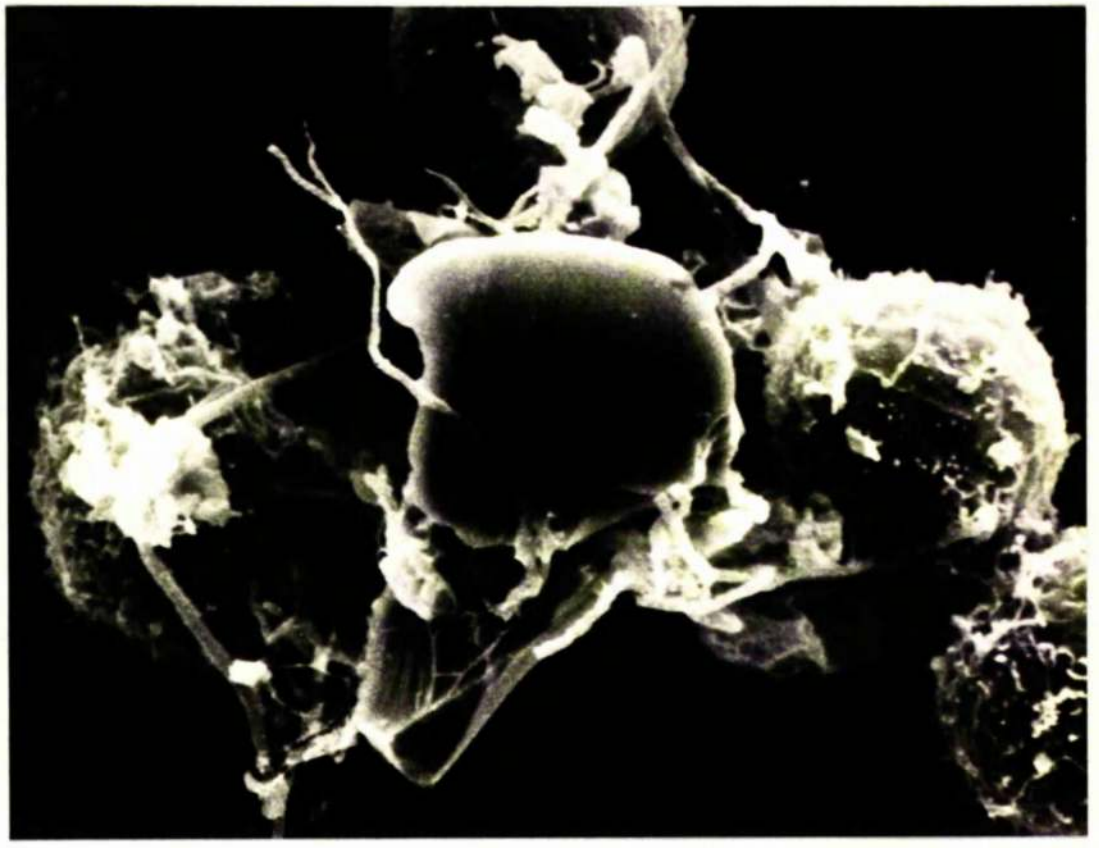

FIGURE 58 : The cell in the centre is in division. It is supported and attached to neighbouring cells by filopodia and ruffles. In regions where cell contact is not present, the cell surface is completely smooth.

SEM x 2,500

FIGURE 59 : Daughter cells are shown in different stages of their separations (arrows). On the left hand side, cells are smooth and closely attached; they represent the early stage. In the upper right corner, cells are in a later stage and have a "bleby" surface.

SEM x 2,500

FIGURE 60 : Cell after division in the early stage of separation. It is small and has a slightly elongated shape. The round nucleus contains heterochromatin distributed along the nuclear wall. The eccentric nucleoli are closely attached to the condensed chromatin. The nucleolar components are well segregated with foci of pars amorpha.

TEM x 7,500

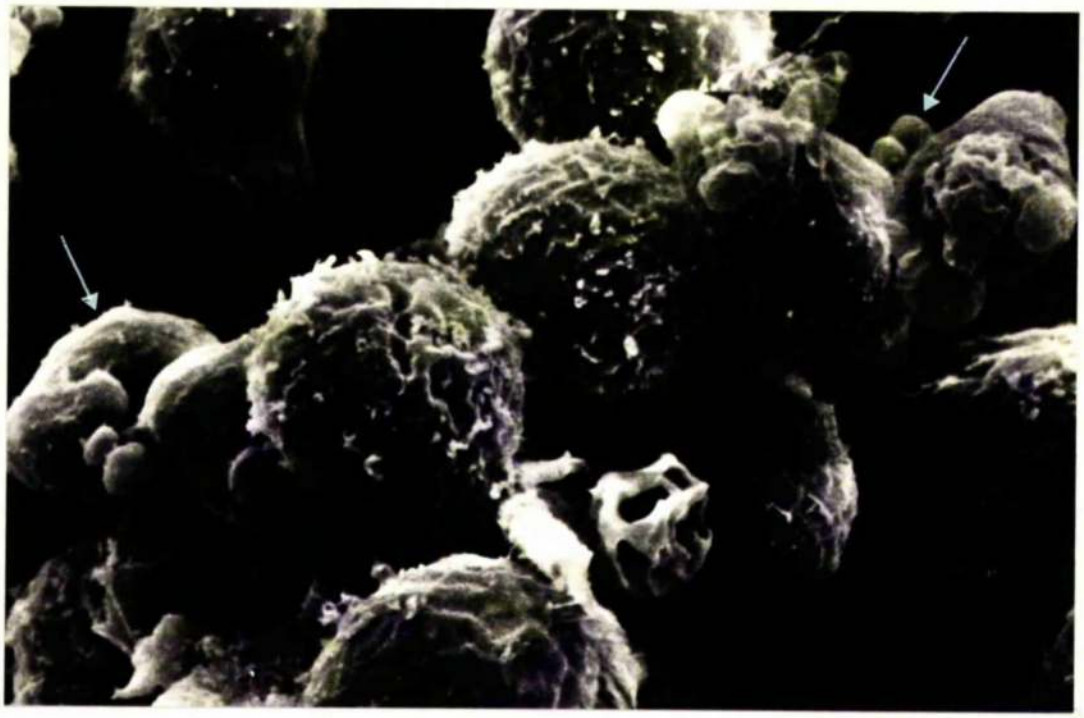

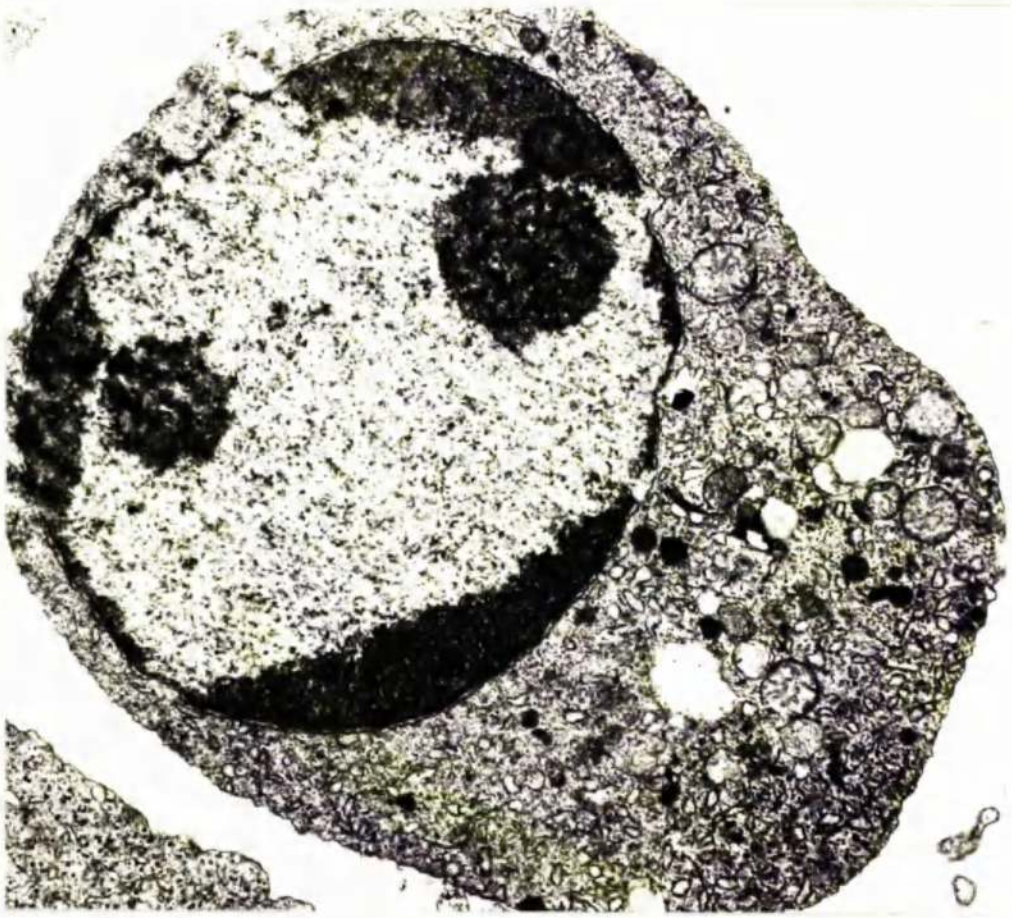

FIGURE 61 : Group of "bleby" cells from the early - G_1 phase. In the upper right corner separating daughter cells can be seen. These and the cells in Fig. 62 represent two different periods in the cell cycle and demonstrate changes in cell surface morphology at their most striking.

SEM x 1,250

FIGURE 62 : Early - S phase - cells with phase-specific small ruffles.

SEM x 1,250

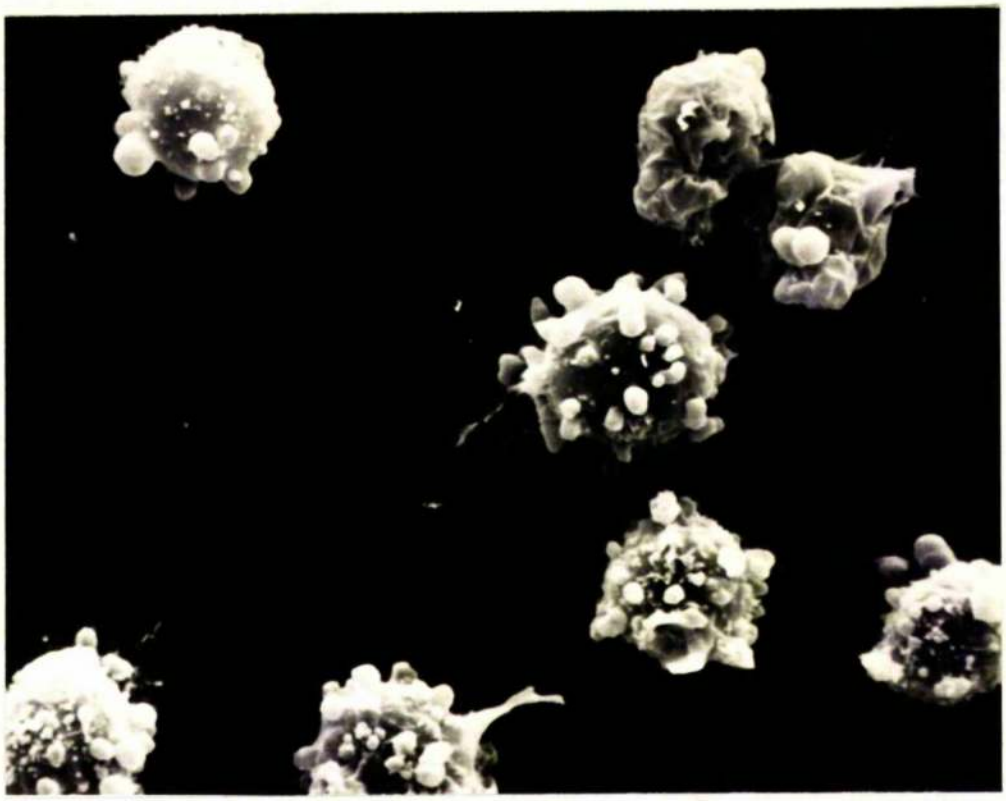

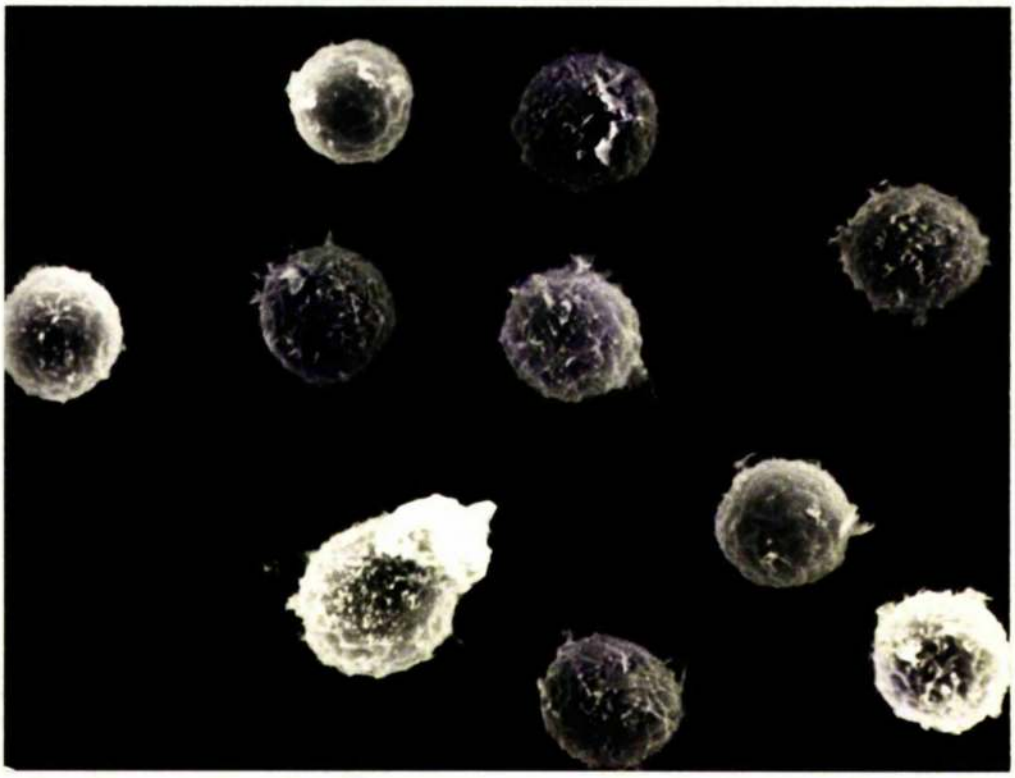

FIGURE 63 : Group of F422 cells. The uropod form is characteristic of this cell line. The appearance of the cells depends on the pole by which they are attached to the substrate.

SEM x 5,000

FIGURE 64 : The uropod morphology can be recognised in this thin section because of the plane of section.

TEM x 5,000

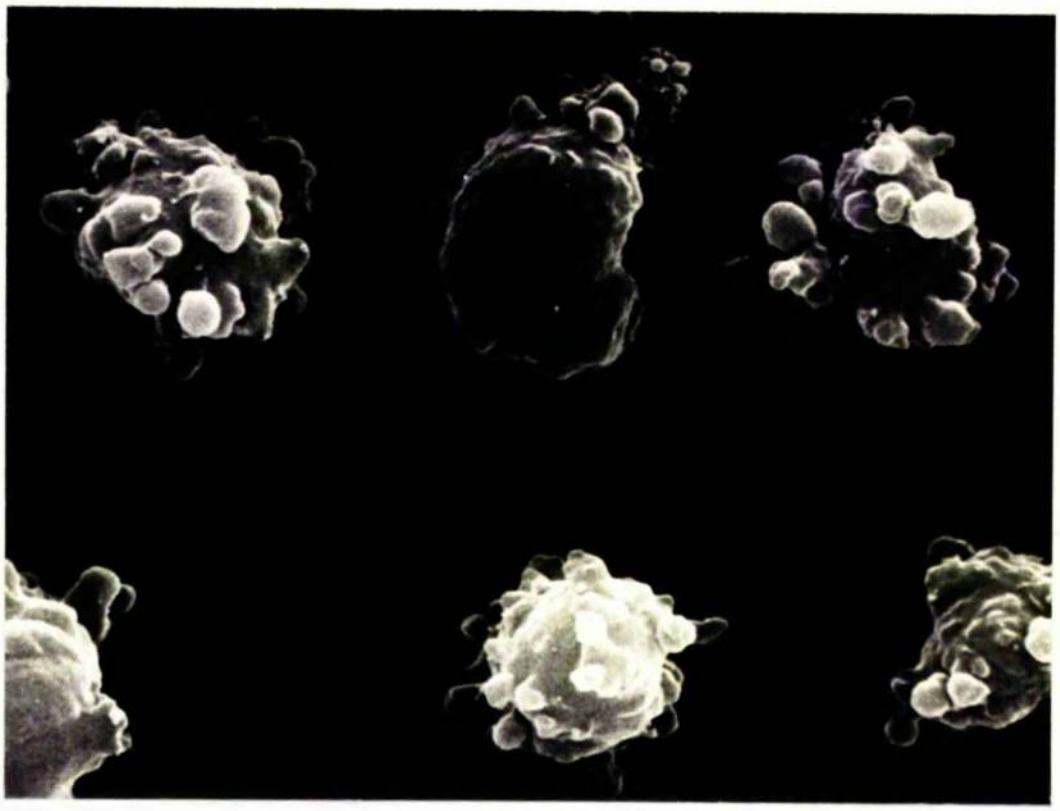

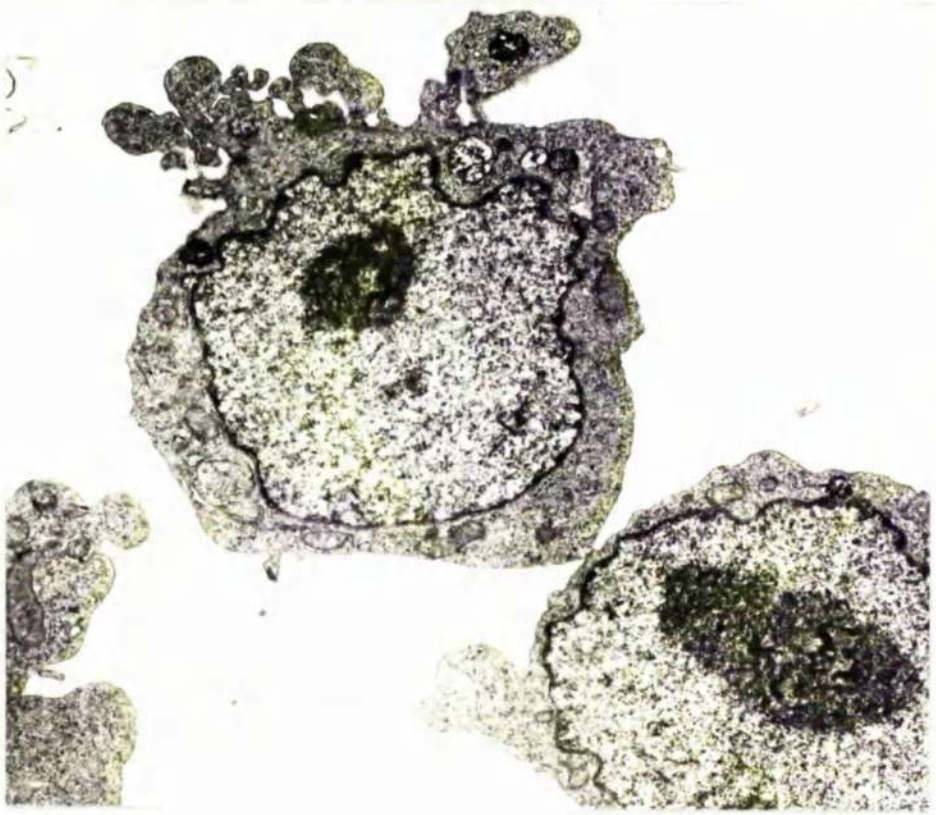

FIGURE 65 : F422 cell with surface protrusions, mainly blebs, accumulated at one pole of the cell. The remaining part of the cell surface is smooth.

SEM x 10,000

FIGURE 66 : F422 cell with cell surface features similar to those shown in Fig. 65. Accumulation of budding particles and the presence of thick, parallel-oriented microfilaments (arrow) can also be observed indicating the importance of contractile elements in uropod formation.

TEM x 15,000

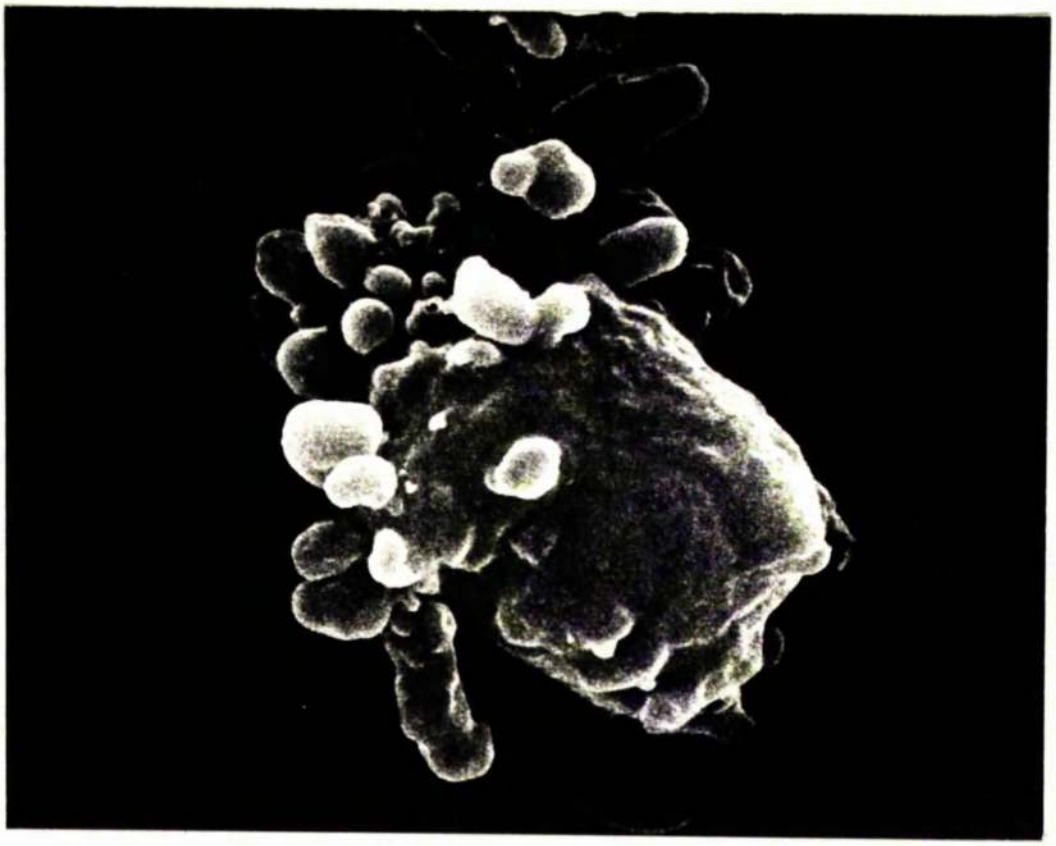

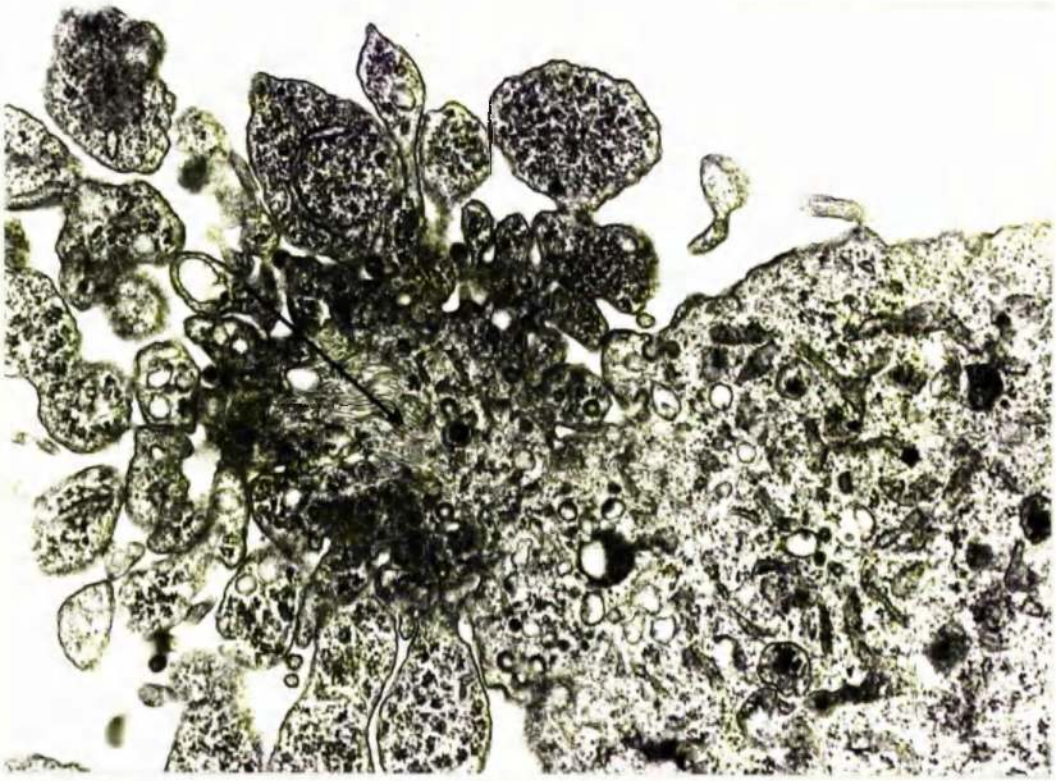

FIGURE 67 : F422 cell. The shape of this uropod is similar to the "hand-mirrow" shape of lymphocytes moving on substrates or interacting with other cells.

SEM x 10,000

FIGURE 68 : F422 cell. The tail of the uropod is shown characteristically facing the nuclear indentation containing the Golgi apparatus and the centrioles. The prominent centriole shown is cut obliquely (arrow).

TEM x 20,000

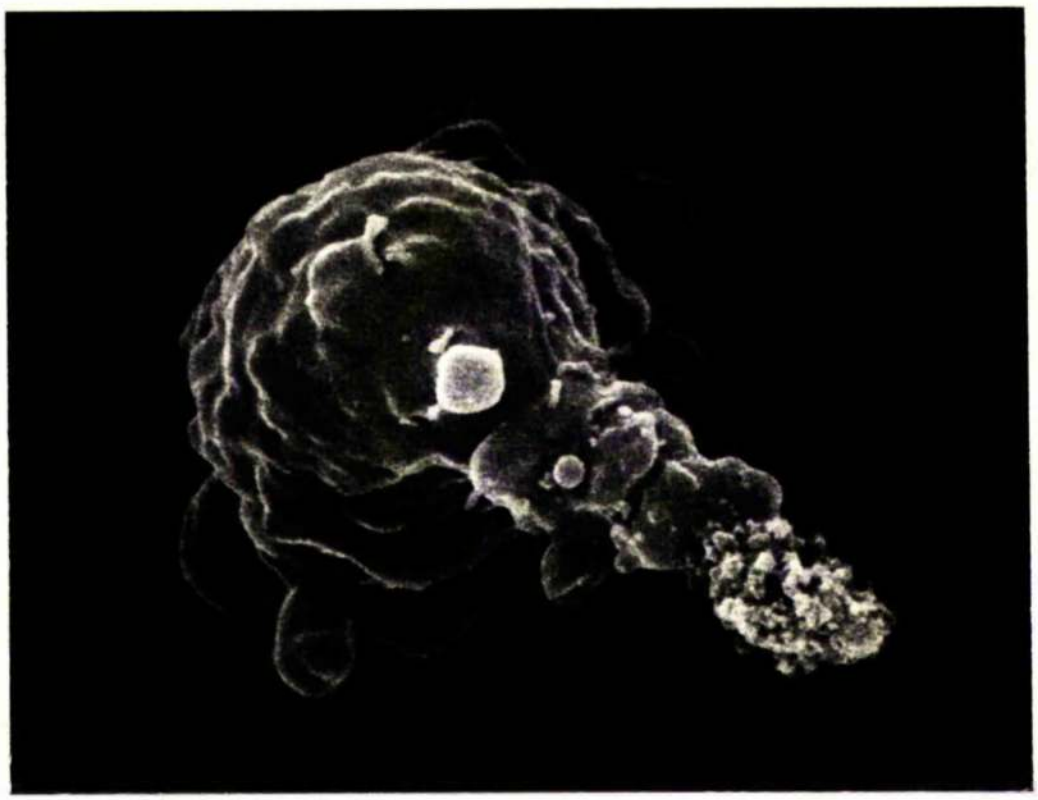

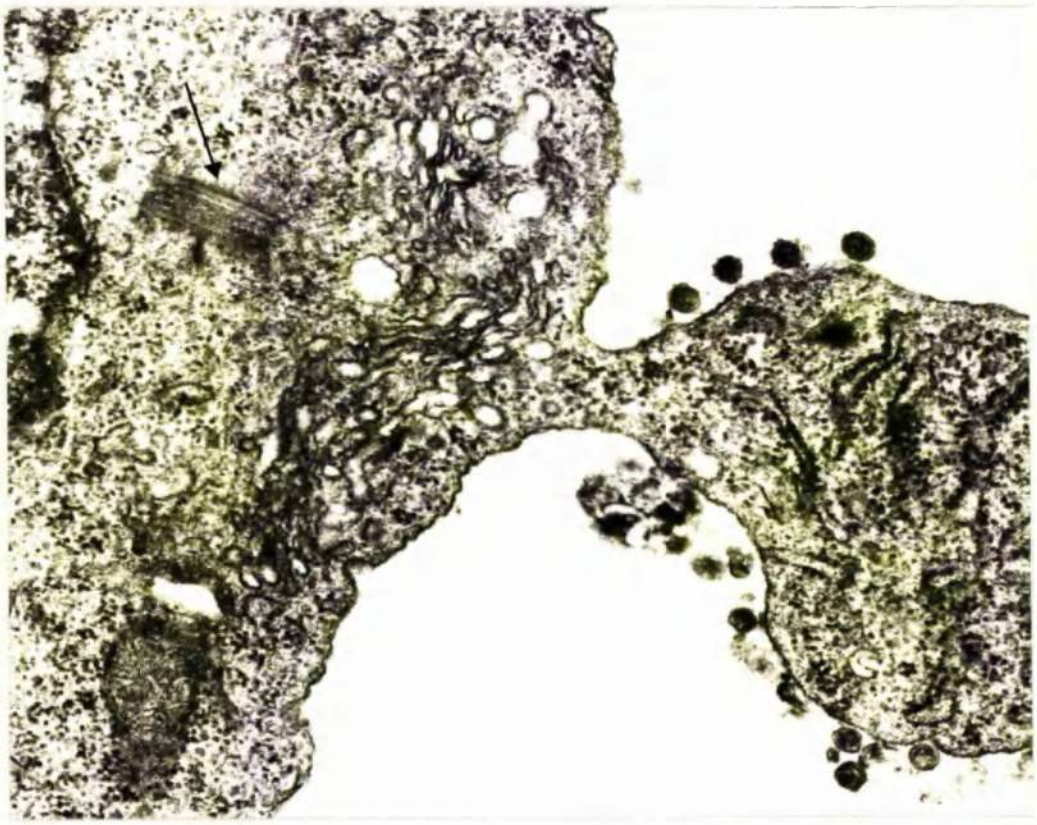

FIGURE 69 : Normal and giant CT45-S cells. The cell surfaces are bizarre, cauliflower-like and most of the cells have a few very long and thick, finger-like protrusions.

SEM x 2,500

FIGURE 70 : The giant CT45-S cell, on the left hand side, is in metaphase. The smaller cells have early - G_1 morphology. Large numbers of C-type particles are present on the cell membranes. The released virions have type-1 morphology.

TEM x 5,000

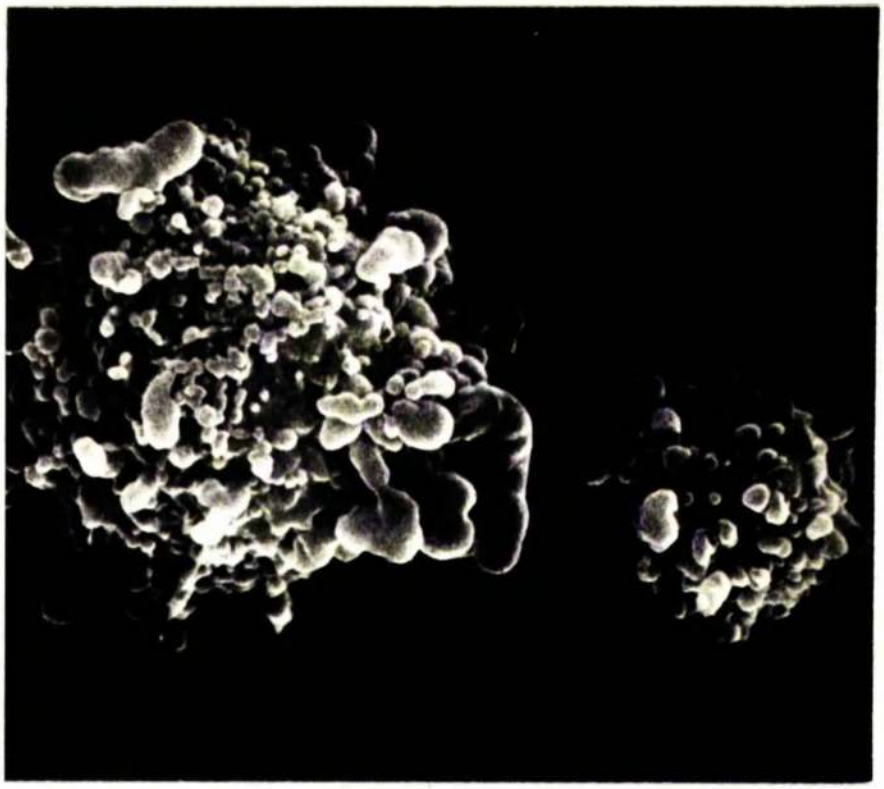

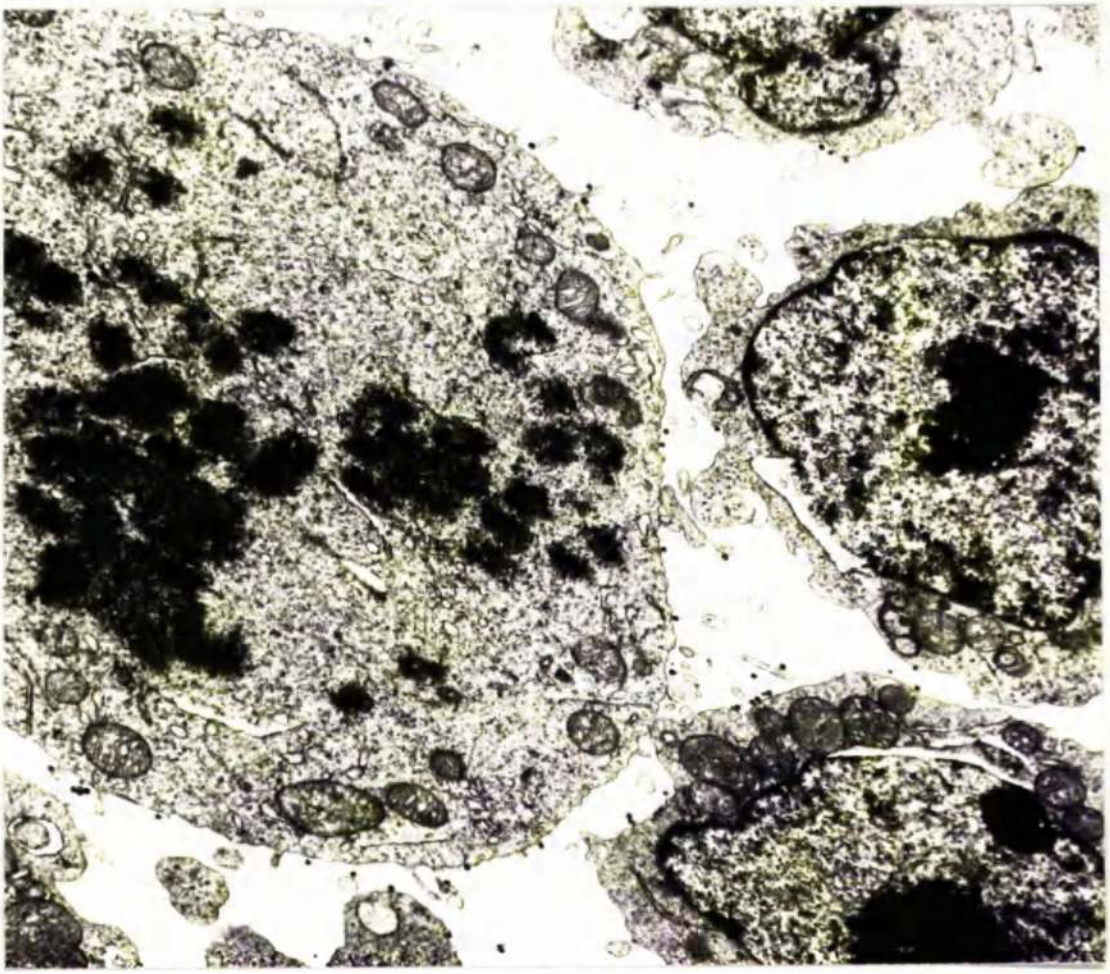

CHAPTER FOUR

INVESTIGATION OF THE EXPRESSION OF VIRAL ANTIGENS AND THE FELINE ONCORNAVIRUS-ASSOCIATED CELL MEMBRANE ANTIGEN (FOCMA) BY IMMUNOFLUORESCENCE TECHNIQUES

CHAPTER FOUR : INVESTIGATION OF THE EXPRESSION OF VIRAL ANTIGENS AND THE FELINE ONCORNAVIRUS-ASSOCIATED CELL MEMBRANE ANTIGEN (FOCMA) BY IMMUNOFLUORESCENCE TECHNIQUES

1. The Structural Proteins of FeLV and their Relationship to FOCMA

2. Review of the Literature

3. Materials and Methods

4. Experiments and Results

   A. Examination of synchronised FL74 cells by the indirect cytoplasmic immunofluorescence technique

   B. Examination of synchronised FL74 cells by the indirect viable immunofluorescence technique

   C. Investigation of FOCMA expression using two different synchronising methods

   D. Investigation of FOCMA and viral antigen expression during logarithmic cell growth

   E. Investigation of FOCMA and gp70 expression on synchronised F422 cells

   F. Investigation of antigen expression on synchronised FeLV-infected CT45-S cells

5. Discussion

I. The Structural Proteins of FeLV and their Relationship to FOCMA

Infection of mammalian cells with oncornavirus results in the non-lytic production of C-type particles which bud from the host cell membrane and are released into the medium. As a consequence of virus infection, host cells begin to express a variety of antigens. Oncornavirus antigens are found in the cytoplasm and cell membrane of both normal and transformed infected cells. These antigens are glycoproteins of the viral envelope or are internal virion proteins.

The expression of gp70 on virus producing cell membranes is predictable since this glycoprotein is the major surface component of budding virions. This glycoprotein is also found on the cell surface of a number of non-virus-producing normal mouse tissues (Lerner et al., 1976), and has been identified as the carrier of the G_{IX} type specific cell surface antigen on G_{IX} + mouse thymocyte cell surfaces (Obata et al., 1975; Tung et al., 1975).

In addition to gp70, internal viral proteins have also been detected on the surface of MuLV and FeLV infected cells. These include the major internal protein p27-30, the smaller gag region proteins p10, p12 and p15 and in the mouse system the lower molecular weight envelope glycoprotein p15(E) and p12(E) (Yoshiki et al., 1974; O'Brien et al., 1976; Grant et al., 1974; Fenyö and Klein, 1976; Lerner et al., 1976; Tung et al., 1976; Van de Ven, 1978).

A membrane antigen designated feline oncornavirus-associated cell membrane antigen (FOCMA) (Essex et al., 1971) was found to be

expressed on FeSV and also on certain FeLV infected cells. The immunological role of anti-FOCMA antibodies was investigated in the FeSV system by Essex et al., (1974) and in the FeLV system by Jarret et al., (1974). In both systems, high FOCMA antibody titres appeared to be protective against tumour development. It was suggested that FOCMA acts as a target for natural immunosurveillance against leukaemia development (Essex et al., 1975). The findings of Jarrett (1975) indicated that a critical factor in the pathogenesis of feline leukaemia was whether or not the virus was able to cause immunodepression before the production of moderately high levels of FOCMA antibodies. It was demonstrated in a series of experiments that horizontal transmission of FeLV commonly took place (Jarrett et al., 1973; Hardy et al., 1973; Essex, 1975). Surveys of normal cat populations showed that 39 - 63% of urban cats had antibodies to FOCMA. However, in rural environments there was a lower percentage of 3 to 5% (Jarrett et al., 1973; Rogerson et al., 1975; Essex, 1975). The higher incidence of antibodies to FOCMA in urban cats was attributed to the horizontal transmission of FeLV (Jarrett, 1976). It was concluded from epidemiological and immunological studies that vaccination against FeLV might be practicable. An experimental vaccine has been developed based on FL74 cells which were producing FeLV of low infectivity and also had a large amount of FOCMA on their surfaces. Vaccinated cats produced high anti-FOCMA antibody titres and were immune to subsequent challenge with FeLV (Jarrett et al., 1974, 1975).

FOCMA is detected by immunofluorescence tests on FL74 cells which are commonly used as target cells. The molecular nature of FOCMA

is as yet unclear. No correlation was found between FOCMA and neutralising antibody titres (Jarrett et al., 1973). It was claimed that absorption of anti-FOCMA sera with FeLV of all three subgroups did not remove anti-FOCMA activity (Essex, 1975). Absorption of immune sera with purified gp70 and p30 also failed to remove anti-FOCMA antibodies (Stephenson et al., 1977a). It was also demonstrated by using radioimmunoassay that antibody response to FOCMA was independent of the antibody response to gp70 and p30 (Stephenson, 1977). The lack of anti-gp70 activity in FOCMA positive viraemic cat sera was attributed to a state of antigen excess of virion antigens. Hardy et al., (1977) claimed to have found FOCMA expression on FeSV transformed cells in vitro and in vivo and on FeLV-induced feline tumour cells. They concluded that FOCMA was a tumour-specific antigen which was induced by FeLV infection and encoded possibly by FeSV. Recently, the term FOCMA-L was suggested for the antigen as it occurs on lymphoid tumour cells while the term FOCMA-S was suggested for the transformation specific antigen on fibroblasts which were non-productively transformed in vitro with FeSV (Sherr et al., 1978). An FeSV transformed non-producer mink cell line was shown to express FOCMA-S but not p30 and gp70 (Sliski et al., 1977). FOCMA-S had a molecular weight of 60,000 - 65,000 daltons or a molecular weight of 80,000 - 100,000 daltons when linked to p15 and p12 (Stephenson et al., 1977b). In the latest study by Sliski and Essex (1979), healthy cats which were naturally exposed to FeLV were examined for the presence of FOCMA-S by immunofluorescence test. Anti-FOCMA sera obtained from viraemic cats showed similar endpoint titres whether tested on FeSV-transformed non-producer mink fibroblasts

or on cat lymphoma cell lines productively infected with FeLV. It was suggested that FOCMA-S shares at least one major antigenic determinant with FOCMA-L. FOCMA might be encoded by a region of the virus genome shared by both FeLV and FeSV. Alternatively, FeLV, by transforming lymphoid cells, might turn on cell sequences related to those carried in the FeSV genome.

Nevertheless, there is some evidence which suggests that a cross-reactive determinant between FeLV-C and FOCMA might also exist (Ruscetti et al., 1976; Russell, 1977).

2. Review of the Literature

Studies of the antigenic properties of cultured mammalian cell lines revealed that even genetically homogeneous cell populations contained both antigen-positive and antigen-negative cells. It was also observed that some cell surface antigens were stable during the growth phase while others disappeared soon after subculture. These observations and the evidence obtained in several studies for the cell cycle dependent expression of cell surface antigens suggest that the expression of certain cell surface antigens is a dynamic phenomenon, a notion in keeping with the concept which views the plasma membrane as a dynamic structure which is able to undergo rapid and reversible change in response to specific stimuli arising in the intra- or extra-cellular environments.

Evidence for the cell cycle-dependent expression of cell surface antigens has been obtained in several studies.

Changes in cytotoxic sensitivity of cells have been investigated by using anti-H-2 immune sera. It was found that the sensitivity of cells was high in the G_1 phase while cells in the S phase were found to be resistant to specific immune lysis (Shipley, 1971; Pasternak, 1971; Summer et al., 1973).

The human HL-A antigens and the so-called i-antigen which is expressed in foetal tissues, transformed cell lines and mitogen-stimulated lymphocytes, were shown to be expressed maximally on human lymphoid cells during the S phase (Pellegrino et al., 1972; Thomas, 1974).

Various mechanisms may be involved in the variations of antigen expression during the cell cycle but several lines of evidence support the hypothesis that the change in the synthesis of antigenic determinants is the most important mechanism underlying these variations.

Substantial data exist which lend support to this hypothesis and which show that the synthesis of specialised cell products and some cell membrane components by cultured cells, bears considerable resemblance to the cell cycle-dependent expression of cell surface antigens.

As long ago as 1930, it was observed that cells ceased to form specialised products when cultured in media which favoured a rapid multiplication (Doljansky, 1930). The specific activity of B-glucuromidase in cultured cells derived from human skin increased considerably in density inhibited cells. This increase in the enzyme activity could be inhibited by puromycin (De Mars, 1964). Similar density-dependent increases of the specific activity of other enzymes have been reported (De Luca, 1966; Eagle, 1968; Ruddle and Rapola, 1970).

Cultured neuroblastoma cells have been used extensively in in vitro studies of morphological and biochemical markers characteristic of the differentiated state. Some of the findings obtained are as follows. The specific activity of acethylcholinesterase and the number of acethylcholin receptors increase in stationary phase cultures (Blume et al., 1970; Simontov and Sachs, 1973). Stationary cells express three additional properties of neurone differentiation : axon-dendrite development, formation of electrically excitable plasma membranes and synthesis of acethylcholin receptors (Rosenberg et al., 1971). Cultured mouse neuroblastoma cells (C 1300) possess surface receptors for nerve growth factor (NGF) as well and the binding of NGF to synchronised C 1300 cells is maximal during the G_1 phase (Revoltella et al., 1974).

The above results suggest that morphological, antigenic and at least some of the biochemical properties characteristic of the differentiated neuronal state are normally expressed in the G_1 phase of the cell cycle.

Other examples of cell cycle-dependent expression of surface receptors were described in a variety of cell types cultured in vitro. Isersky et al., (1975) examined the expression of IgE receptors and basophilic granules in cultured rat basophilic leukaemia cells and found that these two differentiation markers were maximally expressed in stationary phase cultures in which cells are arrested in the G_1 phase.

The inverse relationship between cell growth rate and the production of melanin was observed by several researchers (Doljansky, 1930; Whittaker, 1963; Moore, 1964; Schachtschnabel et al., 1970, 1971; Kitano and Hu, 1971; Kreider and Schmoyer, 1975). The data obtained suggest that changes in melanogenesis during the growth cycle of mouse melanoma cells are the result of the de novo synthesis of melanin.

Collagen synthesis in mouse fibroblast lines was also shown to be cell cycle-dependent (Goldberg and Green, 1964). Myogenesis in cultured cells derived from embryonic skeletal muscles was investigated by Merlic et al., (1975 They found that the synthesis of the differentiation markers, actomyosin and keratin kinase as well as the de novo synthesis of acethycholin receptors increased during the G_1 period.

Abbot and Holtzer (1966) found that cultured chick chondrocytes failed to divide and synthesise chondroitin sulphate after reaching critical density. The morphological differentiation of mouse myeloma cells was also shown to be dependent on cell density (Saunders and Wilder, 1971). The relationship between cell density and the synthesis of cell surface macromolecular components were studied extensively. It was demonstrated that the concentration of several glycolipids increased in confluent normal hamster cells (BHK). However, virus transformed BHK cells had a lower concentration of glycolipids and no longer

exhibited the density-dependent increase of glycolipid concentration found in normal cells (Hakamori et al., 1970). Similarly, in high density cultures of untransformed hamster cells, the levels of the so-called "higher" glycolipids (trihexosyl ceramide, globoside and Forssman antigen) increased (Sakiyama et al., 1972). An increase in the synthesis of higher glycolipids(ceramide tri-, tetra-, and penta-hexoside) in dense cultures as compared with sparse cultures of NIL2 hamster cells was reported by Critchley and Macpherson (1973). Sakiyama and Terasima (1975) also described a gradual increase in the concentration of Forssman antigen in monolayer cultures of NIL cells after cells reached a critical density.

Cell cycle-dependent synthesis of cell surface components was shown more directly in experiments using various synchronising techniques. For example, synchronised 3T3 cells accumulated in the G_1 phase increased the synthesis of a trypsin-labile surface macromolecular glucosamide-containing component (Onodera and Sheinin, 1970). Similar observation was made by Gerner et al., (1971) using a double thymidine block for cell synchronisation. The incorporation of radio-labelled palmitate, glucosamine and galactose into phospholipids and glycolipids was monitored in NIL cells. The maximum labelling of ceramide tri-, tetra-, and penta-hexoside (the Forssman antigen) occurred during the G_1 phase (Wolf and Robbins, 1974).

The synthesis of a variety of products was also studied in synchronised cultures. It was found that in human lymphoblastoid cells, the synthesis of IgG and IgM molecules reached a peak in the G_1 phase (Buell and Fahey, 1969), whereas, maximal production of γG_{2a} immunoglobulins in synchronised mouse myeloma cells occurred during the early S phase (Byars and Kidson, 1970).

The cell cycle-dependence of leukaemia and sarcoma virus production, virus release and viral antigen expression was already reviewed in the Introduction and the Second Chapter. Significant variations in virus replication during synchronous cell growth was detected in a wide range of other virus-host cell systems (Basilico and Marin, 1966; Carp and Gilden, 1966; Pages et al., 1973; Thorne, 1973). Differences in virus replication were also observed between logarithmically growing and stationary phase cells (Fiszman et al., 1974; Poste et al., 1974).

3. Materials and Methods

Cells, the culturing of cells and the synchronising methods are described in the First Chapter.

Sera

(a) Anti-gs serum was prepared in rabbits to Tween-ether-disrupted density-gradient-purified FeLV, which results in a mixture of viral nucleoids, internal virion proteins and some disrupted envelope fragments as antigenic determinants. For immunisation, LV5 was used with subgroup A and B specificities.

(b) Anti-gp70 serum was raised in rabbits to purified glycoprotein. The envelope glycopeptide was obtained from the Theilen strain of FeLV by phosphocellulose column chromatography, and analysed by high resolution electrophoresis in gradient polyacrylamide slab gels containing SDS. The antigen specificity and purity were tested by radioimmunoassay.

(c) Anti-p15 and -p30 sera were raised in rabbits to purified viral proteins. FeLV proteins were separated by guanidine hydrochloride gel filtration (6 M gu HCl) and sodium dodecyl sulfate polyacrylamide (SDS PAGE) separation. Rabbit antisera to FeLV-p15 and p30 gave strong precipitin lines in Ochterlony gel diffusion tests. Reactivities of antisera to FeLV proteins were analysed by immune precipitation and SDS PAGE.

(d) Anti-FOCMA sera were obtained -

(1) from two cats with naturally occurring high FOCMA titres of 1:64 and 1 : 256 respectively. These antisera had virus neutralising activities as well.

(2) from two experimental control cats, Paravac 9/10 and 14 which had high FOCMA titres 1:256 and 1:512 respectively and were viraemic at the same time.

The anti-gs serum and the anti-FOCMA sera were kindly provided by Professor W.F.H. Jarrett, the anti-gp70 serum by Dr. M. Strand and the anti-p15 and -p30 sera by Dr. J. Neil.

Absorption of antisera

Immune sera raised in heterologous species and the fluorescein-conjugated immunoglobulins were absorbed with lyophilised foetal bovine serum (FBS) and with lyophilised extracts of normal liver tissues (30 mg/ml) for 1 hour at 37°C and overnight at 4°C.

When anti-FOCMA serum and anti-gp70 serum were reacted with FeLV-infected CT45-S cells, prior to use, they were absorbed with uninfected CT45-S cells. The antisera (0.5 ml.) diluted within 2 $\log_2$ dilutions above the 50% endpoint titre were incubated with 5×10^7 cells (total volume 0.6 ml.) for 1 hour at room temperature, then overnight at 4°C. Additional absorption steps were performed 2 to 6 times in the same manner and the sera were clarified at 10,000 x g for 5 minutes.

Inactivation of sera

All sera were inactivated for 30 minutes at 56°C and stored undiluted in samples at -20°C. Prior to use, sera were diluted with PBS containing 1% bovine serum albumin.

Fluorescein-conjugated antiglobulins

Conjugates purchased from Miles Laboratories (U.K.) Ltd., were tested in immunoelectrophoresis against whole serum. All conjugates reacted

only with gammaglobulins. Rabbit anti-cat immunoglobulin was used at 1:10 dilution and goat anti-rabbit immunoglobulin was used at 1:20 dilution in PBS.

Immunofluorescence Techniques

A. Cytoplasmic indirect immunofluorescence test

(a) To obtain adequate cell densities on coverslips, the following method was used: 1 ml. from the suspension culture was removed, cells were washed three times in PBS and resuspended in 2 ml. of PBS. 0.5 ml. of the above cell suspension was placed in a holder and the cells were deposited on clean microscopic slides by means of a cytocentrifuge (500 r.p.m. for 5 minutes). Cells were dried for 1 - 2 hours at room temperature, fixed with acetone for 10 minutes and stored at -20°C.

Three slides were prepared from each sample. The cells attached by the above method were slightly extended and showed better differentiation between the cytoplasm and the nucleus.

(b) Cells from each sample were incubated in a drop of antiserum at 1:50, 1:100 and 1:200 dilutions for 1 hour at 37°C in a humidified chamber. The slides were washed twice with PBS pH 7.2 and twice with distilled water with 5 minute intervals for each wash.

(c) Slides were dried and 1 drop of fluorescein-conjugated antiglobulin (goat anti-rabbit) was added at 1:10 or 1:20 dilution. The cells were incubated for 1 hour at 37°C and washed twice in PBS and once in distilled water.

(d) Cells were counterstained by incubation in Evan's blue dye (0.06%) for 5 - 10 minutes, washed twice in distilled water and dried. A drop of glycerin: PBS (1:1) was placed on the cells and the slide was covered

with a coverslip. Slides prepared in this way could be stored at -20°C for many months without diminution of fluorescence.

B. Viable indirect immunofluorescence test

The test was performed by using Dynatech disposable sterile 'U' plates and transfer-plates. 1×10^5 cells were used for every well.

(a) The required number of cells were washed twice with PBS and resuspended in an appropriate amount of PBS (for every well 0.025 ml.). The cell suspension was aliquotted into the 'U' plate with the aid of a microdiluter which is calibrated to pick up and dispense 0.025 ml.

(b) Doubling dilutions of the test sera were made up in the transfer-plate and by placing the transfer-plate directly on top of the 'U' plate, the serum dilutions were transferred to the wells containing the cells.

(c) Cells were incubated for 30 minutes at room temperature and were frequently resuspended with a mechanical shaker during the incubation period. Cells were washed twice with PBS by centrifugation and after the removal of the supernatant by resuspension in PBS.

(d) After washing, 0.025 ml. of fluorescein-conjugated antiglobulin was added to each well and the resuspended cells were incubated for 30 minutes at room temperature. Cells were washed three times and finally resuspended in 0.025 ml. PBS. By using a new pipette for each well, one drop of each dilution was placed on a clean microscopic slide which was covered with coverslip of 13 mm. in diameter. Slides were stored in a moisture chamber at 4°C and examined immediately.

4. Experiments and Results

A. Examination of synchronised FL74 cells by the cytoplasmic indirect immunofluorescence technique

FL74 cells were synchronised by a double thymidine block. Cells were removed at time intervals between 0 and 30 hours post release. Cells were attached to slides and fixed with acetone. The IF test was performed as described in the Materials and Methods part of this Chapter.

From each sample, three slides were prepared and in this way each sample could be incubated with three different dilutions of the anti-gs serum. It was established in previous experiments that the periodicity of the staining could be best demonstrated by using the dilutions 1:50, 1:100 and 1:200, respectively.

Goat anti-rabbit IgG fluorescein conjugate was used at 1:20 dilution.

Normal rabbit serum and fluorescein conjugate without antiserum were used as controls.

In each specimen 200 - 300 cells were examined under code and the number of fluorescent positive and negative cells and the intensity of the fluorescence were evaluated. The brightness of the cells was judged on a 1+ to 3+ scale where 1+ fluorescence represented barely detectable staining and 3+ was very bright.

FL74 cells examined for cytoplasmic immunofluorescence showed a diffuse granular staining throughout the cytoplasm, but not in the nuclei. Control sera and the control fluorescein conjugate did not cause immunofluorescence.

As shown in Fig. 71 and Table 14, p.184 cytoplasmic staining of the cells varied periodically during the cell cycle. The periodicity of the staining could be demonstrated most strikingly with the 1:100 dilution of the anti-gs serum. With that dilution, staining was not detected immediately following release from the double TdR block. It appeared later in the S phase (PR - 4 hr), increased during the G_2 and M periods (PR - 6, -8 hrs.) and reached a peak in the early-G_1 phase (PR - 10 hr.). At that time, 100% of the cells were very intensely fluorescing. In the mid- and late-G_1 periods (PR - 18, - 22 hrs.) all the cells remained positive but the intensity of their fluorescence diminished.

With 1:200 dilution, no cytoplasmic fluorescence was detected during S and G_2 phases. Staining appeared only around mitosis, became much brighter in the early-G_1 phase and disappeared again in the later part of the G_1 period.

Similar staining pattern was observed in the cytoplasm using anti-p30 serum. In the early G_1 phase, 100% of the cells were found to be positive and very bright; the intensity of their fluorescence diminished later the mid-G_1 phase.

B. Examination of synchronised FL74 cells by the viable indirect immunofluorescence technique

Synchronised FL74 cells were stained for membrane fluorescence as described in the Materials and Methods part of this Chapter. Cell membrane fluorescence was measured by end-point-titration with monospecific antisera and anti-FOCMA sera. The antibody endpoint was that dilution of reference antisera beyond which less than 50% of the cells showed membrane fluorescence.

Goat anti-rabbit IgG fluorescein conjugate and rabbit anti-cat IgG fluorescein conjugate were used at 1:20 and 1:10 dilutions, respectively.

Normal rabbit serum, normal cat serum and fluorescein conjugate without immune sera were used as controls. As shown in Fig. 71 by applying the various antisera, the following results were obtained :-

With anti-p15 and -p30 sera, the staining pattern of anti-p15 and -p30 sera closely followed the pattern observed in the cytoplasm. Antigen levels began to climb at PR - 4 hr., reached a peak at PR - 10 hr. in the early-G_1 phase and diminished in the mid- and -late G_1 periods.

With anti-gp70 serum, a peak was also reached at PR - 10 hr. but the titres did not drop afterwards. They remained at the same level during the G_1 phase and were dropping only at the G_1/S border.

Anti-FOCMA sera. Both viraemic and non-viraemic anti-FOCMA sera followed the pattern of the anti-gp70 serum, reaching a peak at PR - 10 hr. and remaining at the same level afterwards. However, there was a second and more prominent peak at PR - 24 hr. in the late-G_1 period which declined again at the beginning of the following S phase.

C. Investigation of FOCMA expression using two different synchronising methods

In order to obtain more synchronous population in the G_1 phase, FL74 cells were synchronised by isoleucine deprivation or by chilling. On cells synchronised by these methods, at least one, but often two log higher FOCMA titres were detected than on cells synchronised by excess thymidine.

FL74 cells were sensitive to isoleucine deprivation and the viability of cells decreased rapidly after the second day in deprived medium. No loss of viability was observed after cold treatment, but occasionally cells failed to

to re-enter the cycle and no cell division occurred. Therefore, in every experiment, cell number counts were performed at PR - 0, PR - 33 and PR - 66 hrs. Mitotic indices were also determined.

Results obtained by the use of the various synchronising techniques are shown in Tables 15 and 16, pp.185 and 186.

D. Investigation of FOCMA and viral antigen expression during logarithmic cell growth

Initially, FL74 cells were examined for viral antigen and FOCMA expression on the first, second and third day after subculturing. It can be seen in Table 17, p.187 that viral antigen titres were fairly constant on each day, no significant variations in endpoint titres being detected. However, when cells were examined at 7 p.m. on the first day, 30 hours after subculturing, the titres appeared to be one log higher as compared to the titres measured on the first, second and third day at 1 p.m. At that time, a large proportion of cells were undergoing mitosis and many of them recently entered the G_1 phase. The one log difference in viral antigen expression was due to the presence of a higher number of early-G_1 cells with peak antigen expression in the growing population.

The highest FOCMA titres were measured on the second day after subculturing the cells, owing to the fact that by that time most of the cells underwent mitosis and approached the late G_1 phase. On the third day, the titres were lower again, which might be the consequence of the extensive exfoliation of the third day cells. From the third day on, an increasing number of shed-off blebs could be seen in cultures by light microscopy and also by transmission- and scanning-electron-microscopy.

E. Investigation of FOCMA and gp70 expression on synchronised F422 cells

F422 cells were synchronised by excess thymidine or by cold treatment. After release from the synchrony-inducing block, at time intervals, cells were stained for membrane immunofluorescence using anti-FOCMA and anti-gp70 immune sera. The results obtained are shown in Table 18, p.188.

On cells synchronised by a double TdR block, both anti-FOCMA and anti-gp70 sera produced similar staining patterns. No additional "FOCMA" peak was detected during the G_1 phase of the cell cycle.

As cells tend to lose their synchrony after mitosis, they were synchronised by chilling to attain a more synchronous population in the G_1 phase. After this treatment, a distinct two log higher "FOCMA peak" was detected in the late G_1 period.

The failure to detect the FOCMA peak after TdR synchronisation on F422 cells, as opposed to FL74 cells, might be explained by the difference in the timing of virus release in these cell lines. There is a 14 hour gap between viral- and FOCMA-peaks in FL74 cells, whereas in F422 cells, both peaks occur in the mid - late G_1 period. Therefore the simultaneous occurrence of gp70 peak is likely to camouflage the FOCMA peak which becomes detectable only when the synchrony of cells is increased in the G_1 phase.

F. Investigation of antigen expression on synchronised FeLV infected CT45-S cells

By using anti-FOCMA sera in both FL74 and F422 feline lymphoid cell lines a significant peak was observed in the late G_1 phase of the cell cycle which appeared to be distinct from the viral antigen peaks. In this experiment, the FeLV infected CT45-S canine cell line was examined by cell membrane IF assay.

According to the findings of Hardy and Zuckerman (1977) these cells do not express FOCMA on their membranes. It was important to establish whether, in addition to the viral antigen peak, another extra peak was detectable or not on these cells, because the absence of the extra peak would provide strong evidence for its being a FOCMA rather than a viral peak.

As discussed in Chapter Two, virus release from CT45-S cells occurred during the mitotic and the early-G_1 periods of the cell cycle. Therefore, synchronisation of the cells by a TdR block seemed to be the suitable method.

Cells were synchronised by excess thymidine, and immunofluorescent staining of the cell membranes was performed at time intervals.

To remove non-specific reactivity immune sera were extensively absorbed with uninfected CT45-S cells. The procedure followed is described in the Materials and Methods part of this Chapter.

The results obtained are shown in Table 19, p.189. It can be seen that the use of both anti-FOCMA and anti-gp70 sera resulted in similar staining patterns, and that no FOCMA peak could be resolved.

Since anti-FOCMA serum is not a monospecific serum and even in viraemic anti-FOCMA serum low titres of virus neutralising activities and possibly other multiple specificities are present, CT45-S cells infected with FeLV were positively reacting not only with anti-gp70 but also with anti-FOCMA serum. However, as stated above, no evidence was found for an extra FOCMA activity.

Control CT45-S cells were negative with anti-gp70 and also with anti-FOCMA serum.

5. Discussion

The experiments presented in this Chapter indicate that the expression of virus-associated antigens and FOCMA antigen(s) are cell cycle-related.

FL74 cells chronically infected with FeLV contained intracellular antigen pools which were not utilised for virion production. Therefore, synchronised FL74 cells tested for cytoplasmic immunofluorescence with low dilution of immune sera gave positive results with similar staining intensity throughout the cell cycle. However, with appropriate serum dilutions, 1:100 or 1:200, it was demonstrated that viral antigen expression significantly increased in the early-G_1 phase and decreased again in the mid- and late-G_1 period. Similar staining patterns were observed by using both anti-gs and anti-p30 sera. The periodic fluctuation in staining intensity are most likely to reflect the periodic synthesis of the viral antigens in the cell cycle.

By using anti-p15 and -p30 sera, the pattern of surface immunofluorescence in synchronised FL74 cells closely followed the pattern seen in the cytoplasm. Antigen peaks were observed in the early-G_1 phase which declined later in the cell cycle.

A different staining pattern was detected by using anti-gp70 serum. Antigen titres began to climb around mitosis and reached a peak in the early-G_1 phase, but remained at the same level and diminished only in the following S phase.

The co-ordinate rise of viral structural proteins p15 and p30 and of the envelope glycoprotein gp70 after mitosis and their corresponding rise with virus production, implies that the time between the translation of viral mRNA and the assembly of virus is very short. Using labelled precursors and

metabolic inhibitors. Baluda (1969) suggested that the time between transcription and virus release was about 2 hours in the avian oncornavirus system.

In this study, the cell-associated viral antigens were detected by immunofluorescence microscopy. Applying IF techniques, the fluctuation in the staining intensity of synchronised cells could be demonstrated but no distinction between precursor and mature viral proteins could be made and also no information about the time of the synthesis and cleavage of the viral precursors, could be gained. Therefore, the findings of Naso and Brown (1977) concerning the synthesis and cleavage of Raucher murine leukaemia virus (R-MLV) precursor proteins in synchronised cells were of great interest. FeLV has a very close relationship to R-MLV and probably the synthesis and post-synthetic processes of FeLV and R-MLV proteins are similar.

Viral precursor protein synthesis in cells chronically infected with R-MLV was shown to occur in three distinct waves corresponding to the G_1, middle-S and late S-G_2 phases of the cell cycle. The G_1 wave of viral precursor proteins did not require new viral RNA synthesis, while the two later waves were apparently dependent upon the presence of newly made viral RNA. SDS-polyacrylamide gel electrophoresis of immunoprecipitates from pulse-labelled and pulse-chased cells identified the viral specific proteins made in each wave of synthesis as those precursors and viral cleavage products characteristic of non-synchronised cells infected with R-MLV.

As FeLV release and viral antigen expression appear to be cell cycle-dependent and occur in the early-G_1 phase, the above observations with R-MLV provide evidence for a synchronised synthesis of viral protein precursors prior to virus release in the middle-S and late S-G_2 phases of the cell cycle.

The differences between the appearance and utilisation of the gag gene products p15 and p30 and the env gene product gp70, demonstrated in this study by membrane immunofluorescent test and shown in Fig. 71 might be due to (1) the quantitative differences between the various antigenic sites expressed per unit length of the cell membrane, (2) the different post-translational processing of the precursor polypeptides and (3) the different fractional turnover of the various molecules per unit time.

According to O'Brien et al., (1978), FL74 cells expressed 5.6×10^5 p30 and 7.5×10^5 gp70 antigenic determinants per single cell surface. It was also found that the major core protein (p27-30) and the major envelope glycoprotein (gp70) antigens were physically sufficiently separated on cell surfaces so that binding of either of the membrane antigens with component-specific antibodies did not interfere with binding of antibodies specific for the other. As it will be discussed in Chapter Six, immuno-electron microscopy also revealed that on the FL74 cell membrane, the gp70 antigenic sites were the most numerous compared to the p30 and p15 antigenic sites, the latter being very sparsely expressed.

Studies of mammalian RNA type-C viruses have led to the demonstration that the gag gene codes for a 76,000 molecular weight precursor polypeptide which undergoes post-translational cleavage to give rise to viral structural proteins with molecular weights of 30,000 (p30), 15,000 (p15), 12,000 (p12) and 10,000 (p10) (Stephenson et al., 1975; Barbacid et al., 1976). Okasinsky and Velicier (1977) demonstrated that the small structural proteins of FeLV were also synthesised as part of a 70,000 dalton precursor.

The evidence regarding the cleavage of the internal non-glycosylated gag proteins points to the cleavage taking place on the plasma membrane. Agents which disrupt membranes inhibit the cleavage (Vogt et al., 1975). This would support the idea that cleavage of the non-glycosylated virion protein precursor is intimately associated with virus assembly on the plasma membrane. The incorporation of precursor polypeptide into assembled virions appears to be a unique phenomenon of FeLV and R-MLV (Jamjom et al., 1975; Okasinsky and Velicier, 1977).

The viral glycoproteins are also derived from a precursor polypeptide encoded for by the env gene (Korshin et al., 1977).

The virion precursor glycoproteins are synthesised and cleaved in the rough endoplasmic reticulum (Witte et al., 1977) Cleavage of the glycoprotein precursor before it reaches the plasma membrane would explain why this precursor is never found in mature virions while the gag precursors can be incorporated in mature virions (Hunter et al., 1976).

Studies undertaken to investigate the kinetics of formation and utilisation of viral membrane glycoproteins of Moloney sarcoma-leukaemia virus (MSV-MLV) revealed that core synthesis (p30) and the appearance of recently synthesised products in extracellular virions, was rapid, whereas appearance of labelled membrane glycoproteins (gp69, 71) was delayed (Witte and Weissman, 1974). The same researchers (1976) concluded from later experiments that the delay in appearance of label in extracellular gp69, 71 was due to some post-synthetic process involving passage of the recently synthesised glycoproteins through one or more large intermediary pools

prior to availability for the budding process. Results of lactoperoxidase iodination pulse-chase and immunoprecipitation suggest that such a large pool of 70,000 dalton exists on the cell membrane.

The prolonged excretion pattern, i.e., the slow fractional turnover per unit time, for gp69, 71 molecules is in striking contrast to the rapid excretion rate per unit time, i.e., fast fractional turnover, for p30. If similar post-synthetic processes were operating in FL74 cells, these might account for the rapid appearance and utilisation of the proteins p30 and p15 in the early-G_1 phase which coincides with peak virus release and for the more prolonged presence of the gp70 antigen peak which persists during the whole G_1 phase. Similarly, if FOCMA were distinct from the viral proteins, its synthesis, post-synthetic processing and peak expression on the cell membrane would most likely be temporally different which would account for the 14 hour gap between the viral antigen peaks and FOCMA peak related to the cell cycle.

The detection of a "FOCMA" peak on the feline tumour cell lines FL74 and F422 chronically infected with FeLV and its absence on the FeLV infected canine CT45-S cell line, might suggest that FOCMA is distinct from the viral antigens which is in accordance with recent findings concerning the nature of FOCMA (antigen(s)) (Hardy and Zuckerman, 1977; Essex, 1975; Stephenson et al., 1977; Hardy et al., 1977).

TABLE 14

Examination of Synchronised FL74 Cells by the Cytoplasmic IF Test

Dilution of anti-gs serum	Hours post release	Phase of the cell cycle	Fluorescence positive cells in %	Fluorescence pattern
1:50	2	S	25	+
	4		25	+
	6	G_2	40	+
	8	M	80	++
	10	E-G_1	100	+++
	12		100	+++
	14		100	++
	18	M-G_1	100	++
	22		100	++
	26	L-G_1	100	++
1:100	2	S	0	-
	4		20	+
	6	G_2	40	+
	8	M	75	+
	10	E-G_1	100	+++
	12		100	+++
	14		100	++
	18	M-G_1	100	++
	22		100	+
	26	L-G_1	100	+
1:200	2	S	0	-
	4		0	-
	6	G_2	0	-
	8	M	75	+
	10	E-G_1	100	++
	12		100	++
	14		100	+
	18	M-G_1	0	-
	22		0	-
	26	L-G_1	0	-

TABLE 15

Expression of FOCMA on FL74 Cells Synchronised by Excess Thymidine

Hours post release	Cell No. x 10^5	M.I. in %	Phase of the cell cycle	FOCMA titre end-points	Fluorescence pattern
0	1.45		G_1/S		
2		0.01	S	1:32	+
4		0.4		1:64	+
6		3.4	G_2	1:64	+
8		32.0	M	1:64	++
10	3.4	5.2	E-G_1	1:128	++
18		0.5	M-G_1	1:128	++
24		0.6	L-G_1	1:512	+++
26		0.5		1:512	+++
32		0.5		1:128	++
38	7.65		M		

TABLE 16

Expression of FOCMA on FL74 Cells Synchronised by Cold Treatment

Hours post release	Cell No. x 10^5	M.I. in %	Phase of the cell cycle	FOCMA titre end-points	Fluorescence pattern
0	4.35	1.8	M/G_1		
4		2.4	$E\text{-}G_1$	1:128	+
8		2.6		1:128	++
18		2.4	$L\text{-}G_1$	1:1024	+++
24			S	1:128	++
32		18.0	M	1:64	++
36	10.6	3.2			

TABLE 17

Viral Antigen and FOCMA Titres during Logarithmic Cell Growth

Time (day)	Cell No. x 10^5	M.I. in %	Phase of growth	Titre end-points				Fluorescence pattern
				FOCMA	gp70	p30	p15	
1 (1 pm)	5.6	3.2	Log phase	1:64	1:64	1:32	1:128	++
1 (7 pm)		5.5		1:64	1:128	1:64	1:256	+++
2 (1 pm)	10.5	2.2		1:128	1:64	1:32	1:128	++
3 (1 pm)	12.3	1.0	Stationary Phase	1:64	1:64	1:32	1:128	++

TABLE 18

Expression of FOCMA and gp70 on Synchronised F422 Cells

Synchronisation by TdR block				Synchronisation by cold block			
Hours post release	Phase of the cell cycle	FOCMA titres	gp70 titres	Hours post release	Phase of the cell cycle	FOCMA titres	gp70 titres
4	S	1:64	1:64	2	E-G_1	1:512	1:512
6	G_2	1:64	1:64	4			
8	M	1:128	1:128	8	M-G_1	1:1024	1:1024
12	E-G_1	1:512	1:512	10	L-G_1	1:4096	1:1024
16	M-G_1	1:512	1:512	20	M	1:512	1:1024
18	L-G_1	1:512	1:512				

TABLE 19

Antigen Expression

on Synchronised FeLV-Infected CT45-S Cells

Cell type	Subgroup of FeLV	Phase of the cell cycle	Titres with a FOCMA serum	Titres with a gp70 serum	Fluorescence pattern
CT45-S	AB	S	1:4	1:128	++
		M	1:8	1:256	
		$E\text{-}G_1$	1:32	1:1024	
		$M\text{-}G_1$	1:32	1:1024	
		$L\text{-}G_1$	1:32	1:1024	
CT45-S	B	S	1:8	1:128	+++
		M	1:16	1:256	
		$E\text{-}G_1$	1:128	1:2048	
		$M\text{-}G_1$	1:128	1:2048	
		$L\text{-}G_1$	1:128	1:2048	
CT45-S	C	S	0	1:64	+
		M	1:2	1:128	
		$E\text{-}G_1$	1:16	1:256	
		$M\text{-}G_1$	1:16	1:256	
		$L\text{-}G_1$	1:16	1:256	

FIGURE 71 : Viral and FOCMA Antigen Expression during the Cell-Cycle.

VIRAL AND FOCMA ANTIGEN EXPRESSION DURING THE CELL-CYCLE

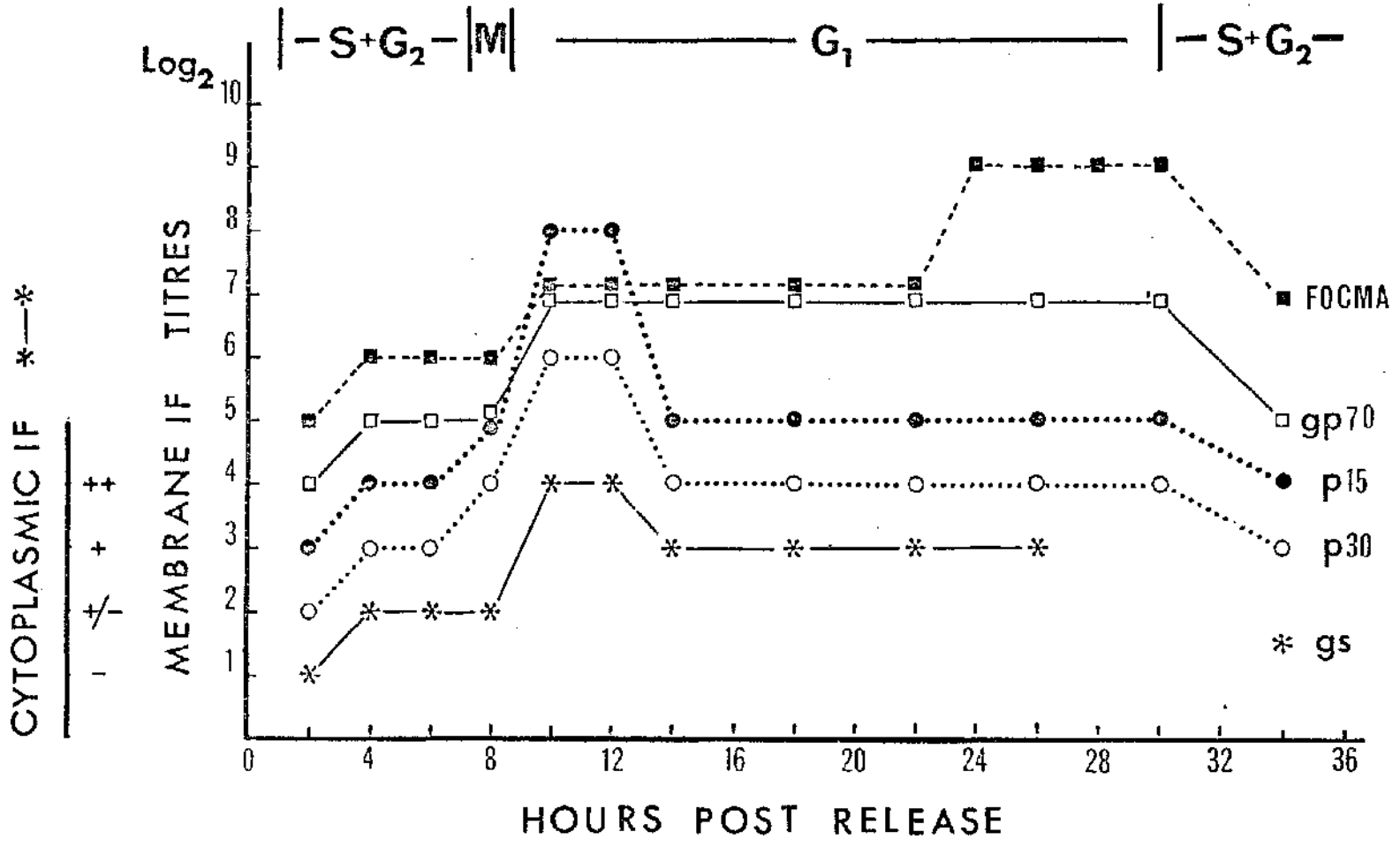

FIGURE 72 : On the cell membranes continuous ring fluorescence can be seen. Viable FL74 cells incubated with cat anti-FOCMA serum and rabbit anti-cat fluorescein-conjugated globulin.

FIGURE 73 : On the cell membranes, patchy fluorescence can be seen. Viable FL74 cells stained as described in Fig. 72. The appearance of the membrane staining is influenced by factors like temperature, titre of the antiserum, and the length of incubation.

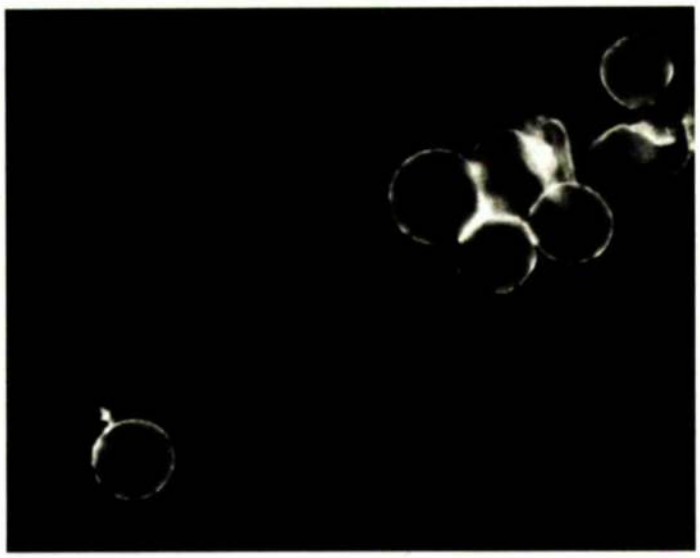

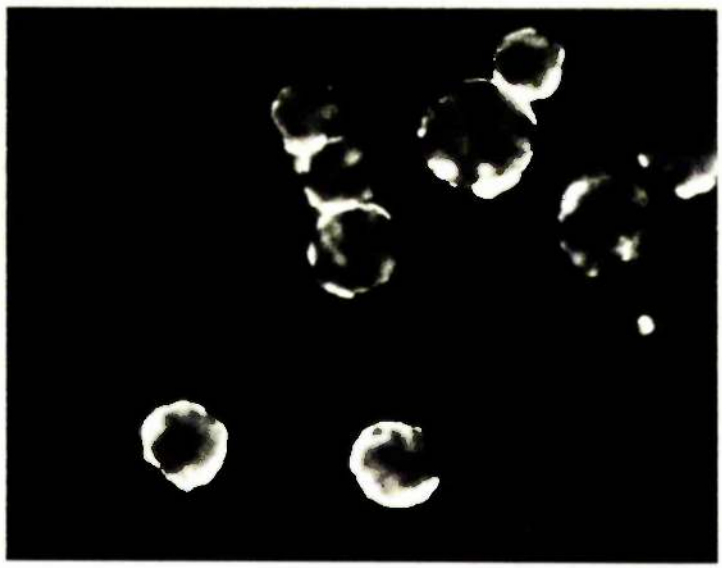

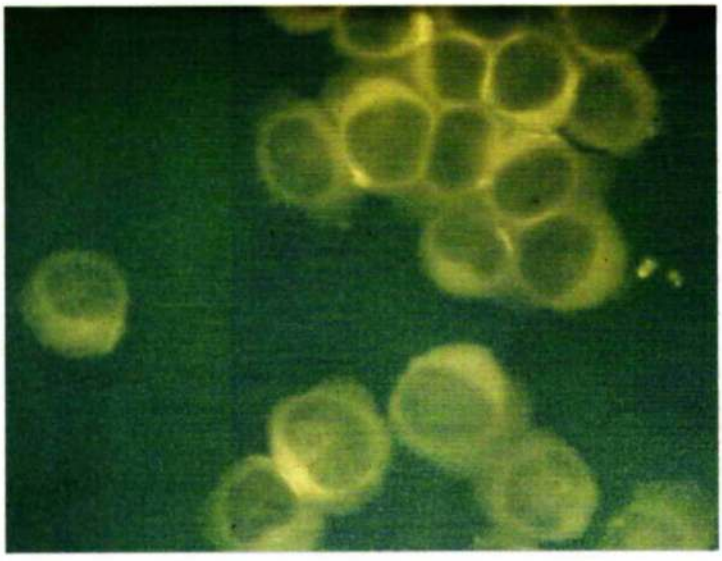

FIGURE 74 : Cytoplasmic fluorescence is shown. Fixed FL74 cells incubated with rabbit anti-p30 serum and goat anti-rabbit fluorescein-conjugated globulin.

CHAPTER FIVE

THE EFFECT OF METABOLIC INHIBITORS ON VIRUS PRODUCTION AND ANTIGEN EXPRESSION

CHAPTER FIVE : THE EFFECT OF METABOLIC INHIBITORS ON VIRUS PRODUCTION AND ANTIGEN EXPRESSION

1. Introduction and Review of the Literature

2. Materials and Methods

3. Experiments and Results

   A. Titration of metabolic inhibitors on FL74 cells

   B. The effect of vinblastine sulfate and cytochalasin B on cell division and virus release

   C. Reversible inhibition of virus release by cytochalasin B

   D. Cell cycle-dependent inhibition of virus release and antigen expression by cytochalasin B

   E. The effect of actinomycin D on virus production and antigen expression

   F. The effect of cycloheximide on virus release

4. Discussion

1. Introduction and Review of the Literature

In order to investigate the kinetics of FeLV production and to explore some of the regulatory mechanisms responsible for the expression of viral antigens in FL74 cells, the effect of various metabolic inhibitors was examined. An attempt was also made to determine the events which impose cell cycle-dependence on virus replication and antigen expression.

Inhibitors of protein synthesis (cycloheximide) and RNA synthesis (actinomycin D) were applied, and also the effect of cytochalasin B and vinblastine sulfate on virus release and antigen expression was investigated.

Cycloheximide ($C_{15}H_{23}NO_4$) is an inhibitor of protein synthesis; it interferes with polypeptide chain elongation in the translation process.

Actinomycin D (AMD) is a potent inhibitor of RNA synthesis in eukaryotic cells. Protein synthesis diminishes in cells treated with AMD. This was originally attributed to decay of messenger RNA (mRNA), but more recently an additional effect of the drug at the level of initiation of protein synthesis has been indicated, although the mechanism of this putative action has not been fully explored (Singer and Penman, 1972; Craig, 1973).

One possible way to approach the problem of the regulation of cell surface antigen expression is to use inhibitors of nucleic acid and protein synthesis.

AMD added to logarithmically growing YCAB mouse lymphoma cells increased the proportion of antigen-positive cells and their antibody absorptive capacity. This effect was dose dependent. The AMD-induced antigen expression was blocked in a dose-response fashion by inhibitors of protein

synthesis (cycloheximide and puromycin). However, inhibitors of DNA sythesis (cytosine arabinoside, hydroxyurea and mitomycin C) had no effect (Cikes and Klein, 1972).

Turner et al., (1972) enzymatically removed the histocompatibility antigens from the surface of intact human peripheral lymphocytes and studied their re-expression in the presence of puromycin and AMD. The HL-A2 antigen was fully expressed during a 6 hour incubation of the cells in fresh growth medium. The re-expression was completely inhibited by puromycin (50 mg/ml). AMD concentrations which caused 98% inhibition of ^{3}H-uridine incorporation allowed a 70% re-expression of the HL-A2 antigenic content. These findings were interpreted as an indication that the antigen was re-synthesised de novo and the synthesis had been taking place on pre-existing templates.

Similar kinetics for the re-expression of cell surface antigens were observed on Meth A ascites fibrosarcoma cells following removal of their H-2 antigen by papain (Schwartz and Nathenson, 1971) and for the regeneration of surface sialoglycoproteins on TA3 mouse mammary adenocarcinoma cells following treatment with neurominidase (Hughes et al., 1972). Ferrone et al., (1972, 1974) also observed a reduced HL-A antigen expression in puromycin-treated WIL_2 cultured human lymphoid cells.

The above results are reminiscent of the superinduction by AMD of the production of enzymes, antibodies and interferon in cultured cells (Garren et al., 1964; Thompson et al., 1970; Reif-Lehrer, 1971; Ambrose, 1969; Sejkalova et al., 1970; Tan et al., 1970).

The finding of an enhanced antigen expression in cells with suppressed RNA synthesis suggests a post-transcriptional control of antigen synthesis. In a model proposed by Tomkins et al., (1969) for the regulation of gene activity in cells of higher animals, this paradoxical effect of AMD was suggested. The model postulates the existence of a short-lived repressor which inactivates the specific mRNA. AMD is envisaged as preferentially inhibiting the short-lived mRNA for repressor(s) of specific mRNAs. The latter RNAs are relatively long-lived and in the absence of their repressor(s) can thus be fully translated.

The replication of oncornaviruses is mediated through proviral DNA. Therefore, AMD can be applied to inhibit the synthesis of viral RNA and subsequently virus production. The primary function of the viral RNA transcribed from DNA is to serve as messenger RNA for viral protein synthesis. It is also encapsulated in the mature virion.

The effect of AMD on the synthesis of reverse transcriptase-containing leukaemia-sarcoma viruses has been studied in great detail. It was shown that virus pnfected cells, upon treatment with AMD, cease viral RNA synthesis (Bader, 1964; Temin, 1963 Duesberg, 1967; Bases, 1967) and markedly reduce virus production (Temin, 1963; Bader, 1964; Vigier, 1964). Baluda and Nayak (1969) and Bader (1970) provided evidence that virus assembly and virus release continued for at least 1 or 2 hours after the addition of AMD. Levin et al., (1974) showed that the production of MuLV persisted for at least 6 hours in AMD-treated cells. Recently, Sarkar et al., (1977) investigated the effect of AMD on the synthesis of MuMTV-RNA and proteins and demonstrated that the treatment of cells with AMD at a concentration

of 0.5 μg/ml. inhibited the production of viral RNA but did not prevent the formation of viral proteins and their assembly into mature virion for a period of approximately 10 hours. It was concluded that a considerable pool of viral RNA for both messenger function and encapsulation existed within the cell system used.

Termination of protein synthesis with cycloheximide in cells producing MuLV resulted in a rapid decay in MuLV production and also in viral structural protein synthesis, whereas AMD-treated cells continued to produce virion proteins (Levine et al., 1974). Levine and Rosenac (1976) postulated the presence of a polyribosomal RNA with a functional half-life of 6 to 8 hours and a genomic virion RNA with a functional half life of 1.5 to 2 hours.

The response of FeLV production and FeLV-associated cell surface antigen synthesis in FL74 cells in the presence of inhibitors of mRNA was examined by O'Brien and Boone (1977). Virus production was affected within 3 hours of exposure to AMD but viral antigen synthesis continued for 10 hours before AMD effect was observed. These data also suggest the existence of two different RNA species which are rate-limiting under conditions of inhibition of RNA synthesis: a short-lived virion-limiting RNA and a more stable mRNA which specified the viral antigens.

The effect of metabolic inhibitors on the production of Ki MSV (Ki MuLV) during synchronous cell growth was studied by Panem and Kirsten (1967). Application of AMD resulted in inhibition of virus release when the drug was applied during late-S and early-G_2 periods. p30 expression

in the cytoplasm was also lowered if RNA synthesis was inhibited during late-S and middle-G_2 phases.

Cytochalsin B (CB) is a metabolite produced by the fungus Helmintosporium dematioideum. A wide variety of transport and motile processes in eukaryotic cells are affected by its application. At relatively low concentrations (0.1 - 10μM) the drug inhibits uptake of glucosamine as well as glycoprotein and mucopolysaccharide synthesis in some cultured cells (Sanger and Holtzer, 1972). CB interferes with glycosylation mainly through inhibition of the transport of certain monosaccharides across the plasma membrane (Kletzien and Perdue, 1973). At higher concentrations (1 - 100 μM/ml.) CB affects cell morphology and inhibits a wide range of motile processes including cell locomotion, cytoplasmic streaming and cytokinesis (Sanger and Holtzer, 1972; Carter, 1972). Recently, Lin et al., (1978) concluded that the effects of CB on sugar transport and on cell motility and morphology were separate and independent events, mediated by the binding of the drug to specific cellular receptors.

Vinblastine sulfate (VB) is a potent inhibitor of cellular proliferation which exerts its action through metaphase arrest. VB poisons the mitotic spindle apparatus by binding to microtubular protein and disaggregating microtubules (Olmsted and Borisy, 1973). VB acts at the biochemical level as an inhibitor of the conversion of glutamic acid to both urea and citric acid cycle intermediates (Pfeiffer, 1967).

CB and VB inhibited the release of KiMSV (KiMuLV). Concentrations of VB which inhibited virus release also inhibited mitosis and cell division. In contrast, low concentrations of CB inhibited virus release without affecting

cell division (Panem and Kirsten, 1976). CB inhibition of virus release from synchronously growing NRK-K cells was shown to be cell cycle-dependent (Panem, 1977).

The effect of impaired glycosylation on the synthesis of envelope proteins of Rauscher murine leukaemia virus was investigated in pulse-labelling experiments. CB did not affect the proteolytic cleavage of the virus-specific precursor polypeptides gag-pr 75 and gag-pr 65. In contrast, CB had an inhibitory effect on the production of the glycosylated precursor polypeptide env-pr 82. This inhibitory effect of CB, however, was reversible (Van de Ven et al., 1977).

Cytochalasin D (CD) which has only one effect, the disruption of microfilaments, inhibited MuLV production in chronically infected mouse thymus-bone marrow cells by 70-80 per cent. Co-capping of MuLV-proteins and actin was demonstrated in the same cells by double immunofluorescent staining. It was proposed that a connection between actin and virus-specific cell surface antigens might exist in a similar fashion as it exists between actin and H-2, and actin and surface immunoglobulins (Mousa and Bechberger, 1978).

2. Materials and Methods

Metabolic inhibitors were purchased from Sigma Chemical Co.

Stock solutions of cytochalasin B in dimethyl sulfoxide (DMSO) containing 10 μg of CB/ml were stored at -20°C.

Vinblastine sulfate was stored at -20°C in a stock solution containing 100 μg of VB/ml.

Actinomycin D was stored at -20°C in lyophilised form and solubilised in ethanol as needed for each experiment.

Cycloheximide was stored at -4°C and freshly prepared for each experiment.

Cells, culturing of the cells, synchronising and immunofluorescence techniques were described in the previous Chapters.

3. Experiments and Results

A. Titration of metabolic inhibitors on FL74 cells

First, the relative viability of FL74 cells was tested by the trypan blue exclusion test over a 24 hour period of growth in the presence of each of the metabolites at various concentrations.

AMD and CH were used at concentrations of 0.1 μg/ml. and 10 μg/ml., respectively. In the first 8 hours, cell viability remained fairly constant, approximately 70 - 75%, whereas all the cells died when incubated with AMD or CH for 15 or 20 hours.

CB and VB appeared to be cytotoxic at high concentrations only (10 - 20 μg/ml. and 1 - 2 μg/ml., respectively).

B. The effect of Vinblastine Sulfate and Cytochalasin B on cell division and virus release

Replicate cultures of logarithmically growing FL74 cells were incubated overnight with fresh growth medium containing inhibitors at various concentrations The following morning cell viability was tested by the trypan blue exclusion test and, in addition, cell number counts and mitotic index determination were performed. The remaining cells were processed for EM. The results are shown in Table 20, p.212. At concentrations of 0.25 - 0.5 μg/ml, VB completely blocked cells from passing through metaphase. The mitotic index was fairly high, 10 - 12% and the cell viability was not greatly affected (71 - 75%). Concentrations greater than 1.0 μg/ml. caused crenelation of the cell membrane along with loss of viability. The lower concentrations were therefore used in subsequent experiments.

Even at low concentrations, VB inhibited virus release by 60% but at the same time inhibited mitosis and cell division. Therefore, its inhibitory

effect on virus release was due to the fact that cells were prevented from undergoing mitosis and reaching the early-G_1 phase where virus release occurred.

At low concentrations of 0.5 - 1.0 μg/ml., CB did not interfere with cell division. The viability of the cells remained high, 81 - 87%. At higher concentrations, 5.0 - 10.0 μg/ml., the number of cells did not increase and large, round, binucleated cells were observed by light and electron microscopy. Apparently, CB at those concentrations inhibited the separation of daughter cells. CB-inhibited, binucleated cells are shown in Fig. 75. At the concentrations of 20 - 25μg/ml., CB also exerted cytotoxic effects on cells as judged by EM. At a low concentration of 1.0 μg/ml., CB inhibited virus release by 50% relative to controls without affecting cell division. The cells inhibited by 0.1 μg/ml of CB did not show accumulation of budding forms on their surfaces when examined in the EM. Therefore, it was concluded that the CB inhibitory effect on virus release was mediated by its interference with the normal glycosylation process of viral envelope proteins.

C. Reversible inhibition of virus release by cytochalasin B.

The reversibility of CB inhibition was examined. Replicate cultures of exponentially growing FL74 cells were incubated in fresh growth medium containing 1.0 μg/ml. CB. After 3 hours, CB was removed by washing the cells twice and resuspending in fresh growth medium without the drug.

Samples were processed for EM at 0, 2 and 4 hours following drug removal. Mitotic indices were also determined. Control cultures were treated similarly but the drug was omitted.

During the time of the experiment, both the control and the CB treated cultures showed unchanged, 3.5%, mitotic indices which were usually

found in exponentially growing cells. When thin sections of cells were examined, it was found that cells at 0 hr after drug removal had fewer budding particles (20/100) than the control cells (40/100). Whereas, cells 2 and 4 hours after drug removal showed a higher number of budding particles (80/100) than the control cells (40/100).

These data suggested that the inhibitory effect of CB was not only rapid, but it was easily reversible.

D. Cell cycle-dependent inhibition of virus release and antigen expression by Cytochalasin B

In order to determine the time of CB inhibitory effect in the cell cycle, FL74 cells were synchronised by excess thymidine and after the removal of the synchrony inducing block, replicate cultures were treated with 1μg/ml. of CB for decreasing times during synchronous growth. At post-release 10 hr., which is the time of the viral peak, samples were taken. From each sample half of the cells were processed for EM and the other half were used for mitotic index determination and for preparation of slides using a cytocentrifuge. Cells were dried, fixed in acetone for 10 minutes and stored at -20°C. Later, cells were stained for cytoplasmic immunofluorescence by using anti-p30 and -gp70 immune sera in 1:100 dilutions.

Table 21, p213 shows that virus release and gp70 expression in the cytoplasm were inhibited by CB in a cell cycle-dependent fashion, whereas the synthesis of p30 antigen was not affected by the drug. When the drug was present during S and early-G_2 periods, the number of budding C-type particles was lowered and the intensity of the cytoplasmic staining by anti-gp70 serum was greatly reduced.

The presence of CB during late-G_2, M and early-G_1 phases did not influence virus release and cells stained for cytoplasmic immunofluorescence showed similar brightness to that of the control cells.

From these data it was concluded that CB was most likely to have affected the glycosylation process of envelope precursor proteins which recently was shown to be synthesised in two distinct waves, during middle-S and late-S-G_2 phases of the cell cycle (Naso and Brown, 1977).

CB had no effect on the synthesis of non-glycosylated gagprecursor polypeptides.

E. . The effect of actinomycin D on virus production and antigen expression

Viral RNA transcription is very sensitive to AMD (Bases and King, 1967; Duesberg and Robinson, 1967; Paskind et al., 1975). 0.1 μg/ml. of drug was shown to be sufficient to reduce by 90% the incorporation of ^{3}H-uridine into extracellular virions.

In these experiments, the response of FeLV production, viral and FOCMA antigen synthesis in the presence of AMD were examined.

Duplicate cultures of FL74 cells were incubated in fresh growth medium containing 0.1 μg/ml. AMD. At 2, 4 and 8 hour intervals, samples were taken. Cells were processed for EM and from each block, 100 cell profiles were examined for budding particles. It was found that virus production was not inhibited after 2 hours, slightly inhibited after 4 hours and more than 50% inhibited after 8 hours incubation in the presence of the drug. After that period, cells showed cytotoxic changes and soon died.

Higher inhibitory effect of AMD was reported when virus release was measured by biological (Paskind et al., 1975) or by reverse transcriptase assays or by the measurement of the incorporation of ^{3}H-uridine in extracellular particles (Levin et al., 1974). Therefore, depending on the virus assay system, results can be strikingly different after AMD treatment of cells. When virus release is measured by counting budding particles, only the inhibition of maturation and budding process can be followed which is, in turn, a secondary effect of the inhibition of viral RNA or viral-precursor mRNA and the resulting reduced protein synthesis. The fact that virions continued to be synthesised and released in the first hours after AMD treatment suggested that virus production was dependent upon a relatively large intracellular viral RNA pool.

Experiments were also performed to establish the exact period(s) in the cell cycle during which in the presence of AMD the inhibition of virus release and antigen expression occurred.

FL74 cells were synchronised by a double TdR block. At various times during synchronous growth, replicate cultures of cells were treated for 2 hours with 0.1 μg/ml. of AMD. After 2 hours, the medium containing the drug was removed, cells were washed twice and fresh growth medium was added. Previously, it had been determined that maximal antigen expression and virus production occurred at 10 hr. post release, therefore samples were taken at PR-10 hr. Each culture was divided into three parts. One part of the cells was processed for EM, the second part was deposited on slides, fixed in acetone and stored at -20°C, while the third part was immediately stained for cell membrane immunofluorescence and also used

for MI determination to assess the degree of synchrony achieved.

The results are shown in Table 22, p.214.

AMD inhibited virus release and viral antigen expression in the cytoplasm when it was applied during early-S and late-S- early-G_2 phases, PR 0-2 and PR 4-6 hr., respectively. Inhibition was more pronounced when AMD was present during late-S -early-G_2 periods. On the cell membrane, similar endpoint titres were measured by using anti-gp70 and an anti-FOCMA sera, irrespective of the presence of the drug. The drastically reduced cytoplasmic immunofluorescence in cells treated with AMD in S and early-G_2 phases was thought to be caused by the inhibition of viral precursor polypeptide mRNA which was also reflected in the reduced rate of virus release. The continuous presence of cell membrane antigens, gp70 and FOCMA, respectively, indicated that a considerable pool of membrane associated proteins existed in these cells and/or that more RNA species with different functional half lives were operating in the viral synthetic process.

Attempts to treat cells with AMD at various times during synchronous cell growth and to collect samples at the time when FOCMA peak occurred (PR-24 hr.) were highly unsuccessful because cells died sooner. Similarly, cells cultured in the continuous presence of AMD died before reaching the time of viral and FOCMA peaks in the cell cycle.

F. The effect of cycloheximide on virus release

As previously described, AMD treatment of exponentially growing cells had minimal effect on virus release during the first 4 hours of growth. This suggested that the viral particles released utilised viral RNA which

existed prior to AMD inhibition. In this experiment, the effect of CH on protein synthesis and virus release was examined.

Duplicate cultures of exponentially growing FL74 cells were incubated with fresh growth medium containing 10 μg/ml. of CH. At 2, 4 and 8 hour intervals, samples were taken. Cells were processed for EM and cell number and viability counts were also performed. Thin sections were examined for budding C-type particles. Control cultures were similarly treated without drug. Results are shown in Table 23, p.215.

No increase in cell number was seen in cultures treated with CH. CH had a far more rapid effect on virus production than AMD did. Virus release was drastically reduced by 2 hours and ceased almost completely by 4 hours after treatment, indicating that virus release was highly sensitive to CH. This sensitivity reflected the requirement for synthesis of rate-limiting viral and/or cellular proteins. As oncornavirus production was shown to be dependent upon cell growth (Temin, 1971), the effect of CH on virus release was possibly the consequence of inhibited cell growth. However, viral protein synthesis was equally inhibited in the presence of the drug (Paskind et al., 1975).

It follows from this that CH must have influenced virus release by inhibiting both cellular and viral protein synthesis.

4. Discussion

Using a variety of metabolic inhibitors, the factors limiting virus release and antigen expression were investigated.

Mitosis has a prominent role in oncornavirus replication. It was shown to be required not only for virus release but also for the appearance of virus specific RNA (Humphries and Temin, 1974) and for the production of viral proteins (Fischinger et al., 1975). Therefore, inhibitors of contractile element functions were first examined.

Vinblastine sulfate which disrupts microtubules greatly inhibited virus release. This was the consequence of cells being blocked in metaphase by the drug and not being able to undergo mitosis.

Cytochalasin B in higher concentrations was shown to affect a later step in the mitotic process. Cytokinesis, the separation of daughter cells was inhibited by this drug. Large, round, binucleated cells were seen in cultures treated with CB. The considerable decrease in virus release caused by high doses of CB was due to its interference with mitosis.

When lower doses of CB were applied, they did not interfere with mitosis. No binucleated cells were seen and the number of cells normally increased. However, in the presence of 1.0 μg/ml. of CB, virus release was still affected. Cells were producing 50% less virus particles than the untreated control cells. Low doses of CB interfered with the transport of certain monosaccharides across the plasma membrane (Kleitzen and Perdue, 1973). CB was shown to prevent the synthesis of the precursor polypeptides of Rauscher murine leukaemia virus glycoproteins (Van de Ven et al., 1977). Therefore, it was concluded that the inhibition of FeLV release by low doses of the drug was due to the impaired glycosylation of the viral glycoprotein precursors.

Cleavage of the glycoprotein precursor was found to take place before it reached the plasma membrane (Van de Ven et al., 1977). Impaired glycosylation might interfere with cleavage and formation of viral glycoproteins. Although cleavage of the precursor polypeptide may not be directly associated with assembly and virus release but the lack of the cleavage products might indirectly influence the normal budding process. Glycoproteins may be important also in controlling the selective incorporation of virion components and the exclusion of host plasma membrane proteins.

It was also established that the inhibitory effect of CB was rapid, reversible and cell cycle-dependent. Virus release and cytoplasmic antigen expression were greatly reduced when CB was applied during S and early-G_2 periods. These results are consistent with the finding that viral precursor polypeptides are synthesised during mid-S and late-S -G_2 phases of the cell cycle (Naso and Brown, 1977).

Replication of oncornavirus is inhibited by Actinomycin D (Bader, 1964; Robinson, 1966; Allen, 1966; Baluda, 1969; Bases, 1967; Bader, 1970; Paskind et al., 1975; Jamjom et al., 1976; Levin, 1976; Panem, 1976; O'Brien and Boone, 1977; Sarkar et al., 1977).

The experiments with AMD showed that the major inhibitory effect of this drug was upon RNA synthesis which was arrested within 30 minutes after application of the drug. Virus release can be measured several ways, and, depending on the virus assay system used, the time by which virus production is affected by AMD will vary.

The interval between completion of the synthesis of RNA and its appearance in released virions was determined to be about 70 minutes. AMD prevented the appearance of viral RNA extracellularly if added within 15 min.

after labelling (Bader, 1970). Comparison of the effect of AMD on the biological titre with its effect on virion-bound reverse transcriptase activity showed strikingly different results. Biological titre of virus (XC assay) was reduced less than 10% after 6 hours of treatment with AMD but the cells were still producing 40% of the normal amount of reverse transcriptase-containing particles (Paskind et al., 1975). Similarly, Levin et al., (1974) reported that AMD treatment of cells allowed the release of viral particles which contained virion-bound reverse transcriptase but lacked viral RNA.

In the present experiments, virus release was monitored by EM. Therefore, only the inhibition of virion assembly and the actual budding process could be observed. AMD inhibited FeLV release gradually. Maximum inhibition was seen after 8 hours; by this time virus release was reduced by 65% which possibly reflected the inhibition of viral protein synthesis.

Contrary to AMD, cycloheximide inhibited virus release rapidly and completely. Not only the synthesis of viral proteins but cell division was also affected in the presence of CH. This suggested that it was necessary for FeLV production that regulatory systems influencing cell division remained unimpaired.

Inhibition of viral antigen synthesis and virus release by AMD was cell cycle-dependent and occurred in the early-S and late-S -G_2 phases of the cell cycle.

Viral precursor polypeptide synthesis in R-MuLV-infected cells was shown to be cell cycle-related and it occurred in the early-S and late-S - early G_2 periods (Naso and Brown, 1977). If similar macromolecular regulatory systems are operating in FeLV infected cells, then the decrease in antigen and FeLV production could be caused by the inhibition of the viral precursor polypeptide synthesis.

The appearance of cell membrane antigens was not affected by AMD no matter at which phase of the cycle it was present. Possibly a large cell membrane antigen pool existed in FL74 cells. That such a large pool of glycoproteins existed in the MSV (MLV)- infected cell membrane was demonstrated by Witte and Weismann (1976). Glycoproteins which were synthesised before AMD inhibition occurred, could also be delayed by intracellular processing, transit and appearance on the cell membrane and prolonged presence in the membrane pre-bud pool(s) before passage to the actual budding complex.

One attempt was made to measure FOCMA expression in the continuous presence of AMD or by treating cells with AMD at various intervals during synchronous cell growth. Unfortunately, cells died before they could have reached the late-G_1 period where FOCMA peak expression occurred. When cells were treated with AMD in early-S and late-S - early-G_2 periods and were stained with anti-FOCMA serum in the early-G_1 phase, their viability remained fairly high. However, on both AMD treated and untreated cells similar endpoint titres were measured. Thus, anti-FOCMA serum produced similar results to anti-gp70 serum. This might be explained in several ways. For example, it is possible that anti-FOCMA serum contained anti-gp70 specificities and in early-G_1 phase these were measured on cells instead of FOCMA. Alternatively, synthesis of FOCMA was specified by a mRNA which responded to AMD inhibition in the same way as the viral specific mRNA did. To ascertain the precise nature of the underlying mechanism, however, would have required further experiments which would have been beyond the scope of the present study.

To sum up, in this study, the effects of various metabolic inhibitors on FeLV replication in chronically infected cells were investigated. It was found that virus production was regulated by a complex, cell cycle-dependent RNA, mRNA, viral and cellular protein synthesis which was co-ordinated by mitosis.

TABLE 20

Inhibition of Cell Division

by Vinblastine Sulfate and Cytochalasin B

Inhibitor Concentrations µg/ml	No. of cells x 10^5/ml.	Mitotic Index in %	Viability in %	No. of buds/ 100 cell profiles
Vinblastine SO_4				
Control	6.5	3.2	78	120
0.25	5.0	10.2	75	60
0.5	5.0	12.0	71	40
1.0	3.2	Cytotoxicity		20
2.0	2.5	"		-
Cytochalasin B				
Control	8.9	3.5	87.2	112
0.5	6.15	3.5	81.0	84
1.0	6.05	3.4	85.2	56
5.0	3.85	3.4	72.0	40
10.0	3.95	3.4	69.0	-

TABLE 21

Cell Cycle-Dependent Inhibition of Virus Release and Antigen Expression by Cytochalasin B

Time of CB treatment Hours post release	No. of budding C-type particles/ 100 cell profiles	Pattern of cytoplasmic fluorescence a gp70	Pattern of cytoplasmic fluorescence a p30
2 - 10	68	+	+++
4 - 10	70	+	+++
6 - 10	100	+++	+++
8 - 10	110	+++	+++
9 - 10	105	+++	+++
Control	110	+++	+++

TABLE 22

The Effect of Actinomycin D on Virus Release and Antigen Expression during Synchronous Cell Growth

Time of AMD treatment Hours post Release	No. of budding C-type particles/ 100 cell profiles	Pattern of cytoplasmic fluorescence a gs serum	Membrane endpoint titres a gp70 serum	Membrane endpoint titres a FOCMA serum
0 - 2	60	++	1:256	1:128
2 - 4	100	+++	1:256	1: 128
4 - 6	32	+/-	1:256	1:128
6 - 8	102	+++	1:256	1:128
Control[a]	108	+++	1:256	1:128

[a] Both AMD treated and untreated control cells were examined at 10 hr post release in the early-G_1 phase.

TABLE 23

Inhibition of Virus Release

by Actinomycin D and Cycloheximide

Hours after treatment	Drugs Present				No drug present			
	AMD		CH		Viability in %	No. of buds/ 100 cell profiles	Cell number x 10^5/ ml.	Viability in %
	No. of buds/ 100 cell profiles	Cell number x 10^5/ ml.	No. of buds/ 100 cell profiles	Cell number x 10^5/ ml.				
2	36	5.5	10	5.5	75	40	5.5	8(
4	28	5.6	2	5.5	72	38	5.8	8:
8	12	5.8	0	5.4	68	39	6.0	8(

FIGURE 75 : Cytochalasin B-treated binucleated FL74 cell.

CHAPTER SIX

DETECTION OF CELL SURFACE ANTIGENS BY IMMUNOELECTRON MICROSCOPY

CHAPTER SIX : DETECTION OF CELL SURFACE ANTIGENS BY IMMUNOELECTRON MICROSCOPY

1. Immunoferritin Technique

2. Review of the Literature

3. Materials and Methods

4. Experiments and Results

   A. Determination of the distribution of ferritin monomers, dimers and higher oligomers in glutaraldehyde cross-linked IgG preparations

   B. Comparison of various prefixation methods and their effects on the preservation of antigenic sites

   C. Appearance and distribution of viral structural antigens and FOCMA on the surface of FL74 cells

   D. Ferritin labelling of CT45-S cells using FOCMA antiserum

   E. Ferritin labelling of synchronised FL74 cells

   F. Investigation of cell membrane antigens under capping conditions. An immunofluorescence-immunoferritin study

5. Discussion

1. Immunoferritin Technique

The investigation of the molecular architecture and dynamic organisation of biological membranes received considerable impetus from technical progress in biochemistry and biophysics, e.g., polyacrylamide gel electrophoresis in the presence of detergents and the measurement of lipid viscosity. However, with these methods alone no information can be obtained concerning the topographic arrangement and interaction of membrane constituents. Another approach to membrane research is based on immuno- histo- and cytochemical methods and in particular, on the immunoferritin labelling technique at the electron microscopic level.

Conventional transmission electron microscopy is based on the different electron scattering intensities of the components in the object under investigation. The electron density of biological specimens consisting mainly of carbon, hydrogen, oxygen and sulphur is often so weak that it has to be increased by artificial contrasting. This is achieved by making use of the varying affinity of different chemical groups to heavy metal atoms such as lead citrate and uranyl acetate.

Antigenic changes on the cell surface following transformation of a normal cell are of great theoretical and practical interest. While antigens are not detectable in the EM, antibodies are large enough to be resolved, but even in stained preparations they do not display sufficient electron dense properties. Application of labelled antibody of known specificity permits localisation of its respective antigen in the antigen-antibody complex.

In 1954, Farrant proposed horse spleen ferritin as a suitable marker for EM and in 1959, Singer prepared covalent ferritin-antibody conjugates

using bivalent di-isocyanates as coupling reagents. Such conjugates were first used by Morgan et al., (1960) for the detection of influenza virus structural antigens. The immunoferritin technique was later modified by using heavy atoms such as uranium and gold (Sternberger et al., 1963, 1965; Faulk and Taylor, 1971) or enzyme-substrate complexes (Avrameas, 1969, 1970; Sternberger et al., 1970) as marker molecules. Since di-isocyanates react with every lysin residue, they produce aggregation and the specific binding regions of the antibody are often sterically hindered. In addition, the coupling conditions destroy part of the antibody activity so that only 10% of the initial activity of the native antibody is available. These drawbacks were greatly overcome by the hybrid-antibody technique (Hämmerling et al., 1968). Ferritin labelling by this technique is not dependent on covalent binding of ferritin to antibody but on the specific combination of ferritin with anti-ferritin antibody globulin. Hybrid-antibody molecules of dual specificity can be obtained by combining univalent fragments of pepsin-treated antibodies of different specificities. While the technique is highly sensitive and specific, the preparation of hybrid antibodies requires the use of a variety of buffer-systems and immunoadsorbents.

Recently, glutaraldehyde (GA) was found to be suitable as a coupling reagent for attaching ferritin to antibody. Unlike other conjugants which are almost insoluble in water, GA is totally water-soluble. The coupling reaction with GA leads to reproducible amounts of conjugates and can be standardised easily. The conjugates are stable, they can be stored at $4^{o}C$ for several months. The stability of the conjugates may be explained by the finding that the cross linkages produced in proteins by GA are mainly the result of stable

Michael-type adducts formed between amino groups and α, β unsaturated aldehydes (Richards and Knowles, 1968; Payne, 1973).

Initially, GA was used in a one-stage reaction in which antibody and ferritin were simultaneously exposed to GA (Avrameas, 1969; Siess et al., 1971; Neauport-Santes and Slivester, 1972, Micheel, 1972).. Although this method was quick, easy and fairly reliable, it was not entirely satisfactory since, as a consequence of direct exposure of antibodies to GA, reduction in antibody activity and formation of undesirable aggregates might occur. Both of these disadvantages were avoided by the use of a two-stage method whereby antibody was conjugated to ferritin pre-treated with GA (Otto et al., 1973; Takamiya et al., 1974, 1975; Kishida et al., 1975). Although both aldehyde groups of the GA molecule have the same intrinsic reactivity, the properties of the ferritin molecule permit a two-stage reaction. In contrast to globulin, or albumin, intermolecular cross-linkages between ferritin molecules are less frequently formed.

Ferritin is an iron storage protein. The molecule has a diameter of about 100 - 200 A^{o} and has a high, 20% iron content up to 4,000 iron atoms per molecule are contained in a micellar core of 60 A^{o} in diameter which has a high electron scattering potential in spite of the relatively low atomic weight of Fe (=56). The core is surrounded by a protein shell. Ferritin has a molecular weight ranging between 600,000 - 750,000 daltons. The iron-depleted protein shell, called apoferritin, has a molecular weight of 465,000 daltons.

2. Review of the Literature

Since its introduction in 1959, the immunoferritin technique (IFT) has been used in a variety of immunological investigations. These include the identification of viral antigens (Morgan et al., 1961; Rezko et al., 1962; Biberfield et al., 1966; Howe et al., 1967; Levinthal et al., 1967; Oshiro et al., 1967; Duc-Nguyen et al., 1967; Nii et al., 1968; Breeze, 1969, 1970; Micheel, 1970; Hampar et al., 1970, 1971; Wagner et al., 1970); the localisation of surface antigens on bacteria (Walker et al., 1966, 1967; Katz, 1970; Fukushi et al., 1968; Kushnarev et al., 1969); red blood cells (Davis et al., 1968; Mardiney et al., 1968; Silvestre et al., 1969; Kourlisky et al.; 1971); mouse lymphocytes (Aoki et al., 1969; Taylor et al., 1971; Parr and Oei, 1973) and on human fibroblasts (Hedman et al., 1978); the localisation of the production of enzymes and myosin in cells (Shimazakin et al., 1966; Olsen et al., 1975; Samosudova et al., 1968); studies on the mechanism of certain experimental and human diseases (Porter et al., 1968; Andres et al., 1970).

In the oncornavirus system, the first study with IFT was by Tanaka et al., (1967) who examined the localisation of viral antigens in mouse mammary tumours. It was found that only mature and budding virus particles were labelled, while the cell membrane was free from specific staining. In another study, Rous sarcoma virus-infected rat cells were treated with chicken antibody to RSV. Conglomerates of ferritin were found in the outer third of cytoplasm, sometimes also in vesicles (Lindberg et al., 1967). In order to investigate the localisation of Graffi virus-induced cell surface antigens, IFT was applied. Graffi-specific antibodies reacted with budding

and extracellular virus particles and also with the non-budding sites of the cell membrane (Micheel and Bierwolf, 1968). Aoki et al., (1970) found in the mouse system that the Gross antigen was situated on the surface of Gross leukaemia cells and this antigen was not identical with the virus envelope antigen. They did not specify the envelope antigen as a cell surface antigen. Micheel et al., (1972) demonstrated by IFT the presence of a membrane-bound group-specific antigen in Graffi and Gross leukaemia systems. No difference was found between the localisation of the type-specific and group-specific leukaemia antigens in the cell. It was assumed that the antigenic determinants were located either on one molecule or on two adjacent molecules. Gelderblom et al., (1972) found two kinds of antigens on the surface of chicken cells infected or transformed by avian RNA-tumour virus. The first, designated as Ve antigen, was identical with the viral envelope antigen and was found to be expressed on both virions and non-budding areas of productively infected cell membranes. The second antigen was group-specific and restricted to transformed cells. Since it was not observed on virions, it was called tumour-specific cell surface antigen (TSSA). A new common cell surface antigen associated with murine and feline leukaemia viruseses was demonstrated by membrane immunofluorescence test (Yoshiki et al., 1973). The subsequent IF study by the same group of murine leukaemia cells revealed that the antigen was located on the cell surface, but budding and complete virions were not labelled. Antibody activity could be adsorbed with purified viral protein containing gs antigen. It was concluded that the common cell surface antigen was closely related to or identical with gs antigen.

Randal and Fritz (1975) investigated the immunological properties of the surface of chick embryo cells (CEC) following their infection with avian leukosis virus. They found that cells stained soon after infection. The staining was time- and dose-dependent and was not decreased after treatment of cells with actinomycin D which implied entry by fusion. This was in contrast with an earlier report by Dales and Hanafusa (1972) who suggested that avian oncornaviruses penetrated the host cell by endocytic process. It was also found that CEC transformed by an avian leukosis virus had a group-specific TSSA associated with the cell surface. This antigen either cross-reacted or was identical with an antigen found on CEC transformed by RSV, and was distinct from viral envelope antigens of the different transforming viruses. Only 25 - 30% of the transformed cells stained for TSSA. Gelderblom et al., (1972) also reported that not all cells transformed by RSV would stain for TSSA. It was suggested that the expression of TSSA might be cell cycle-dependent.

A wide range of transformed and normal mouse cells were examined by IFT (Holder et al., 1976). Specific rabbit antisera to the major glycoproteins of Friend leukaemia virus (gp71) and mouse mammary tumour virus (gp52) were used. Antiserum to gp71 showed reactivity with all the mouse cells tested regardless of strain, virus production or state of transformation, demonstrating the ubiquitous expression of gp71. In virus producing cells, both budding virus particles and non-budding areas of the cell surface were consistently labelled with anti-gp71 serum. Similarly, anti-gp52 serum stained both cell surfaces and virions. gp52 was expressed predominantly in cells from mice with high mammary tumour incidence. The finding that

all the mouse cells observed expressed gp71 was in contrast with the results obtained by Schwartz et al., (1976) according to whom gp71 was detectable only on cells producing MuLV. However, the anti-gp71 serum utilised by Schwartz et al., was absorbed with STU cells which were found by Holder's group to be positive with anti-gp71 serum. The latter finding and the variable degrees of expression among the various cultures as well as the release of antigen into medium might all be related to the controversial results concerning gp71 expression on mouse cells.

Although immunoelectron microscopy was used by many scientists as a means for demonstrating viral antigens and associated antibodies, only a few studies had been carried out in which sera were tested for the presence of naturally-occurring antibodies. The first study was by Calafat et al., (1974) where sera of mice were tested for the presence of naturally-occurring antibodies to mouse mammary tumour virus (MMTV). MMTV-specific antigens were demonstrated on plasma membranes of virus-infected cells. Miller et al., (1977) also found anti-MMTV antibodies in mouse sera, confirming previous reports that mice were not tolerant to MMTV.

The appearance and distribution of the Friend mouse leukaemia virus infected cell surface antigens were investigated by Schwartz et al., (1976). Their immunoelectron microscopic studies confirmed most of the results obtained by cytotoxic tests (Hunsmann et al., 1976). The viral structural proteins p12 and gp71 were expressed on virus producing but not on non-producing transformed cells. p10, p15 and p31 antigens were not detected in significant amounts, with the exception of p31 on high virus producing cells. gp71 occurred on virions and non-budding areas of the cell

membrane. p12 antigen was absent on viral particles and relatively abundant on non-budding areas of the cell surface. An interspecies reactivity of gp71 serum with FeLV-producing cells, but not with simian virus producing ones, was reproducibly detectable by cytotoxic test, whereas IFT provided no clear evidence for such an activity. This was attributed to the low antibody titre and to the possible low valency of antibodies and/or changes in accessibility of the interspecies antigenic determinant caused by fixation. p10, p15 and p31 antisera possessing mainly group and/or interspecies serological activities reacted in the cytotoxic test exclusively with the high virus producer Eveline cell line, but to a much lower degree than anti-gp71 or -p12 sera. By IFT, no labelling was seen with anti-p10 serum, low amount of labelling was obtained with anti-p15 and -p31 sera. Neither p31 nor p15 antigens were found on budding sites or on free virions. It was concluded that gp71 and p12 antigens were integral constituents of the cell membrane. It was also suggested that p10, p15 and p31 antigens were passively adsorbed because these antigens were detected only on high producer cells and were shown to be released into the medium. Adsorption of viral constituents was not observed in the avian system (Bauer, 1974). Furthermore, Schwartz and his group confirmed previous suggestions by Micheel et al., (1972) and Aoki et al., (1972) that the type- and group-specific murine Ve antigens were located in a single molecule and that this molecule was represented by gp71. If this molecule or part of it was expressed on a particular productive or non-productive cell of certain mouse strains, it represented the G_{IX} antigen (Obota et al., 1975; Tung et al., 1975). Ve and G_{IX} antigens were also found in "soluble" form in the plasma of mice.

Results obtained by IFT clearly indicated the usefulness, reliability and sensitivity of this method in immunological studies. Expression of viral and virus-induced antigens were detected and their type- or group-specificities were established by IFT far before their molecular properties became known. In many instances IF studies were used to confirm or to interpret results obtained by other immunological methods such as immunofluorescence or cytotoxicity tests. Conversely, immunofluorescent studies carried out prior to the application of ferritin labelling could be used for determination of the potency and specificity of the antisera and also a variety of controls could easily be run with the more simple method of immunofluorescence.

A number of factors may influence the successful outcome of immunoferritin labelling. The use of adequate conjugants and fixatives is as necessary as the standardisation of the labelling procedure. However, being a highly sensitive immunological method with resolution at the molecular level, the application of well defined, possibly monospecific antisera seems to be the most important factor.

3. Materials and Methods

70% glutaraldehyde was purchased from Ladd Research Industries, Burlington, U.S.A.

Purified horse-spleen ferritin, containing 100 mg ferritin/ml was obtained from Sigma.

Lyophilised rabbit anti-cat globulin and goat anti-rabbit globulin were obtained from ICN.

Cells, maintenance of cells, synchronising and immunofluorescent techniques were described in the previous Chapters.

Preparation of γ - globulins

Lyophilised antisera were first rehydrated with 5 ml of distilled water, placed in an ice bath and stirred with a magnetic stirrer. Saturated ammonium sulphate $(NH_4)_2 SO_4$ was added drop-wise until the mixture was 33% saturated. Stirring was continued for 30 minutes. 33% $(NH_4)_2 SO_4$ precipitates out mainly the IgG fraction of the globulins. For immunoferritin work, this technique is satisfactory, but globulins can be further purified by DEAE-cellulose or Protein-A-Sepharose chromatography.

The precipitated globulins were sedimented in a refrigerated centrifuge at 2,500 r.p.m. for 30 mins. The sediment was washed twice with cold 33% saturated $(NH_4)_2SO_4$ and dissolved in 1 ml of phosphate buffer, 0.1M, pH 6.8. Remaining $(NH_4)_2SO_4$ was removed by dialysing extensively against phosphate buffer, changed four times.

The protein concentration of the IgG preparation was determined by the method of Lowry (1954).

One-stage method for cross-linking antibody globulin to ferritin by glutaraldehyde

a. IgG and ferritin were mixed in a ratio of 5:1 protein weight. This was roughly the equimolar ratio assuming a molecular weight of 160,000 for IgG (Tristram and Smith, 1963) and 750,000 molecular weight for ferritin (Harrison, 1959). The final concentration of the mixture contained 5 mg of IgG and 25 mg of ferritin/ml.

Protein content was determined by the method of Lowry.

Ferritin concentration was determined densitometrically.

IOD unit at 440 nm = 650 μg of ferritin/ml. Alternatively, at 310 nm = 10μg ferritin iron/ml. Ferritin has 20% iron and 15% N content.

b. Freshly diluted 0.5% GA in phosphate buffer, 0.1 M, pH6.8, was added drop-wise with gentle stirring. 0.2 ml of 0.5% GA/200 mg of total protein was used.

The mixture was stirred for 2 hours at room temperature. In order to block remaining free aldehyde groups, 0.01M lysin was added.

Alternatively, untreated GA was removed by dialysis against PBS.

c. The conjugate was separated from untreated IgG because these molecules would compete for antigenic sites. Isolation of the conjugate from the reaction mixture was by $(NH_4)_2\ SO_4$ precipitation at 25% saturation. According to Siess et al., (1970) neither γ-globulin nor ferritin nor a mixture of the two precipitated at less than 30% saturation. γ-globulin and γ-globulin complexes which were formed in the reaction mixture were also precipitated out at 25% saturation but they failed to go into solution again.

d. The precipitate was washed twice with 25% $(NH_4)_2SO_4$ and dissolved in phosphate buffer.

e. After extensive dialysis against four changes of PBS, the insoluble precipitate was removed by low speed centrifugation at 2,500 r.p.m. for 30 minutes.

f. Finally, 0.01M lysin and 0.02% NaN3 were added to prevent aggregation and bacterial growth. The conjugate was stored at $4^{o}C$; it remained reactive for several months.

Two-stage method for cross-linking antibody globulin to ferritin by glutaraldehyde

1. Activation of ferritin

Freshly diluted GA was added to ferritin in phosphate buffer, 0.05M, pH 6.8. The final concentration of ferritin and GA were 50 mg and 1 mg/ml, respectively. Ferritin was exposed to GA for 2 hours at $37^{o}C$. At the end of the reaction, to remove unreacted GA, the ferritin pre-treated with GA (FGA) was filtered through a Sephadex G-25 column (25 cm. x 1.6 cm). To avoid undesirable dilution only the middle section of the peak of the effluent FGA was used. Concentrations of FGA were determined by means of a spectrophotometer.

2. Coupling of IgG to activated ferritin

FGA was added to IgG in phosphate buffer in 5:1 ratio to give a final concentration of 15 mg. of FGA and 3 mg. of IgG/ml. 0.02% NaN_3 was added and the mixture was incubated for 12 hours at $37^{o}C$. At the end of the conjugation, 0.01M of lysin was added.

Conjugates were separated by $(NH_4)_2 SO_4$ precipitation at 25% saturation or by gel filtration (Bio gel A 1.5M) where the middle peak contained the 1:1 antibody + ferritin conjugate.

0.01M lysin and 0.02% NaN_3 were added and the conjugate was stored at 4^oC.

Indirect ferritin labelling technique (IFT)

Labelling of cells grown in suspension cultures is technically more difficult than labelling of monolayers. Cells have to be carefully resuspended and kept in suspension at every step of the labelling procedure in order to prevent aggregation and to ensure the labelling of the entire cell surface and the removal of the non-specifically bound ferritin.

a. Prefixation of cells

Cells, 2×10^6 per sample, were washed twice with cold phosphate buffered saline (PBS) containing 5% foetal bovine serum (FBS) (PBS-FBS).

Cells were resuspended in ice cold 0.25% GA for 30 minutes or in 1% GA for 5 minutes.

Alternatively, cells on ice were prefixed with 1% paraformaldehyde for 1 hour.

Prefixed cells were washed first with cold PBS-FBS containing 0.01M lysin and with PBS-FBS. This step was omitted when cells were labelled without prefixation. Cells were only washed twice and kept on ice.

b. Labelling of cells

Fixed and unfixed cells were resuspended in 0.2 ml. of the appropriate dilution of the antiserum which was approximately 3 times the pellet volume. Cells were incubated at room temperature or, in the case of unfixed cells,

on ice for 30 minutes and were frequently resuspended during incubation. At the end of the incubation period, they were washed twice with PBS-FBS and resuspended, using individual Pasteur pipettes for each sample, in 0.2 ml of appropriate dilution of Fe-Ab conjugates. After 30 minutes incubation at room temperature or on ice, cells were washed three times to remove unbound ferritin. Gentle centrifugation was used to obtain the final pellet. Had the cells been packed too tightly, the labelling of the surface would have been difficult to observe.

c. Preparation of cells for EM

The final pellets were fixed in cold 2.5% GA in Millonig's buffer without sucrose for 30 minutes at $4^{o}C$. Pellets were kept overnight in Millonig's buffer containing sucrose.

After post-fixation with cold 1% osmium tetroxide, pellets were dehydrated by graded series of ethanol and embedded in Araldite. Thin sections were cut, stained and finally examined in the EM. In certain experiments, cells were stained with 1% uranyl acetate at the 70% ethanol step. After sectioning, these cells were not stained with lead citrate and uranyl acetate.

4. Experiments and Results

The aim of this immunoelectron microscopic study was to examine the occurrence and distribution of FeLV structural proteins on the surface of FL74 cells. In addition, the appearance of FOCMA was investigated on FeLV-infected homologous and heterologous cell membranes. Synchronised FL74 cells were also labelled with ferritin in various phases of the cell cycle, in order to see the quantitative differences in the expression of antigenic sites. The possible ability of monospecific viral antisera to influence the expression of FOCMA and vice versa were examined by competition experiments. Finally, a series of immunofluorescence and immunoferritin experiments were performed in capping conditions to study the possible independent behaviour of FL74 cell membrane antigens including FOCMA.

A. Determination of the distribution of ferritin monomers, dimers and higher oligomers in glutaraldehyde cross-linked IgG preparations

For preparing ferritin-antibody conjugates, both the one-stage and the two-stage GA coupling methods were used. The ferritin preparation obtained from Sigma contained mainly monomers but the naturally occurring dimer, called β-ferritin, and a few larger aggregates were also present. The degree of conjugation and aggregate formation was examined by negative staining.

First, a series of dilutions were made from a sample of known ferritin density to establish the best dilution for negative staining. It was found that at the dilution of 1:1,000, individual ferritin molecules could easily be distinguished and subsequently this dilution was used in the experiments.

Three samples with equal ferritin densities were negatively stained. The first was a control containing uncoupled ferritin, the second and third

contained ferritin-antibody conjugates obtained by the one- and two-stage methods, respectively. The samples were diluted with phosphate buffer and negatively stained with 2% phosphotungstic acid pH 7.0 on carbon-coated copper grids.

Figs. 76, 77 illustrate pure ferritin molecules with electron dense centres. Without contrasting, only the central iron containing core is revealed. Ferritin label is seen in this form in the EM. After negative staining, the protein shell also appears in the form of a clear circle.

Representative fields from the different preparations, having fairly low and approximately equal densities of ferritin molecules, were counted to determine the proportions of solitary, paired, trimeric and oligomeric molecules present. Ferritin oligomers occurred in all three preparations with varying frequency. Only a few oligomers were observed in the control, which was possibly due to naturally occurring cross-linkages between ferritin molecules during storage. The one-stage method produced more oligomers than the two-stage method, but in both cases the majority of the conjugates consisted of monomers and dimers.

The occurence of ferritin oligomers, especially in the one-stage method, indicated that a higher percentage of ferritin molecules were covalently associated via GA and also via IgG molecules to which they had been independently cross-linked.

The presence of ferritin oligomers in these preparations explains the appearance of small ferritin clusters seen on labelled cell membranes and virus particles in situations where the antigens themselves are dispersed.

B. Comparison of various prefixation methods and their effects on the preservation of antigenic sites

The distribution of independent molecules in a perfectly fluid plasma membrane would be expected to be random, but interactions between membrane molecules or between membrane molecules and cellular structures, which must occur at least to some extent in any living cell, would necessarily induce some deviations from complete randomness. Experimental determination of the true distribution of individual molecules at the ultrastructural level is based on immunoelectron microscopic techniques. The interpretation of the observations gained by these techniques presents some difficulties because, due to the fluid nature of the membrane, the binding of any label perturbs the random distribution. This difficulty is minimised by labelling the surface components with monovalent ligands or by immobilising the distribution by prefixation with aldehydes.

Aldehyde prefixation was found particularly useful for the examination of the carbohydrate lectin receptors which were not modified by aldehydes. It was not successful for the immobilisation and preservation of protein molecules, such as surface Ig (de Petris and Raff, 1972).

Prefixed cells are widely used in immunoelectron microscopy. In virology, reports concerning preservation of cell membrane antigens by prefixation, at first sight, appear to be contradictory.

Upon analysing 11 experiments the following picture emerged: GA was used in 6, paraformaldehyde (PA) in 3 cases, while formaldehyde and a mixture of GA-PA was used in 1 case each. In cases where PA was successfully used, GA seemed to have quite a deleterious effect. This

might be explained by the fact that in those experiments, enzymes and cell surface globulins were treated with GA and appeared to be greatly affected by it (Parr and Oei, 1973; Olsen et al., 1973, 1975; de Petris, 1978). On the other hand, in cases where application of GA proved to be satisfactory, mainly viral antigens were investigated (Gelderblom et al., 1972; Calafat et al., 1974; Morris and Fritz, 1975; Birdwell and Strauss, 1974; Schwartz et al., 1976).

Selective impairment of cell surface and viral antigenicity by altering fixation protocols was reported by Gatti et al., (1974). Calafat et al., (1974) using GA prefixation, were able to detect cell membrane labelling in MMTV infected cells while Miller et al., (1977) using acreolin and PA to prefix MMTV infected cells, detected only the labelling of virus particles, but not that of the cell membrane.

In the present experiment, FL74 cells were prefixed prior to ferritin labelling with either 0.25% GA for 30 minutes

or 0.5 % GA for 5 minutes

or 1.0 % PA for 1 hour

In addition, unfixed cells were labelled on ice which served as controls. After prefixation, cells were labelled by the indirect immunoferritin technique as described in the Materials and Methods part of this Chapter.

For the labelling procedure, the following antisera were used:

1. anti-p15 serum raised in rabbits.
2. anti-p30 serum raised in rabbits
3. anti-gp70 serum raised in rabbits
4. naturally-occurring high titre FOCMA serum from a virus

negative cat, and

5. from a viraemic cat

6. cat serum with neutralising antibody activity of FeLV-AC.

1, 2 and 3 antisera were labelled with ferritin conjugated goat anti-rabbit IgG; 4, 5 and 6 antisera with ferritin conjugated rabbit anti-cat IgG.

Electron microscopic examination of labelled cells revealed the following:

The labelling intensity of budding or extracellular viral particles after GA and PA treatment when compared to unfixed controls, varied depending on the particular antiserum used.

Ferritin densities on virions were reduced by GA prefixation when viraemic FOCMA serum or cat serum with neutralising activity were applied. Virus labelling with gp70 antiserum was not noticably affected by GA.

On the other hand, after PA prefixation, virions remained heavily labelled with FOCMA serum, but labelling was greatly affected on virions stained with cat antiserum to FeLV-AC. In the latter case, in many instances, the surface of the virions appeared to be fuzzy and had a halo-like appearance without presence of any ferritin label. This suggested that initially, an antigen-antibody reaction took place but the binding of the antibody was weak and it was removed by the extensive washings.

Ferritin labelled virions after GA and PA prefixations and without prefixation are shown in Figs. 78, 79, 80, 81, 82 and 83.

Cell membranes also displayed variation in labelling intensity which was related mainly to the prefixation method used and was not influenced so much by the various antisera.

Labelling of non-budding areas of the cell membrane by anti-FOCMA serum was considerably reduced in the case of PA treatment and reduced, but less so, in the case of GA prefixation. Similar results were obtained with cat anti-FeLV-AC and rabbit anti-gp70 sera. Cell membrane staining by p15 and p30 antisera was affected by PA but not so much by GA.

To sum up, preservation of antigenic sites after prefixation with GA appeared to be satisfactory on virions and on cell membranes as well, although a slight reduction in the labelling intensity was observed. PA prefixation did not reduce the labelling intensity of virions, but considerably reduced that of the cell membranes when FOCMA sera were used. Virions as well as cell membranes were greatly affected by PA in the case of all the other antisera.

Prefixation with 0.25% GA for 30 minutes appeared to be the best compromise for the preservation of most of the antigenic sites. Subsequently, this method was used in all labelling experiments. 0.25% GA prefixed virions and cell membranes can be seen in Figs. 84, 85 and 86.

Based on the immunoferritin studies of Aoki et al., (1969), the concept was developed that antigens on lymphocyte surface were arranged in a mosaic of discrete patches of variable sizes and patterns characteristic of each antigen. In those studies, the antibodies were applied on living, unfixed cells. The distribution patterns obtained under these conditions are now known to be the result of ligand-induced redistribution. The redistribution pattern is dependent on ligand characteristics, mainly on valency and other general experimental conditions, such as temperature (Taylor et al., 1971; de Petris and Raff, 1972). Three basic patterns of redistribution of the labelled

components were observed: 1. Dispersed; after labelling with monovalent antibody or using prefixation. 2. Patches; when cells were labelled with divalent antibody at low temperature, 0 - 4°C, the label appeared to be concentrated in discrete "spots" or "patches" separated by unlabelled areas. In immunofluorescence techniques, "spotty" or "broken rings" could be seen. 3. Caps; when cells labelled at 4°C were brought to higher temperature or were labelled at high temperature, 15 - 37°C, under normal metabolic conditions all the label coalesced rapidly (1 - 5 mins) into a single "cap" at one pole of the cell. Capping was usually accompanied by endocytosis of the areas of labelled membrane which resulted in the progressive disappearance of the label from the surface.

Viral and FOCMA antigens showed the characteristic redistribution pattern of patching when unfixed FL74 cells were labelled on ice, which are shown in Figs. 87, 88, 89 and 90.

C. Appearance and distribution of viral structural antigens and FOCMA on the surface of FL74 cells

FL74 cells were prefixed with 0.25% GA for 30 minutes. After washings, they were pre-incubated with 2% bovine serum albumin in PBS for 30 minutes, then washed again and labelled by the indirect IFT as described in the Materials and Methods part of this Chapter.

Immune sera used are described in experiment B. All sera were applied at a dilution of 1:2 which in pilot experiments was found to give the best labelling results. Ferritin-conjugated rabbit anti-cat IgG and ferritin-conjugated goat anti-rabbit IgG were applied at dilutions of 1:4 and 1:2, respectively.

The following controls were used:

1. Specific immunológic blocking of the reaction. Samples were treated with specific unconjugated antibody prior to their treatment with ferritin conjugated antibody.

2. Treatment of samples with non-specific ferritin conjugates.

3. Treatment of samples with pure ferritin.

4. Lymphocytes from a FeLV and FOCMA negative cat.

After labelling, cells were fixed with 2.5% GA in Millonig's buffer for 30 minutes and prepared for EM.

Results

Cell membranes exhibited various degrees of labelling depending on the antisera used. In each case the labelled antigenic sites were randomly distributed and tagged with a single ferritin or small clusters of ferritin molecules. Cells were heavily stained by the cat serum which contained neutralising antibodies to FeLV-AC. Both viral envelopes and non-budding areas of the cell membrane were labelled.

Anti-gp70 serum which originally was prepared from FeLV-AB also stained virions as well as non-budding areas of the cell membrane. The intensity of the membrane labelling was considerably less than when using cat serum, while virions were more intensely labelled.

p15 and p30 antisera did not stain budding and intact virus particles, while the cell membranes appeared to be labelled. Much higher amount of label was obtained by anti-p30 than by anti-p15 serum.

Viral envelopes were found to be labelled by both viraemic and virus-negative anti-FOCMA sera and so were the non-budding areas of the cell

membranes. Ferritin density on the cell membranes was less than that of the gp70 but more than that of p30.

Ferritin labelling was not observed on any of the controls used, see Fig. 91.

The appearance of labelling by various antisera is demonstrated in Figs. 92, 93, 94, 95 and 96.

D. Ferritin labelling of CT45-S cells using FOCMA antiserum

As discussed in Chapter Four, by immunofluorescence test, no FOCMA expression was found in the FeLV-infected CT45-S cell membrane. In order to confirm this finding, CT45-S cells infected either with FeLV-AB or FeLV-B or FeLV-C and also uninfected controls were labelled by the indirect IFT. Cells were prefixed, incubated with viraemic FOCMA serum extensively absorbed with uninfected CT45-S cells and labelled with ferritin-conjugated rabbit anti-cat IgG.

Interpretation of the results was made slightly complicated by the fact that anti-FOCMA serum was found by neutralisation test to contain neutralising activities to FeLV-A (1:8) and FeLV-C (1:4). It is most likely that there is a difference between the sensitivity of virus neutralisation and immunoferritin tests because low titres of anti-FeLV antibodies were able to stain antigenic sites by IFT. The following results were obtained.

Non-budding areas of FeLV-AB and B infected cells were weakly labelled and large areas of the cell membranes appeared to be free of label. All FeLV-AB particles were labelled with normal labelling intensity while FeLV-B particles showed a strikingly heavy labelling.

FeLV-C infected cell membranes were sporadically labelled. No

label could be seen on the majority of the virus particles and only one or two ferritin tags were attached to the few positive ones.

The intense labelling of FeLV-B particles was quite unexpected because the serum did not have anti-B activity. It was thought, at first, that the cells might have been contaminated with other subgroups but this was not the case. Therefore, this was one more finding in line with the various observations concerning the curious nature of FeLV-B.

It was shown that the major glycoproteins of FeLV isolates varied in molecular weight in SDS PAGE. FeLV-B had a range of 74,000 - 82,000 Mr (Neil, personal communication). FeLV-B/Boston showed a high degree of cross-neutralisation with FeLV-A isolates (Russell, 1977) as well as similar molecular weight for the major glycoproteins. FeLV-B was found to be dependent on FeLV-A for contact transmission in the field and also under experimental conditions (Jarrett et al., 1978; Jarrett and Russell, 1978). It was suggested that a phenotypically mixed population of FeLV-B with A might enhance the growth of B by widening the range of permissive cells which would imply a differential cytotropism of the subgroups.

Not only subgroups A and B but subgroups A and C were shown to have strange properties. For example, neutralising antibodies to FeLV-C occur frequently in cats but FeLV-C is seldom isolated. Cats experimentally infected with FeLV-A have antibodies to FeLV-C (Russell, 1977) which points to a possible existence of a group-specific determinant shared by both subgroups.

In view of the above findings, labelling of FeLV-B infected cells might be due to a cross-reactivity between subgroups A and B. The heavier

labelling as well as the more intense immunofluorescence pattern might be explained by the presence of more antigenic sites per unit length in the virion envelopes. Alternatively, glycoproteins of the subgroups might undergo changes during incorporation into budding particles. This would also explain the differences in the distribution of labelling found in FeLV-B and C infected cells. In the case of FeLV-B, virions were preferentially labelled while anti-FeLV-C antibodies failed to label most of the viral particles.

The lack of any considerable amount of label on FeLV-infected, especially on FeLV-C infected, CT45-S cell membranes, in spite of the high anti-FOCMA titre of the serum, suggested that FOCMA was not expressed on these cells.

Ferritin labelled FeLV-AB, -B and -C infected CT45-S cells and control cells are shown in Figs. 97, 98, 99 and 100.

E. Ferritin labelling of synchronised FL74 cells

The use of immunoferritin labelling technique is not limited to the detection of antigens alone. It is equally applicable to the quantitative assessment of antigenic sites on the cell membrane.

As discussed in the previous Chapters, FeLV release and antigen expression appeared to be cell cycle-dependent and occurred in the E - G_1 phase. In order to examine differences in the number of labelled antigenic sites, synchronised FL74 cells were ferritin labelled in the S and E - G_1 phase of the cell cycle.

FL74 cells were synchronised by excess thymidine. After release from the synchrony-inducing block, cells were prefixed; one half of the cells

were labelled by the indirect IFT at 2 hours post-release in the S phase, and the second half at 10 hours post-release in the E - G_1 phase. Anti-gp70 and anti-FOCMA sera, and ferritin-conjugated rabbit-anti-cat and goat anti-rabbit globulins were used. Labelled cells were prepared for EM.

From each block, fifty cell profiles were examined. Only intact cells which had nuclei and exhibited the morphology characteristic of the particular cell cycle phase under investigation were considered.

Cells in the S phase were sparsely labelled. The density of ferritin was considerably increased on E - G_1 phase cells, which was easily noticed by a simple viewing of the cells. When the number of labelled gp70 antigenic sites was counted, two and a half times more ferritin labels per unit length were found on cells in the E - G_1 phase than on cells in the S phase. The number of FOCMA antigens increased less in the E - G_1 phase.

As indicative mean values, the ferritin concentration per unit length of membrane was as follows:

In the case of gp70	:	116.5 in S phase
		289.6 in E - G_1 phase
In the case of FOCMA:		96.6 in S phase
		185.6 in E - G_1 phase.

These values were in accordance with results obtained by immunofluorescence staining of synchronised FL74 cells. According to the latter, highest gp70 titres were measured in the E - G_1 phase. FOCMA titres also increased in that period but peak expression occurred later in the G_1 phase.

S and E - G_1 phase-cells with various ferritin densities are demonstrated in Figs. 101, 102, 103 and 104.

F. Investigation of cell membrane antigens under capping conditions. An immunofluorescence-immunoferritin study

I

In contrast to the essentially diffusional nature of the patching process, capping represents a non-diffusional, polarised and metabolically dependent process. Capping of particular surface components occurs only if they are cross-linked by a multivalent ligand. Generally, capping requires the prior formation of patching. It is dependent on the valency of the reactants and on the concentration of the ligand. Excess ligand (prozone or antibody excess) or too little ligand (antigen excess) leads to the formation of smaller patches and are less effective in inducing capping. Capping in lymphocytes occurs by a co-ordinated polarised movement of the cross-linked complexes towards that pole of the cell which is facing the nuclear indentation and contains most of the cytoplasm and the cellular organelles. This pole corresponds to the "tail" or "uropod" of locomoting cells. Only the cross-linked molecules appear to move to the cap while physically independent molecules which are unlabelled or insufficiently cross-linked remain dispersed over the surface.

Independence of membrane components can be demonstrated. For example, one component labelled with one marker is capped completely and the distribution of the second component labelled with a second marker is examined under non-capping conditions. If the second component is also allowed to cap normally it moves to the same pole where the first cap is located. The movement characteristics of the cross-linked molecules and their dependence on metabolic energy indicate that some relationship exists between certain cellular framework located in the cytoplasm which, somehow,

generates the motive force to the movement. Very little is known about the precise nature and organisation of this structure but putative structural elements in lymphocytes as well as in other cells are the microfilaments and the microtubules. Motility and cell shape alterations are inhibited in all surface systems by cytochalasin B and capping is also affected to a variable extent (de Petris, 1974).

The fact that individual cross-linked surface components move independently towards one pole of the cell can be used for the selective investigation of surface antigens. In the following experiments, the behaviour of viral and FOCMA antigens were examined in capping conditions.

An immunofluorescence study was performed prior to ferritin labelling whereby cells were first incubated for various lengths of time, at 37^{o}C with p15, p30, gp70 and FOCMA antisera at the dilutions of 1:2, 1:4, 1:8 and 1:16 and were subsequently stained with fluorescein-conjugates.

When cells were incubated at 37^{o}C for 30 minutes at the dilution of 1:4, the following results were obtained. Complete caps were produced by p15 and p30 antisera. In the UV microscope, only the small, round, very bright, often internalised caps were visible; p15 molecules needed only 10 - 15 minutes for the formation of a complete cap.

FOCMA antisera also induced cap formation but the size of the caps was much larger and their internalisation did not take place in the first 30 minutes.

gp70 did not induce capping in the first 30 minutes and cells showed ring fluorescence, but after longer incubation, gathering of the fluorescein-

stained molecules towards one pole of the cell could be observed. The differences in the length of time needed for cap formation could be explained by the results of experiment C which demonstrated that gp70 had the most numerous antigenic sites followed by FOCMA, p30 and p15, in descending order. Cap formation is shown in Figs. 111 and 112.

To investigate the independent movement and distribution of viral and FOCMA antigens, FL74 cells were labelled by the indirect IFT in capping conditions. Antisera, dilution of sera and the time of incubation were the same as those used for immunofluorescence staining.

Ferritin labelling of antigens was detectable in the EM only when the sections were cut through or parallel with the capped area of the cell. Cell membranes away from the capped area were free from any label. Antisera to viral and FOCMA antigens all induced the capping of their respective antigens. Not only could the capped antigen molecules be visualised in the EM, but by gradually increasing the incubation periods from 10 minutes to 1 hour, the consecutive steps in the capping process could also be followed. In the first step, large, continuously labelled areas of cell membrane were seen and ferritin molecules were as dense as physically possible. In the next step, invagination of the labelled membrane occurred which was followed by the pinching off of the vesicle from the membrane as in the typical pinocytosis process. At first, fairly small vesicles were seen which possibly fused to form larger ones in the Golgi area. Ferritin molecules were found along the inner surface of the otherwise empty vesicles which later appeared to detach from the membrane and had a condensed appearance. This probably indicated the beginning of hydrolytic degradation caused by fusion of

the pinocytic vesicles with lysosomes. Eventually all the labels were removed by the above process and after incubation of cells for much longer than 1 hour, they appeared to be unlabelled and intensively vacuolated. Cap formation in consecutive steps is demonstrated in Figs. 105, 106, 107 and 108.

The time needed for cap formation and for the subsequent removal of the cross-linked molecules by pinocytosis differed with every antisera tested. The more numerous the antigenic sites were, the larger was the time needed for cap formation and its subsequent removal. Hence, p15 molecules needed the shortest and gp70 molecules, the longest time. To summarise, viral and FOCMA antigens appeared to move and form caps independently on the surface of FL74 cells. Quantitative differences between the various antigens greatly influenced the length of time needed for cap formation and its removal by pinocytosis. Results obtained by both immunofluorescence and immunoferritin techniques were essentially the same.

II

Most of the observations gained during the course of this study concerning FL74 cell membrane antigens suggested that FOCMA was distinct and independent from the viral antigens. However, the finding that viral particles were heavily labelled with both viraemic and virus-negative FOCMA antisera indicated that either virus neutralising antibodies were present which were not detectable by virus neutralisation test and/or FOCMA cross-reacted with the viral envelope glycoproteins. To explore these possibilities, further investigations were carried out.

To compare the sensitivity of the virus neutralisation and IF tests, the following experiment was performed: FL74 cells were ferritin-labelled

using high titre (1:512) viraemic FOCMA serum which had neutralising activity of less than 2 to FeLV-A determined by virus neutralisation test according to Russell and Jarrett (1978). The serum was used at dilutions of 1:2, 1:10, 1:20, 1:40 and 1:80 respectively, and the following results were obtained:

At a dilution of 1:2 some of the virus particles were labelled in normal density but the majority of them were not labelled at all. Non-budding areas of the cell membrane were moderately labelled. 1:40 was the highest dilution which could be used for IFT, above which it was very difficult to detect any labelling. At 1:40 dilution, the proportion of labelled and unlabelled virions remained the same while the intensity of labelling was considerably reduced. Interestingly, the positive virions had always one ferritin tag attached as shown in Figs. 109, 110. Cell membranes remained labelled although with slightly reduced intensity.

This experiment demonstrated the sensitivity of IFT which appeared to be greater than that of the neutralisation test. Similarly, the specificity of the IFT was also proved by the labelling of subgroup A virions only.

It was concluded that the labelling of virions by both viraemic and virus-negative FOCMA sera in experiment C was possibly caused by neutralising antibodies undetected by neutralisation tests.

Finally, the possible cross-reactivity between FOCMA and gp70 molecules was examined by competition experiments in normal and capping conditions.

An immunofluorescence study was first performed with the following staining protocols:

1. First serum FOCMA for 1 hour at 37°C
   Second serum gp70 for 30 mins at room temperature (r.t.)
   Third serum fluorescein-conjugated goat anti-rabbit IgG (GaR-IgG-Fl) for 30 minutes at r.t.

As a result, most of the cells exhibited thin, patchy ring fluorescence and some of them had half moons on their surfaces. This fluorescence pattern was similar to that of the controls. As a control, cells were incubated with gp70 and with the appropriate conjugate at room temperature.

2. First serum FOCMA for 1 hour at 37°C
   Second serum gp70 for 30 mins at room temperature
   Third serum RaC-IgG-Fl* for 30 mins at room temperature

The above staining protocol resulted in the formation of caps in the majority of the cells. Few half moons were also seen. This was identical with the control group's pattern. Control cells were incubated with FOCMA at 37°C for 1 hour and with the appropriate conjugate.

3. Additionally, cells were incubated first with anti-p30 serum at 37°C, secondly with FOCMA at r.t. and stained with GaR-IgG-Fl. All the cells were completely capped and the caps appeared to be internalised. In a similar protocol where FOCMA was stained instead of p30, ring fluorescence and half-moons were observed on the cell membrane instead of caps.

4. First serum gp70 1 hour at r.t.
   Second serum FOCMA 30 mins at r.t.
   Third serum GaR-IgG-Fl 30 mins at r.t.

Patchy ring-fluorescence was seen on the cells which pattern was similar to that of the controls.

5. First serum gp70 1 hour at 37°C
   Second serum FOCMA 30 mins at r.t.
   Third serum RaC-IgG-Fl 30 mins at r.t.

Patchy ring fluorescence was seen on the cells which was different from the controls where continuous rings were seen.

The above results suggested that FOCMA was independent of gp70 and of p30. However, the result of the fifth staining protocol indicated that capping of gp70 molecules might induce patching of FOCMA molecules.

To investigate the extent to which the capping process of one molecular component influenced the behaviour of other components, FL74 cells were stained by the above staining protocols but instead of fluorescein-conjugates, ferritin conjugates were used. Electron microscopic examination of the cells showed the following:

When cells were first capped with gp70 and thereafter incubated with FOCMA and stained for FOCMA at r.t., FOCMA molecules seemed to co-cap with the gp70 molecules but the intensity of their staining was not decreased.

When cells were first capped with FOCMA and afterwards incubated with gp70 at r.t., and stained for gp70, the co-capping was not as intense. gp70 molecules were gathered on large areas of the cell membrane, but were not capped entirely. This difference in the degree of co-capping was possibly due to the quantitative differences of FOCMA and gp70 antigens.

The co-capping of FOCMA and gp70 molecules could be due to several factors. The two components might be identical. The two components might be parts of the same mobile molecular unit, in other words, the two antigens might be present on the same polypeptide chain, like some H-2 and HL-A antigens, or on two linked polypeptide chains, like β_2 microglobulin and human HL-A. Both mobile molecules might be independent but they might carry the same antigenic or receptor site and therefore are cross-

reacting similarly to the ConA receptors and surface IgG or to H-2 and θ-antigens. Finally, the two components could be normally independent but became secondarily associated as a result of some change in the configuration or state of aggregation of one of the two components due to labelling and cross-linking by the ligand. This seems to be the case, for example, for surface IgM and Fc receptors of B lymphocytes. Which of the above situations between FOCMA and gp70 contributed to the observed co-capping phenomenon is not known. The fact that, in spite of co-capping, the labelling intensity of FOCMA was not influenced by pre-incubation with gp70 and vice versa, and also the results of experiments 1, 2, 3 and 4, all strongly supported the interpretation that FOCMA and gp70 were not identical. On the other hand, if labelling of virus particles was not entirely due to the undetected presence of neutralising antibodies, then, as an alternative, the cross-reactivity of the two molecules might be responsible for the labelling. However, the exact nature of the relationship between FOCMA and gp70 is yet to be determined.

5. Discussion

During the course of this immunoelectron microscopic study, valuable information was gained about the occurrence and distribution as well as about the interactions of the various antigens expressed on FeLV infected cell membranes. The combination of immunofluorescence and immunoferritin techniques contributed greatly to a better understanding of the results obtained.

Although all prefixation methods seemed to reduce reactivity, it was nevertheless possible to find one which was satisfactory for the system under investigation.

Examination of unfixed cells by IFT revealed that the viral antigens p15, p30 and gp70 as well as FOCMA were freely moving and upon cross-linkage by the ligands all formed patches. When antigenic sites were immobilised by 0.25% GA prefixation, the distribution of the antigens appeared to be random all over the cell surface. Determination of their true densities created some difficulty because labelling of unfixed cells induced redistribution while GA prefixation reduced the number of the reacting sites. However, quantitative comparison could be made between the individual antigens each of which displayed a characteristic density pattern. gp70 was the most numerous followed by FOCMA, p30 and p15 in descending order. These quantitative differences determined the behaviour of the antigens when investigated under capping conditions.

gp70 and FOCMA antisera as well as the cat serum with FeLV-AC specificities all stained both the viral particles and the non-budding areas of the cell membrane. While gp70 antiserum labelled virions well, its

labelling of the non-budding areas of the cell membrane was slightly less intense.

The antigenic sites labelled with FOCMA antisera were not too numerous but the virions were fairly heavily labelled by both viraemic and virus-negative FOCMA sera. The possible cause of this unexpected labelling of virions was investigated. High titre FOCMA serum with very low titre subgroup A activity was used at a dilution of 1:40 which was twenty times over the sensitivity of the virus neutralisation test. It was found that a proportion of virus particles, corresponding to subgroup A, was still labelled although the virions had only one ferritin tag attached. It was concluded that labelling of virus particles by viraemic and virus-negative FOCMA serum, might have been due to the undetected presence of neutralising antibodies. The possible cross-reactivity between FOCMA and gp70 molecules was also examined in capping conditions. The results clearly indicated that FOCMA was distinct and independent from gp70. Most likely, there was no cross-reactivity between the two molecules but another kind of association between them could not be ruled out. It should be mentioned that all these observations were performed with anti-gp70 serum with FeLV-AB activities. Therefore the properties of FeLV-C glycoprotein and especially its relationship to FOCMA could not be investigated.

Anti FeLV-AC cat serum preferentially labelled cell membranes. The highest numbers of antigenic sites on FL74 cell membrane were labelled by this serum. FL74 cells release FeLV-ABC but not in equal proportions. More sub-group C is released than A and B, and consequently more subgroup C glycoprotein is expressed on the cell membrane. This would explain the heavy labelling by a serum which had FeLV-AC specificities.

Another interesting observation concerning subgroup C was made when FeLV-infected CT45-S cells were labelled with FOCMA serum which had anti-FeLV-AC specificities. With this serum, FeLV-C was not labelled while FeLV-AB and especially B was heavily labelled. Such difference in the labelling of the cell membranes was not detected. It might be possible that subgroup C glycoprotein underwent some change during or after incorporation into the viral envelope and as a consequence antigen-antibody binding could not take place, or their binding was too weak. The finding that paraformaldehyde prefixation affected only the binding of FeLV-AC but not that of FeLV-AB or FOCMA antibodies supports this assumption. It was not only in canine cells but also in FL74 cells that virions of subgroup C were not as heavily labelled as those of subgroup A or B. There was another unexpected result which concerned subgroup B. FeLV-B infected CT45-S cells and especially the viral particles were heavily labelled with anti-FeLV-AC antibodies. Several theories could be put forward to explain this curious behaviour of the subgroups. It was already suggested that some cross-reactivity might exist between subgroups A and B. As an alternative, in this situation, also a putative alteration of glycoprotein B incorporated in the virion might play a role.

p15 and p30 antisera did not stain intact and budding virions, while the non-budding areas of the cell membrane were labelled. More p30 than p15 molecules were expressed on the FL74 cell membrane. Both p15 and p30 molecules appeared to be independent; they readily showed patching and capping in favourable conditions. In competition and capping experiments they did not seem to influence the labelling intensity and the behaviour of FOCMA.

FIGURE 76 : Unstained ferritin molecules, only the electron dense cores are visible.

x 80,000

FIGURE 77 : Negatively stained ferritin molecules. The protein shells of the molecules are visible in the forms of clear circles.

x 80,000

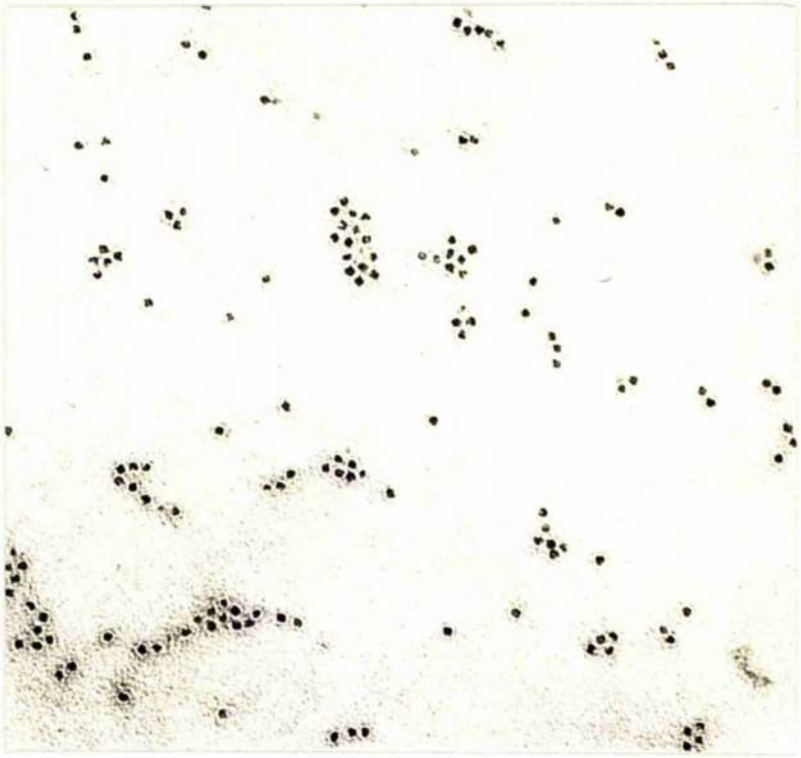

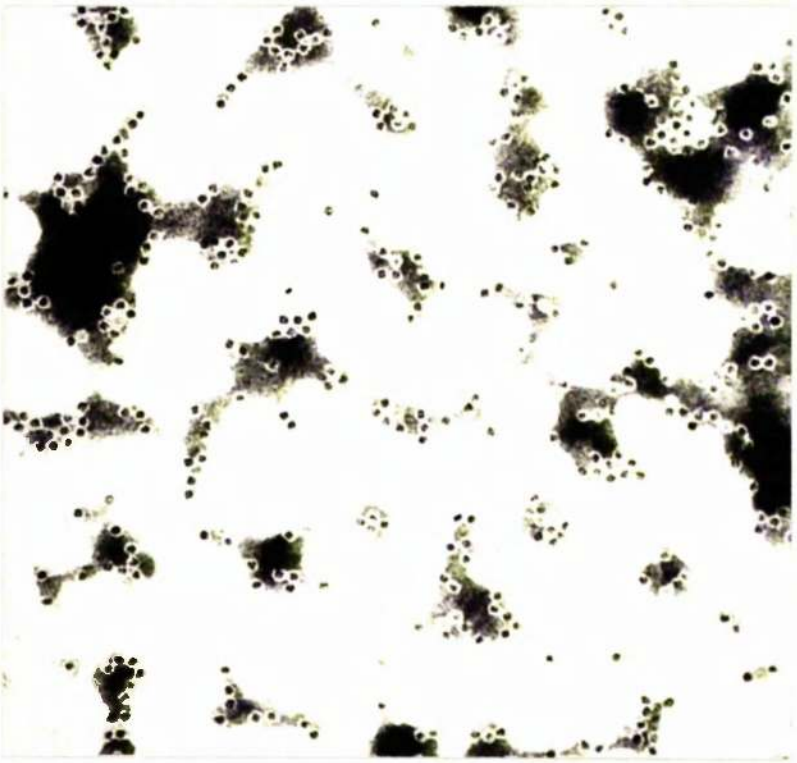

FIGURE 78 : Unfixed FeLV particles incubated with cat anti-FeLV-AC serum.

x 40,000

FIGURE 79 : Glutaraldehyde-prefixed FeLV particles incubated with cat anti-FeLV-AC serum. Unstained section.

x 40,000

FIGURE 80 : Paraformaldehyde-prefixed FeLV particles incubated with cat anti-FeLV-AC serum. The surfaces of the virions are "fuzzy".

x 40,000

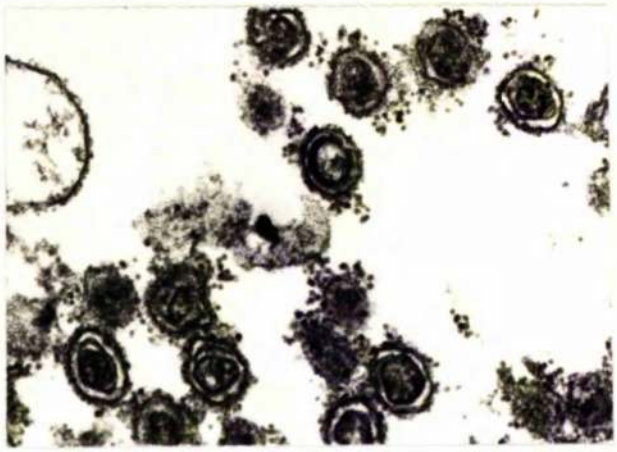

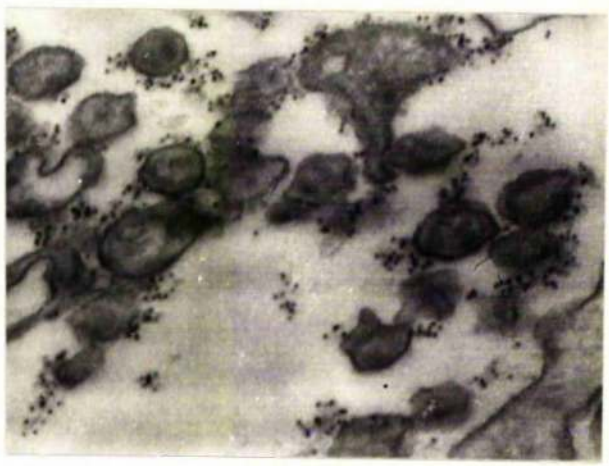

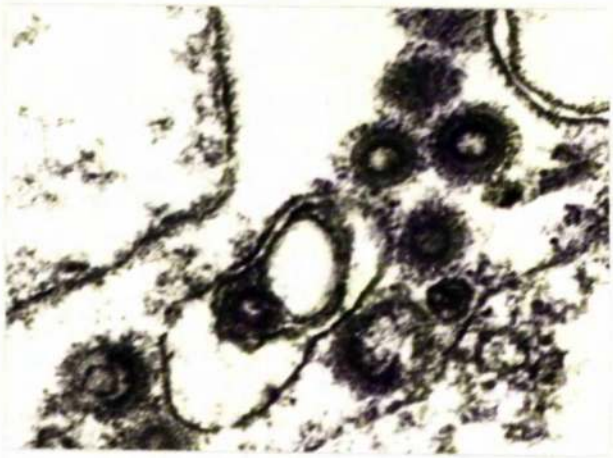

FIGURE 81 : Unfixed FL74 cell incubated with cat anti-FOCMA serum. Antigenic sites are patchily distributed (arrow).

x 30,000

FIGURE 82 : Glutaraldehyde-prefixed FL74 cells incubated with cat anti-FOCMA serum. Antigenic sites are randomly distributed. Unstained section.

x 30,000

FIGURE 83 : Paraformaldehyde-prefixed FL74 cell incubated with cat anti-FOCMA serum. The cell membrane is not labelled, budding and released virions are heavily labelled.

x 30,000

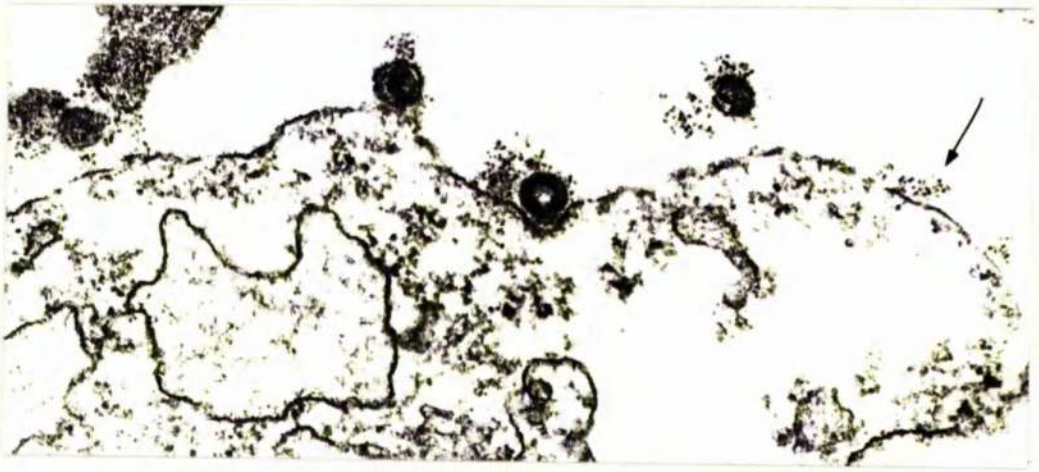

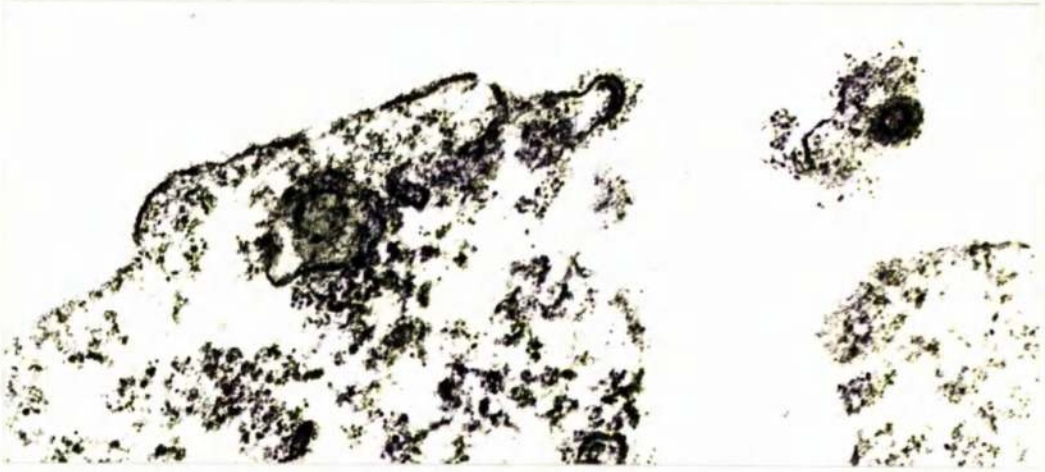

FIGURE 84 : Glutaraldehyde-prefixed FL74 cell incubated with cat anti-FeLV-AC serum. The cell membrane is heavily labelled. Unstained section.

x 30,000

FIGURE 85 : Glutaraldehyde-prefixed FL74 cell incubated with cat anti-FOCMA serum. Unstained section.

x 30,000

FIGURE 86 : Glutaraldehyde-prefixed FL74 cell incubated with rabbit anti-gp70 serum. Unstained section.

x 30,000

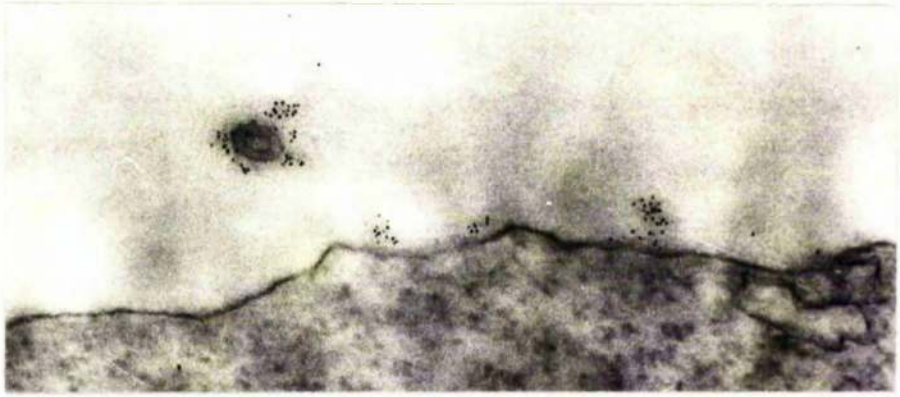

FIGURE 87 : Ligand-induced patchy distribution of p15 antigenic sites on unfixed FL74 cells.

x 30,000

FIGURE 88 : Ligand-induced patchy distribution of p30 antigenic sites on unfixed FL74 cells.

x 30,000

FIGURE 89 : Ligand-induced patchy distribution of gp70 antigenic sites on unfixed FL74 cells.

x 30,000

FIGURE 90 : Ligand-induced patchy distribution of FOCMA antigenic sites on unfixed FL74 cells.

x 30,000

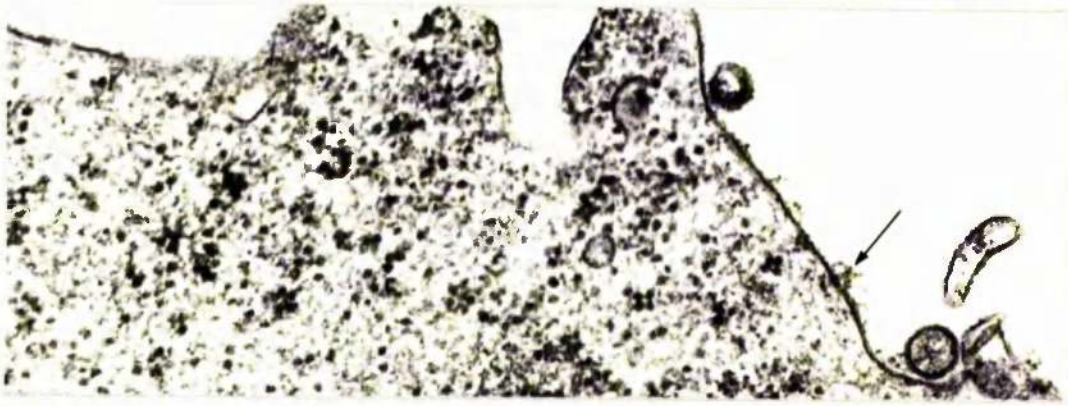

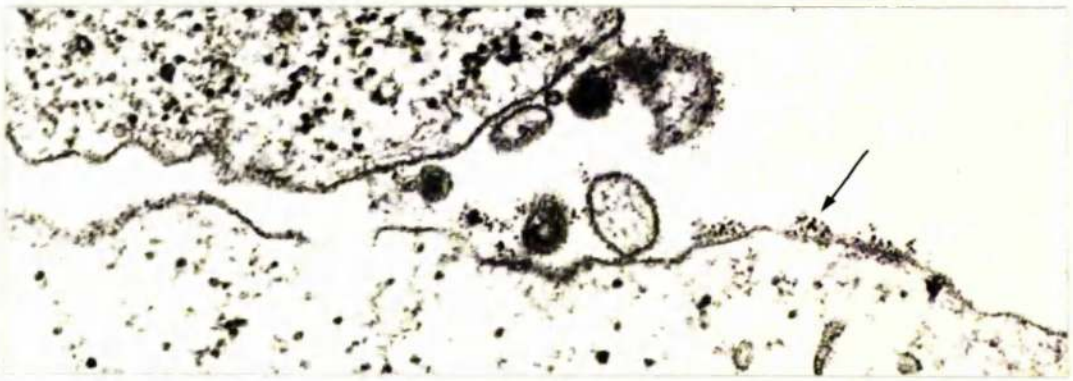

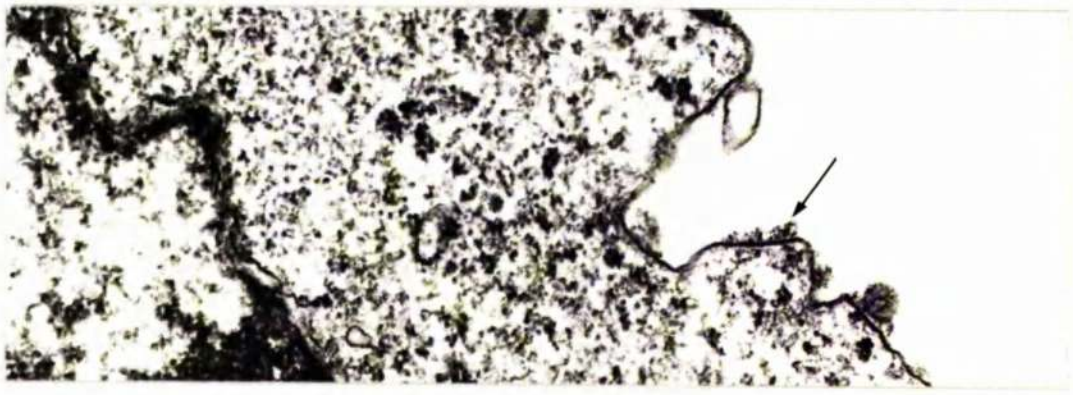

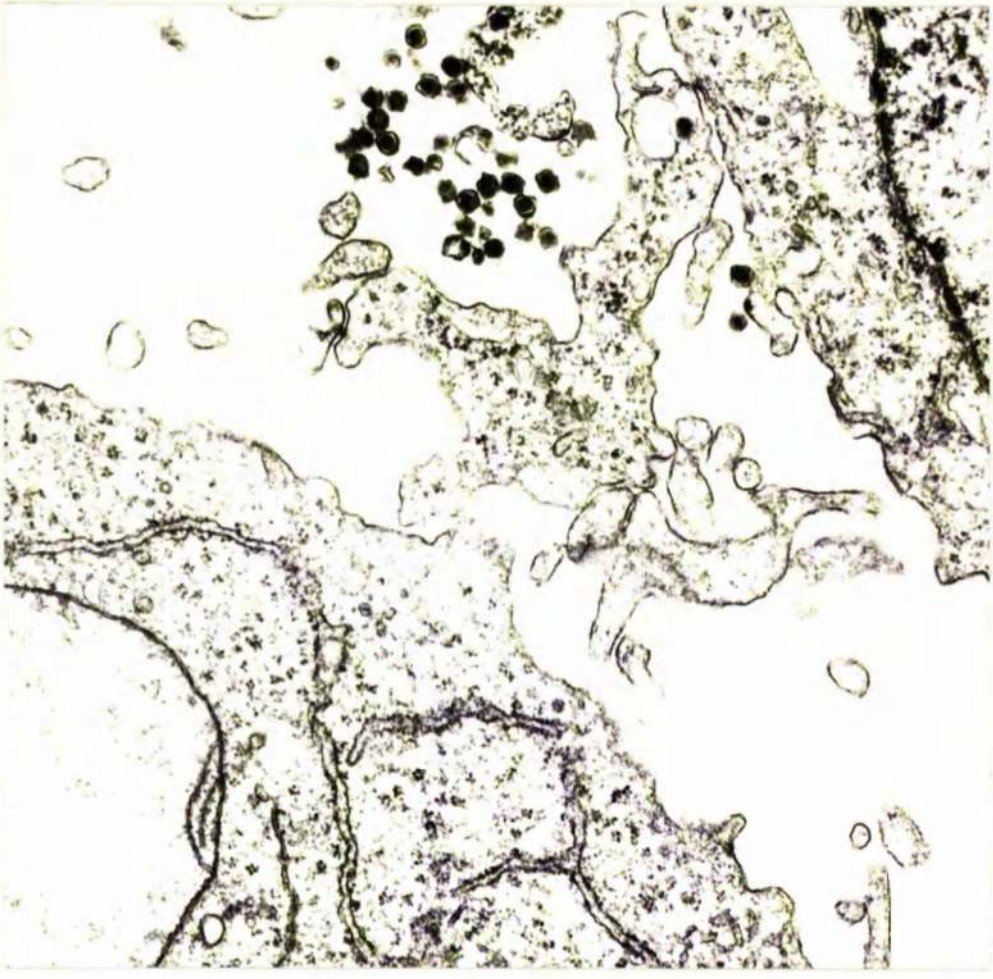

FIGURE 91 : Control cells. Cell membranes and virus particles are unlabelled.

x 15,000

FIGURE 92 : FL74 cell incubated with anti-p15 serum. Intact virus particles are not labelled. The cell membrane is sparsely labelled. Unstained section.

x 40,000

FIGURE 93 : FL74 cell incubated with anti-p30 serum. Intact virus particles are not labelled. The cell membrane is moderately labelled. Unstained section.

x 40,000

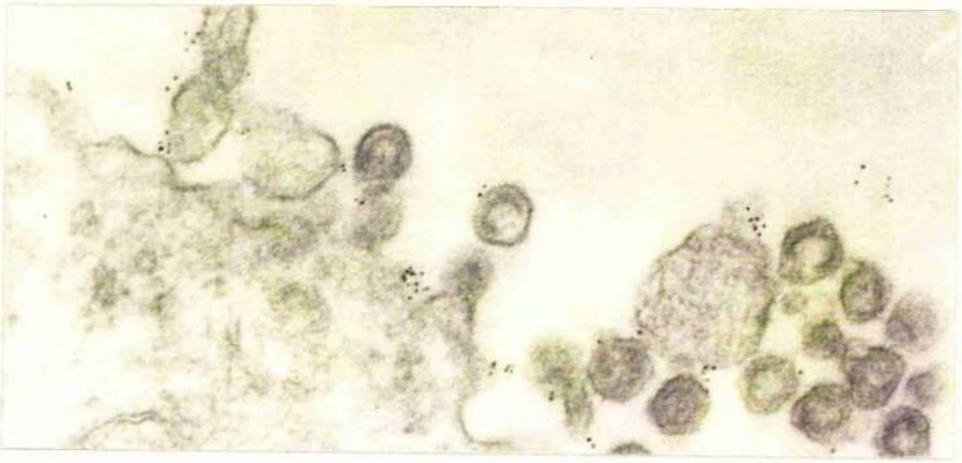

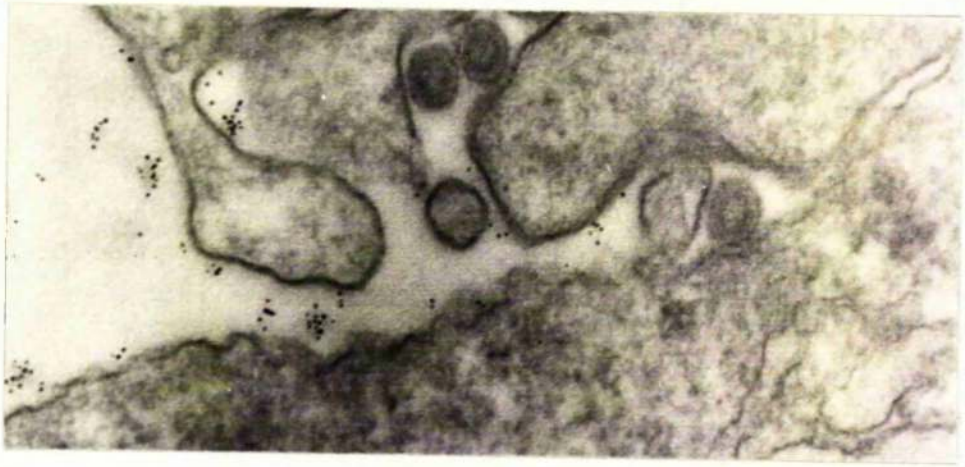

FIGURE 94 : FL74 cell incubated with anti-gp70 serum. The cell membrane and the viral surfaces are moderately labelled. Unstained section.

x 40,000

FIGURE 95 : FL74 cell incubated with anti-FeLV-AC serum. The viral surfaces are moderately labelled. The cell membranes are more heavily labelled with this serum than with the anti-gp70 serum (see Fig. 94) or with anti-FOCMA serum (see Fig. 96). Unstained section.

x 40,000

FIGURE 96 : FL74 cell incubated with anti-FOCMA serum. The cell membranes and virus particles are labelled. The cell membrane is less heavily labelled with this serum than with the anti-gp70 (see Fig. 94) or with the anti-FeLV-AC serum (see Fig. 95). Unstained section.

x 40,000

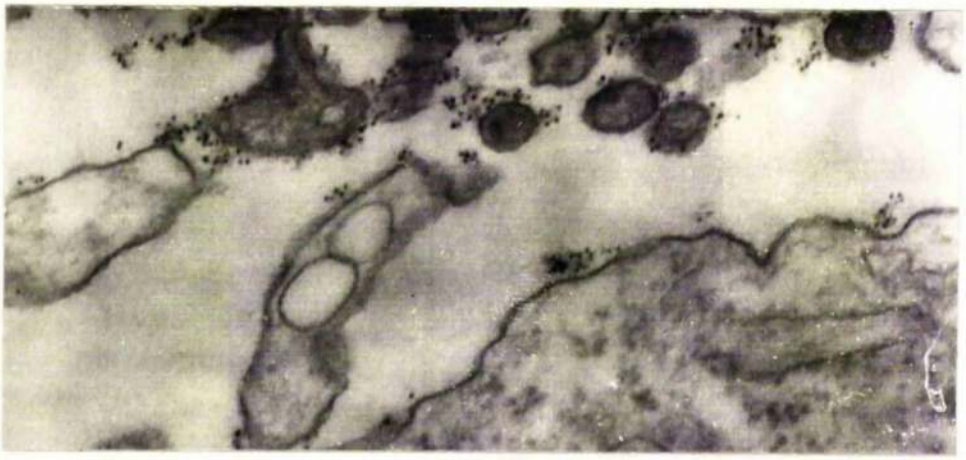

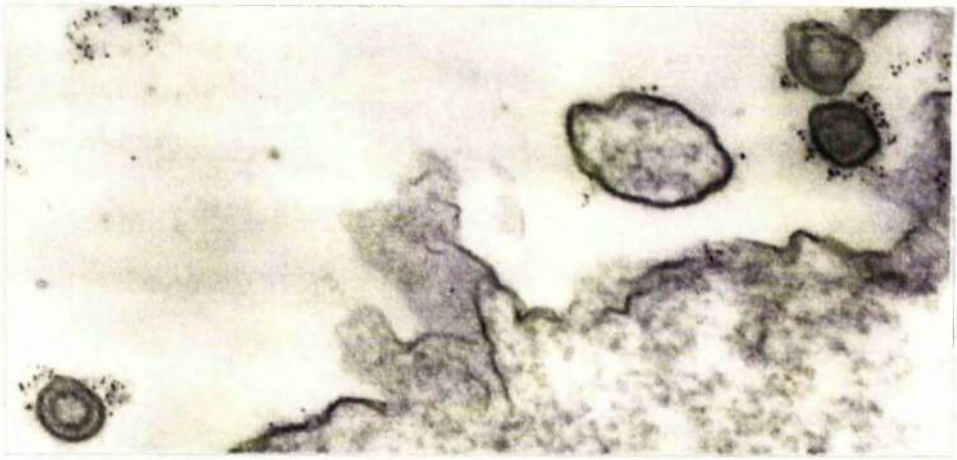

FIGURE 97 : CT45-S cells infected with FeLV-B and incubated with anti-FOCMA serum with anti-FeLV-A and -C activities. Note the heavy labelling of the virions.

x 20,000

FIGURE 98 : CT45-S cells infected with FeLV-AB. Cells were incubated with the serum described in Fig. 97. Virions are slightly less labelled than those in Fig. 97.

x 20,000

FIGURE 99 : CT45-S cells infected with FeLV-C. Cells were incubated with the serum described in Fig. 97. The cell membranes are sparsely labelled (arrows) and the virions are unlabelled.

x 20,000

FIGURE 100 : Control CT45-S cells. Cells were incubated with normal cat serum. Cell membranes and virions are unlabelled.

x 20,000

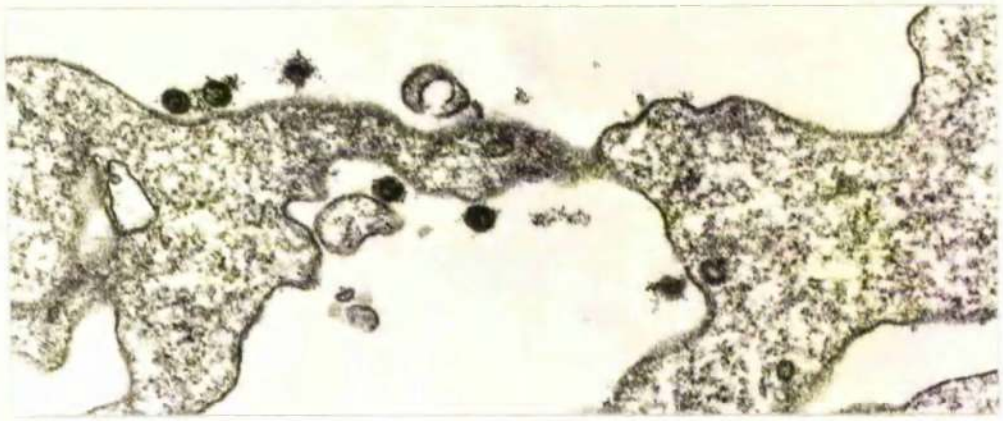

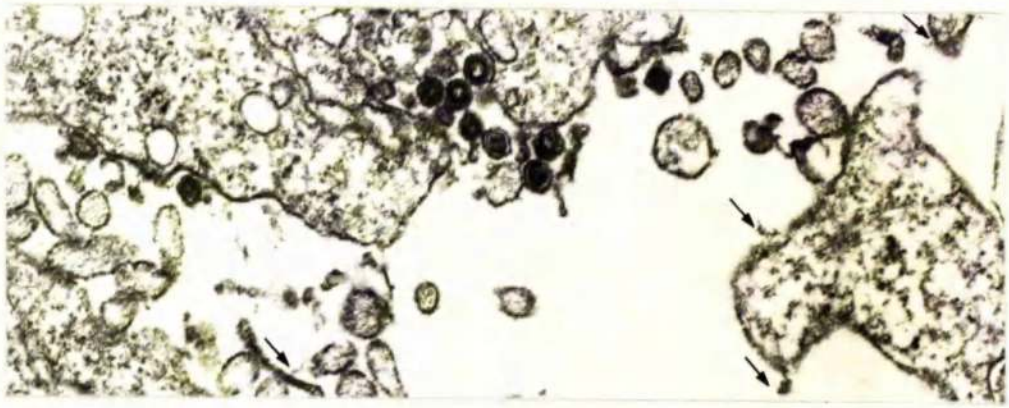

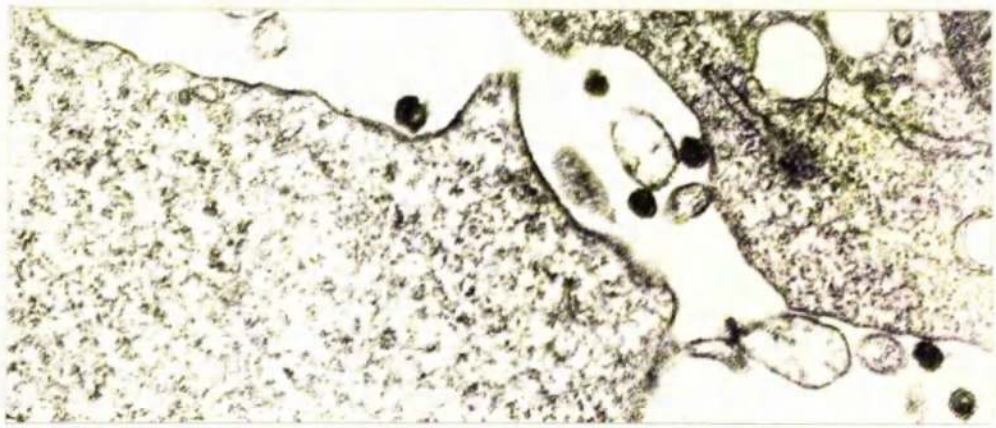

FIGURE 101 : Synchronised FL74 cells in the E - G_1 phase incubated with anti-gp70 serum. Cell membranes are heavily labelled.

x 20,000

FIGURE 102 : Synchronised FL74 cells in the S phase incubated with anti-gp70 serum. Cell membranes are sparsely labelled.

x 20,000

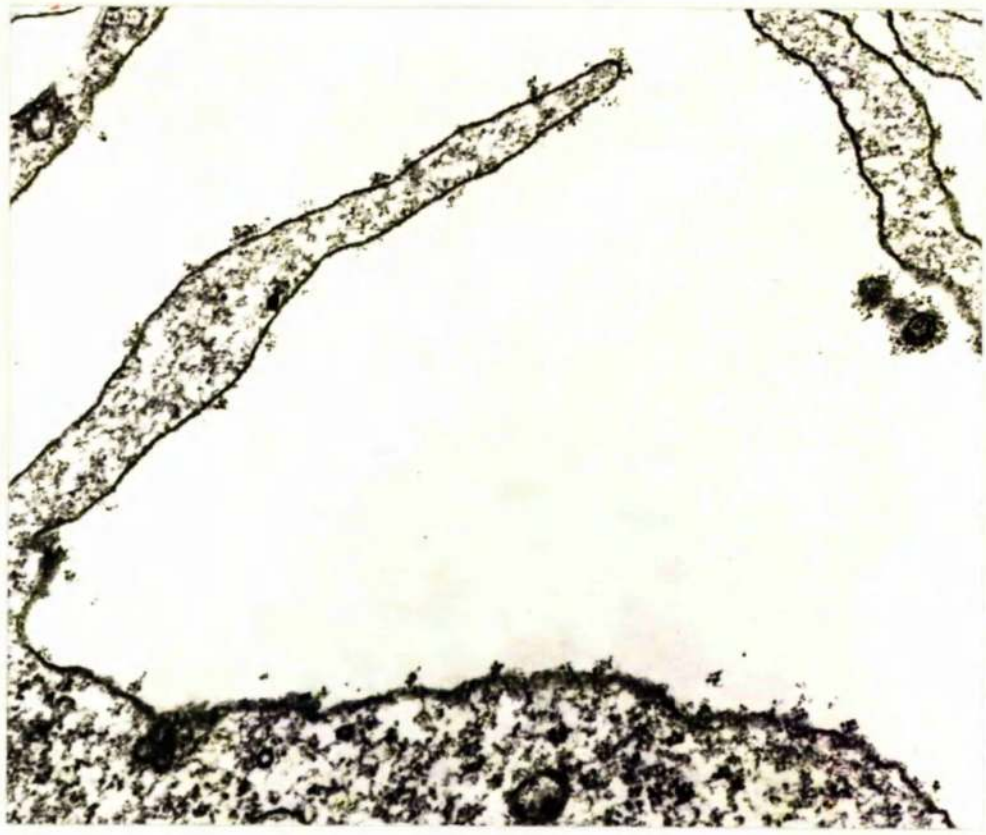

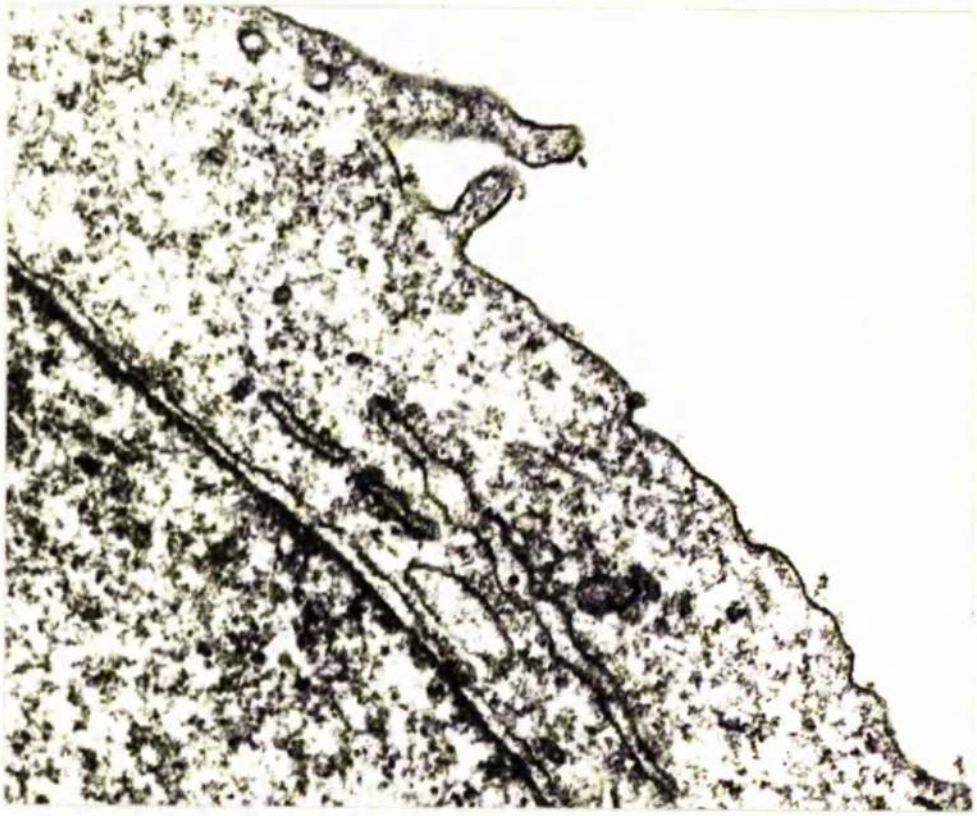

FIGURE 103 : Synchronised FL74 cells in the E - G_1 phase incubated with anti-gp70 serum. The number of antigenic sites per unit length is greater than in the -S phase. See Figs. 102 and 104.

x 20,000

FIGURE 104 : Synchronised FL74 cells in the S phase. The cell membranes are sparsely labelled. Budding and released virions have similar labelling intensities throughout the cycle. See Figs. 101 and 104.

x 20,000

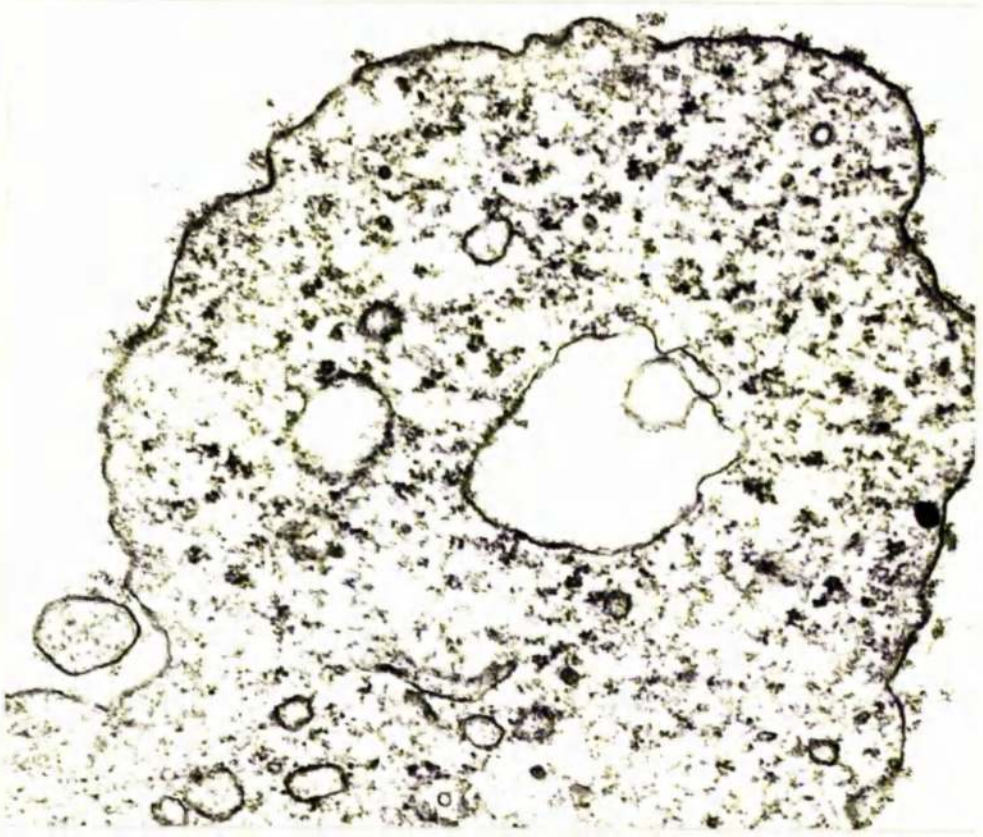

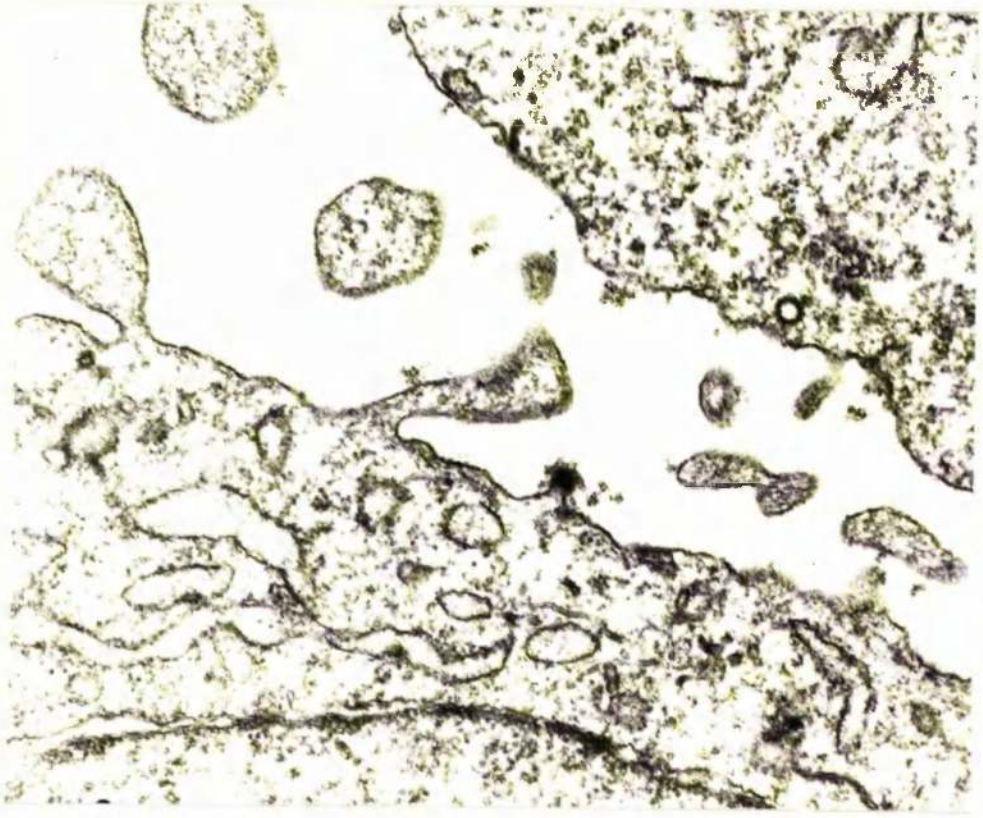

FIGURE 105 : Capping process. Stage one. Long length of the cell membrane is heavily labelled (arrows).

x 30,000

FIGURE 106 : Capping process. Stage two. The labelled cell membrane is invaginated, pinched off and appears in the form of a small vesicle (arrow).

x 30,000

FIGURE 107 : Capping process. Stage three. Vesicles are larger than those in Fig. 106. Their inner surfaces, with budding virions, are heavily labelled (arrow).

x 30,000

FIGURE 108 : Capping process. Stage four. Detached and clumped ferritin molecules are in the lumen of the vesicles (arrow). The cell is intensively vacuolated.

x 20,000

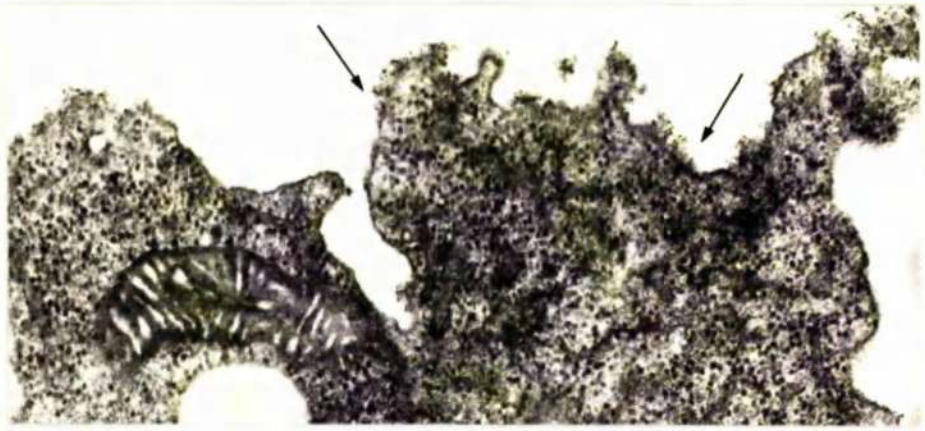

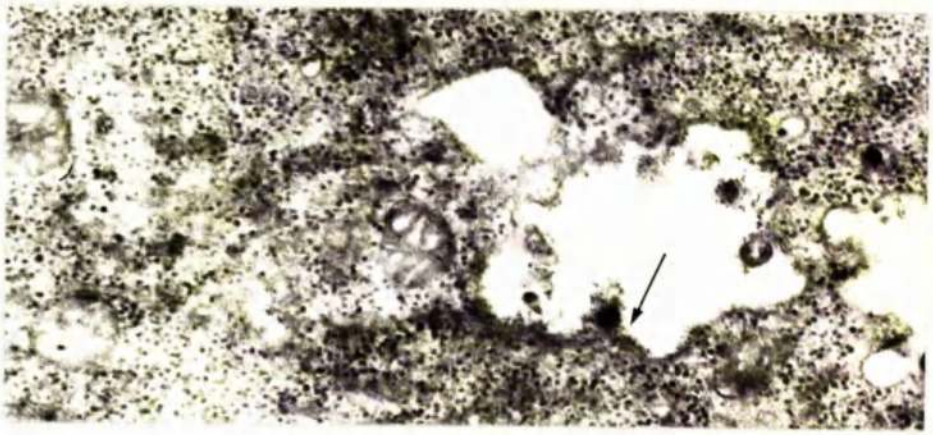

FIGURE 109 : FL74 cell incubated with high titre viraemic FOCMA serum with low neutralising activity to FeLV-A, 1:40 dilution. One virus particle, presumably FeLV-A, is labelled (arrow) the others are not.

x 30,000

FIGURE 110 : FL74 cell incubated with the antiserum described in Fig. 109. Virions are labelled with only one ferritin tag (arrows).

x 30,000

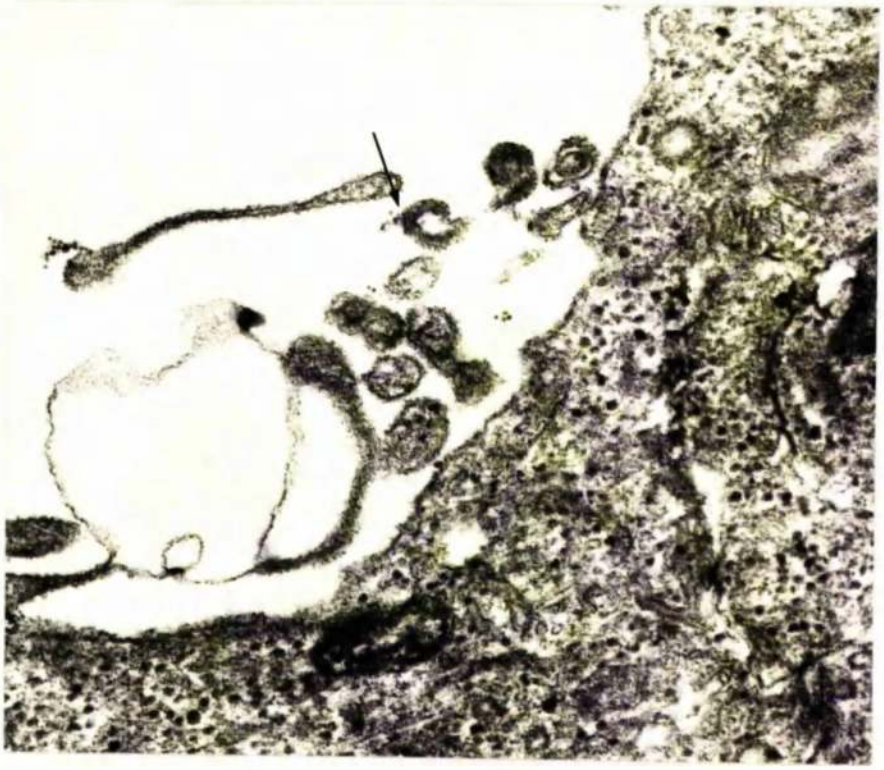

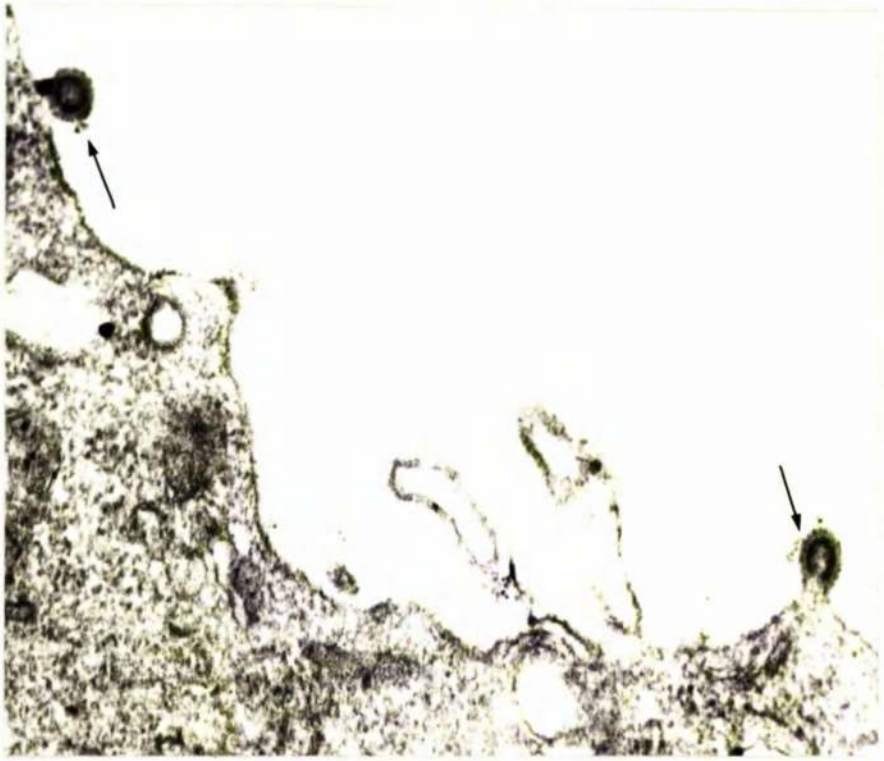

FIGURE 111 : Ring fluorescence. FL74 cells incubated for 30 minutes with gp70 antiserum and goat anti-rabbit fluorescein-conjugated globulin.

FIGURE 112 : Patchy ring fluorescence and caps (arrow). FL74 cells incubated, for 1 hour, with gp70 antiserum and goat anti-rabbit fluorescein-conjugated globulin.

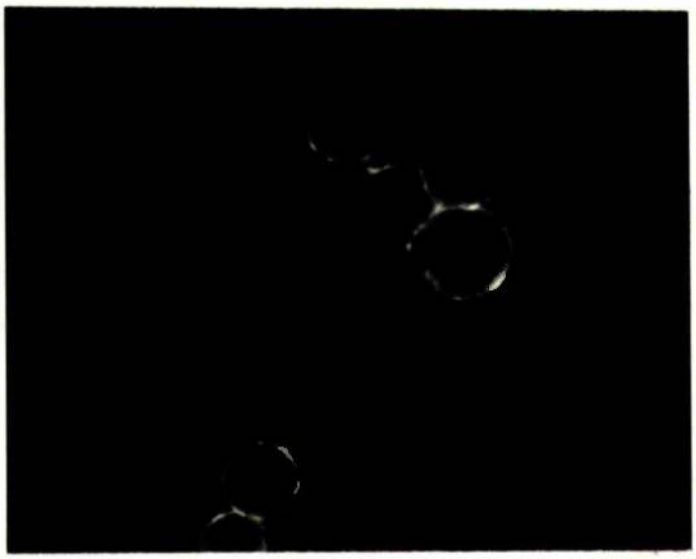

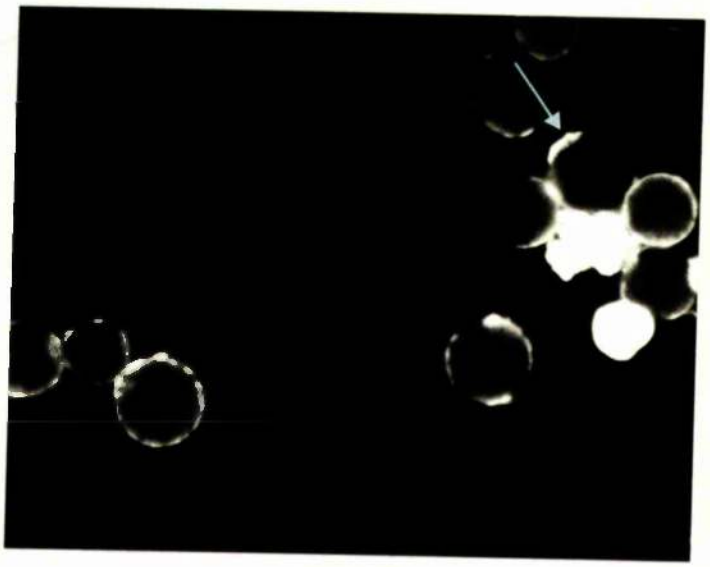

FINAL DISCUSSION AND CONCLUSIONS

FINAL DISCUSSION AND CONCLUSIONS

In the course of this study a variety of cell cycle-related changes were examined in feline leukaemia virus-infected lymphoid cell lines. These included an investigation of the cell cycle-dependence of virus release and antigen expression, a study of the effects of metabolic inhibitors, and the transmission, scanning and immunoelectron microscopy of cells.

Generally, this type of investigation requires the use of a wide range of methods and especially the use of synchronous cell populations in which most of the cells are at a similar stage of biochemical development. To gain well synchronised populations and to be able to interpret data obtained on synchronised cells the phases of the cycle have to be analysed and their duration determined. The fact that in all the experiments, lymphoid cell lines in suspension culture were used, restricted the choice of synchronisation procedures and life cycle analysis methods. After preliminary experiments, the double thymidine block, cold treatment, and isoleucine deprivation of cells were selected as the most suitable techniques. For life cycle analysis pulse-labelling with ^{3}H-TdR and mitotic index determination of synchronised cells were used.

By using two assay systems and applying two different synchronising methods it was established that FeLV production was cell cycle-dependent. It occurred in the G_1 period in both homologous and heterologous cell lines. However, there was some difference between them concerning the exact time of the viral peak in the G_1 phase itself. Particular attention was paid to the FL74 cell line which expressed FOCMA and which released virus in

the early part of the G_1 phase. There was only a 2 - 3 hour gap between the mitotic and the viral peaks, and the question arose which particular cells in the cycle were releasing most of the virus. To establish this, it was necessary to be able, morphologically, to identify individual cells or groups of cells belonging to a certain phase of the cell cycle. For that purpose a detailed ultrastructural study of synchronised FL74 cells was carried out by transmission and scanning electron microscopy.

An analysis of morphological data obtained by TEM and SEM revealed that synchronised FL74 cells exhibited distinct ultrastructural variations which were closely related to the cell cycle. When morphologically characterised cells were examined for budding C-type particles it was found that in both TEM and SEM preparations it was the early-G_1-cells that were releasing the highest number of virus particles. In addition, a number of important observations was made by TEM and SEM. Thus, it was established, for the first time, that lymphoid cells showed characteristic cell surface changes which were highly cell cycle-specific. In many instances, these surface changes were similar to those reported by Porter et al., (1973) and Hale et al., (1975) for monolayer cells. This finding gave rise to the assumption that all proliferating cells, normal or transformed, go through a sequence of cell cycle-dependent phenotypic expression. The fact that the main morphological types of mononuclear cells described by Dantchev and Belpomme (1977) bore a striking resemblance to the phenotypes of synchronously growing FL74 cells greatly supports this theory. It would also follow from this that the prevalence of one morphological type in a certain leukaemic cell population merely reflects the position of the cells in the cycle.

The formation of certain surface structures by a membrane assembly process as well as the shedding off of membrane projections were also followed up and demonstrated. These observations contributed to a better understanding of the changing nature of the cell surface structure, and gave morphological evidence for the shedding off of surface components which had already been demonstrated by radioimmunoassay (Neil, personal communication).

Evidence for the cell cycle-dependent expression of antigens was obtained in a series of experiments using immunofluorescence techniques. It was established that the viral structural proteins p15 and p30 reached a peak in the early-G_1 phase which declined later in the G_1 period. The pattern of surface immunofluorescence closely followed the pattern seen in the cytoplasm. gp70 also reached a peak in early-G_1 phase but remained at the same level and diminished only in the following S phase. Anti-FOCMA sera produced a staining pattern similar to that of gp70 antiserum with the difference that there was a second prominent peak 14 hours later in the late-G_1 period. The presence of the second "FOCMA peak" on the feline tumour cell lines FL74 and its absence from the FeLV-infected canine CT45-S cell line suggested that FOCMA was distinct from the viral antigens.

It is thought that the periodic fluctuation in staining intensity reflects the periodic synthesis of the antigens. This view is supported by the findings of other researchers, made at about the same time as the present experiments were carried out, concerning the synthesis and cleavage of R-MLV precursor proteins (Naso and Brown, 1977). They provided

evidence for the synchronised synthesis of viral precursors prior to virus release in the middle - S and late - S - G_2 phases of the cycle. Considerable difference was found between the post-synthetic processing of gag and env precursor polypeptides in MSV-MLV-infected cells (Witte and Weissman, 1974, 1976). The prolonged excretion pattern for gp69-71 molecules was in striking contrast to the rapid excretion rate per unit time for p30 molecules. The assumption that similar post-synthetic processes take place in FL74 cells would explain the rapid appearance and utilisation of the proteins p15 and p30 in the early -G_1 phase which coincides with peak virus release, and the more prolonged presence of the gp70 antigen peak which persists during the whole G_1 phase. Moreover, the synthesis and post-synthetic processing of FOCMA precursors would also be different from those of the viral precursors and this would account for the 14 hour gap between the viral antigen and FOCMA peaks.

In order to investigate more closely the regulatory mechanisms responsible for the expression of antigens and to determine the events which impose cell cycle-dependence on virus replication and antigen expression, the effects of various metabolic inhibitors were examined. Mitosis has a prominent role in oncornavirus replication. Drugs, such as vinblastine sulfate and high doses of cytochalasin B, which interfered with the mitotic process also inhibited virus release. Low dises of CB did not affect mitosis but still inhibited virus release which was possibly caused by its known effect on the glycosylation of the viral precursors. The inhibitory effect of CB was found to be rapid, reversible and cell cycle-dependent. Virus production and cytoplasmic antigen expression were greatly reduced when CB was applied

during S and early-G_2 periods. Actinomycin D, a potent inhibitor of RNA synthesis, inhibited virus release in log phase cells gradually. In synchronised cells AMD inhibited virus release and cytoplasmic antigen expression most when applied during the late -S and early -G_2 periods. It did not affect the expression of cell membrane antigens. Inhibition by AMD was thought to have been caused by its effect on viral precursor polypeptide mRNA. This was also reflected in the reduced rate of virus release. The continuous presence of cell membrane antigens, notably gp70 and FOCMA, indicated that a considerable pool of membrane associated proteins existed in these cells and/or that more RNA species with different functional half lives were operating in the viral synthetic process. Cycloheximide, which affects protein synthesis, inhibited virus release rapidly and completely. Cell division was also affected by this drug suggesting that it was necessary for FeLV production that regulatory systems influencing cell division remained unimpaired. These results indicated that virus production and antigen expression were regulated by a complex cell cycle-dependent synthesis of RNA, mRNA, viral and cellular proteins, which in turn was co-ordinated by mitosis.

To obtain data on the topographic arrangements of cell surface antigens, including FOCMA, immunoelectron microscopy of cells was performed. Prior to the labelling procedures, experiments were carried out to compare various prefixing methods and their effects on the preservation of antigenic sites. Prefixation with 0.25% glutaraldehyde for 30 minutes appeared to be the best method and was consequently used during the experiments. When unfixed cells were labelled on ice the viral antigens as well as FOCMA showed the characteristic redistribution pattern of patching.

Ferritin labelling of cells revealed that the cell surface antigens were randomly distributed. gp70 was found to be the most numerous followed by FOCMA, p30 and p15 in descending order. p30 and p15 antisera did not stain intact virus particles, while the non-budding areas of the cell membrane were labelled. Both gp70 and FOCMA antisera stained viral particles as well as non-budding areas of the cell membrane. In order to investigate the unexpected labelling of viral particles by viraemic FOCMA antiserum, an immunofluorescence-immunoferritin study in capping conditions and a series of competition experiments were performed. The results indicated that FOCMA was distinct from gp70 and that labelling of virions was possibly due to the undetected presence of neutralising antibodies in the FOCMA antisera used. After labelling of cells in capping conditions, viral antigens and FOCMA appeared to move and form caps independently. Quantitative differences between the various antigens influenced the length of time needed for cap formation. When synchronised FL74 cells were labelled in the S and early -G_1 phases of the cycle it was found that the number of labelled antigenic sites per unit length was two and a half times higher on early-G_1- cells than on cells in the S phase. This was in accordance with results obtained by immunofluorescence staining and indicated that during peak antigen expression the number of antigenic sites per unit length increased.

It is hoped that the findings made in the course of these investigations have cast some new light on the inter-relationship between the cell cycle and feline leukaemia viruses and have reaffirmed the overall importance of the cell cycle concept in a variety of fields.

REFERENCES

Aaronson, S.A., and Dunn, C.Y. (1974). High frequency C-type virus induction by inhibitors of protein synthesis. Science 183, 422-424.

Abbot, J., and Holtzer, H. (1966). The loss of phenotypic traits by differentiated cells. III. The reversible behaviour of chondrocytes in primary cultures. J. Cell Biol. 28, 473-487.

Alexander, E.L., and Wetzel, B. (1975). Human Lymphocytes: Similarity of B and T Cell Surface Morphology. Science 188, 732-734.

Ambros, V.R., Chen, L.B., and Buchanan, J.M. (1975). Surface ruffles as markers for studies of cell transformation by Rous Sarcoma Virus. Proc. Nat. Acad. Sci. (U.S.A.) 72, 3144-3148.

Ambrose, Ch.T. (1969). Regulation of the secondary antibody response in vitro. Enhancement by actinomycin D and inhibition by a macromolecular product of stimulated lymph node cultures. J. Exp. Med. 130, 1003-1029.

Amos, H., Leventhal, M., Chu, L., and Karnovsky, M.T. (1976). Modification of mammalian cell surfaces induced by sugars: scanning electron microscopy. Cell 7, 97-103.

Andres, G.A., Accini, L., Hsu, K.C., Penn, I., Porter, K.A., Rendall, J.M., Seegal, B.C., and Starzl, T.E. (1970). Human renal transplants. III. Immunopathologic studies. Lab. Invest. 22, 588.

Aoki, T., Hämmerling, U., De Harven, E., Boyse, E.A., and Old, L.J. (1969). Antigenic structure of cell surface. J. Exp. Med. 130, 979.

Aoki, T., Boyse, E.A., Old, L.J., De Harven, E., Hämmerling, U., and Wood, H.A (1970). G (Gross and H-2 cell surface antigens: Location on Gross leukaemia cells by electron microscopy with visually labelled antibody. Proc. Nat. Acad. Sci. U.S.A., 65, 569-576.

Aoki, T., Herberman, R.B., Johnson, P.A., Lin, M., and Sturm, M.M. (1972). Wild type Gross Leukaemia Virus: Classification of soluble antigen (GSA). J. Virol. 10, 1208-1219.

Augenlicht, L.H., and Baserga, R. (1974). Changes in the G_0 state of Wi-38 fibroblasts at different times after confluence. Exptl. Cell Res. 89, 255-262.

Avrameas, S. (1969). Coupling of enzymes to proteins with glutaraldehyde. Use of the conjugates for the detection of antigens and antibodies. Imunochemistry 6, 43.

Avrameas, S., and Leduc, E.H. (1970). Detection of simultaneous antibody synthesis in plasma cells and specialised lymphocytes in rabbit lymph nodes. J. Exp. Med. 131, 1137.

Bader, J.P. (1964). The role of deoxyribonucleic acid in the synthesis of Rous sarcoma Virus. Virology 22, 462-468.

Bader, J.P., (1966). Metabolic requirements for infection by Rous sarcoma virus. II. The participation of cellular DNA. Virology 29, 452.

Bader, J.P. (1968). A change in growth potential of cells after conversion by Rous sarcoma virus. J. Cell Physiology 70, 301.

Bader, J.P. (1970). Synthesis of the RNA of RNA-containing tumor viruses. I. The interval between synthesis and envelopment. Virology 40, 494-504.

Baltimore, D. (1974). Tumor Viruses. Cold Spring Harbor Symposium. Quant. Biol. 39, 1187-1200 (1975).

Baluda, M.A., and Nayak, D.P. (1969). Incorporation of precursors into ribonucleic acid, protein, glycoprotein and lipoprotein of avian myeloblastosis virions. J. Virol. 4, 554-566.

Barbacid, M., Stephenson, J.R., and Aaronson, S.A. (1976). The gag gene of mammalian type-C RNA tumor viruses. Nature (London) 262, 554-559.

Barranco, S.C., Haenelt, B.R., and Bolton, W.E. (1977). Cell cycle time determinations based on liquid scintillation counting of ^{3}H-TdR labelled mitotic cells. Cell Tissue Kinet. 10, 335-340.

Baserga, R., and Lisco, E. (1963). Duration of DNA synthesis in Ehrlich ascites cells as estimated by double-labelling with C^{14} and ^{3}H-TdR and autoradiography. J. Natl. Cancer Inst. 31, 1559-1571

Baserga, R. (1976). Multiplication and Division in Mammalian Cells. New York. Marcel Dekker.

Baserga, R., Huang, C., Rossini, M., Chang, H., and Ming, P.L. (1976). The role of Nuclei and Nucleoli in the Control of Cell Proliferation. Cancer Res. 36, 4297-4300.

Bases, R.E., and King, A.S. (1967). Inhibition of Rauscher murine leukaemia virus growth in vitro by actinomycin D. Virology 32, 175-183.

Basilico, C., and Marin, G. (1966). Susceptibility of cells in different stages of the cell cycle to transformation by polyoma virus. Virology 28, 150-162.

Bauer, H., Kurth, R., Rohrschneider, L., Pauli, G., Friis, R.R., and Golderbloom, H. (1974). The Role of Cell Surface Changes in RNA Tumor Virus-transformed Cells. Cold Spring Harbor Symp. Quant. Biol. 39, 1181-1185.

Belpomme, D., Dantchev, D., Joseph, R., Santoro, A., Feuilhade de Chauvin, F., Lelarge, N., Grandjon, D., Pontvert, D., and Mathe, G. (1976). Classification of leukaemias and hematosarcomas based on cell membrane markers and scanning electron microscopy. Europ. J. Cancer 1, 131.

Bennett, G., and Leblond, C.P. (1970). Formation of cell coat material for the whole surface of columnar cells in the rat small intestine visualised by radioautography with L-fucose-^{3}H. J. Cell Biol. 46, 409-416.

Bernhard, W., and Guerin, M. (1958). Presence de particules d'aspect virusal dans les tissus tumoraux de souris atteintes de leucemie spontanee.

Biberfeld, P., and Ringertz, N.Y. (1966). The application of immune electron microscopy to the demonstration of polyoma virus antigen in cultured mouse embryo cells. J. Natl. Cancer Inst. 37, 451.

Birdwell, C.R., and Strauss, J.H. (1974). Replication of Sindbis Virus. IV. Electron Microscope Study of the Insertion of Viral Glycoproteins into the Surface of Infected Chick Cells. J. Virol. 14, 366-374.

Blume, A., Gilbert, G., Wilson, S., Farber, J., Rosenberg, R., and Nirenberg, M. (1970). Regulation of acetylcholine in neuroblastoma cells. Proc. Natl. Acad. Sci. U.S.A. 67, 786-792.

Bolognesi, D.P., Hüper, G., Green, R.W., and Graf, T. (1974). Biochemical properties of oncornavirus polypeptides. Biochim. Biophys. Acta. 355, 220-235.

Bootsma, D., Budke, L., and Vos, O. (1964). Studies on synchronous division of tissue culture cells initiated by excess thymidine. Exp. Cell Res. 33, 301.

Bostoc, D.J., Prescott, D.M., and Kirkpatrick, J.B. (1971). An evaluation of the double thymidine block for synchronising mammalian cells at the G_1 - S border. Exp. Cell Res. 68, 163-168.

Boyde, A., Weiss, R.A., and Vesely, P. (1972). Scanning electron microscopy of cells in culture. Exptl. Cell Res. 71, 313-324.

Breeze, S.S. (1969). Reactions of intracellular crystals of foot and mouth disease virus with ferritin-tagged antibody. J. Gen. Biol. 4, 343.

Breeze, S.S. (1970). An indirect ferritin-tagged antibody system for foot and mouth disease virus. J. Gen. Virol. 8, 153.

Brunk, U., Bell, P., Collins, P., Forsby, N., and Fredricksson, B.A. (1975). SEM of in vitro cultivated cells, osmotic effects during fixation. In "SEM/IITRI/1975", 379-386.

Buell, D.H., Fahey, J.C. (1969). Limited periods of gene expression in immunoglobulin synthesising cells. Science 164, 1524-1525.

Burger, M.M. (1973). Surface changes in transformed cells detected by lectins. Fed. Proc. 32, 91.

Bürk, R.R. (1958). Reduced adenyl cyclase activity in a polyoma virus transformed cell line. Nature (London), 219. 1272-1275.

Byars, N., and Kidson, C. (1970). Programmed synthesis and export of immunoglobulin by synchronised myeloma cells. Nature (London), 226, 648-650.

Calafat, J., Buijs, F., Hageman, P.C., Links, J., Hilgers, J., and Heckman, A. (1974). Distribution of virus particles and mammary tumor virus antigens in Mouse Mammary Tumors, Transformed BALB/c Mouse Kidney Cells and GR Ascites Leukemia Cells. J. Natl. Cancer Inst. 53, 977-991.

Carp, R.I., and Gilden, R.V. (1966). Comparison of the replication cycles of simian virus 40 in human diploid and African green monkey kidney cells. Virology 28, 150-162.

Carteaud, J.P., Muir, M.D., and Cataigne, G. (1973). A Morphological investigation in the SEM of haemagglutination with influenza and vaccinia viruses. In "SEM/IITRI/1973", pp.497-504.

Carter, S.B. (1972). The cytochalasins as research tools in cytology. Endeavour 31, 77-82.

Cikes, M. (1970a). Antigenic Expression of a Murine Lymphoma during Growth in vitro. Nature 225

Cikes, M. (1970b). Relationship between Growth Rate, Cell Volume, Cell Cycle Kinetics and Antigenic Properties of Cultured Murine Lymphoma Cells. J. Natl. Cancer Inst. 45, 979-988.

Cikes, M., and Friberg, Jr., S. (1971). Expression of H-2 and Moloney leukaemia virus-determined cell-surface antigens in synchronised cultures of mouse cell line. Proc. Natl. Acad. Sci. (U.S.A.) 68, 566-569.

Cockerell, G.L., and Hoover, E.A. (1977). Inhibition of Normal Lymphocyte Mitogenic Reactivity by Serum from FeLV-infected Cats. Cancer Res. 37, 3985-3989.

Cohnen, G., Fischer, K., Ludwig, H., and Brittinger, G. (1976). Surface Morphology of Normal and Chronic Lymphocytic Leukaemia Lymphocytes. Eur. J. Cancer 12, 199-202.

Craig, N. (1973). The Effects of Inhibitors of RNA and DNA synthesis on Protein Synthesis and Polysome Levels in Mouse L-cells. J. Cell Physiol. 82, 133-150.

Critchley, D.R., and MacPherson, I. (1973). Cell density-dependent glycolipids in NIL_2 hamster cells derived malignant and transformed cell lines. Biochim.Biophys. Acta. 296, 145-159.

Dales, S., and Hanafusa, H. (1972). Penetration and Intracellular Release of the Genomes of Avian RNA Tumor Viruses. Virology, 50, 440-458.

Dantchev, D., and Belpomme, D. (1977). Critical Study of the Mononuclear Leukocyte Morphology Based on Scanning Electron Microscopy in Normal Subjects and in Patients with Lymphoid or Monocytoid Proliferative Disorders. Comparison with the T, B or Null Cell Membrane Phenotypes. Biomed. 27, 202-222.

Davis, W.C., Douglas, S.P., Petz, L.D., and Fadenberg, H.H. (1968). Ferritin-antibody localisation of erythrocyte antigenic sites in immuno-haemolytic anaemias. J. Immunol. 101, 621.

De Cosse, J.J., and Gelfant, S. (1968). Non-cycling Tumor Cells: Mitogenic Response to Anti-lymphocytic Serum. Science 162, 698.

De Harven, E., Lampen, N., and Bayard, D.C. (1978). The significance of scanning electron microscopy in the diagnosis of hairy cell leukaemias. In Sixty-Ninth Annual Meeting of the American Association for Cancer Research (AACR Abstracts), p.199.

De Luca, C. (1966). Effects of mode of culture and nutrient medium on cyclic variations in enzyme activities of mammalian cells cultured in vitro. Exp. Cell. Res. 43, 39-50.

De Mars, R. (1964). Some studies of enzymes in cultured human cells. Natl. Cancer Inst. Monogr. 13, 181-195.

De Petris, S., and Raff, M.C. (1972). Distribution of immunoglobulin on the surface of mouse lymphoid cells as determined by immunoferritin electron microscopy. Antibody-induced, temperature dependent re-distribution and its implications for membrane structure. Eur. J. Immunol. 2, 523-535.

De Petris, S. (1974). Inhibition and reversal of capping by cytochalasin B, vinblastine and colchicine. Nature (London) 250, 54-56.

De Petris, S. (1978). Non-uniform Distribution of Concanavalin-A Receptors and Surface Antigens on Uropod-Forming Thymocytes. J. Cell. Biol. 79, 235-251.

Doljanski, L. (1930). Sur le rapport entre la proliferation et l'activite pigmentogene dansles cultures d'epithelium de l'iris. C.R. Soc. Biol. 105, 343-345.

Duc-Nguyen, H., and Rosenblum, E N. (1967). Immunoelectron microscopy of the morphogenesis of mumps virus. J. Virol. 1, 415.

Eagle, H. (1968). Growth-regulatory effects of cellular interactions in vitro, and their relevance to cancer. In "Proliferation and Spread of Neoplastic Cells". Twenty-First Annual Symposium on Fundamental Cancer Research. William and Wilkins, Baltimore, pp. 7 - 20.

Eckhart, W., Dulbecco, R., and Burger, M.M. (1971). Temperature dependent surface changes in cells infected or transformed by a temperature sensitive mutant of polyoma virus. Proc. Natl. Acad. Sci. USA. 68, 283.

Engelberg, J. (1964). The decay of synchronisation of cell division. Exp. Cell Res. 36, 647-662.

Enger, M.D., and Tobey, R.A. (1972). Effects of isoleucine deficiency on nucleic acid and protein metabolism in cultured Chinese hamster cells. Continued RNA and protein synthesis in the absence of DNA synthesis. Biochemistry 11, 269.

Enlander, D., Drew, L., Hoo, R., Everhart, T.E., and Scott, T. (1974). The cytopathic effect of herpes simplex virus on HEp-2 cells as shown by scanning electron microscopy. J. Gen. Virol. 25, 313-316.

Epifanova, O.I., and Terskikh, V.V. (1969). On the Resting Periods in the Cell Life Cycle. Cell Tissue Kinet. 2, 75-93.

Essex, M., Klein, G., Snyder, S.P., and Harrold, J.B. (1971). Antibody to feline oncornavirus-associated cell membrane antigen in neonatal cats. Int. J. Cancer 8, 384.

Essex, M. (1974). The Immune Response to Oncornavirus Infections. In "Virus Evolution and Cancer". (E. Kurstak and K. Maramarosch, Eds.), p.832. New York : Academic Press.

Essex, M., Sliski, A., Cotter, M. Jakowski, R.M., and Hardy, Jr., W.D. (1975). Immunosurveillance of Naturally Occurring Feline Leukaemia. Science, 190, 790.

Essex, M. (1975). Horizontally and Vertically Transmitted Oncornaviruses of Cats. Adv. Cancer Res. 21, 175.

Essex, M., Jakowski, R.M., Hardy, W.D. Jr., Cotter, S.M., Hess, P., and Slisky, A. (1975). Feline oncornavirus-associated cell membrane antigen. III. Antibody titres in cats from leukaemia cluster households. J. Natl. Cancer Inst. 54, 637-641.

Farrant, J.F. (1954). An Electron Mixroscopic Study of Ferritin. Biochim. Biophys. Acta 13, 569.

Faulk, P.W., and Taylor, M.G. (1971). An immunocolloid method for the electron microscope. Immunochemistry 8, 1081.

Ferrone, S., De Villano, B., Pellegrino, M.A., Lerner, R.A., Reisfeld, R.A. (1972). Expression of HL-A antigens on the surface of cultured lymphoid cells: Effects of inhibitors of protein and nucleic acid synthesis. Tissue Antigens 2, 477-453.

Ferrone, S., Cooper, N.R., Pellegrino, M.A., and Reisfeld, R.A. (1973). Interaction of histocompatibility (HL-A) antibodies and complement with synchronised human lymphoid cells in continuous culture. J. Exp. Med. 137, 55-68.

Ferrone, S , Pellegrino, M.A , Dierich, M.P., and Reisfeld, R.A. (1974). Effects of inhibitors of macromolecular synthesis on HL-A antibody mediated lysis of cultured lymphoblasts. Tissue Antigens 4, 275-282.

Fischinger, P.J . (1974) Simple, quantitative assay for both xenotropic Murine Leukemia and ecotropic Feline Leukemia Viruses. J. Virol. 14, 177-179,

Fischinger, P.J. (1975). Efficient Release of Murine Xenotropic Oncornavirus after MuLV Infection of Mouse Cells. Virology 65, 304-307.

Fiszman, M., Reynier, M., Bucchini, D., and Girard, M (1974). Retarded growth of poliovirus in contact inhibited cells. J. Gen. Virol. 23, 73-82.

Folett, E.A.C., and Goldman, R.D. (1970) The occurrence of microvilli during spreading and growth of BHK21/C13 fibroblasts. Exp. Cell Res. 124.

Fonte, V G , and Porter, K.R. (1974) Visualisation in whole cells of herpes simplexvirus using SEM and TEM. In "SEM/IITRI/1974", pp.827-834.

Frei and Ritchie (1963). "Cell Proliferation". A Guiness Symposium held at University of Dublin Trinity College. I.L.F. Lamarton and R.J.M. Fry, eds), F.A. Davis Co., Philadelphia.

Friedman, M., Lilly, F., and Nathenson, S.G. (1974). Cell surface antigen induced by Friend murine leukemia virus is also in the virion. J. Virol. 14, 1126-1131.

Fukushi, K., Fumio, A., and Oka, S. (1968). Electronmicroscopy of bacterial endotoxin-antibody complexes by use of ferritin-conjugated antibody. J. Electron Micr. (Tokyo) 17, 74.

Galavazi, G., and Bootsma, D. (1966). Synchronisation of mammalian cells in vitro by inhibition of the DNA synthesis. Exp. Cell Res. 41, 438.

Gambari, R., and Masaaki, T. (1978) Synthesis of globin mRNA in relation to the cell cycle during induced murine erythroleukemia differentiation. Proc. Natl. Acad. Sci. USA. 75, 3801-3804.

Gani, R. (1976). The Nucleoli of Cultured Human Lymphocytes. I. Nucleolar Morphology in Relation to Transformation and the DNA cycle. Exptl. Cell Res. 97, 249-258.

Garren, L.D., Howell, R.R., Tomkins, G.M., and Grocco, R.M. (1964). A paradoxical effect of actinomycin D: The mechanism of regulation of enzyme synthesis by hydrocortison. Proc. Natl. Acad. Sci. USA, 52, 1121-1129.

Gatti, R.A., Ostborn, A., and Fagraeus, A. (1974). Selective Impairment of Cell Antigenicity by Fixation. J. Iminunol. 113, 1361-1368

Gelderblom, H., Bauer, H., and Graf, T. (1972). Cell-Surface Antigens Induced by Avian RNA Tumor Viruses: Detection by Immunoferritin Technique. Virology 47, 416-425.

Gelfant, S. (1977). A New Concept of Tissue and Tumor Cell Proliferation. Cancer Res. 37, 3845-3862.

Gerner, E.W., Glick, M.C., and Warren, L. (1971). Membranes of animal cells. V. Biosynthesis of the surface membrane during the cell cycle. J. Cell Physiol. 79, 79-90.

Gilbert, L.W., and Lajtha, L.G. (1965). "Cellular Radiation Biology". Williams and Wilkins, Baltimore.

Goessens, G., and Lepoint, A. (1974). The Fine Structure of the Nucleolus during Interphase and Mitosis in Ehrlich Tumor Cells Cultivated in vitro. Exptl. Cell Res. 87, 63-72.

Goessens, G. (1976). High Resolution Autoradiographic Studies of Ehrlich Tumor Cell Nucleoli. Exptl. Cell Res. 100, 88-94.

Goldberg, B., and Green, H. (1964). An analysis of collagen secretion by established mouse fibroblast lines. J. Cell Biol. 22, 227-258.

Golomb, H.M., Braylan, R., and Polliack, A. (1975). "Hairy" Cell Leukaemia (Leukaemic Reticuloendotheliosis): A Scanning Electron Microscopic Study of Eight Cases. Br. J. Haemat. 29, 455-460.

Gonda, M.A., Aaronson, S.A., Ellmore, N., Zeve, V.H., and Nagashima, K. (1976). Ultrastructural studies of surface features of human, normal and tumor cells in tissue culture by scanning and transmission electron microscopy. J. Nat. Cancer Inst. 56, 245-263.

Gonzalez, P., and Nardone, R.M. (1968). Cyclic Nucleolar Changes during the Cell Cycle. Exptl. Cell Res. 50, 599-615.

Grant, J.P., Bigner, D.D., Fischinger, P.J., and Bolognesi, D.P. (1974). Expression of murine leukemia virus structural antigens on the surface of chemically induced murine sarcomas. Proc. Natl. Acad. Sci. USA. 71, 5037-5041.

Gray, J.W., Carver, J., and Mendelsohn, M.L. (1975). Rapid cell cycle analysis - method and model. In "Workshop on Mathematical Techniques of Cell Cycle Analyses," Copenhagen, Denmark.

Gray, J.W., and Mendelsohn, M.L. (1975). A rapid technique of cell cycle analyses based on sorting cells in S phase. Radiation Research Society Meeting, Miami, Florida.

Greenberger, J.S., and Aaronson, S.A. (1975). Cycloheximide induction of xenotropic type-C virus from synchronised mouse cells: Metabolic requirement for virus activation. J. Virol. 15, 64-70.

Hakomory, S., and Kijomo, S. (1972). Forssman reactivity and cell contacts in cultured hamster cells. Nature (London) New Biol. 239, 87-88.

Hale, A.H., Winkelhake, J.L., and Weber, M.J. (1975). Cell Surface Changes and Rous Sarcoma-Virus Gene Expression in Synchronised Cells. J. Cell Biol. 64, 398-407.

Hämmerling, U., Aoki, T., De Harven, E., Boyse, E.A., and Old. L.J. (1968). Use of hybrid antibody with anti-G and anti-ferritin specificities in locating cell surface antigens by electronmicroscopy. J. Exp. Cell Res. 128, 1461.

Hampar, B., Gerber, P., Hsu, K.C., Martos, L.M., Walker, J.L., Siguenza, R.F., and Wells, G.A. (1970). Immuno-ferritin and immuno-fluorescent studies with Epstein-Barr virus and herpes simplex virus by use of human sera and hyperimmune rabbit sera. J. Nat. Cancer Inst. 45, 75.

Hampar, B., Hsu, K.C., Martos, L.M., and Walker, J.L. (1971). Serologic evidence that herpes-type virus is the etiologic agent of heterophile-positive infectious mononucleosis. Proc. Nat. Acad. Sci. USA, 68, 1407.

Hampar, B., Derge, J.G., Martos, L.M., Tagamets, M.A., Chang, S.Y., and Chakrabarty, M. (1973). Identification of a critical period during the S phase for activation of the Epstein-Barr virus by 5 - iododeoxyuridine. Nature (New Biol.) 244, 214-217.

Hampar, B., Derge, J.A., Nonoyama, M., Chang, S.Y., Tagamets, M., and Showalter, S.D. (1974a). Programming of events in Epstein-Barr virus-activated cells induced by 5-iododeoxyuridine. Virology, 62, 71-89.

Hampar, B , Tanaka, A., Nonoyama, M., and Derge, J. (1974b). Replication of the resident repressed Epstein-Barr virus genome during the early S phase (S-1 period) of non-producer Raji cells. Proc. Natl. Acad. Sci. USA, 71, 631-633.

Hampar, B., and Gilbert, L. (1976). Cell Cycle-Dependence for Activation of EB Virus by Inhibitors of Protein Synthesis of Medium Deficient of Arginine. Virology 69, 660-668.

Hardy, W.D. Jr., Old, L.J., Hess, P.W., Essex, M., and Cotter, S.M. (1973). Horizontal Transmission of Feline Leukaemia Virus. Nature 244, 266.

Hardy, W.D. Jr., Zuckerman, E.E. MacEwen, E.G., Hayes, A.A., and Essex, M. (1977). A feline leukemia virus and sarcoma virus-induced tumor specific antigen. Nature 270, 249-351.

Hayflick, L (1973) Subculturing human fibroblast cultures. In "Tissue Culture, Methods and Applications. Eds. P.F. Kruse and M.K. Patterson.

Hedman, K. (1978). External Fibronectin of Cultured Human Fibroblasts Predominantly a Matrix Protein. J. Cell Biol. 76, 748-760.

Hobom-Schnegg, B., Robinson, H.L., Robinson, W.S. (1970). Replication of Rous Sarcoma Virus in Synchronised Cells. J. Gen. Virol. 7, 85-93

Holder, W., Peer, G., Bolognesi, D.P. (1976). Detection of the major glycoprotein of Friend Leukemia Virus (gp71) and the murine mammary tumour virus (gp52) on the surface of mouse cells. Cancer Res. 36, 3217-3224.

Holmes, K.V. (1975). Scanning electronmicroscopic studies of virus infected cells. I. Cytopathic effects and maturation of vesicular stomatitis virus in L2 cells. J. Virol. 15, 355-362.

Howard, A., and Pelc, S.R. (1953). Synthesis of DNA in normal and irradiated cells and its relation to chromosome breakage. Heredity Suppl. 6, 261.

Howe, C., Morgan, C., De Vaux St. Cyr, C., Hsu, K.C., and Rose, H.M. (1967). Morphogenesis of type 2 parainfluenza virus examined by light and electron microscopy. J. Virol. 1, 215.

Hsie, A.W., and Puck, T.T. (1971). Morphological transformation of Chinese hamster cells by dibutyryl adenosine cyclic 3' 5' - monophosphate and testosterone. Proc. Nat. Acad. Sci. USA. 68, 358-361.

Hughes, R.C., Sanford, B., and Jeanloz, R.W. (1972). Regeneration of the surface glycoproteins of a transplantable mouse tumor cell after treatment with neuraminidase. Proc. Nat. Acad. Sci. USA. 69, 942-945.

Humphries, E.H., Temin, H.M. (1972). Cell Cycle-Dependent Activation of Rous Sarcoma Virus-Infected Stationary Chicken Cells: Avian Leukemia Virus Group-Specific Antigens and Ribonucleic Acid. Virology 10, 82-87.

Hunsmann, G., Claviez, M., Moennig, V., Schwartz, H., and Schäfer, W. (1976). Properties of mouse leukemia viruses. X. Occurrence of viral structural antigens on the cell surfaces as revealed by a cytotoxicity test. Virology, 69, 157-168.

Hunter, E., Hayman, M.J., Rongey, R.W., and Vogt, P.K. (1976). An avian sarcoma virus mutant that is temperature sensitive for virion assembly. Virology 69, 35-49.

Iserzky, C., Metzger, H., Buell, D.N. (1975). Cell Cycle-Associated Changes in Receptors for IgE during Growth and Differentiation of a Rat Basophilic Leukemia Cell Line. J. Exp. Med. 141, 1147-1162.

Jamjom, G., Karshin, W.L, Naso, R.B., Arcement, L.J., and Arlinghous, R.B. (1975). Proteins of Rauscher murine leukemia virus: resolution of a 70,000 dalton, non-glycosylated polypeptide containing p30 peptide sequences. Virology 68, 135-145.

Jarrett, O., Pitts, J.D., Whalley, J.M., Clason, A.E., and Hay, D. (1971). Isolation of the nucleic acid of feline leukemia virus. Virology 43, 317-320.

Jarrett, O., Hardy, W.D. Jr., Golder, M.C., and Hay, D. (1978). The frequency of occurrence of feline leukemia virus subgroups in cats. Int. J. Cancer 21, 334-337.

Jarrett, O., and Russell, P.H. (1978). Differential Growth and Transmission in Cats of FeLV viruses of Subgroups A and B. Int. J. Cancer, 21, 466-472.

Jarrett, W.F.H., Crawford, E., Martin, W.B., and Davie, F. (1964). Leukaemia in the cat. A virus-like particle associated with leukemia (lymphosarcoma). Nature, 202, 567-569.

Jarrett, W.F.H., Jarrett, O., Mackey, L.J., Laird, H.M., Hardy, W.D. Jr., and Essex, M. (1973). Horizontal transmission of Leukemia Virus and Leukemia in the Cat. J. Nat. Cancer Inst. 51, 833.

Jarrett, W.F.H., Mackey, L., Jarrett, O., Laird, H.M., and Hood, C. (1974). Antibody Response and Virus Survival in Cats Vaccinated against Feline Leukaemia. Nature 248, 230.

Jarrett, W.F.H. (1975). The relation of immune response to pathogenesis, vaccination and epidemiology in virus-induced leukaemia. Br. J. Cancer 31. 147-151.

Jarrett, W.F.H., Jarrett, O., Mackey, L., Laird, H.M., Hood, C., and Hay, D. (1975). Vaccination against feline leukaemia virus using a cell membrane antigen system. Int. J. Cancer 16, 134.

Jarrett, W.F.H. (1976). The Epidemiology of Feline Leukaemia Virus Infection. Comp. Leuk. Res. Bibl. Haemat. 43, 209-211, Karger, Basel.

Jeter, J.R. Jr., Glas, P.S., and Kupetz, I.S. (1978). Changes in the nuclear activity of cyclic AMP and cyclic GMP phosphodiesterase during the cell cycle of physarium polycephalum. In: Abstracts, The American Society for Cell Biology. Eighteenth Annual Meeting. 4-8 November 1978. San Antonio, Texas.

Johnson, G.S., Friedman, R.M., and Pastan, I. (1971). Restoration of several morphological characteristics of normal fibroblasts in sarcoma cells treated with adenosine 3', 5'-cyclic monophosphate and its derivatives. Proc. Nat. Acad. Sci. USA. 68, 425-429.

Johnson; R.G., and Sheridan, J.D. (1971). Junctions between cancer cells in culture: Ultrastructure and permeability. Science (Wash. D.C.) 174, 717.

Johnson, G.S., Morgan, W.D., and Pastan, I. (1972). Regulation of Cell Motility by Cyclic AMP. Nature (London) 235, 54.

Johnson, G.S., and Pastan, I. (1972). Cyclic AMP increases the adhesion of fibroblasts to substratum. Nature New Biol. 236, 247-249.

Jones, P.A., Taderera, J.V., and Hawtrey, A.O. (1972). Transformation of Hamster Cells in vitro by 1-β-D-Arabinofuranosylcytosin, 5-Fluorodeoxyuridine and Hydroxyurea. European J. Cancer 8, 595-599.

Jones, P.A., Baker, M.S. (1977). Cell cycle-specific oncogenic transformation of C3H/10 $T\frac{1}{2}$ Clone 8 Mouse Embryo Cells by 1-β-D-Arabinofuranosylcytosin. Cancer Res. 37, 2214-2217.

Kaplan, J.C., Wilbert, S.M., and Blach, P.H. (1972). Analysis of simian virus 40-induced transformation of hamster kidney tissue in vitro. VIII. Induction of infectious simian virus 40 from virogenic transformed hamster cell by amino acid deprivation or cycloheximide treatment. J. Virol. 9, 448-453.

Karnovsky, M.J., Leventhal, M., and Unanue, E.R. (1975). Correlated fluorescent and scanning microscopy of immunoglobulin-induced capping and movement of B lymphocytes. J. Cell Biol. 67, 201a.

Karshin, W.L., Arcement, L.J., Naso, R.B., and Arlinghaus, R.B. (1977). Common precursor for Rauscher leukemia virus for gp69/71, p15 and p12E. J. Virol. 23, 787-798.

Katz, L.N., Mescheryakova, I.S., and Oghievetskaya, M.M. (1970). Electron microscopic study of localisation of antigens in Francisella tularensis by means of ferritin-labelled antibodies. Zh. Mikrobiol. Epidemiologic i immunobiologi 47, 51.

Kerr, J.M., Olshevsky, U., Lodish, H.F., and Baltimore, D. (1976). Translation of murine leukemia virus RNA in cell-free systems from animal cells. J. Virol. 18, 627-635.

Kirschner, M.W., Williams, R.C., Weingarten, M., and Gerhard, J.C. (1974). Microtubules from mammalian brain: Some properties of their depolymerisation products and a proposed mechanism of assembly and disassembly. Proc. Natl. Acad. Sci. USA. 71, 1159-1163.

Kishida, Y., Olsen, B.R., Berg, R.A., and Prockop, D.J. (1975). Two improved methods for preparing ferritin-protein conjugates for electron microscopy. J. Cell Biol. 64, 331-339.

Kitano, Y., and Hu, F. (1971). Proliferation and differentiation of pigment cells in vitro. J. Invest. Dermatol. 55, 444-451.

Kletzien, R.F., and Perdue, J.F. (1973). The inhibition of sugar transport in chick embryo fibroblasts by cytochalasin B. Evidence for a membrane-specific effect. J. Biol. Chem. 248, 711-719.

Kourlisky, F.M., Silvestre, D, Levy, P.J., Dausset, J., Nicolai, M.G., and Senik, A. (1971). Immunoferritin study of the distribution of HL-A antigens on human blood cells. J. Immunol. 106, 454.

Koury, R.E., Kurtz, S.A., Price, P.J., and Benedict, W.F (1975). A-β-D Arabinofuranosylcytosin-induced Malignant Transformation of Hamster and Rat Cells in Culture. Cancer Res. 35, 2413-2419.

Krakowka, S., Olsen, R., and Cockerell, G.(1977)The effect of cell synchronisation upon the detection of T and B lymphoid cell receptors on two continuous lymphoid cell lines. In Vitro 13, 119-123.

Kreider, J.W., and Schmoyer, M.E. (1975). Spontaneous maturation and differentiation of B16 melanoma cells in culture. J. Nat. Cancer Inst. 55, 641-647.

Kuhns, W.J. (1978). Biosynthesis of blood group H gene-associated ∝ - 2 - L - fucosyltransferase during the cell cycle. In: Abstracts, The American Society for Cell Biology. Eighteenth Annual Meeting 1978, San Antonio, Texas.

Kushnarev, V.M., Smirnova, T.A., and Mikhailova, I.M. (1969). Electron microscopic study of the secretion of the toxin of U. perfringens by means of specific ferroglobulin. Zh. Mikrobiol. Epidemiologic i immunobiologi, 46, 24.

Laird, H.M., Jarrett, W.F.H., Jarrett, O., and Crighton, G.W. (1967). Virus-like particles in three field cases of feline lymphosarcoma. Vet. Rec. 80, 606.

Lazarides, E. (1975a). Immunofluorescence studies on the structure of actin filaments in tissue culture cells. J. Histochem. Cytochem. 23, 507-528.

Lazarides, E. (1975b). Tropomyosin antibody: the specific localisation of tropomyosin in non-muscle cells. J. Cell Biol. 65, 549-561.

Leblond, C.P., and Bennett, G. (1974). Elaboration and turnover of cell coat glycoproteins. In: A.A. Moscona (Ed.), The Cell Surface in Development. Wiley, New York, pp.29-49.

Leong, J.A., Warren, L., and Bishop, J.M. (1972). Synchronisation of Rous Sarcoma Virus Production in Chick Embryo Cells. Virology 47, 133-141.

Lerner, R.A., Oldstone, M.B.H., and Cooper, N.R. (1971). Cell Cycle-Dependent Immune Lysis of Moloney Virus-Transformed Lymphocytes: Presence of Viral Antigens, Accessibility to Antibody and C.A. Proc. Nat. Acad. Sci. USA, 68, 2584-2588.

Lerner, R.A., Wilson, C.B., Del Villano, B.C., McConahey, P.J., and Dixon, F.J. (1976). Endogenous oncornaviral gene expression in adult and fetal mice: quantitative, histologic and physiologic studies of the major viral glycoprotein, gp70. J. Exp. Med. 143, 151-166.

Lettre, R., and Siebs, W. (1954). Beobachtungen zur Struktur des Nucleolus in Normallen Zellen Sowie Tumorzellen. Z. Krebsforsch 60, 564-580.

Levin, J.G., Grimley, P.M., Ramseur, J.M. and Berezesky, I.K. (1974). Deficiency of 60 - 70S RNA in murine leukaemia virus particles assembled in cells treated with actinomycin D. J. Virol. 14, 152-161.

Levin, J.G., and Rosenac, M.J. (1976). Synthesis of murine leukemia virus proteins associated with virions assembled in actinomycin D-treated cells, evidence for persistence of viral messenger RNA. Proc. Natl. Acad. Sci. USA, 73, 1154-1158.

Levinthal, J.D., Cerottini, J.C., Ahmad-Zadeh, C., and Witcher, R. (1967). The detection of intracellular adenovirus type 12 antigens by indirect immunoferritin technique. J. Cancer 2, 85.

Ley, K.D., and Tobey, R.A. (1970). Regulation of initiation of DNA synthesis in CHO cells. II. Induction of DNA synthesis and cell division by isoleucine and glutamine in G_1-arrested cells in suspension cultures. J. Cell Biol. 47, 453-459.

Lin, P.S., Wallach, D.F.H., and Tsai, S. (1973). Temperature induced variations in the surface topology of cultured lymphocytes are revealed by scanning electron microscopy. Proc. Natl. Acad. Sci. USA, 70, 2492-2496.

Lin, P.S. (1978). Specificity of the effects of cytochalasin B on transport and motile processes. Proc. Natl. Acad. Sci. USA, 75, 329-333.

Lindahl, P.E., and Sörenby, L. (1966). A New Method for the Continuous Selection of Cells in Mitosis. Exptl. Cell Res. 43, 424-434.

Lindberg, L.G., and Biberfeld, C. (1967). Rous rat sarcoma studied with ferritin-conjugated antibodies. Acta. Path. et Microbiol. Scandinav. 69, 481.

Lipkin, M. (1971). The Cell Cycle and Cancer. Ed. R. Baserga, p.6 New York, M. Dekker.

Littlefield, J.W. (1962). DNA synthesis in partially synchronised L cells. Exp. Cell Res. 26, 318.

Loor, F. (1976). Cell surface design. Nature 264, 272-273.

Love, R., and Walsh, R.J. (1968). The Relation of Nucleolini to Nucleolar Vacuoles in Living Cells. Exptl. Cell Res. 53, 432-466.

Lowry, O.H., Rosebrough, N.H., Farr, A.L., and Randall, R.J. (1951). Protein measurements with the folin phenol reagent. J. Biol. Chem. 193, 265-275.

Mardiney, M.R., Muller-Eberhard, H.J., and Feldman, J.D. (1968). Ultrastructural localisation of the third and fourth components of complement on complement-cell complexes. Am. J. Path. 53, 253.

Mazia, D. (1975). Adhesion of Cells to Surfaces Coated with Polylysine. J. Cell Biol. 66, 198-200.

McFairland, W., Heilman, D., and Moorhead, J.F. (1966). Functional anatomy of the lymphocyte in immunological reactions in vitro. J. Exptl. Med. 124, 851-858.

McPherson, I., and Stoker, M. (1962). Polyoma transformation of hamster cell clones, an investigation of genetic factors affecting cell competence. Virology 16, 147-151.

Melli, M., Spinelli, G., and Arnold, E. (1977). Synthesis of Histone Messenger RNA of HeLA Cells during the Cell Cycle. Cell 12, 167-174.

Merlie, J.P., Sobel, A., Changeux, J.P., and Gros, F. (1975). Synthesis of acethylcholine receptors during differentiation of cultured embryonic muscle cells. Proc. Natl. Acad. Sci. USA, 72, 4028-4032.

Micheel, B., and Bierwolf, D. (1968). Demonstration of Graffi virus-induced surface antigens of leukemia cells by indirect immunoferritin technique. Exptl. Cell Res. 54, 268-271.

Micheel, B. (1970). Ferritin-labelled antibodies and their use in experimental cancer research. Arch. Geschwulst Forsch 36, 17.

Micheel, B., Pasternak, D., and Bierwolf, D. (1972). Immunologische Untersuchungen an virusinduzierten Maus - und Ratten-leukämien. Acta. Biol. Med. Germ. 28, 167-175.

Miller, M.F., Dmochowsky, L., and Bowen, J.M. (1977). Immunoelectron Microscopic Studies of Antibodies in Mouse Sera directed against Mouse Mammary Tumor Virus. Cancer Res. 37, 2086-2091.

Milner, G. (1969). Nuclear morphology and the ultrastructural localisation of deoxyribonucleic acid synthesis during interphase. J. Cell. Sci. 4, 569-582.

Mitchinson, J.M. (1971). The Biology of the Cell Cycle. London, Cambridge University Press.

Mittermayer, C., Kaden, P., and Sandritter, W. (1968). Untersuchungen an teilungssynchronen L-Zellen. Histochemie 12, 67-74.

Miura, T., and Utakoji, T. (1961). Studies on Synchronous Division of FL Cells by Chilling. Exp. Cell Res. 23, 452-459.

Mohberg, T., and Johnson, M.J. (1963). Amino acid utilisation by 929-L fibroblasts in chemically defined media. J. Nat. Cancer Inst. 31, 611.

Moore, G.E. (1964). In vitro cultures of a pigmented hamster melanoma cell line. Exp. Cell Res. 36, 422-423.

Morgan, C., Hsu, K.C., Rifkind, R.A., Knox, A.W., Rose, H.M. (1961). The application of ferritin conjugated antibody to electron microscopic studies of influenza virus-infected cells. I. The cellular surface. J. Exptl. Med. 114, 825-832.

Morgan, C., Rifkind, R.A., Hsu, K.C., Holden, M., Seegal, B.C., and Rose, H.M. (1961). Electron microscopic localisation of intracellular viral antigen by the use of ferritin-conjugated antibody. Virology 14, 292.

Mouse, G.Y., Trevithick, J.R., Bechberger, J., and Blair, D.G. (1978). Cytochalasin D induces the capping of both leukaemia viral proteins and actin in infected cells. Nature 274, 808-809.

Obata, Y., Ikeda, H., Stockert, E., and Boyse, E.A. (1975). Relation of G IX antigen of thymocytes to envelope glycoprotein of murine leukemia virus. J. Exp. Med. 14, 188-197.

O'Brien, S.J., Simonson, J.M., and Boone, C.W. (1976). Expression of viral structural proteins on murine cell surfaces in association with the production of murine leukaemia virus. J. Gen. Virol. 33, 355-360.

O'Brien, S.J., Simonson, J.M., and Davis, S. (1978). Deposition of Retrovirus Associated Antigens (p30 and gp70) on Cell Membranes of Feline and Murine Leukaemia Virus Infected Cells. J. Gen. Virol. 38, 483-496.

Okasinski, G.F., and Velicier, L.F. (1977). Analysis of intracellular feline leukaemia virus proteins. II. Generation of feline leukaemia virus structural proteins from precursor polypeptides. J. Virol. 22, 74-85.

Olmsted, J.B., and Borisy, G.G. (1973). Microtubules. Ann. Rev. Biochem. 42, 507-539.

Olsen, B.R., Berg, R.A., Kishida, Y., and Prockop, D.J. (1973). Collagen synthesis: Localisation of prolyl hydroxylase in tendon cells detected with ferritin-labelled antibodies. Science (Wash. D.C.), 182, 825.

Olsen, B.R., Berg, R.A., Kishida, Y., and Prockop, D.J. (1975). Further characterisation of embryonic tendon fibroblasts and the use of immuno-ferritin techniques to study collagen biosynthesis. J. Cell. Biol. 64, 340-355.

Olsen, R.G., Milo, G.E., Schaller, J.P., Heding, L., and Yohn, D.S. (1976). Influence of culture conditions on growth of FL74 cells and feline oncornavirus associated cell membrane antigen production. In Vitro 12, 37-43.

Onodera, K., and Sheinin, R. (1970). Macromolecular glucosamine-containing component on surface of cultivated mouse cells. J. Cell Sci. 7, 337-355.

Ooka, T., and Daillie, J. (1974). A new method for cell culture synchronisation. Exp. Cell Res. 84, 219-222.

Oshiro, L.S., Rose, H.M , Morgan, C , and Hsu, K.C. (1967). Electron microscopic study of the development of simian virus 40 by use of ferritin-labelled antibodies. J. Virol. 1, 384.

Otten, J., Johnson, G.S., and Pastan, I. (1971). Cyclic AMP levels in fibroblasts: relationship to growth rate and contact inhibition of growth. Biochem. Biophys. Res. Commun. 44, 1192-1198.

Otten, J., Bader, J.P., Johnson, G.S., and Pastan, I. (1972). A mutation in Rous sarcoma virus gene that controls adenosine 3', 5'-cyclic monophosphate levels and transformation. J. Biol. Chem. 247, 1632-1633.

Pages, J., Mantenil, S., Stehelin, D., Fiszman, M., Marx, M., and Girard, M (1973). Relationship between replication of simian virus 40 DNA and specific events in the host cell cycle. J. Virol. 12, 99-107.

Palade, G. (1959). Functional changes in the structure of cell components. In: T. Haysky (Ed.) 'Subcellular Particles' Ronald Press, New York. pp.64-83.

Panem, S., and Kirsten, W.H. (1973). Release of mouse leukaemia-sarcoma virus from synchronised cells. J. Nat. Cancer Inst. 50, 563-565.

Panem, S., and Schauf, V. (1974). Cell Cycle Dependent Appearance of Murine Leukaemia-Sarcoma Virus Antigens. J. Virol. 13, 1169-1175.

Panem, S., and Kirsten, W.H. (1975). Secondary scanning electron microscopy of cells infected with murine oncornaviruses. Virology 63, 447-458.

Panem, S., and Kirsten, W.H. (1976). Effects of Metabolic Inhibitors on Oncornavirus Production during Synchronised Cell Growth. Comp. Leuk. Res. 1975, Bibl. Haemat. 43, 472-474 (Karger, Basel 1976).

Panem, S (1977). Cell Cycle-Dependent Inhibition of Kirsten Murine Sarcoma-Leukemia Virus Release by Cytochalasin B. Virology 76, 146-151.

Pardee, A.B. (1974). A Restriction Point for Control of Normal Animal Cell Proliferation. Proc. Natl. Acad. Sci. USA, 71, 1286-1290.

Pardee, A.B. (1975). The cell surface and fibroblast proliferation. Some current research trends. Biochim. Biophys. Acta 417, 153-174.

Parmley, R.T., Dow, L.W., and Mauer, A.M. (1977). Ultrastructural cell cycle-specific nuclear and nucleolar changes of human leukemic lymphoblasts. Cancer Res. 37, 4313-4325.

Parr, E.L., and Oei, J.S. (1973). Immobilisation of Membrane H-2 Antigens by Paraformaldehyde Fixation. J. Cell Biol. 59, 537-542.

Paskind, M.P., Weinberg, R.A., and Baltimore, D. (1975). Dependence of Moloney Mu LeV Production on Cell Growth. Virology 67, 242-248.

Pasternak, C.A., Warmsley, A.M.H., and Thomas, D.B. (1971). Structural alterations in the surface membrane during the cell cycle. J. Cell Biol. 50, 562-564.

Payne, J.W. (1973). Polymerization of proteins with glutaraldehyde. Biochem. J. 135, 867.

Pederson, T., and Gelfant, S. (1970). G_2-Population Cells in Mouse Kidney and Duodenum and their Behaviour during the Cell Division Cycle. Exptl. Cell Res. 59, 32-36.

Pederson, T. (1972). Chromatin structure and the cell cycle. Proc. Natl. Acad. Sci. USA, 69, 2224-2228.

Pederson, T., and Robbins, E. (1972). Chromatin structure and the cell division cycle, actinomycin binding in synchromised HeLa cells. J. Cell Biol. 55, 322-327.

Pellegrino, M.A., Ferrone, S., Natali, G.G., and Reisfeld, R.A. (1972). Expression of HL-A antigens in synchronised cultures of human lymphocytes. J. Immunol. 108, 573-576.

Perecko, J.P , Berezesky, I K., and Grimley, P.M (1973). Surface features of some established murine cell lines under various conditions of oncogenic virus infection. In "SEM/IITRI/1973, pp.521-528.

Petersen, D.F., and Anderson, E.C (1964). Quantity Production of Synchronised Mammalian Cells in Suspension Culture. Nature 203, 642-643.

Petersen, D.F., Tobey, R.A., and Anderson, E.C. (1969). Synchronously dividing mammalian cells. Fed. Proc. 28, 1771-1779.

Pfeiffer, S.E , and Tolmach, C.J. (1967). Selecting Synchronous Populations of Mammalian Cells. Nature (Jan. 14), 139-142.

Polliack, A., Lampen, N., Clarkson, β.D., and Harven, E.D. (1973). Identification of Human B and T Lymphocytes by Scanning Electron Microscopy. J. Exp. Med. 138, 607-624.

Polliack, A., Touraine, J.L., De Harven, E., Lampen, N., and Hadden, J.W. (1975). Scanning electron microscopy of mitogen transformed human lymphocytes. Israel J. Med. Sci. 11, 1285-1295.

Polliack, A., Froimovici, M., Pozzoli, E., and Lambertenghi-Deliliers, G. (1976). Acute Lymphoblastic Leukemia: A Study of 25 cases by Scanning Electron Microscopy. Blut 33, 359-366.

Porter, K.A., Andres, G.A., Calder, N.W., Dossetor, J.B , Hsu, K.C., Rendall, J.M., Seegal, B.C., and Starzl, T.L. (1968). Human renal transplants. II. Immunofluorescent and immunoferritin studies. Lab. Invest. 18, 159.

Porter, K.R., Kelley, D., and Andrews, P.M. (1972). The Preparation of Cultured Cells and Soft Tissues for Scanning Electron Microscopy. In 'Proceedings of the Fifth Annual Stereoscan Colloquium' 1972, Kent. Cambridge Scientific Inc., Morton Grove, Ill.

Porter, K.R., and Todaro, G.J., and Fonte, V. (1973). Scanning Electron Microscopic Study of Surface Features of Viral and Spontaneous Transformants of Mouse BALB/3T3 Cells. J. Cell Biol. 59, 633-642.

Porter, K.R., Prescott, D., and Frye, J. (1973). Changes in Surface Morphology of Chinese Hamster Ovary Cells during the Cell Cycle. J. Cell Biol. 57, 815-836.

Porter, K.R , and Fonte, V. (1973). Observations on the topography of normal and cancer cells. Scanning Electron Micros copy. IIT Research. Institute, Chicago, 683-688.

Porter, K.R., Fonte, V., and Weiss, G. (1974). A scanning microscope study of the topography of HeLa cells. Cancer Res. 34, 1385-1394.

Poste, G., Schaeffer, B., Reeve, P., and Alexander, D.J. (1974). Rescue of simian virus 40 (SV40) from SV40-transformed cells by fusion with anucleate monkey cells and variation in the yield of virus rescued by fusion with replicating or non-replicating monkey cells. Virology 60, 85-95

Potmesil, M., and Smetana, K. (1969). Significance of Ring-Shaped Nucleoli and Micronucleoli in Human Lymphocytes. Folia Biol. (Prague) 15, 300-305.

Potmesil, M., and Goldfeder, A. (1972). Nucleolar Morphology and Maturation of Thymic Lymphocytes. J. Cell Biol. 53, 832-837.

Potmesil, M., and Goldfeder, A. (1973). Nucleolar Morphology and Cell Proliferation Kinetics of Thymic Lymphocytes. Exptl. Cell Res. 77, 31-40.

Potmesil, M., and Goldfeder, A.(1977). Identification and Kinetics of G_1 Phase-confined Cells in Experimental Mammary Carcinoma. Cancer Res. 37, 857.

Prescott, D.M. (1976). The Cell Cycle and the Control of Cellular Reproduction. Adv. Genet. 18, 99-177.

Prescott, D.M. (1976). Reproduction of Eukaryotic Cells. Academic Press New York.

Puck, T.T., and Steffen, J. (1963). Life cycle analysis of mammalian cells. I. A method for localising metabolic events within the life cycle, and its application to the action of colcemide and sublethal doses of X-irradiation. Biophys. J. 3, 379-397.

Randal, E.M., and Fritz, R.B. (1975). Expression of Virion and Tumor-specific Antigens on the Surface of Chick Embryo Cells Infected with Strain MC29 Avian Leukosis Virus. Cancer Res. 36, 414-418.

Rao, P.N., and Johnson, R.T. (1974). Induction of chromosome condensation in interphase cells. Adv. Cell Mol. Biol. 3, 135-189.

Recher, L., Whitescarver, J., and Briggs, L. (1969). The Fine Structure of a Nucleolar Constituent. J. Ultrastruct. Res. 29, 1-14.

Reif-Lehrer, L. (1971). Actinomycin-D enhancement of glutamine synthetase activity in chick embryo retina cultures in the presence of cortisol. J. Cell Biol. 51, 303-311.

Revoltella, R , Bertolini, L., and Pediconi, M. (1974). Unmasking of nerve growth factor membrane specific binding sites in synchronised murine C13oo neuroblastoma cells. Exp. Cell. Res. 85, 89-94.

Reynolds, E.S. (1963). The Use of Lead Citrate at High pH as an Electron-Opaque Stain in Electron Microscopy. J. Cell Biol. 17, 208.

Rezko, E., and Bogel, K. (1962). Elektron Mikroskopische Untersuchungen über das Verhalten eines vom Kalb isolierten parainfluenza-3 Virus in Kalbernieren Zellkulturen. Arch. Ges. Virus Forsch. 12, 404.

Richards, F.M., and Knowles, J. (1968). Glutaraldehyde as a protein cross-linking reagent. J. Mol. Biol. 37, 231.

Roath, S., and Newell, D.G. (1975). T and B Lymphocytes. Lancet 1, 221.

Robbins, E., and Marcus, P.I. (1964). Mitotically synchronised mammalian cells: a simple method for obtaining large populations. Science 144, 1152-1153.

Robinson, S.H., Brecher, G., Lourie, J.S., and Haley, J. (1965). Leukocyte labelling in rats during and after continuous infusion of tritiated thymidine: implications for lymphocyte longevity and DNA re-utilisation. Blood 26, 281-295.

Robinson, A.G., Butcher, R.W., and Sutherland, E.W. (1972). Cyclic AMP. Academic Press, New York.

Rogerson, P., Jarrett, W.F.H., and Mackey, L.J. (1975). Epidemiological studies on feline leukaemia virus infection. I. A serological survey in urban cats. Int. J. Cancer 15, 781.

Rosenberg, R.N., Van De Venter, L., De Francesco, L., and Friedkin, M.E. (1971). Regulation of the synthesis of choline-o-acetyltransferase and thymidylate synthetase in mouse neuroblastoma in cell culture. Proc. Natl. Acad. Sci. USA, 68, 1436-1440.

Rosenfeld, C., Dore, J.F., Choquet, C., Venaut, A.M., Ajuria, E., Marholev, L., and Vastiaux, J.P. (1973a). Variations in expression of cell membrane antigens by cultured cells. A study of antilymphocytic-globulin binding by human lymphoblastoid cells before, during, and after their establishment as culture lines. Transplantation 16, 279-286.

Rosenfeld, C., Dore, J.F., Choquet, C., Venaut, A.M., Vastiaux, J.P., Guibout, C., and Pico, J.C. (1973b). Variations au cours du cycle cellulaire de l'expression des cellules d'une lignee lymphoblastoide. C.R. Acad. Sci. Paris. Ser. D. 277, 2829-2832.

Rubin, R.W., and Everhart, L.P. (1973). The Effect of Cell-to-Cell Contact on the Surface Morphology of CHO Cells. J. Cell Biol. 57, 837-844.

Ruddle, F.H., and Rapola, J. (1970). Changes in lactate dehydrogenase and esterase specific activities, isozymic patterns, and cellular distribution during the growth cycle of PK cells in vitro. Exp. Cell Res. 59, 399-412.

Rueckert, R.R., and Mueller, G.C. (1960). Studies on unbalanced growth in tissue culture. I. Induction and consequences of thymidine deficiencies. Cancer Res. 20, 1584.

Ruscetti, S.K., Scolnick, E.M., and Parks, W.P. (1976). Characterisation of the feline oncornavirus-associated cell membrane antigen. In 'Proceedings of the Cold Spring Harbor Meeting on Oncornaviruses', p.45.

Russell, P.H. (1977). Neutralising Antibodies in Feline Leukaemia Virus Infections. Ph.D. thesis, University of Glasgow.

Sakayima, H., Gross, S.K., and Robbins, P.W. (1972). Glycolipid synthesis in normal and virus transformed hamster cell line. Proc. Natl. Acad. Sci. USA, 69, 872-876.

Sakayima, H., and Terasima, T. (1975). The synthesis of Forssman glycolipid in clones of Nil2 hamster fibroblasts grown in monolayer or spinner culture. Cancer Res. 35, 1723-1726.

Salden, M., Asselbergs, F., and Bloemendal, H. (1976). Translation of oncogenic virus RNA in Xenopus laevis oocytes. Nature 259, 696-699.

Samosudova, N.V., Ogievetskaya, M.M., Kalam-Karova, M.B., and Frank, G.M. (1968). Use of ferritin antibodies for the electron-microscopic study of myosin. 3. Localisation of ferritin actinomyosin in the sarcomere. Biofizike 13, 877.

Sanger, J.W., and Holtzer, H. (1972). Cytochalasin B: Effects on Cell Morphology, Cell Adhesion, and Mucopolysaccharide Synthesis. Proc. Natl. Acad. Sci. USA, 69, 253-257.

Sarkar, N.H., Pomenti, A.A., and Dion, A.S. (1977). Replication of Mouse Mammary Tumor Virus in Tissue Culture. II. Kinetics of Virus Production and the Effect of RNA and Protein Inhibitors on Viral Synthesis. Virology 77, 31-44.

Saunders, G.C., and Wilder, M. (1971). Repetitive maturation cycles in a cultured mouse myeloma. J. Cell Biol. 51, 344-348.

Schachtschnabel, D. (1970). Speziphische Zellfunkzionen von Zell and Gewebekulturen. I. Züchtung von Melanin-bildenden Zellen des Haroling-Passey-Melanomas in Monolayer Kultur. Virchows Archiv. Abt. Zell pathol. 7, 27-36.

Schachtschnabel, D., Fischer, R.D., und Zilliken, F. (1971). Speziphische Zellfunctionen von Zell - und Gewebekulturen. II. Untersuchungen zur Kontrolle der Melanin - Synthese in Zellkulturen des Harding - Passey - Melanomas. Z. Physiol. Chem. 351, 1402-1410.

Schwartz, B.D., and Nathenson, S.G. (1971). Regeneration of transplantation antigens on mouse cells. Transplan. Proc. 3, 180-182.

Schwartz, S.A., Panem, S., and Kirsten, W.H. (1975). Distribution and virogenic effects of 5-bromodeoxyuridine in synchronised rat embryo cells. Proc. Natl. Acad. Sci. USA, 72, 1829-1833.

Schwartz, H., Hunsmann, G., Moenning, V., and Schäfer, W. (1975). Properties of Mouse Leukemia Viruses. XI. Immunoelectron Microscopic Studies on Viral Structural Antigens on the Cell Surface. Virology 69, 169-178.

Sheppard, J.R. (1971). Restoration of contact-inhibited growth to transformed cells by dibutyryl adenosine 3', 5'-cyclic monophosphate. Proc. Natl. Acad. Sci. USA, 68, 1316-1320.

Sheppard, J.R. (1972). Differences in the cyclic adenosine 3', 5'- monophosphate levels in normal and transformed cells. Nature New Biol. 236, 14-16.

Sternberger, L.A., Donati, E.J., Cuculis, J.J., and Petrali, J.P. (1965). Indirect immunouranium technique for staining of embedded antigen in electron microscopy. Exp. Mol. Path. 4, 112.

Sternberger, L.A., Hardy, P.H. Jr., Coculis, J.J., and Meyer, H.G. (1970). The unlabelled enzyme method of immuno-histochemistry, preparation of antigen-antibody complex (peroxidase-antiperoxidase) in identification of spirochetes. J. Histochem. Cytochem. 18, 315.

Stubblefield, E., and Klevecz, R.R. (1965). Synchronisation of Chinese hamster cells by reversal of colcemide inhibition. J. Cell Biol. 40, 660-664.

Studzinski, G.P., and Lambert, W.G. (1969). Thymidine as a synchronising agent. I. Nucleic acid and protein formation in synchronous HeLa cultures treated with excess thymidine. J. Cell Physiol. 73, 109.

Summer, M.C.B., Collin, R.C.L.S., and Pasternak, C.A. (1973). Synthesis and expression of surface antigens during the cell cycle. Tissue Antigens 3, 477-484.

Swift, H. (1963). Cytochemical Studies on Nucleolar Fine Structure. Exptl. Cell Res. Suppl. 9, 54-67.

Tan, Y.H., Armstrong, J.A., Ke, Y.H., and Ho, M. (1970). Regulation of cellular interferon production. Enhancement by anti-metabolites. Proc. Natl. Acad. Sci, USA, 67, 464-471.

Tanaka, H., and Moore, D.H. (1967). Electron Microscopic Localisation of Viral Antigens in Mouse Mammary Tumors by Ferritin-Labelled Antibody. I. The Homologous System. Virology 33, 197-214.

Taylor, R.B., Duffus, P.H., Raff, M.C., and De Petris, S. (1971). Redistribution and pinocytosis of lymphocyte surface immunoglobulin molecules induced by anti-immunoglobulin antibody. Nature New Biol. 233, 225.

Temin, H.M. (1963). The effects of actinomycin D in Rous sarcoma virus production. Virology 23, 486-494.

Temin, H.M. (1967). Studies on Carcinogenesis by Avian Sarcoma Viruses. V. Requirement for new DNA synthesis and for cell division. J. Cell Physiol. 69, 53-64.

Temin, H.M. (1971). Mechanism of Cell Transformation by RNA Tumor Viruses. Annual Rev. of Microbiol. 25

Temin, H.M. (1971). Stimulation by Serum of Multiplication of Stationary Chicken Cells. J. Cell Physiol. 78, 161-170.

Terasima, T., and Tolmach, L.J. (1963). Growth and nucleic acid synthesis in synchronously dividing populations of HeLa cells. J. Exp. Cell Res. 30, 344-362.

Terasima, T., and Yokoyama, T. (1966). Further supports for harvesting procedure of synchronising mammalian cells in culture. Gann 57, 95-98.

Terasima, T., Fujivara, Y., Tanaka, S., and Yasukawa, M. (1968). Synchronous culture of L cells and initiation of DNA synthesis. In: Cancer Cells in Culture. H. Katsuta, (Ed.), University of Tokyo Press, Tokyo, pp.73-84.

Theilen, G.H., Kawakami, T.G., Rush, J.D., and Munn, R.J. (1969). Replication of cat leukemia virus in cell suspension cultures. Nature 222, 589-590.

Thomas, D.B. (1971). Cyclic expression of blood group determinants in murine cells and their relationship to growth control. Nature (London) New. Biol. 233, 225-229.

Thomas, D.B., and Phillips, B. (1973). Membrane antigens specific for human lymphoid cells in the dividing phase. J. Exp. Med. 138, 64-70.

Thomas, D.B. (1974). The i antigen complex: a new specificity unique to dividing human cells. Eur. J. Immunol. 4, 819-824.

Thompson, E.B., Granner, D.K., and Tomkins, G.M. (1970). Super-induction of tyrosine aminotransferase by actinomycin D in rat hepatoma (HTC) cells. J. Mol. Biol. 54, 159-175.

Thorne, H.V. (1973). Cyclic variations in the susceptibility of BALB/c 3T3 cells to polyoma virus. J. Gen. Virol. 23, 73-82.

Tobey, R.A., and Ley, K.D. (1970). Regulation of initiation of DNA synthesis in Chinese hamster cells. I. Production of stable, reversible G_1-arrested populations in suspension cultures. J. Cell Biol. 46, 151.

Tobey, R.A., Petersen, D.F., and Anderson, E.C. (1971). The Cell Cycle and Cancer. R. Baserga, (Ed.), New York, M. Dekker.

Todaro, G.T., and Green, H. (1966). Cell growth and initiation of transformation by SV40. Proc. Natl. Acad. Sci. USA, 55, 302-308.

Tokuyasu, K., Madden, S.C., and Zeldis, L.J. (1968). Fine structural alterations of interphase nuclei of lymphocytes stimulated to growth activity in vitro. J. Cell Biol. 39, 630-660.

Tomkins, G.M., Gelehrter, T.D., Grauner, D., Martin, D. Jr., Samuels, H.H., and Thompson, E.B. (1969). Control of specific gene expression in higher organisms. Science 166, 1474-1480.

Tung, J.S., Vitetta, E., Fleissner, E., and Boyse, E.A. (1975). Biochemical evidence linking the G_{IX} thymocyte surface antigen to the gp69/71 envelope glycoprotein of murine leukemia virus. J. Exp. Med. 141, 198-205.

Tung, J.S., Yoshiki, T., and Fleissner, W. (1976). A core polyprotein of murine leukemia virus on the surface of mouse leukemia cells. Cell 9, 573-578.

Turner, M.J., Strominger, J.L., and Sanderson, A.R. (1972). Enzymic removal and re-expression of histocompatibility antigen HL-A2 at the surface of human peripheral lymphocytes. Proc. Natl. Acad. Sci. USA, 69, 200-202.

Van De Ven, W.J.M., Vermorken, A.J.M., Onnekink, C., Bloemers, H.P.J., and Bloemendal, H. (1978). Structural Studies on Rauscher Murine Leukemia Virus. Isolation and Characterisation of Viral Envelopes. J. Virol. 27, 595-603.

Vasiliev, J.M., Gelfand, I.M., Domnina, L.V., Ivanova, O.Y., Komm, J.G., and Olshevskaja, L.V. (1970). Effect of Colcemid on the locomotory behaviour of fibroblasts. J. Embryol. Exp. Morph. 24, 625-640.

Veseley, P., and Boyde, A. (1973). The significance of SEM evaluation of the cell surface for tumor cell biology. In: SEM (IITRI) 1973, pp.689-695.

Vogt, V.M., Eisenman, R., and Diggelmann, H. (1975). Generation of avian myeloblastosis virus structural proteins by proteolytic cleavage of a precursor polypeptide. J. Mol. Biol. 96, 471-493.

Van Der Helm, K., and Duesberg, P. (1975). Translation of Rous sarcoma virus RNA in a cell-free system from ascites Krebs II Cells. Proc. Natl. Acad. Sci. USA, 72, 614-618.

Wagner, M., and Veckenstedt, A. (1970). Electron microscopic detection of mengovirus in L ells with ferritin-labelled antibodies. Arch. Gesamte Virus Vorsch. 32, 147.

Walker, P.D., Baillie, A., Thompson, R.D., and Batty, I. (1966). Use of ferritin-labelled antibodies in the location of spore and vegetative antigens of B. cereus. J. Appl. Bact. 29, 512.

Walker, P.D., Thompson, R.O., and Baillie, A. (1967). Use of ferritin-labelled antibodies in the location of spore and vegetative antigens in B. subtilis. J. Appl. Bact. 30, 317.

Watson, M.L. (1958). Staining of Tissue Sections for Electron Microscopy with Heavy Metals. J. Biophys. Biochem. Cytol. 4, 475-478.

Westbrook, E., Wetzel, B., Cannon, G.B., and Berard, D. (1975). The impact of culture conditions on the surface morphology of cells in vitro. In: SEM/IITRI/1975, pp.351-360.

White, J.D., and McManus, A.T. (1975). SEM of vesicular stomatitis virus infection in cell cultures grown on aluminium foil. In: SEM/IITRI/1975, pp.411-416.

Whitmore, G.F., and Gulyas, S. (1966). Synchronisation of Mammalian Cells with Tritiated Thymidine. Science 151, 691.

Whittaker, J.R. (1963). Changes in melanogenesis during the differentiation of chick pigment cells in cell culture. Dev. Biol. 8, 99-127.

Willingham, M.C., and Pastan, I. (1975). Cyclic AMP and cell morphology in cultured fibroblasts. Effects on cell shape, microfilament and microtubule distribution and orientation to substratum. J. Cell Biol. 67, 146-159.

Witte, O.N., and Weissman, I.L. (1974). Polypeptides of Moloney sarcoma-leukemia virions: Their resolution and incorporation into extra-cellular virions. Virology 61, 575-587.

Witte, O.N., Tsukamoto-Adey, A., and Weissman, I.L. (1977). Cellular maturation of oncornavirus glycoproteins: topological arrangement of precursor and product forms in cellular membranes. Virology 76, 539-553.

Wolf, B.A., and Robbins, P.W. (1974). Cell mitotic cycle synthesis of NIL hamster glycolipids including the Forssman antigen. J. Cell Biol. 61, 676-687.

Yamaguchi, H., Ishiguro, S., Oka, Y., and Miyamoto, H. (1977). L-cells in Mitosis Selected by an Improved Technique. Effects of Cold Storage. Cell Struct. and Function 2, 111-118.

Yoshinaka, Y., and Luftig, R.B. (1977). Partial characterisation of a P70 proteolytic factor that is present in purified virions of Rauscher leukemia virus (RLV). Biochem. Biophys. Res. Commun. 76, 54-63.

Yoshikura, H. (1968). Requirement of cellular DNA synthesis for the growth of Friend leukemia virus. Exp. Cell Res. 52, 445.

Yoshikura, H., and Hirokava, Y. (1968). Induction of cell replication. Exp. Cell Res. 52, 439.

Yoshikura, H. (1970). Dependence of murine sarcoma virus infection on the cell cycle. J. Gen. Virol. 6, 183.

Yoshiki, T., Mellors, R.C., and Hardy, W.D. Jr. (1973). Common Cell-Surface Antigen Associated with Murine and Feline C-Type RNA Leukemia Viruses. Proc. Natl. Acad. Sci. USA, 70, 1878-1882.

Yoshiki, T., Mellors, R.C., Hardy, W.D. Jr., and Fleissner, E. (1974). Common cell surface antigen associated with mammalian C-type RNA viruses. J. Exp. Med. 139, 925-941.

Xeros, N. (1962). Deoxyribose control and synchronisation of mitosis. Nature (London) 194, 682.

Zeilig, C.E., Johnson, R.A., Friedman, D.L., and Sutherland, E.W. (1972). Repetitive Synchronisation of Human Lymphoblast Cultures. J. Cell Biol. 55, 296a.

Zeilig, C.E., Johnson, R.A., Sutherland, E.W., and Friedman, D.L. (1974). Cyclic AMP Levels in Synchronised HeLa Cells and a Dual Effect on Mitosis. Fed. Proc. 33 (II), 948.

Zeilig, C.E., Johnson, R.A., Sutherland, E.W., and Friedman, D.L. (1976). Adenosine 3':5'-Monophosphate Content and Actions in Division Cycle of Synchronised HeLa Cells. J. Cell Biol. 71, 515-534.

Zeilig, C.F., and Goldberg, N.D. (1977). Cell cycle-related changes of 3':5'-cyclic GMP levels in Novikoff hepatoma cells. Proc. Natl. Acad. Sci. USA, 74, 1052-1056.